Design of kidney-targeted drug-carrier conjugates for the inhibition of profibrotic signaling cascades

Maria Emma Maartje Dolman

2011

The printing of this thesis was financially supported by:

Utrecht Institute for Pharmaceutical Sciences, Utrecht, The Netherlands

LinXis B.V., Amsterdam, The Netherlands

J.E. Jurriaanse Stichting, Rotterdam, The Netherlands

tebu-bio, Heerhugowaard, The Netherlands

Design of kidney-targeted drug-carrier conjugates for the inhibition of profibrotic signaling cascades

By Maria Emma Maartje Dolman

Ph.D. thesis, with a summary in Dutch
Department of Pharmaceutics, Utrecht University, The Netherlands

ISBN: 978-90-393-5572-5

Cover design: Roberta Censi, Negar Babae and Aart-Jan Dolman

Printed by Ipskamp Drukkers B.V., Enschede, The Netherlands

Design of kidney-targeted drug-carrier conjugates for the inhibition of profibrotic signaling cascades

Het ontwerpen van nierspecifieke geneesmiddel conjugaten voor het remmen van profibrotische signaleringsroutes
(met een samenvatting in het Nederlands)

Proefschrift

ter verkrijging van de graad van doctor aan de Universiteit Utrecht op gezag van de rector magnificus, prof. dr. G.J. van der Zwaan, ingevolge het besluit van het college voor promoties in het openbaar te verdedigen op maandag 27 juni 2011 des middags te 4.15 uur

door

Maria Emma Maartje Dolman

geboren op 31 oktober 1981 te Utrecht

Promotoren: Prof. dr. ir. W.E. Hennink
Prof. dr. G. Storm

Co-promotor: Dr. R.J. Kok

Dit proefschrift werd (mede) mogelijk gemaakt met financiële steun van het zesde kaderprogramma voor onderzoek van de EU (FP6, LSHB-CT-2007-036644, DIALOK).

Voor mijn familie

Table of Contents

General introduction

1. Tubulointerstitial fibrosis in chronic kidney disease

Chronic kidney disease (CKD) is a major health problem in the world, associated with increased morbidity and mortality (1-6). Patients with other serious health problems such as diabetes, hypertension and/ or obesity are at increased risk for CKD (1, 2, 7, 8). Currently, the treatment of CKD is focused on prevention of further deterioration of kidney function by treatment of the underlying disease, *e.g.* normalization of blood glucose levels or blood pressure (9). However, due to the asymptomatic nature of CKD in the early stages, CKD is often diagnosed in the late stage in which treatment of the underlying cause is not sufficient to cure the patient (4). As a consequence, patients develop end-stage renal disease (ESRD) (3, 10), which means that the renal function is so low that renal dialysis or kidney transplantation are essential for survival (11). Because there is a lack of clinically available therapeutics that can halt or reverse the progression of CKD (12), we need to follow innovative approaches to develop them. The underlying mechanism responsible for the progression of CKD to ESRD is renal fibrosis, commonly characterized by glomerulosclerosis, capillary loss, tubular atrophy and dilatation and tubulointerstitial fibrosis (12-14). In this thesis we focused on the development of novel therapeutics that can intervene in the progression of CKD by inhibiting tubulointerstitial fibrosis.

2. Kinase-mediated activation of proximal tubular cells

An important step in the pathogenesis of tubulointerstitial fibrosis is the activation of proximal tubular cells (**Figure 1**) (15-17). Activated proximal tubular cells induce an inflammatory response and undergo epithelial-to-mesenchymal transition (EMT) into myofibroblasts which start to produce excessive amounts of extracellular matrix (ECM), eventually resulting in the formation of scar tissue and loss of renal function (18-27). These profibrotic actions of the proximal tubular cells are mediated by a complex intracellular network of signaling cascades, with a key role for growth factor activated- and stress activated kinases (12, 16, 28). Kinases are enzymes that modulate the activity of downstream targets by transferring a phosphate group from adenosine triphosphate (ATP) to its substrates (*e.g.* kinases and transcription factors). Examples of kinases that have been associated with the development of tubulointerstitial fibrosis are the transforming growth factor-β receptor (TGFR-β) kinases (29-32), the platelet-derived growth factor receptor (PDGFR) kinases (12, 33), p38 mitogen activated protein kinase (p38 MAPK) (34-36) and Rho-associated kinase (ROCK) (37-39). Because of the importance of these kinases in the profibrotic actions of activated proximal tubular cells, kinase inhibitors are promising drug candidates for the treatment of tubulointerstitial fibrosis. The therapeutic use of small molecule kinase inhibitors is, however, frequently associated with severe unwanted side effects. This is especially true for multitargeted kinase inhibitors, such as sunitinib (40-42).

3. Delivery of kinase inhibitors into the proximal tubular cells

A strategy to avoid unwanted side effects of kinase inhibitors and simultaneously enhance their efficacy is to selectively deliver the kinase inhibitors into the cell type in which they need to exert their therapeutic effects and to prevent the entry of the kinase inhibiters in other cell types. As will be clear from this thesis, a rational strategy for the intracellular delivery of kinase inhibitors into the proximal tubular cells is to design kinase inhibitor-carrier conjugates that are internalized at the luminal side of the proximal tubular cells.

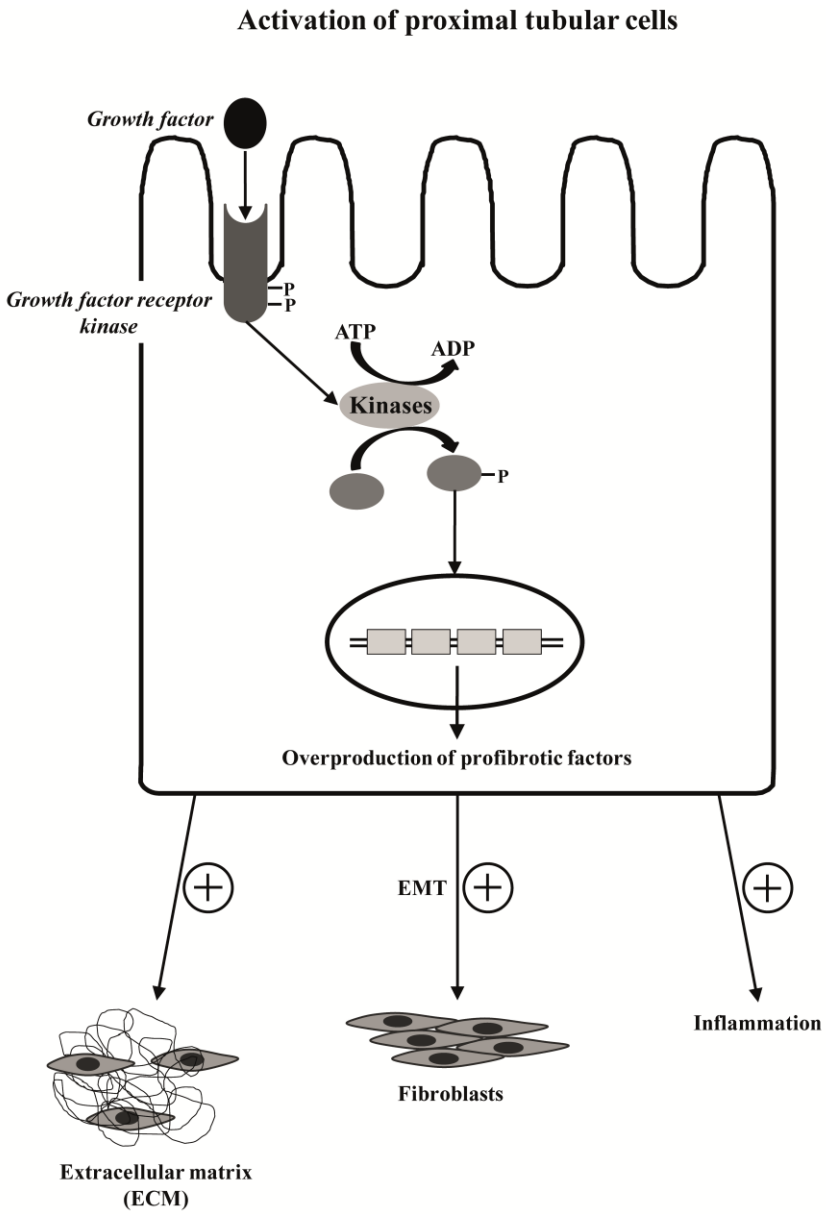

Figure 1. Schematic illustration of the activation of proximal tubular cells in the pathogenesis of tubulointerstitial fibrosis. Upon activation, growth factors bind to their receptors, which results in the onset of kinase-mediated signaling cascades. The activated signaling cascades ultimately induce the transcription of profibrotic genes, responsible for the inflammatory response, EMT and ECM production observed in tubulointerstitial fibrosis.

Kinase inhibitor-carrier conjugates (< 5-7 nm) can reach the luminal side of the proximal tubular cells after glomerular filtration from the circulation (43-45). Once the luminal side of the proximal tubular cells has been reached, the kinase inhibitor-carrier conjugates can be internalized via receptor-mediated endocytosis. The proximal tubular cells contain different internalizing receptors on their luminal membranes (46-48), that are able to internalize small molecules as well as macromolecular kinase inhibitor-carrier conjugates (49-51). As shown by the schematic illustration in **Figure 2**, in the development of kinase inhibitor-carrier conjugates the right combination needs to be chosen between carrier, linker and kinase inhibitor.

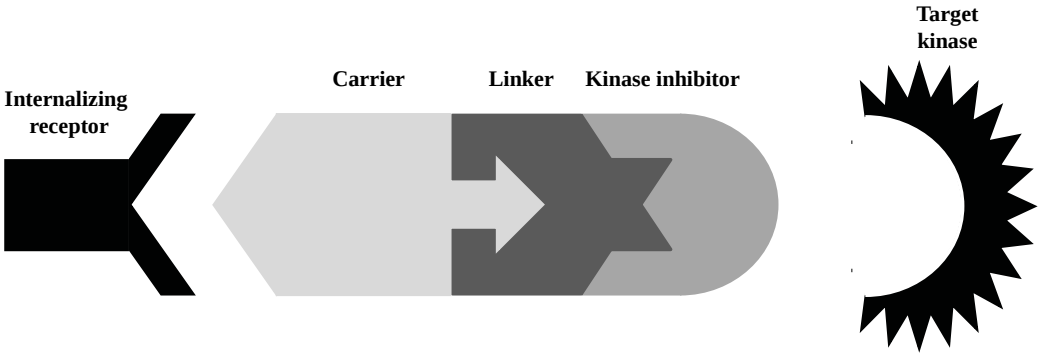

Figure 2. Schematic representation of kinase inhibitor-carrier conjugates. Such a product consists of three different functional parts: 1) a ligand or carrier that can bind to one of the internalizing receptors on the luminal membrane of the proximal tubular cells; 2) a kinase inhibitor that can inhibit a disease-related kinase within the targeted proximal tubular cells and 3) a linker that couples the kinase inhibitor to the carrier. The choice for a specific linker depends on the chemical constraints of the kinase inhibitor and carrier system as well as on pharmacokinetic considerations.

4. Megalin receptor-mediated endocytosis and lysosomal escape

Figure 3 illustrates the megalin receptor-mediated internalization of kinase inhibitor-carrier conjugates. Binding of the kinase inhibitor-carrier conjugate to megalin results in internalization of the conjugate-receptor complex in clathrin-coated vesicles. Via these coated vesicles the conjugate-receptor complex is routed to the endosomes and subsequently lysosomes of the cells. Within the late endosomes and lysosomes the megalin receptor is released from the conjugate due to the low environmental pH and recycled to the luminal membrane of the proximal tubular cells (49, 52, 53). Since the pharmacological targets of the kinase inhibitors are localized in the cytosolic compartment of the proximal tubular cells, lysosomal escape of the delivered kinase inhibitor is essential to obtain a pharmacological effect. Intact kinase inhibitor-carrier conjugates are too large for transport across the lysosomal membrane. The biodegradability of the carrier as well as the linker used for the coupling of the kinase inhibitor to the carrier will therefore have a major influence on the capability of the kinase inhibitor to reach its pharmacological targets and to exert its renoprotective effects.

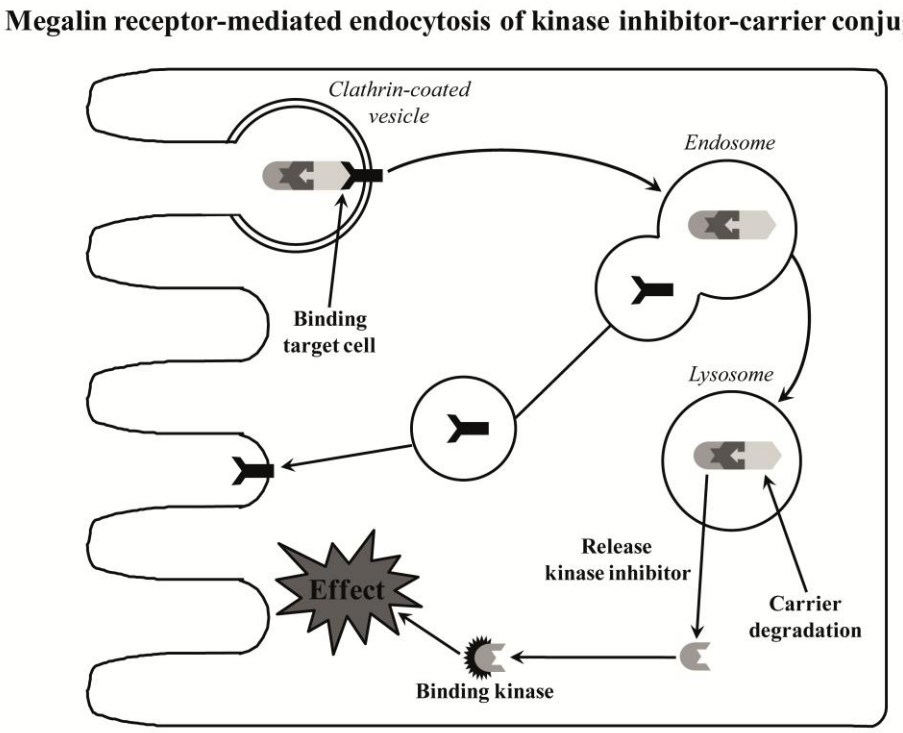

Figure 3. Illustration of the megalin receptor-mediated internalization of kinase inhibitor-carrier conjugates in the proximal tubular cells of the kidneys.

5. Aim and outline of the thesis

The aim of the current thesis is the development of kinase inhibitor-carrier conjugates for the cell-specific inhibition of profibrotic signaling cascades in proximal tubular cells. More specifically, strategies to improve the active kinase inhibitor levels within the proximal tubular cells of the kidneys are exploited. Furthermore, the potential of kinase inhibitor-carrier conjugates in the treatment of tubulointerstitial fibrosis is investigated. **Figure 4** shows the chemical structures of the kinase inhibitors that have been conjugated to a proximal tubular cell-specific carrier.

Chapter 1 describes carrier systems that can be used for the delivery of drugs to the glomerulus and tubular cells of the kidneys. It explains why drug targeting of kinase inhibitors to the proximal tubular cells may be beneficial in the treatment of tubulointerstitial fibrosis. Particular attention is paid to the design and characteristics of proximal tubular cell-specific kinase inhibitor-ULS-lysozyme conjugates. The results of the *in vitro* and *in vivo* antifibrotic effects obtained with LY364947-ULS-lysozyme, SB202190-ULS-lysozyme and Y27632-ULS-lysozyme, directed to TGFR-β kinase, p38 MAPK and ROCK, respectively are shown and discussed.

Chapter 2 focuses on drug delivery to the proximal tubular cells of the kidneys. The capability of drug-carrier conjugates to reach and enter the proximal tubular cells at either the apical or basolateral side is discussed, based on important characteristics such as size and charge, and on the presence of internalizing receptors. This chapter furthermore gives an overview of the carrier systems that have been investigated for drug delivery to the proximal tubular cells as well as potential carriers and of the linkage technologies that can be applied for the coupling of drugs to these carriers. Since the applied carrier and linker greatly influence the intracellular fate of the delivered drug, the cellular processing of drug-carrier conjugates is also discussed.

Chapter 3 describes the conjugation of the kinase inhibitors LY364947 (directed to TGFR-β kinase) and erlotinib (directed to epidermal growth factor receptor (EGFR) kinase) to lysozyme. The low molecular weight protein lysozyme is an attractive carrier for the intracellular delivery of kinase inhibitors into the proximal tubular cells, because it is a ligand of the internalizing megalin receptor on the luminal membrane of the cells that is almost freely filtered through the glomerulus. Both kinase inhibitors were conjugated to lysozyme via the platinum (II)-based Universal Linkage System™ (ULS)™. The *in vitro* cellular handling of the resulting conjugates, *i.e.* LY364947-ULS-lysozyme and erlotinib-ULS-lysozyme, was investigated in immortalized human kidney proximal tubular (HK-2) cells. Lastly, the *in vitro* capability of LY364947-ULS-lysozyme and erlotinib-ULS-lysozyme to inhibit the cellular responses to, respectively, the growth factors TGF-β and EGF was studied.

The profibrotic actions leading to tubulointerstitial fibrosis are mediated by a complex intracellular network of signaling cascades. Inhibition of multiple cascades with a multitargeted kinase inhibitor may therefore be advantageous. **Chapter 4** reports the synthesis of imatinib-ULS-lysozyme. This conjugate is directed against the receptor kinases PDGFR-α and PDGFR-β as well as against Abelson tyrosine kinase (c-Abl), which is a downstream target of TGFR-β kinase. Because tubulointerstitial fibrosis is associated with overactivation of both the PDGFR- and TGFR-β kinase mediated signaling cascades, drug delivery of imatinib to the proximal tubular cells may be promising in the management of tubulointerstitial fibrosis. The pharmacokinetics of imatinib-ULS-lysozyme was evaluated after intravenous and intraperitoneal administration in healthy mice. To investigate the potential of imatinib-ULS-lysozyme in the treatment of tubulointerstitial fibrosis, the *in vivo* efficacy of imatinib-ULS-lysozyme was investigated in the mouse unilateral ureteral obstruction (UUO) model for tubulointerstitial fibrosis.

Chapter 5 reports the development of a novel sunitinib derivative, *i.e.* 17864, which can be conjugated to lysozyme via the ULS linker. Because the multitargeted kinase inhibitor sunitinib lacks functional groups that can be used for the coupling reaction with the ULS linker, the *N*-2-(diethylamino)ethylene moiety of sunitinib was replaced by *N*-4-methylpyridine. This chapter describes the conjugation of 17864-ULS to lysozyme and its *in vitro* capability to inhibit kinase activities in proximal tubular cells. The pharmacokinetics of 17864-ULS-lysozyme was investigated after intravenous administration in healthy mice, and its *in vivo* efficacy in the mouse UUO model for tubulointerstitial fibrosis.

Chapter 6 focuses on the *in vitro* evaluation of 17864-ULS-lysozyme. Sunitinib is a type I ATP-competitive kinase inhibitor that exerts its effects on target kinases by binding to and around the adenine binding site of the ATP-binding pocket. Our hypothesis is that the activity of 17864 is retained after coupling to the ULS linker, because the *N*-4-methylpyridine is protruding outwards when 17864 binds to its target kinases. As a consequence, the proximal tubular cells will be exposed to higher levels of active kinase inhibitor. The orientation of ULS-bound 17864 inside the ATP-binding pocket was studied by molecular modeling. These findings were corroborated by inhibition studies using recombinant kinases and tyrosine kinase microarrays.

Chapter 7 describes the conjugation of 17864-ULS to generation-3 amine-terminated poly(amidoamine) dendrimers (NH_2-PAMAM-G3). Amine-terminated PAMAM dendrimers have been shown to accumulate in the proximal tubular cells to a greater extent than lysozyme. BIAcore receptor interaction studies were performed to study whether NH_2-PAMAM-G3 binds to the megalin receptor. The *in vitro* activity of 17864-ULS-NH_2-PAMAM-G3 as well as the cytotoxicity was investigated in HK-2 cells. Accumulation of 17864-ULS-NH_2-PAMAM-G3 in the kidneys was investigated after intravenous administration in healthy mice and compared with the renal accumulation of 17864-USL-lysozyme.

The thesis is concluded with a **summarizing discussion**. With the chapters of this thesis as guiding principle, the choice between different carriers, linkage technologies and kinase inhibitors is discussed. Furthermore, the *in vivo* evaluation of the antifibrotic effects of kinase inhibitor-carrier conjugates as well as the future perspectives of proximal tubular cell-specific kinase inhibitor-carrier conjugates will be discussed.

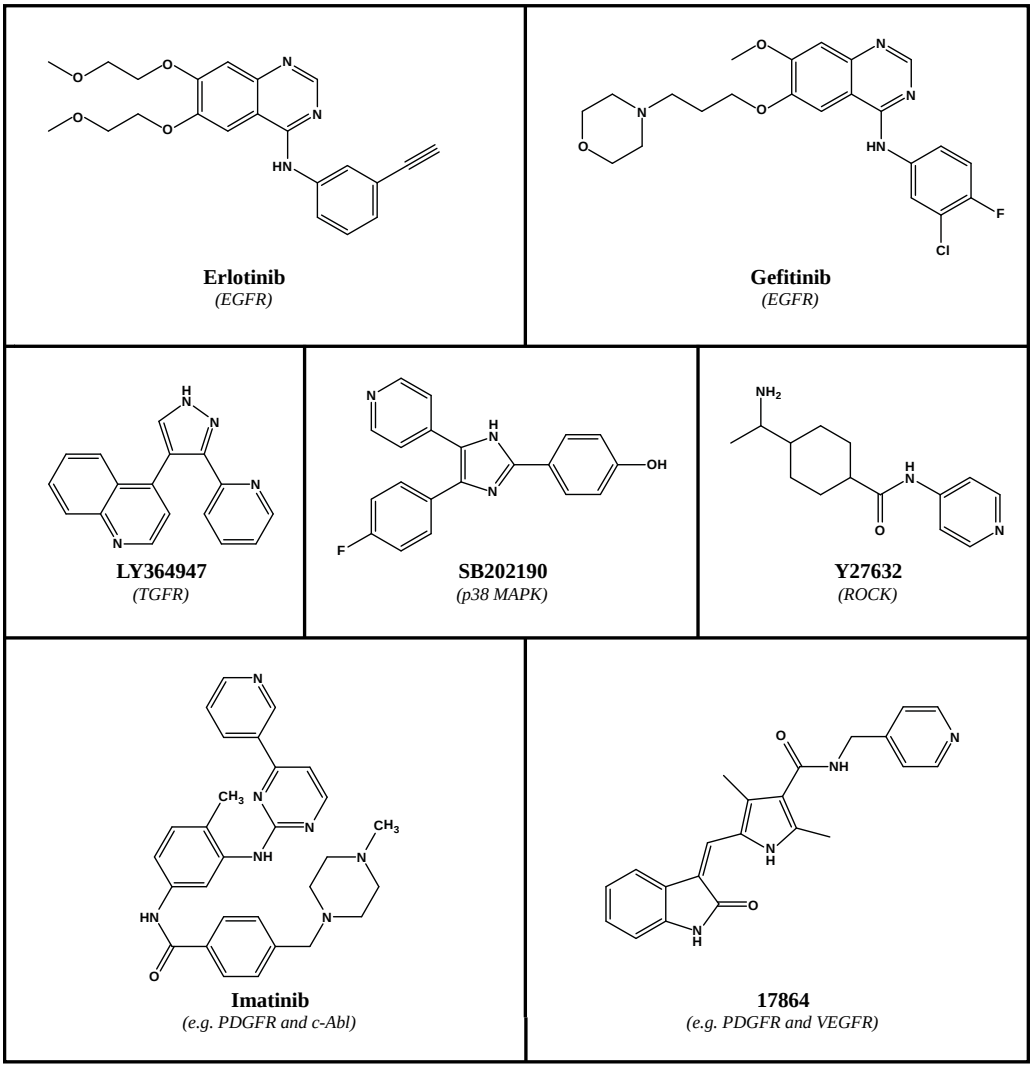

Figure 4. Chemical structures of the kinase inhibitors that have been conjugated to a proximal tubular cell-specific carrier. EGFR = epidermal growth factor receptor kinase; TGFR = transforming growth factor receptor kinase; p38 MAPK = p38 mitogen activated protein kinase; ROCK = Rho-associated kinase; PDGFR = platelet-derived growth factor receptor kinase; c-Abl = Abelson tyrosine kinase; VEGFR = vascular endothelial growth factor receptor kinase.

References

1. M.K. Haroun, B.G. Jaar, S.C. Hoffman, G.W. Comstock, M.J. Klag and J. Coresh. Risk factors for chronic kidney disease: a prospective study of 23,534 men and women in Washington County, Maryland. J Am Soc Nephrol. 14:2934-2941 (2003).
2. A.S. Levey, R. Atkins, J. Coresh, E.P. Cohen, A.J. Collins, K.U. Eckardt, M.E. Nahas, B.L. Jaber, M. Jadoul, A. Levin, N.R. Powe, J. Rossert, D.C. Wheeler, N. Lameire and G. Eknoyan. Chronic kidney disease as a global public health problem: approaches and initiatives - a position statement from Kidney Disease Improving Global Outcomes. Kidney Int. 72:247-259 (2007).
3. A. Meguid El Nahas and A.K. Bello. Chronic kidney disease: the global challenge. Lancet. 365:331-340 (2005).
4. T.P. Ryan, J.A. Sloand, P.C. Winters, J.P. Corsetti and S.G. Fisher. Chronic kidney disease prevalence and rate of diagnosis. Am J Med. 120:981-986 (2007).
5. M. Tonelli, N. Wiebe, B. Culleton, A. House, C. Rabbat, M. Fok, F. McAlister and A.X. Garg. Chronic kidney disease and mortality risk: a systematic review. J Am Soc Nephrol. 17:2034-2047 (2006).
6. A.B. Fogo. Progression versus regression of chronic kidney disease. Nephrol Dial Transplant. 21:281-284 (2006).
7. K. Iseki. Factors influencing the development of end-stage renal disease. Clin Exp Nephrol. 9:5-14 (2005).
8. J.M. Lopez-Novoa, C. Martinez-Salgado, A.B. Rodriguez-Pena and F.J. Hernandez. Common pathophysiological mechanisms of chronic kidney disease: therapeutic perspectives. Pharmacol Ther. 128:61-81 (2010).
9. A.A. Eddy. Can renal fibrosis be reversed? Pediatr Nephrol. 20:1369-1375 (2005).
10. A.M. el Nahas, E.C. Muchaneta-Kubara, M. Essawy and O. Soylemezoglu. Renal fibrosis: insights into pathogenesis and treatment. Int J Biochem Cell Biol. 29:55-62 (1997).
11. Y. Liu. Renal fibrosis: new insights into the pathogenesis and therapeutics. Kidney Int. 69:213-217 (2006).
12. P. Boor, T. Ostendorf and J. Floege. Renal fibrosis: novel insights into mechanisms and therapeutic targets. Nat Rev Nephrol. 6:643-656 (2010).
13. P. Boor, K. Sebekova, T. Ostendorf and J. Floege. Treatment targets in renal fibrosis. Nephrol Dial Transplant. 22:3391-3407 (2007).
14. M. Nangaku. Mechanisms of tubulointerstitial injury in the kidney: final common pathways to end-stage renal failure. Intern Med. 43:9-17 (2004).
15. G.J. Becker and T.D. Hewitson. The role of tubulointerstitial injury in chronic renal failure. Curr Opin Nephrol Hypertens. 9:133-138 (2000).
16. H. Okada and R. Kalluri. Cellular and molecular pathways that lead to progression and regression of renal fibrogenesis. Curr Mol Med. 5:467-474 (2005).
17. G.A. Muller, M. Zeisberg and F. Strutz. The importance of tubulointerstitial damage in progressive renal disease. Nephrol Dial Transplant. 15 Suppl 6:76-77 (2000).
18. A.A. Eddy. Molecular basis of renal fibrosis. Pediatr Nephrol. 15:290-301 (2000).
19. M. Eikmans, J.J. Baelde, E. de Heer and J.A. Bruijn. ECM homeostasis in renal diseases: a genomic approach. J Pathol. 200:526-536 (2003).
20. E. Healy and H.R. Brady. Role of tubule epithelial cells in the pathogenesis of tubulointerstitial fibrosis induced by glomerular disease. Curr Opin Nephrol Hypertens. 7:525-530 (1998).
21. H.W. Schnaper and J.B. Kopp. Renal fibrosis. Front Biosci. 8:e68-86 (2003).
22. T.A. Wynn. Cellular and molecular mechanisms of fibrosis. J Pathol. 214:199-210 (2008).
23. M. Zeisberg and R. Kalluri. The role of epithelial-to-mesenchymal transition in renal fibrosis. J Mol Med. 82:175-181 (2004).
24. F. Strutz and M. Zeisberg. Renal fibroblasts and myofibroblasts in chronic kidney disease. J Am Soc Nephrol. 17:2992-2998 (2006).
25. M.S. Razzaque and T. Taguchi. Cellular and molecular events leading to renal tubulointerstitial fibrosis. Med Electron Microsc. 35:68-80 (2002).
26. H.Y. Lan. Tubular epithelial-myofibroblast transdifferentiation mechanisms in proximal tubule cells. Curr Opin Nephrol Hypertens. 12:25-29 (2003).
27. M.R. Daha and C. van Kooten. Is the proximal tubular cell a proinflammatory cell? Nephrol Dial Transplant. 15 Suppl 6:41-43 (2000).

28. J. Rosenbloom, S.V. Castro and S.A. Jimenez. Narrative review: fibrotic diseases: cellular and molecular mechanisms and novel therapies. Ann Intern Med. 152:159-166 (2010).
29. E.P. Bottinger and M. Bitzer. TGF-beta signaling in renal disease. J Am Soc Nephrol. 13:2600-2610 (2002).
30. J.B. Kopp. TGF-beta signaling and the renal tubular epithelial cell: too much, too little, and just right. J Am Soc Nephrol. 21:1241-1243 (2010).
31. X.M. Meng, X.R. Huang, A.C. Chung, W. Qin, X. Shao, P. Igarashi, W. Ju, E.P. Bottinger and H.Y. Lan. Smad2 protects against TGF-beta/ Smad3-mediated renal fibrosis. J Am Soc Nephrol. 21:1477-1487 (2010).
32. J. Prakash, M.H. de Borst, A.M. van Loenen-Weemaes, M. Lacombe, F. Opdam, H. van Goor, D.K. Meijer, F. Moolenaar, K. Poelstra and R.J. Kok. Cell-specific delivery of a transforming growth factor-beta type I receptor kinase inhibitor to proximal tubular cells for the treatment of renal fibrosis. Pharm Res. 25:2427-2439 (2008).
33. J. Floege, F. Eitner and C.E. Alpers. A new look at platelet-derived growth factor in renal disease. J Am Soc Nephrol. 19:12-23 (2008).
34. C. Stambe, R.C. Atkins, G.H. Tesch, T. Masaki, G.F. Schreiner and D.J. Nikolic-Paterson. The role of p38alpha mitogen-activated protein kinase activation in renal fibrosis. J Am Soc Nephrol. 15:370-379 (2004).
35. J. Prakash, M. Sandovici, V. Saluja, M. Lacombe, R.Q. Schaapveld, M.H. de Borst, H. van Goor, R.H. Henning, J.H. Proost, F. Moolenaar, G. Keri, D.K. Meijer, K. Poelstra and R.J. Kok. Intracellular delivery of the p38 mitogen-activated protein kinase inhibitor SB202190 [4-(4-fluorophenyl)-2-(4-hydroxyphenyl)-5-(4-pyridyl)1H-imidazole] in renal tubular cells: a novel strategy to treat renal fibrosis. J Pharmacol Exp Ther. 319:8-19 (2006).
36. Y. Liu. New insights into epithelial-mesenchymal transition in kidney fibrosis. J Am Soc Nephrol. 21:212-222 (2010).
37. K. Hayashi, S. Wakino, T. Kanda, K. Homma, N. Sugano and T. Saruta. Molecular mechanisms and therapeutic strategies of chronic renal injury: role of rho-kinase in the development of renal injury. J Pharmacol Sci. 100:29-33 (2006).
38. J. Prakash, M.H. de Borst, M. Lacombe, F. Opdam, P.A. Klok, H. van Goor, D.K. Meijer, F. Moolenaar, K. Poelstra and R.J. Kok. Inhibition of renal rho kinase attenuates ischemia/ reperfusion-induced injury. J Am Soc Nephrol. 19:2086-2097 (2008).
39. K. Nagatoya, T. Moriyama, N. Kawada, M. Takeji, S. Oseto, T. Murozono, A. Ando, E. Imai and M. Hori. Y-27632 prevents tubulointerstitial fibrosis in mouse kidneys with unilateral ureteral obstruction. Kidney Int. 61:1684-1695 (2002).
40. T. Force, D.S. Krause and R.A. Van Etten. Molecular mechanisms of cardiotoxicity of tyrosine kinase inhibition. Nat Rev Cancer. 7:332-344 (2007).
41. W.J. Lee, J.L. Lee, S.E. Chang, M.W. Lee, Y.K. Kang, J.H. Choi, K.C. Moon and J.K. Koh. Cutaneous adverse effects in patients treated with the multitargeted kinase inhibitors sorafenib and sunitinib. Br J Dermatol. 161:1045-1051 (2009).
42. A. Arora and E.M. Scholar. Role of tyrosine kinase inhibitors in cancer therapy. J Pharmacol Exp Ther. 315:971-979 (2005).
43. J.C. Atherton. Renal blood flow, glomerular filtration and plasma clearance. Anaesthesia & Intensive Care Medicine. 10:271-275 (2009).
44. M.L. Schipper, G. Iyer, A.L. Koh, Z. Cheng, Y. Ebenstein, A. Aharoni, S. Keren, L.A. Bentolila, J. Li, J. Rao, X. Chen, U. Banin, A.M. Wu, R. Sinclair, S. Weiss and S.S. Gambhir. Particle size, surface coating, and PEGylation influence the biodistribution of quantum dots in living mice. Small. 5:126-134 (2009).
45. Y. Takakura, R. Mahato, M. Nishikawa and M. Hashida. Control of pharmacokinetic profiles of drug-macromolecule conjugates. Adv Drug Deliv Rev. 19:377-399 (1996).
46. H. Birn. The kidney in vitamin B_{12} and folate homeostasis: characterization of receptors for tubular uptake of vitamins and carrier proteins. Am J Physiol Renal Physiol. 291:F22-36 (2006).
47. H. Birn, O. Spiegelstein, E.I. Christensen and R.H. Finnell. Renal tubular reabsorption of folate mediated by folate binding protein 1. J Am Soc Nephrol. 16:608-615 (2005).
48. A. Saito, H. Sato, N. Iino and T. Takeda. Molecular mechanisms of receptor-mediated endocytosis in the renal proximal tubular epithelium. J Biomed Biotechnol:403272 (2010).
49. E.I. Christensen and H. Birn. Megalin and cubilin: multifunctional endocytic receptors. Nat Rev Mol Cell Biol. 3:256-266 (2002).

50. E.I. Christensen, P.J. Verroust and R. Nielsen. Receptor-mediated endocytosis in renal proximal tubule. Pflugers Arch. 458:1039-1048 (2009).
51. S.K. Moestrup and P.J. Verroust. Megalin- and cubilin-mediated endocytosis of protein-bound vitamins, lipids, and hormones in polarized epithelia. Annu Rev Nutr. 21:407-428 (2001).
52. P.J. Verroust and E.I. Christensen. Megalin and cubilin - the story of two multipurpose receptors unfolds. Nephrol Dial Transplant. 17:1867-1871 (2002).
53. K.R. West and S. Otto. Reversible covalent chemistry in drug delivery. Curr Drug Discov Technol. 2:123-160 (2005).

Chapter 1

Renal targeting of kinase inhibitors

M.E.M. Dolman[1], M.M. Fretz[1], G.J. Segers[1], M. Lacombe[2], J. Prakash[3], G. Storm[1], W.E. Hennink[1] and R.J. Kok[1]

[1] Department of Pharmaceutics, Utrecht Institute of Pharmaceutical Sciences, Utrecht University, Utrecht, The Netherlands

[2] KREATECH Biotechnology B.V., Amsterdam, The Netherlands

[3] Department of Pharmacokinetics and Drug Delivery, University Center for Pharmacy, University of Groningen, Groningen, The Netherlands

International Journal of Pharmaceutics 364:249-257 (2008)

Abstract

Activation of proximal tubular cells by fibrotic and inflammatory mediators is an important hallmark of chronic kidney disease. We have developed a novel strategy to intervene in renal fibrosis, by means of locally delivered kinase inhibitors. Such compounds will display enhanced activity within tubular cells and reduced unwanted systemic effects. In our approach kinase inhibitors are linked to the renal carrier lysozyme using a platinum-based linker that binds drugs via a coordinative linkage. Many kinase inhibitors contain aromatic nitrogen atoms able to bind to this linker without the need of prior derivatization. The resulting drug-lysozyme conjugates are rapidly filtered in the glomerulus into the tubular lumen and subsequently reabsorbed via the endocytic pathway for clearance of low-molecular weight proteins. An important property of the formed conjugates is their *in vivo* stability and the sustained drug release profile within target cells.

This review summarizes the state-of-the-art of drug targeting to the kidney. Furthermore, we will highlight recent results obtained with kinase inhibitor-lysozyme conjugates targeted to different kinases, *i.e.* the TGF-β receptor kinase, p38 MAPkinase and Rho-associated kinase. Both *in vitro* and *in vivo* results demonstrated their efficient tubular uptake and beneficial therapeutic effects, superior to treatment with free kinase inhibitors. These proof-of-concept studies clearly indicate the feasibility of drug targeting for improving the renal specificity of kinase inhibitors.

1. Introduction

The number of patients with chronic kidney disease (CKD) has markedly increased during the last decades (1-3). Partly, the increase in CKD incidence relates to the increased incidence of diabetes, systemic hypertension, and obesity (1, 4). In addition to this, patients develop diabetes and hypertension more frequently and at younger age, which also leads to an increased incidence of CKD (5-7). Lastly, since worldwide ageing of the population takes place, the incidence of CKD is expected to further increase (8). In many cases CKD results in renal fibrosis, characterized by inflammation and fibrosis of glomeruli and/ or tubulointerstitium (9).

Increased insight in the pathology of renal diseases along with the development of potent antifibrotic agents may lead to improved therapies for CKD. Kinase inhibitors targeted to fibrotic signaling cascades may serve as such antifibrotic agents. However, kinase inhibitors can also display many other undesired actions within the body. A more focused action in the kidney may improve their potential effectivity for CKD. This article provides (1) a short overview of different strategies used for targeted renal drug delivery, (2) explains how kinase inhibitors can be of benefit for the treatment of renal fibrosis and how they can be targeted to the kidney, and (3) addresses future potential application areas of renal drug delivery and the linkage technology used by our group to couple the kinase inhibitors to the kidney-targeted carrier systems.

2. Targeted renal drug delivery

Each kidney consists of millions of nephrons, which are the functional part of the kidney. Each nephron consists of a glomerulus, located in Bowman's capsule, and a tubular system composed of a proximal tubule, the loop of Henle, a distal tubule ending in the collecting duct. The blood is filtered in the glomerulus, where the primary urine is formed. Along the tubule, the primary urine is concentrated and many compounds are either reabsorbed or secreted from or into the urine, before it finally ends-up in the bladder.

When targeting drugs to the kidney, it is essential to identify which part of the nephron or cell type needs to be targeted. Important considerations in this are which cell types are involved in the disease pathology, the mechanism of action of the drug and the renal handling of the drug-carrier system. Different targeting approaches have been investigated for the delivery of drugs to either the glomerulus or to renal tubuli.

2.1. Targeting to the glomerular cells

The glomerulus is in direct contact with the blood stream. Glomerular cells can hence be targeted by intravenously administered particulate carrier systems that do not filter into the urine. Both endothelial cells which line up the vessel walls and mesangial cells can be reached from the bloodstream, because the glomerular endothelium is fenestrated and lacks a basement membrane between the glomerular capillaries and the mesangial cells. Tuffin *et al.* investigated the possibilities to target mesangial cells with immunoliposomes decorated with OX7 F(ab') fragments, which bind Thy 1.1. antigen expressed by this cell type (10). When tested in rats, a rapid clearance of the particles from the bloodstream was observed together with a significant accumulation in mesangial cells. As a proof-of-concept, tissue specific damage in the glomeruli was inflicted with OX7-immunoliposomes loaded with doxorubicin. Recently, immunoliposomes have also been used for the delivery of anti-inflammatory drugs to the glomerular endothelial cells (11). Successful targeting to glomerular endothelial cells was achieved by immunoliposomes

decorated with anti-E-selectin antibodies, which bind to inflamed endothelium. When evaluated in a glomerulonephritis model, this type of dexamethasone-immunoliposomes inhibited proinflammatory gene expression in the glomeruli and reduced renal damage, while systemic glucocorticoid activity was diminished (12).

2.2. Targeting to tubular cells

Targeting of drugs to the proximal tubular epithelial cells in the kidney can be relatively easily achieved from the tubular lumen, since there is no endothelial layer between the epithelial cells and the tubular fluid. Furthermore, proximal epithelial cells express high levels of internalizing receptors at their luminal membrane, which are able to take up a broad variety of the compounds that have been filtered in the glomerulus into the urine (13, 14). This reabsorptive capacity of proximal tubular cells opposes the loss of valuable endogenous molecules into the urine. The efficiency of this system is for instance exemplified by the absence of glucose and proteins in the urine of normal subjects.

Glomerular filtration is the gateway to the tubular lumen and it sets a limit to the maximum size of drug carriers applicable to tubular cell targeting. It has been proven that particles with a hydrodynamic diameter below 5-7 nm are rapidly cleared by renal filtration and urinary excretion (15). As most particulate drug carriers have a size in the 10-200 nm range, renal drug targeting to tubular cells has not been studied with these systems. Rather, renal-selective proteins and small synthetic polymers have been used for renal tubular cell targeting.

One of the best studied carriers for tubular cell targeting is the low molecular weight protein lysozyme. Previously, it has been shown that low molecular weight proteins with different p*I* such as cytrochrome C, aprotinin and lysozyme are extensively accumulated in the kidney in proximal tubular epithelial cells (16). Later studies have revealed that the tubular accumulation is mediated via the internalizing megalin receptor (14). **Figure 1** shows the principle of drug delivery to the kidneys using lysozyme. After glomerular filtration lysozyme is recognized by the megalin receptor at the luminal membrane of the proximal tubular epithelial cells. Binding results in internalization and routing to the lysosomes, where degradation of lysozyme occurs. Drugs attached to lysozyme are released during this process and may act intracellularly or be transferred into the tubular lumen of the kidney. This approach has been applied successfully for delivery of drugs like the non-steroidal anti-inflammatory drug naproxen and the angiotensin converting enzyme inhibitor captopril (17-19).

Polymeric carriers that have been described for renal drug delivery are anionized derivatives of polyvinylpyrrolidone (PVP) (20, 21), and low molecular weight chitosan (LMWC) (22). Derivatives of another type of polymer, *N*-(hydroxypropyl)methylacrylamide (HPMA), may also end-up in the kidneys when its size is below the glomerular threshold and its modification enhances interactions with renal cells (23, 24). Lastly, dendritic polymers have been used for renal imaging and may also be of use as carrier systems for tubular drug targeting.

In vivo studies in mice have shown that low molecular weight anionized PVP derivates accumulate extensively in the proximal tubular epithelial cells (20). In contrast, normal neutral PVP does not accumulate in the tubular cells and is excreted in the urine. Of special importance is the type of anionic groups introduced in the PVP polymers. While carboxylated PVPs showed relatively high renal accumulation, sulfonated PVPs showed only little renal accumulation. The highest renal accumulation was obtained with 20% carboxylated PVP, of which 30% of the

injected dose accumulated in the kidneys after intravenous administration. Both non-carboxylated and 100% carboxylated PVP hardly accumulated in the kidneys. Another carboxylated PVP, poly(vinylpyrrolidone-co-dimethyl maleic acid) (PVD) also showed extensive kidney accumulation (21). Intravenous administration of PVD in mice resulted in a remarkable accumulation of almost 80% in the proximal tubular cells 24 hours after administration. Approximately 60% of the administered PVD had been eliminated in the urine 4 days after its administration, indicating that PVD stays in the body for a long time. PVD was used as a carrier for the delivery of the protein drug superoxide dismutase (SOD). The PVD-SOD conjugate showed therapeutic effects in an acute renal failure model. Until now, it has not been investigated whether this type of carrier can be applied for the delivery of small molecule drugs.

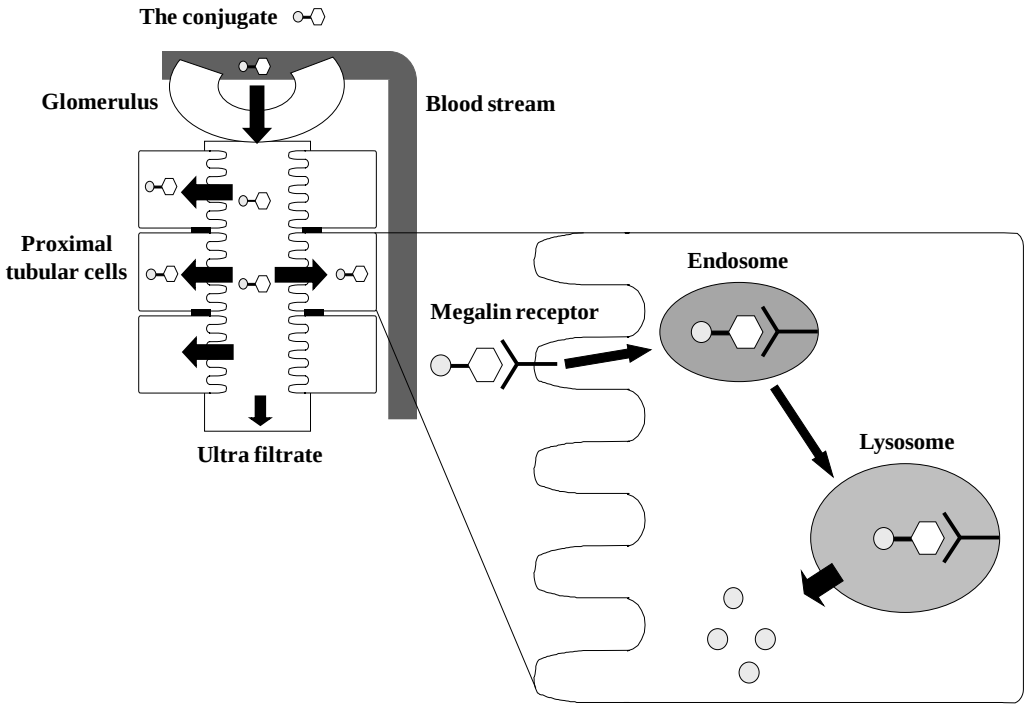

Figure 1. Principle of drug delivery to the kidneys with lysozyme conjugates. Nephrons are the functional part of the kidney, each consisting of a glomerulus and the renal tubuli. The glomerulus is the basic filtration unit of the kidney, responsible for the formation of a plasma ultra filtrate. In the first part of the tubule (also called the proximal tubule), reabsorption of many endogenous compounds like amino acids, glucose and proteins occurs. The property of proximal tubular cells to reabsorb small molecules is used in our delivery approach to target kinase inhibitors to the kidney. In short, after glomerular filtration drug-LZM conjugates specifically accumulate in proximal tubular epithelial cells by recognition of the megalin receptor, which is responsible for reabsorption of proteins. The megalin receptor is expressed in high density at the luminal membrane of the cells. Free drug will be released intracellularly from the conjugate after lysosomal degradation of the drug-LZM conjugate.

LMWC which had been randomly acetylated for 50% was used to deliver prednisolone to the renal tubular cells (22). Delivery of prednisolone using LMWC with a molecular weight of 19 kDa resulted in the highest renal accumulation. A maximum accumulation of approximately 15% was obtained 15 minutes after intravenous administration in mice, which is comparable to the accumulation observed for low molecular weight proteins (as depicted in **Figure 4**). The mechanism by which LMWC is being taken up by the renal tubular cells is unknown. Despite the efficient renal targeting by prednisolone-LMWC, the amount of drug in the kidneys decreased quickly, indicating the rapid release of the delivered drug from the carrier and its rapid elimination or redistribution from the renal tissue.

Another polymer for which accumulation in the kidney has been reported is HPMA. Kissel *et al.* investigated the *in vivo* biodistribution of biotinylated HPMA in rats and compared this with the biodistribution of non-biotinylated HPMA (24). It was found that the biodistribution profiles of 26 kDa polymers were comparable except for the kidneys, which showed an increased uptake of biotinylated HPMA at day 7 after intravenous injection. The accumulation of biotin-HPMA in proximal tubular cells was 33 times higher than normal HPMA. Of note, for both polymers, the highest accumulation was found in spleen, liver and tumour. Biotin-HPMA showed a renal uptake of 4.7% of the initial dose per gram of tissue, while in case of HPMA this percentage was only 0.14%. Assuming that the weight of both kidneys in rats is about 0.9% of total body weight (25), the total accumulation of biotin-HPMA as percentage of the injected dose in both kidneys was 8.5%. The renal accumulation may be explained by the presence of a biotin transporter on the brush border of proximal tubular cells (26), which binds the renally filtered polymers.

More recently, renal accumulation of RGD-decorated HPMA was also reported. Although developed for the purpose of targeting to tumour endothelium, RGD-fK-HPMA 43 kDa showed extensive renal accumulation, far exceeding the attained levels in the tumour tissue. Similar to biotinylated HPMA, a prolonged retention was found which lasted for days, indicating the slow renal degradation of these polymers.

Although dendrimers have not been investigated for renal drug targeting yet, they have been successfully applied for the purpose of magnetic resonance imaging (MRI) to detect structural and functional abnormalities of the kidneys (27). Dendrimers that were used for the development of renal MRI contrast agents are polyamidoamine (PAMAM) and diaminobutane (DAB). PAMAM-based macromolecular MRI contrast agents with a hydrodynamic diameter of less than 8 nm were rapidly cleared from the circulation by glomerular filtration and subsequently excreted by the kidneys or taken up by the renal tubuli (27, 28). Both dendrimers of the 4^{th} (G4D) and 5^{th} generation were used to prepare gadolinium loaded contrast agents. When examined in mice, a rapid and extensive accumulation in the kidneys was found, with highest renal tissue levels obtained with G4D (29). Although the uptake by proximal tubular cells was not studied directly, indirect evidence was obtained by simultaneous injection of G4D contrast agent and lysine, which competes for megalin binding. An increased urinary excretion of G4D was observed (29).

2.3. Gene targeting to the kidney

Also in the field of gene delivery, attention has been given to the targeting of the glomerulus and renal tubuli. This topic has been reviewed excellently by others and we will not elaborate on this subject (see for instance (30-32). Examples of targeting approaches and systems that have been

used for renal gene delivery are liposomes, adenoviruses, as well as naked plasmids or antisense oligonucleotides. Besides the choice between vectors, also the route of administration plays an important role in the renal targeting of the different cell types in the kidney (30).

3. Renal fibrosis

Renal fibrosis is the result of activation of renal cells by inflammatory cytokines (*e.g.* IL-1 and TNF-α) and proteinuria, leading to the production of chemokines, adhesion molecules and other mediators, which leads to tubulointerstitial inflammation (33, 34). Besides inflammation, also epithelial-to-mesenchymal transition (EMT) of proximal tubular epithelial cells into fibroblasts occurs (34). Stimulation of fibroblasts by cytokines and growth factors (*e.g.* TGF-β, CTGF, PDGF, and EGF) leads to the excessive formation of extracellular matrix and the replacement of nephrons by scar tissue (33, 34).

Although the kidneys have a overcapacity of nephrons, it is not infinite and loss of kidney function eventually can lead to the development of end-stage renal disease (ESRD) (8). Patients with ESRD need renal replacement therapy, by dialysis or transplantation, which is a high burden for the patient and very expensive (8).

One of the approaches in the treatment of renal fibrosis is prevention by treatment of the underlying cause, *e.g.* hypertension or diabetes mellitus. However, since renal diseases are often diagnosed in a late stage, it is also important to develop other therapeutic possibilities to arrest the progression of renal fibrosis, or even to reverse it. Activation of proximal tubular epithelial cells leading to the onset of different signaling pathways plays an important role in the progression of renal fibrosis. Kinases play an important role in these signaling pathways and offer an interesting target in the treatment of renal fibrosis (7, 9, 35, 36). Both *in vitro* studies with proximal tubular cells and studies in animal models have shown the beneficial effects of kinase inhibitors in renal fibrotic disease (37-42). We therefore have investigated the specific targeting of kinase inhibitors to the proximal tubular cells. Targeted delivery of kinase inhibitors has several potential benefits. Firstly, high concentrations of kinase inhibitors in the proximal tubular epithelial cells will result in an enhanced efficacy within the kidneys. Secondly, specific targeting will reduce unwanted systemic effects. Until now kinase inhibitors are only clinically used for the treatment of cancer (43-45). Kinase inhibitors are considered targeted drugs. However, this targeted feature refers to their specific mode of action (46), rather than to targeted delivery. Kinase inhibitors are not cell- or tissue specific and will thus act in both unhealthy and healthy cells in which the molecular target is expressed and activated. Kinases play an important role in many physiological activities in the human body (47-49) and, consequently, their inhibition in healthy cells may result in adverse effects. Recently, it has been shown that tyrosine kinase inhibitors are associated with cardiotoxicity (50, 51), bleeding, and neurological complications (52). An example of such an inhibitor is the well-known breakpoint cluster region-Abelson (BCR-ABL) tyrosine kinase inhibitor imatinib (50, 51). One of the techniques used to prevent cardiac toxicity of imatinib is structural reengineering, which yielded a derivative with an altered kinase inhibitory profile (53). This new compound showed decreased cardiac side effects but maintained the antitumour properties of imatinib. Adverse reactions can be divided in on-target and off-target side effects. Once the toxicity of the kinase inhibitor is directly related to the intended pharmacological response it is called an ‘on-target’ side effect. Off-target side effects are related to inhibition of off-target kinases or to other non-kinase dependent mechanisms (54). Structural

reengineering is a valid approach for drug molecules in which the toxicity can be dissected from the intrinsic activity of the compound but cannot be used to reduce toxicity directly associated with the pharmacological activity. In the latter case, cell-specific targeting of kinase inhibitors is an attractive approach.

4. Design and synthesis of kinase inhibitor-lysozyme conjugates

When using a carrier system for the specific targeting of kinase inhibitors to the proximal tubular cells, it is important to use a carrier which is biodegradable. If a polymeric carrier is poorly degradable, its lysosomal accumulation may result in toxicity. Proteins are natural polymers which display excellent lysosomal biodegradability, while in case of many synthetic polymers a lack of biodegradability is a concern. We therefore applied the low molecular weight protein lysozyme as tubular cell-specific carrier for the delivery of kinase inhibitors.

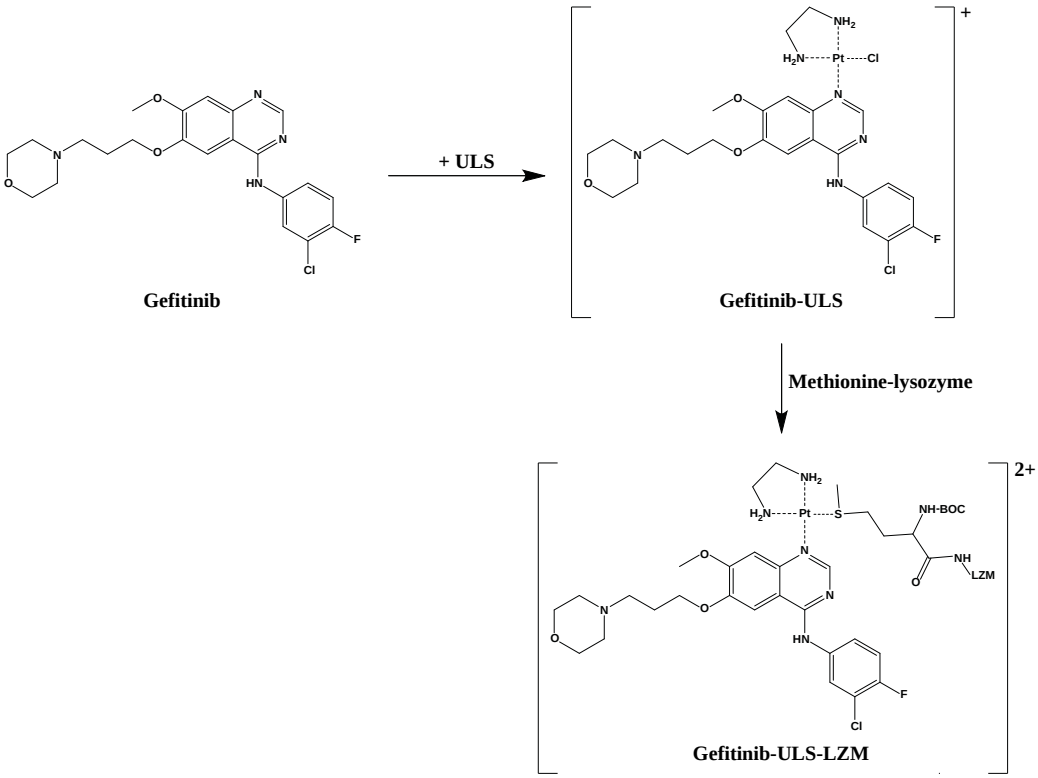

Figure 2. Reaction scheme of the linkage of gefitinib to the platinum linker, and its subsequent conjugation to lysozyme by reaction to methionine residues in lysozyme. Gefitinib was reacted with ULS in DMF at 37 °C for 9 hours. During this reaction the platinum atom in ULS bound the aromatic nitrogen atom present in gefitinib. After characterization and purification of gefitinib-ULS, gefitinib-ULS-LZM was synthesized by reacting gefitinib-ULS to methionine-LZM for 24 hours at 37 °C and pH 8.5. The platinum atom in ULS bound the thioether present in the methionine residue of LZM.

Kinase inhibitors were linked to lysozyme using the platinum (II)-based Universal Linkage System (ULS)™ as a new coupling agent (39, 41, 55). ULS binds to thioether groups (present in methionine residues of the proteinaceous carrier protein) and aromatic nitrogens. Many kinase inhibitors contain an aromatic nitrogen atom, and can therefore be coupled to ULS via a coordinative bond without prior derivatization steps. An important property of platinum-ligand bindings is that coordinative bindings dissociate very slowly, thereby providing adequate stability of the conjugates (41, 56, 57). On the other hand, the platinum coordination bonds are also bioreversible and can intracellularly release the conjugated drug via competitive displacement with gluthathione (58, 59).

Figure 2 shows the linkage of the kinase inhibitor gefitinib (Iressa®) to the platinum linker, and the subsequent conjugation of gefitinib-ULS to lysozyme. Typically, these conjugates are synthesized by coupling the drug to the platinum linker at a slight excess of the drug. Consumption of the parent drug is detected by HPLC analysis of small aliquots of the reaction mixture. Once the reaction has been completed, the remaining traces of non-reacted linker were precipitated by addition of NaCl, yielding the poorly water-soluble ULS-dichloride linker. Gefitinib-ULS was synthesized using equimolar amounts of ULS and gefitinib and subsequently coupled to methionine groups in lysozyme by overnight incubation at 37 °C.

Although lysozyme contains two methionine residues, it does not bind drug-ULS readily since these residues are buried in the core of the protein. We therefore introduced surface-exposed methionine residues into lysozyme by chemical derivatization of lysyl residues with methionine-NHS. Such a chemically derivatized methionine-lysozyme (met-LZM) carrier prototype can be replaced in the future by a recombinantly produced protein with surface-accessible Pt (II) targets. Typically, the chemical derivatization of LZM yielded a carrier equipped with approximately one extra methionine residue, as determined by mass spectrometry (41).

HPLC analysis of gefitinib-ULS-LZM provided a broad peak (**Figure 3B**), likely consisting of different topological isomers. Those isomers result from the ability of methione-NHS residues to bind to different lysine residues in lysozyme, and also have been observed for other types of lysozyme-derivatives (60-62).

Incubation with an excess of KSCN, a known ligand for platinum, resulted in drug release from the conjugate by competitive displacement (**Figure 3C**). This result clearly demonstrates that binding of gefitinib to LZM via ULS is reversible. Similar results were obtained for other kinase inhibitor conjugates. On the other hand, no release of the drug was observed upon incubation of drug-ULS-LZM conjugates in PBS for up to 24 hours and at 37°C. This indicates adequate stability of the conjugates during storage (41, 57, 59, 63).

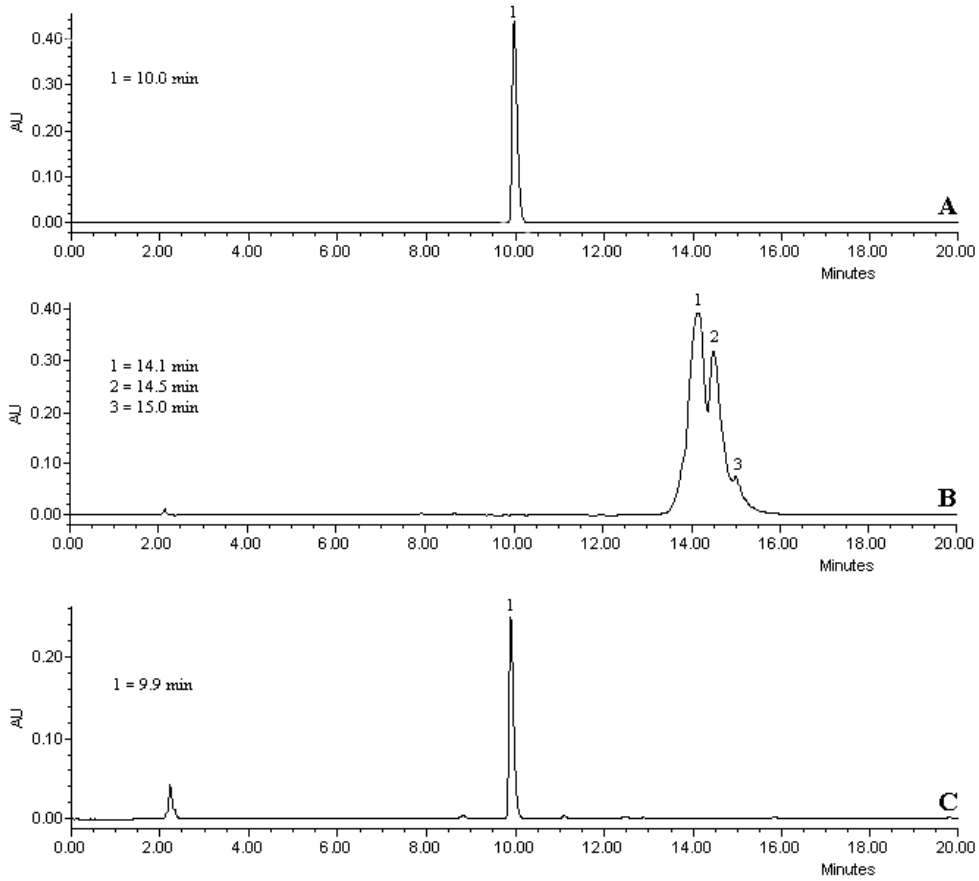

Figure 3. HPLC chromatograms of free gefitinib (A), gefitinib-ULS-LZM (B) and gefitinib-ULS-LZM after incubation with an excess of KSCN at 80 °C (C). Compared to free gefitinib (A) the conjugate gives a broad peak, consisting of different topological isomers (B). This results from the ability of methionine-NHS to bind to different lysine residues in lysozyme. Subpart B also shows there is no free gefitinib present after synthesizing the conjugate, as shown by the absence of a peak at a retention time of approximately 10 minutes. Neither is gefitinib-ULS present, which gives peaks at 8.7, 10.4 and 11.9 minutes (data not shown). It furthermore can be concluded that binding of gefitinib to LZM via ULS is reversible, as shown by figure C which shows the disappearance of the gefitinib-ULS-LZM peak and reappearance of the parent drug after competitive drug displacement with KSCN. Samples were separated on a C_4 reversed-phase column, using a water-acetonitrile-trifluoroacetic acid gradient, and monitored at a wavelength of 270 nm.

5. Biological stability drug-ULS-LZM conjugates

The biological stability of drug-ULS-LZM conjugates has been studied by *in vitro* incubation of conjugates in either rat serum or kidney homogenates, or by incubating the conjugates in 5 mM glutathione (41, 58). Typically, less than 2% release of the drug was observed upon incubation in serum for up to 24 hours at 37 °C (39, 41). On the other hand, slow-release of the coupled drug was observed in the presence of competing glutathione or in the presence of kidney homogenate

(at pH 5.0 and 7.4), suggesting that the drug can be released once the conjugates have been reabsorbed by proximal tubular cells (41, 58).

Adequate stability in the circulation can be expected on the basis of two observations: firstly, the *in vitro* drug release rate in serum is much slower than the rate at which the conjugates will be accumulated in proximal tubular cells. While the $t_{1/2}$ of drug release is in the order of days, drug-ULS-lysozyme conjugates disappear from the circulation with a $t_{1/2}$ of 25 min, providing maximal renal accumulation within 2 hours (18, 64). Secondly, the drug release rate in kidney homogenate was much higher than the release in serum, in line with the different levels of thiols in both matrices (41). We confirmed these expectations in our pharmacokinetic studies with drug-ULS-LZM conjugates prepared with three different kinase inhibitors, directed to either p38 MAPkinase, TGF-β type 1 receptor kinase (ALK5) or Rho-associated kinase (ROCK) (39, 41, 65). These conjugates showed similar distribution and clearance profiles to the lysozyme carrier, and accumulated in the kidneys at about 20% of the injected doses (**Figure 4**) in the first hours (1-6 hours) post injection (41). Furthermore, we observed a prolonged residence of the delivered drug within the kidneys, as evidenced by the persistence of renal drug levels of the p38 MAPK inhibitor SB202190 for several days after a single dose administration (41). Pharmacokinetic data of the free kinase inhibitors are not available and we have not performed in depth pharmacokinetic studies for each of the individual test drugs, due to the large amounts needed of these costly compounds. However, the intravenous administration of one of these compounds, SB202190, showed that less than 0.5% of the free drug accumulated in the kidneys (66). The renal accumulation of the SB202190-ULS-LZM conjugate greatly exceeded the accumulation of the free drug, indicating the feasibility of our delivery approach.

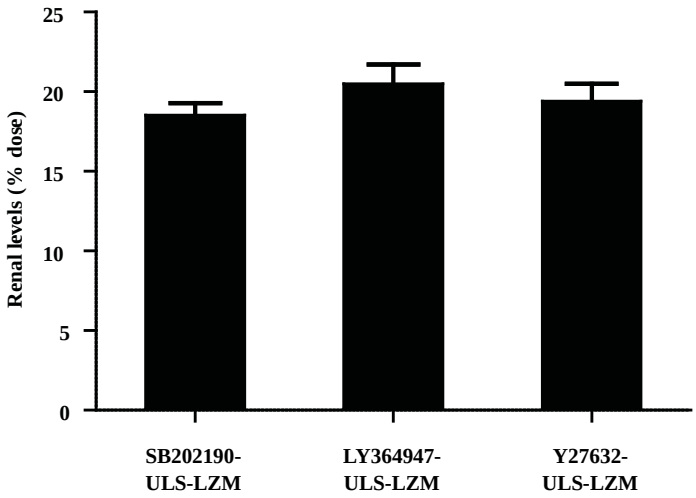

Figure 4. Renal accumulation levels of drug-LZM conjugates. Single dose intravenous injection in rats with three different conjugates resulted in comparative renal accumulation. Shown values are the average values of renal C_{max}, as calculated from the renal concentrations between 1-6 hours (mean ± SEM) (39, 41, 65).

The biodistribution of drug-ULS-lysozyme conjugates to other organs has also been investigated. Immunostaining for drug-ULS-lysozyme conjugates furthermore showed the absence of the conjugate in liver, spleen and lungs (39). The preferential renal accumulation can be explained by the rapid glomerular filtration of low molecular weight proteins, and the efficient tubular reabsorption via megalin. Although megalin is predominantly expressed by the proximal tubular

cells in the kidney and much lower levels of expression are found in other cell types, such as epithelial cells of the small intestine (14), this does not largely diminish the renal accumulation of lysozyme. A plausible explanation is that the megalin receptor is expressed at the luminal side of the epithelial cells of the small intestine making it not accessible for intravenously administered lysozyme.

6. *In vitro* and *in vivo* effects of drug-LZM conjugates

The above mentioned conjugates directed to profibrotic cascades, LY364947-ULS-LZM, SB202190-ULS-LZM and Y27632-ULS-LZM, have been investigated for efficacy *in vitro* in cultured kidney cells and *in vivo* in rats.

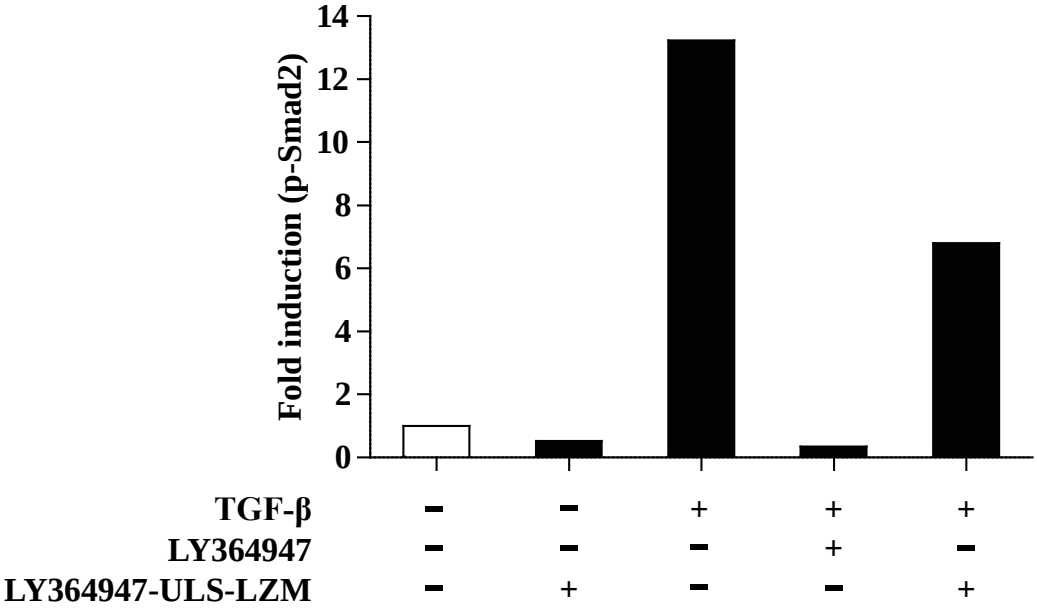

Figure 5. Effects of LY364947 and LY364947-ULS-LZM on TGF-β1-induced phosphorylation of Smad2. Cells were grown to 80% confluency in a 6-well plate and then deprived from serum for 24 hours. Cells were preincubated for 24 hours with LY364947-ULS-LZM (10µM) or for 30 minutes with LY364947 (10 µM) and then activated with 10 ng/ ml TGF-β1 for 30 minutes. Phospho-Smad2 levels were detected by anti-phospho-Smad2 Western blotting (Cell Signaling Antibody #3101S) directed to phosphorylated amino acids in Smad2 (Ser465 and Ser467) and normalized to resting cells by β-actin levels (white bar).

The first conjugate, LY364947-ULS-LZM, is a TGF-β type I receptor kinase inhibitor. TGF-β plays a pivotal role in renal fibrosis by inducing synthesis of matrix proteins and by decreasing their degradation. It furthermore induces tubular epithelial-to-mesenchymal transdifferentiation (EMT) and the proliferation of fibroblasts (67-71). Recent *in vitro* and *in vivo* experiments demonstrated the inhibitory effects of LY364947-ULS-LZM on the MCP-1 mRNA expression and on the fibrosis marker α-SMA (39). We furthermore demonstrated that LY364947-ULS-LZM effectively inhibited the phosphorylation of Smad2, a downstream target of the activated TGF-β

receptor, in HK-2 cells (**Figure 5**). We found a reduction in TGF-β1-induced phosphorylation of Smad2 of approximately 50% when treated with LY364947-ULS-LZM. In case of an equimolar concentration of unbound LY364947 a reduction of approximately 95% was found. An explanation for the relative higher potency of the free drug is that LY364947-ULS-LZM needs to be internalized and processed by the cells to release free drug from the conjugate. In contrast, unbound LY364947 can readily pass the cell membranes by passive diffusion because of its relatively high lipophilicity (calculated log P is 2.85). The pharmacological superiority of LY364947-ULS-LZM can therefore not be demonstrated *in vitro*, but requires *in vivo* testing in which local delivery provides increased concentrations of LY364947 in the kidneys.

The second drug-LZM conjugate investigated is SB202190-ULS-LZM, which targets the p38 MAPK pathway. *In vitro* research in HK-2 cells demonstrated a reduction in TGF-β1 induced procollagen-Iα1 mRNA expression. Single dose administration of SB202190-ULS-LZM in a unilateral renal ischemia-reperfusion rat model resulted in a reduction of intrarenal p38 MAPK phosphorylation and α-SMA protein expression (41).

The third conjugate investigated, prepared with the Rho kinase inhibitor Y27632, has also been evaluated in the unilateral renal ischemia-reperfusion rat model (65). Upon daily treatment for four days, Y27632-ULS-LZM improved histological parameters as well as gene-expression levels of fibrotic and inflammatory markers. The collective results of the three conjugates have been summarized in **Table 1**. In all studies the reported effects were compared to untreated control animals. Inhibitory effects were detected on gene expression levels of profibrotic and inflammatory mediators and genes related to extracellular matrix production, and on immunohistochemical markers of fibrosis and EMT. Furthermore a reduction in the number of infiltrated macrophages was observed. No antifibrotic effects of lysozyme were observed in control experiments with cultured tubular cells, while kinase inhibitor-lysozyme conjugates are clearly effective. This illustrates that the observed effects can be attributed to the attached drug, rather than to the carrier itself. Windt *et al*. investigated the antifibrotic effects of lysozyme, and a captopril-lysozyme conjugate *in vivo* in adriamycin-induced proteinuric rats (72). It was found that captopril-LZM had antifibrotic effects, while lysozyme alone had no effects.

We also investigated the safety of the applied platinum-linker, which is important in view of the nephrotoxicity of cisplatin-based cytostatics. Cisplatinum exerts its effect by cross-linking DNA, which is the result of the availability of free reactive sites at the platinum atom (54). No toxic effects were observed when studying the acute toxicity of SB202190-ULS-LZM in rats (41).

7. Future perspectives

Drug targeting may play an important role in the development of more specific agents for the treatment of all kinds of renal diseases. Renal drug targeting aims for a higher efficacy of the drug along with the avoidance of unacceptable side effects. Different drug targeting approaches are attractive, depending on the type of kidney cells that are involved in the pathogenesis of the disease. Liposomal carriers seem promising systems for glomerular targeting. For drug targeting to the proximal tubular cells, carboxylated PVP derivates, 4th generation dendrimers and small proteins like lysozyme are promising carrier systems. These carrier systems exploit the rapid glomerular filtration of medium-sized macromolecules and give a high renal accumulation. The advantage of proteinaceous carriers is that they are efficiently degraded in the lysosomes of the targeted cells.

Table 1. In vivo inhibitory effects of drug-LZM conjugates on profibrotic markers.

Animal model + conjugate	Gene expression	Immunohistochemical markers
UUO + LY364947-ULS-LZM	MCP-1 ↓	α-SMA ↓ Macrophage influx ↓ Vimentin ↓
I/R + SB202190-ULS-LZM		α-SMA ↓ p-p38 ↓
I/R + Y27632-ULS-LZM	MCP-1 ↓↓ Procollagen Iα1 ↓ TGF-β1 ↓ TIMP-1 ↓ α-SMA ↓↓	Macrophage influx ↓ Vimentin ↓

In vivo experiments are performed in the unilateral ureteral obstruction (UUO) rat model and ischemia-reperfusion (I/ R) rat model. Mentioned profibrotic markers in this table are elevated in both animal models. The symbol ↓ means drug treatment resulted in a significant decrease in gene expression or immunohistochemical staining up to 50%, the symbol ↓↓ means a decrease of 50-90%. All results reported in this table are against non-treated control animals.
UUO rats were injected intravenously with a single dose of 25 mg/ kg LY364947-ULS-LZM (equivalent to 630 µg/ kg LY364947). Rats were sacrificed after three days. Treatment with LY364947-ULS-LZM resulted in a decrease in the gene expression level of MCP-1 and a decrease in α-SMA, macrophage influx and vimentin (39). Treatment of I/ R rats with a single intravenous injection of 32 mg/ kg SB202190-ULS-LZM (equivalent to 752 µg/ kg free SB202190) resulted in a decrease in α-SMA and p-p38 4 days after administration (41). In case of Y27632-ULS-LZM I/ R rats were daily treated with an intravenous injection of 20 mg/ kg conjugate (equivalent to 555 µg/ kg Y27632) for four days. Treatment resulted in a decrease in gene expression levels of MCP-1, procollagen Iα1, TGF-β1, TIMP-1 and α-SMA and in a decrease of vimentin and macrophage influx (65).

Although not described extensively in this article, targeted gene delivery also offers interesting possibilities for inhibiting renal diseases processes. As compared to other organs, an advantage of targeting to the kidneys is that the proximal tubular cells are able to reabsorb different substances including nucleic acids.
This paper discussed a new type of kinase inhibitor-lysozyme conjugates for the delivery of kinase inhibitors to tubular cells in the kidney. These products may find future application in the treatment of renal fibrosis and other types of kidney diseases. Besides kinase inhibitors, other types of drugs can be linked via the ULS linker technology to lysozyme, as long as the drugs contain an aromatic nitrogen atom or other donor group that can coordinate to platinum. Also other carriers than lysozyme can be used, directed to the kidney cells or to other types of target cells outside the kidney, providing that the linker can be reacted to the carrier system. We already have explored two other classes of kinase inhibitor-carrier conjugates, either directed to angiogenic endothelial cells in tumours or to hepatic stellate cells in the liver (57, 63). In the near future, we will explore the feasibility of targeting kinase inhibitors to tumour cells, by means of monoclonal antibody carriers.

Conclusion

Renal drug targeting is an interesting technique for improving the treatment of renal diseases for which no adequate therapies exist, such as renal fibrosis. Both glomerular and tubular targeting strategies have been developed successfully. A great part of the kidney consists of specialized tubular cells, able to reabsorb endogenous compounds from the tubular lumen by receptor-mediated uptake. The unique properties of this cell type offer good opportunities for tubular cell-specific drug delivery, exemplified in this manuscript by the megalin-mediated uptake of lysozyme-drug conjugates. This targeting approach makes it possible to specifically deliver kinase inhibitors, but also other drugs, to the kidney.

Acknowledgements

This work was made possible by a grant from the European Framework program FP6 (LSHB-CT-2007-036644). We thank Mies van Steenbergen for his technical assistance in performing chromatographic experiments.

References

1. K. Iseki. Factors influencing the development of end-stage renal disease. Clin Exp Nephrol. 9:5-14 (2005).
2. T.P. Ryan, J.A. Sloand, P.C. Winters, J.P. Corsetti and S.G. Fisher. Chronic kidney disease prevalence and rate of diagnosis. Am J Med. 120:981-986 (2007).
3. A.S. Levey, K.U. Eckardt, Y. Tsukamoto, A. Levin, J. Coresh, J. Rossert, D. De Zeeuw, T.H. Hostetter, N. Lameire and G. Eknoyan. Definition and classification of chronic kidney disease: a position statement from Kidney Disease: Improving Global Outcomes (KDIGO). Kidney Int. 67:2089-2100 (2005).
4. M. Cignarelli and O. Lamacchia. Obesity and kidney disease. Nutr Metab Cardiovasc Dis. 17:757-762 (2007).
5. R.J. Koopman, A.G. Mainous, 3rd, V.A. Diaz and M.E. Geesey. Changes in age at diagnosis of type 2 diabetes mellitus in the United States, 1988 to 2000. Ann Fam Med. 3:60-63 (2005).
6. A.H. Rubenstein. Obesity: a modern epidemic. Trans Am Clin Climatol Assoc. 116:103-111; discussion 112-103 (2005).
7. W.C. Burns, P. Kantharidis and M.C. Thomas. The role of tubular epithelial-mesenchymal transition in progressive kidney disease. Cells Tissues Organs. 185:222-231 (2007).
8. A. Meguid El Nahas and A.K. Bello. Chronic kidney disease: the global challenge. Lancet. 365:331-340 (2005).
9. Y. Liu. Renal fibrosis: new insights into the pathogenesis and therapeutics. Kidney Int. 69:213-217 (2006).
10. G. Tuffin, E. Waelti, J. Huwyler, C. Hammer and H.P. Marti. Immunoliposome targeting to mesangial cells: a promising strategy for specific drug delivery to the kidney. J Am Soc Nephrol. 16:3295-3305 (2005).
11. S.A. Asgeirsdottir, J.A. Kamps, H.I. Bakker, P.J. Zwiers, P. Heeringa, K. van der Weide, H. van Goor, A.H. Petersen, H. Morselt, H.E. Moorlag, E. Steenbergen, C.G. Kallenberg and G. Molema. Site-specific inhibition of glomerulonephritis progression by targeted delivery of dexamethasone to glomerular endothelium. Mol Pharmacol. 72:121-131 (2007).
12. S.A. Asgeirsdottir, P.J. Zwiers, H.W. Morselt, H.E. Moorlag, H.I. Bakker, P. Heeringa, J.W. Kok, C.G. Kallenberg, G. Molema and J.A. Kamps. Inhibition of proinflammatory genes in anti-GBM glomerulonephritis by targeted dexamethasone-loaded AbEsel liposomes. Am J Physiol Renal Physiol. 294:F554-561 (2008).
13. S.K. Moestrup and P.J. Verroust. Megalin- and cubilin-mediated endocytosis of protein-bound vitamins, lipids, and hormones in polarized epithelia. Annu Rev Nutr. 21:407-428 (2001).
14. E.I. Christensen and P.J. Verroust. Megalin and cubilin, role in proximal tubule function and during development. Pediatr Nephrol. 17:993-999 (2002).
15. H.S. Choi, W. Liu, P. Misra, E. Tanaka, J.P. Zimmer, B. Itty Ipe, M.G. Bawendi and J.V. Frangioni. Renal clearance of quantum dots. Nat Biotechnol. 25:1165-1170 (2007).
16. M. Haas, D. de Zeeuw, A. van Zanten and D.K. Meijer. Quantification of renal low-molecular-weight protein handling in the intact rat. Kidney Int. 43:949-954 (1993).
17. M. Haas, A.C. Kluppel, E.S. Wartna, F. Moolenaar, D.K. Meijer, P.E. de Jong and D. de Zeeuw. Drug-targeting to the kidney: renal delivery and degradation of a naproxen-lysozyme conjugate in vivo. Kidney Int. 52:1693-1699 (1997).
18. R.J. Kok, F. Grijpstra, R.B. Walthuis, F. Moolenaar, D. de Zeeuw and D.K. Meijer. Specific delivery of captopril to the kidney with the prodrug captopril-lysozyme. J Pharmacol Exp Ther. 288:281-285 (1999).
19. J. Prakash, R.J. Kok, A. van Loenen-Weemaes, M. Haas, J.H. Proost, D.K. Meijer and F. Moolenaar. Renal targeting of captopril using subcutaneous administration of captopril-lysozyme conjugate. J Control Release. 101:350-351 (2005).
20. H. Kodaira, Y. Tsutsumi, Y. Yoshioka, H. Kamada, Y. Kaneda, Y. Yamamoto, S. Tsunoda, T. Okamoto, Y. Mukai, H. Shibata, S. Nakagawa and T. Mayumi. The targeting of anionized polyvinylpyrrolidone to the renal system. Biomaterials. 25:4309-4315 (2004).
21. H. Kamada, Y. Tsutsumi, K. Sato-Kamada, Y. Yamamoto, Y. Yoshioka, T. Okamoto, S. Nakagawa, S. Nagata and T. Mayumi. Synthesis of a poly(vinylpyrrolidone-co-dimethyl maleic anhydride) co-polymer and its application for renal drug targeting. Nat Biotechnol. 21:399-404 (2003).

22. Z.X. Yuan, X. Sun, T. Gong, H. Ding, Y. Fu and Z.R. Zhang. Randomly 50% N-acetylated low molecular weight chitosan as a novel renal targeting carrier. J Drug Target. 15:269-278 (2007).
23. H. Ghandehari. Polymer-peptide conjugates for targeted delivery to sites of angiogenesis. European symposium on controlled drug delivery, Noordwijk, April 2-4 2008 (2008).
24. M. Kissel, P. Peschke, V. Subr, K. Ulbrich, A.M. Strunz, R. Kuhnlein, J. Debus and E. Friedrich. Detection and cellular localisation of the synthetic soluble macromolecular drug carrier pHPMA. Eur J Nucl Med Mol Imaging. 29:1055-1062 (2002).
25. E.S.R. de Cassia da Silveira and M. de Oliveira Guerra. Reproductive toxicity of lapachol in adult male Wistar rats submitted to short-term treatment. Phytother Res. 21:658-662 (2007).
26. B. Baur and E.R. Baumgartner. Na(+)-dependent biotin transport into brush-border membrane vesicles from human kidney cortex. Pflugers Arch. 422:499-505 (1993).
27. H. Kobayashi, S.K. Jo, S. Kawamoto, H. Yasuda, X. Hu, M.V. Knopp, M.W. Brechbiel, P.L. Choyke and R.A. Star. Polyamine dendrimer-based MRI contrast agents for functional kidney imaging to diagnose acute renal failure. J Magn Reson Imaging. 20:512-518 (2004).
28. H. Kobayashi, S. Kawamoto, S.K. Jo, H.L. Bryant, Jr., M.W. Brechbiel and R.A. Star. Macromolecular MRI contrast agents with small dendrimers: pharmacokinetic differences between sizes and cores. Bioconjug Chem. 14:388-394 (2003).
29. H. Kobayashi, N. Sato, S. Kawamoto, T. Saga, A. Hiraga, T. Ishimori, J. Konishi, K. Togashi and M.W. Brechbiel. Novel intravascular macromolecular MRI contrast agent with generation-4 polyamidoamine dendrimer core: accelerated renal excretion with coinjection of lysine. Magn Reson Med. 46:457-464 (2001).
30. E.A. van der Wouden, M. Sandovici, R.H. Henning, D. de Zeeuw and L.E. Deelman. Approaches and methods in gene therapy for kidney disease. J Pharmacol Toxicol Methods. 50:13-24 (2004).
31. Y. Isaka. Gene therapy targeting kidney diseases: routes and vehicles. Clin Exp Nephrol. 10:229-235 (2006).
32. D.C. Han, B.B. Hoffman, S.W. Hong, J. Guo and F.N. Ziyadeh. Therapy with antisense TGF-beta1 oligodeoxynucleotides reduces kidney weight and matrix mRNAs in diabetic mice. Am J Physiol Renal Physiol. 278:F628-634 (2000).
33. A.A. Eddy. Molecular basis of renal fibrosis. Pediatr Nephrol. 15:290-301 (2000).
34. F. Strutz and E.G. Neilson. New insights into mechanisms of fibrosis in immune renal injury. Springer Semin Immunopathol. 24:459-476 (2003).
35. C.C. Sharpe and B.M. Hendry. Signaling: focus on Rho in renal disease. J Am Soc Nephrol. 14:261-264 (2003).
36. K. Hayashi, S. Wakino, T. Kanda, K. Homma, N. Sugano and T. Saruta. Molecular mechanisms and therapeutic strategies of chronic renal injury: role of rho-kinase in the development of renal injury. J Pharmacol Sci. 100:29-33 (2006).
37. M. De Borst, J. Prakash, W. Melenhorst, M. van den Heuvel, R. Kok, G. Navis and H. van Goor. Glomerular and tubular induction of the transcription factor c-Jun in human renal disease. J Pathol. 213:219-228 (2007).
38. H. Francois, S. Placier, M. Flamant, P.L. Tharaux, D. Chansel, J.C. Dussaule and C. Chatziantoniou. Prevention of renal vascular and glomerular fibrosis by epidermal growth factor receptor inhibition. Faseb J. 18:926-928 (2004).
39. J. Prakash, M.H. de Borst, A.M. van Loenen-Weemaes, M. Lacombe, F. Opdam, H. van Goor, D.K. Meijer, F. Moolenaar, K. Poelstra and R.J. Kok. Cell-specific delivery of a transforming growth factor-beta type I receptor kinase inhibitor to proximal tubular cells for the treatment of renal fibrosis. Pharm Res. 25:2427-2439 (2008).
40. J. Prakash, K. Poelstra, H. van Goor, F. Moolenaar, D.K.F. Meijer and R.J. Kok. Novel therapeutic targets for the treatment of tubulointerstitial fibrosis. Current Signal Transduction Therapy. 3:97-111 (2008).
41. J. Prakash, M. Sandovici, V. Saluja, M. Lacombe, R.Q. Schaapveld, M.H. de Borst, H. van Goor, R.H. Henning, J.H. Proost, F. Moolenaar, G. Keri, D.K. Meijer, K. Poelstra and R.J. Kok. Intracellular delivery of the p38 mitogen-activated protein kinase inhibitor SB202190 [4-(4-fluorophenyl)-2-(4-hydroxyphenyl)-5-(4-pyridyl)1H-imidazole] in renal tubular cells: a novel strategy to treat renal fibrosis. J Pharmacol Exp Ther. 319:8-19 (2006).
42. M. Zhang, J. Tang and X. Li. Interleukin-1beta-induced transdifferentiation of renal proximal tubular cells is mediated by activation of JNK and p38 MAPK. Nephron Exp Nephrol. 99:e68-76 (2005).

43. S. Madhusudan and T.S. Ganesan. Tyrosine kinase inhibitors in cancer therapy. Clin Biochem. 37:618-635 (2004).
44. J.S. Ross, D.P. Schenkein, R. Pietrusko, M. Rolfe, G.P. Linette, J. Stec, N.E. Stagliano, G.S. Ginsburg, W.F. Symmans, L. Pusztai and G.N. Hortobagyi. Targeted therapies for cancer 2004. Am J Clin Pathol. 122:598-609 (2004).
45. G. Keri, Z. Szekelyhidi, P. Banhegyi, Z. Varga, B. Hegymegi-Barakonyi, C. Szantai-Kis, D. Hafenbradl, B. Klebl, G. Muller, A. Ullrich, D. Eros, Z. Horvath, Z. Greff, J. Marosfalvi, J. Pato, I. Szabadkai, I. Szilagyi, Z. Szegedi, I. Varga, F. Waczek and L. Orfi. Drug discovery in the kinase inhibitory field using the Nested Chemical Library technology. Assay Drug Dev Technol. 3:543-551 (2005).
46. M.A. Fabian, W.H. Biggs, 3rd, D.K. Treiber, C.E. Atteridge, M.D. Azimioara, M.G. Benedetti, T.A. Carter, P. Ciceri, P.T. Edeen, M. Floyd, J.M. Ford, M. Galvin, J.L. Gerlach, R.M. Grotzfeld, S. Herrgard, D.E. Insko, M.A. Insko, A.G. Lai, J.M. Lelias, S.A. Mehta, Z.V. Milanov, A.M. Velasco, L.M. Wodicka, H.K. Patel, P.P. Zarrinkar and D.J. Lockhart. A small molecule-kinase interaction map for clinical kinase inhibitors. Nat Biotechnol. 23:329-336 (2005).
47. J.P. Adams and J.D. Sweatt. Molecular psychology: roles for the ERK MAP kinase cascade in memory. Annu Rev Pharmacol Toxicol. 42:135-163 (2002).
48. C.J. Vlahos, S.A. McDowell and A. Clerk. Kinases as therapeutic targets for heart failure. Nat Rev Drug Discov. 2:99-113 (2003).
49. S.J. Harper and P. LoGrasso. Signalling for survival and death in neurones: the role of stress-activated kinases, JNK and p38. Cell Signal. 13:299-310 (2001).
50. R. Kerkela, L. Grazette, R. Yacobi, C. Iliescu, R. Patten, C. Beahm, B. Walters, S. Shevtsov, S. Pesant, F.J. Clubb, A. Rosenzweig, R.N. Salomon, R.A. Van Etten, J. Alroy, J.B. Durand and T. Force. Cardiotoxicity of the cancer therapeutic agent imatinib mesylate. Nat Med. 12:908-916 (2006).
51. T. Force, D.S. Krause and R.A. Van Etten. Molecular mechanisms of cardiotoxicity of tyrosine kinase inhibition. Nat Rev Cancer. 7:332-344 (2007).
52. F.A. Eskens and J. Verweij. The clinical toxicity profile of vascular endothelial growth factor (VEGF) and vascular endothelial growth factor receptor (VEGFR) targeting angiogenesis inhibitors; a review. Eur J Cancer. 42:3127-3139 (2006).
53. A. Fernandez, A. Sanguino, Z. Peng, E. Ozturk, J. Chen, A. Crespo, S. Wulf, A. Shavrin, C. Qin, J. Ma, J. Trent, Y. Lin, H.D. Han, L.S. Mangala, J.A. Bankson, J. Gelovani, A. Samarel, W. Bornmann, A.K. Sood and G. Lopez-Berestein. An anticancer C-Kit kinase inhibitor is reengineered to make it more active and less cardiotoxic. J Clin Invest. 117:4044-4054 (2007).
54. K. Temming, M.M. Fretz and R.J. Kok. Organ- and Cell-Type Specific Delivery of Kinase Inhibitors: A Novel Approach in the Development of Targeted Drugs. Current Molecular Pharmacology 1:1-12 (2008).
55. M.M. Fretz, J. Prakash, M.E.M. Dolman, M. Lacombe, M.d. Borst, H.v. Goor, K. Poelstra and R.J. Kok. Renal Delivery of Kinase Inhibitors Ameliorates Experimental Inflammation and Fibrosis. ASN Renal Week 2007, October 31-November 5:Abstract SU-FC141 (2007).
56. J. Reedijk. Metal-Ligand Exchange Kinetics in Platinum and Ruthenium Complexes. Platinum Metals Review. 52:2-11 (2008).
57. T. Gonzalo, L. Beljaars, M. van de Bovenkamp, K. Temming, A.M. van Loenen, C. Reker-Smit, D.K. Meijer, M. Lacombe, F. Opdam, G. Keri, L. Orfi, K. Poelstra and R.J. Kok. Local inhibition of liver fibrosis by specific delivery of a platelet-derived growth factor kinase inhibitor to hepatic stellate cells. J Pharmacol Exp Ther. 321:856-865 (2007).
58. T. Gonzalo, E.G. Talman, A. van de Ven, K. Temming, R. Greupink, L. Beljaars, C. Reker-Smit, D.K. Meijer, G. Molema, K. Poelstra and R.J. Kok. Selective targeting of pentoxifylline to hepatic stellate cells using a novel platinum-based linker technology. J Control Release. 111:193-203 (2006).
59. K. Temming, M. Lacombe, P. van der Hoeven, J. Prakash, T. Gonzalo, E.C. Dijkers, L. Orfi, G. Keri, K. Poelstra, G. Molema and R.J. Kok. Delivery of the p38 MAPkinase inhibitor SB202190 to angiogenic endothelial cells: development of novel RGD-equipped and PEGylated drug-albumin conjugates using platinum(II)-based drug linker technology. Bioconjug Chem. 17:1246-1255 (2006).
60. T. Masuda, N. Ide and N. Kitabatake. Effects of chemical modification of lysine residues on the sweetness of lysozyme. Chem Senses. 30:253-264 (2005).
61. M. Salmain, J.C. Blais, H. Tran-Huy, C. Compain and G. Jaouen. Reaction of hen egg white lysozyme with Fischer-type metallocarbene complexes. Characterization of the conjugates and determination of the metal complex binding sites. Eur J Biochem. 268:5479-5487 (2001).

62. C.A. Teske, R. Simon, A. Niebisch and J. Hubbuch. Changes in retention behavior of fluorescently labeled proteins during ion-exchange chromatography caused by different protein surface labeling positions. Biotechnol Bioeng. 98:193-200 (2007).
63. K. Temming, M. Lacombe, H.E. Moorlag, S.A. Asgeirsdottir, L. Orfi, G. Keri, K. Poelstra, G. Molema and R.J. Kok. Targeting of the VEGF-kinase inhibitor PTK787 to angiogenic vasculature using RGD-equipped albumin carrier molecules. J Control Release. 116:e57 (2006).
64. J. Prakash, A.M. van Loenen-Weemaes, M. Haas, J.H. Proost, D.K. Meijer, F. Moolenaar, K. Poelstra and R.J. Kok. Renal-selective delivery and angiotensin-converting enzyme inhibition by subcutaneously administered captopril-lysozyme. Drug Metab Dispos. 33:683-688 (2005).
65. J. Prakash, M.H. de Borst, M. Lacombe, F. Opdam, P.A. Klok, H. van Goor, D.K. Meijer, F. Moolenaar, K. Poelstra and R.J. Kok. Inhibition of renal rho kinase attenuates ischemia/ reperfusion-induced injury. J Am Soc Nephrol. 19:2086-2097 (2008).
66. J. Prakash, V. Saluja, J. Visser, F. Moolenaar, D.K. Meijer, K. Poelstra and R.J. Kok. Bioanalysis and pharmacokinetics of the p38 MAPkinase inhibitor SB202190 in rats. J Chromatogr B Analyt Technol Biomed Life Sci. 826:220-225 (2005).
67. M.S. Razzaque, N. Ahsan and T. Taguchi. Role of apoptosis in fibrogenesis. Nephron. 90:365-372 (2002).
68. J.M. Fan, Y.Y. Ng, P.A. Hill, D.J. Nikolic-Paterson, W. Mu, R.C. Atkins and H.Y. Lan. Transforming growth factor-beta regulates tubular epithelial-myofibroblast transdifferentiation in vitro. Kidney Int. 56:1455-1467 (1999).
69. E.P. Bottinger and M. Bitzer. TGF-beta signaling in renal disease. J Am Soc Nephrol. 13:2600-2610 (2002).
70. N.J. Laping. ALK5 inhibition in renal disease. Curr Opin Pharmacol. 3:204-208 (2003).
71. N.G. Docherty, O.E. O'Sullivan, D.A. Healy, M. Murphy, J. O'Neill A, J.M. Fitzpatrick and R.W. Watson. TGF-beta1-induced EMT can occur independently of its proapoptotic effects and is aided by EGF receptor activation. Am J Physiol Renal Physiol. 290:F1202-1212 (2006).
72. W.A. Windt, J. Prakash, R.J. Kok, F. Moolenaar, C.A. Kluppel, D. de Zeeuw, R.P. van Dokkum and R.H. Henning. Renal targeting of captopril using captopril-lysozyme conjugate enhances its antiproteinuric effect in adriamycin-induced nephrosis. J Renin Angiotensin Aldosterone Syst. 5:197-202 (2004).

Chapter 2

Drug targeting to the kidney: advances in the active targeting of therapeutics to proximal tubular cells

M.E.M. Dolman[1], S. Harmsen[1], G. Storm[1], W.E. Hennink[1] and R.J. Kok[1]

[1] Department of Pharmaceutics, Utrecht Institute of Pharmaceutical Sciences, Utrecht University, Utrecht, The Netherlands

Advanced Drug Delivery Reviews 62:1344-1357 (2010)

Abstract

Activated signaling cascades in the proximal tubular cells of the kidneys play a crucial role in the development of tubulointerstitial fibrosis. Inhibition of these signaling cascades with locally delivered therapeutics is an attractive approach to minimize the risk of unwanted side effects and to enhance their efficacy within the renal tissue.

This review describes the potential avenues to actively target drugs to proximal tubular cells by recognition of internalizing receptors and how drug carriers can reach this cell type from either the apical or basolateral side. Important characteristics of drug carrier systems such as size and charge are discussed, as well as linking technologies that have been used for the coupling of drugs to the presented carrier systems. Lastly, we discuss the cellular handling of drugs by proximal tubular cells after their delivery to the kidneys.

1. Introduction

Renal diseases can be divided in acute kidney injury (AKI) and chronic kidney disease (CKD) (1-3). Patients with AKI suffer from a sudden decline in glomerular filtration rate (GFR) that takes place within hours to days after an acute kidney insult, but is often reversible (2). When the reduced kidney function persists for several months and the initial renal damage has resulted in tissue remodeling and an ongoing process of renal function loss, the term CKD is used. CKD is often diagnosed in a late stage, in which the therapeutic options to prevent or delay the progression are limited (3-5). Hypertension, diabetes, and hyperlipidaemia are important risk factors for the development of CKD (6).

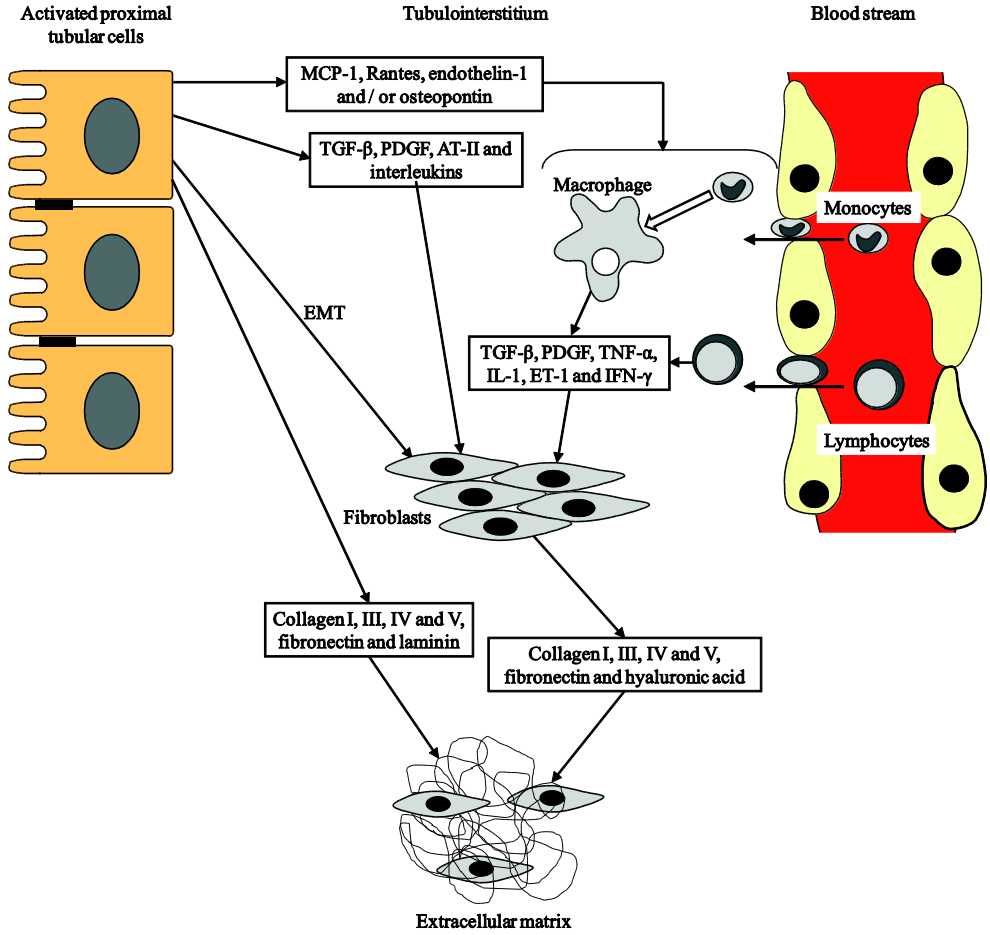

Figure 1. Schematic representation of the molecular and cellular events in tubulointerstitial fibrosis (derived from (26)).

In most cases CKD results in glomerulosclerosis and/ or tubulointerstitial fibrosis (7-9). Although fibrosis of the glomerulus and tubulointerstitium often occurs in parallel, this review focuses on tubulointerstitial fibrosis. One of the hallmarks of tubulointerstitial fibrosis is increased production of chemokines, adhesion molecules and growth factors by activated proximal tubular epithelial cells. As a consequence, inflammatory cells such as macrophages and lymphocytes are attracted into the renal interstitium and further activated, thereby promoting an ongoing cycle of inflammation and tissue remodeling. In addition, epithelial-to-mesenchymal transition (EMT) of normal proximal tubular epithelial cells is triggered by profibrotic growth factors and cytokines, resulting in increased levels of myofibroblasts and the excessive formation of extracellular matrix (ECM) (6, 10-14) (**Figure 1**).

One of the most important growth factors involved in the pathogenesis of tubulointerstitial fibrosis is transforming growth factor - β1 (TGF-β1), which stimulates both EMT and ECM deposition (11-13, 15-20). Other important profibrotic mediators in tubulointerstitial fibrosis are epidermal growth factor (EGF) and platelet-derived growth factor (PDGF) (21, 22). They exert their effects by activating downstream signaling cascades, in which kinases play a major role (23, 24). Progression of the above mentioned profibrotic processes will eventually result in established CKD/ stage 5 CKD, which requires renal replacement therapies such as dialysis or renal transplantation (25).

1.1. Treatment of tubulointerstitial fibrosis

Since the early stages of CKD are usually asymptomatic, CKD is often only diagnosed in the advanced stage, in which the disease progresses irrespective of its initial underlying pathology (5). Drugs that inhibit the function of angiotensin II (AT II), such as angiotensin-converting enzyme (ACE) inhibitors and AT_1 receptor antagonists, are the preferred choice of treatment and have clinically been proven to retard the progression of CKD. However, monotherapy with AT II inhibitors will not prevent the final development of end-stage renal disease (ESRD) (27, 28). Combination therapy of spironolactone (*i.e.* an aldosterone inhibitor) with an AT II inhibitor has been investigated in small clinical trials and seems to be beneficial in the treatment of renal fibrosis. Larger clinical trials need to be performed to estimate if the addition of spironolactone to therapy with an AT II inhibitor prevents the development of ESRD (29). Another drug that is currently under clinical investigation for the treatment of renal fibrosis is pirfenidone (30, 31), initially developed for the treatment of idiopathic pulmonary fibrosis. At the moment it is too early to conclude if treatment of renal fibrosis with pirfenidone prevents ESRD. In clinical trials treatment with pirfenidone, however, was associated with adverse reactions such as dyspepsia and sedation requiring dosage adjustment (31). The lack of clinically available drugs that are able to stop or reverse tubulointerstitial fibrosis requires the development of new and advanced therapeutic strategies.

In view of the pivotal role of proximal tubular epithelial cells in the pathogenesis of tubulointerstitial fibrosis (32, 33), targeting the disease-activated pathways in tubular cells seems an attractive and straightforward strategy to stop or reverse the progression of renal disease. Different *in vitro* and *in vivo* studies have shown promising effects of kinase inhibitors in the treatment of renal fibrosis. Examples of successfully tested kinase inhibitors are TGF-β kinase inhibitors (34-36), p38 mitogen activated protein kinase (p38 MAPK) inhibitors (37-39), Rho-associated kinase (ROCK) inhibitors (20, 40) and PDGF receptor kinase inhibitors (22, 41). Apart

from kinase inhibitors also small interfering RNAs against growth factors (such as connective tissue growth factor (42) and TGF-β1 (43)) and other profibrotic molecules (such as induced in high glucose-1 (44) and heat shock protein 47 (45)) have successfully been tested in preclinical trials for the treatment of tubulointerstitial fibrosis. This review gives an overview of the different strategies that can be used for the delivery of such therapeutic agents to the proximal tubular cells of the kidney and, secondly, addresses the linkage technologies that can be used for the coupling of a therapeutic agent to a carrier system. Cell specific targeting of antifibrotic agents to proximal tubular cells is an attractive method to increase their efficacy and/ or minimize their side effects, as the preferred renal accumulation of the drugs will result in higher tubular drug concentrations, while simultaneously the distribution to other tissues will be avoided. It is well known that advanced drug targeting can be used for the delivery of cytostatic drugs to tumour cells or angiogenic blood vessels (46-48). We will outline that advanced drug targeting approaches can also be of value for drug delivery to the kidney.

Many of the above discussed antifibrotic compounds target processes that are also relevant to physiological processes elsewhere in the human body (49-52). As a consequence, inhibition of the same molecular targets in healthy cells may result in unwanted side effects. Small molecule inhibitors and antibodies directed to the epidermal growth factor receptor (EGFR) kinase, for example, are associated with serious cutaneous side effects (53). And the well known kinase inhibitors imatinib and sunitinib, clinically used in the treatment of several types of cancer (54, 55), have been associated with cardiotoxicity (55, 56). Cell specific delivery of these agents to the afflicted tissue can improve the therapeutic potential of these potent drugs, and opens up new opportunities for the treatment of renal disease.

2. The proximal tubule as target site

Drug targeting to the proximal tubular cells may offer new tools for the treatment of tubulointerstitial fibrosis, by reducing toxicity of drugs that exert unwanted side effects and/ or by increasing the renal efficacy of antifibrotic drugs. The same targeting strategies may be used for the treatment of other renal diseases in which the proximal tubular cells play a crucial role. An exception is the treatment of renal cell carcinoma (RCC). Although RCC in most cases originate from the proximal tubular cells, drug targeting to renal tumours may be best performed with a tumour-directed approach. First of all because the architecture of the nephron is lost when tubular cells transform into cancer cells and the carcinoma cells dedifferentiate during their transformation to cancer cells. As a consequence, they may lose the expression of internalizing receptors that are discussed in this review as potential entry ports for active uptake by proximal tubular cells. Second, when tubular cell-directed carriers are used for the delivery of anticancer agents to renal cell carcinoma, the targeted anticancer drug will concomittantly accumulate in the remaining healthy parts of the kidney. Hence, delivery of cytotoxic drugs to RCC with the targeting approaches discussed in this review may result in tubular cell death. Tubular cell-targeted drug delivery requires a carrier system that can reach the target cells and that is subsequently internalized by this cell type. The following chapter will describe how drug-carrier conjugates directed to proximal tubular cells are handled by the kidney, and how they can enter the proximal tubular cells (**Figure 2**). We will start by briefly describing the nephron, the basic functional unit of the kidney.

2.1. Role of the proximal tubule in the reabsorption and secretion of substances

Nephrons are composed of a filtration unit (*i.e.* the glomerulus) and a tubular system (composed of a proximal tubule, the loop of Henle, a distal tubule and a collecting duct) along which substances can be exchanged between the blood stream and urine. The tubular system is responsible for the reabsorption of endogenous compounds, such as water, salts and glucose, but also allows the reabsorption of other filtered compounds, including drug molecules that can cross the tubular cells either by passive or active transport. The proximal tubuli represent the biggest part of the kidneys and play by far the most prominent role in the recovery of substances from the urine, as they are involved in reabsorption of about two-third of the filtrate volume, along with recovery of many compounds that have been filtered into the urine (57). In addition, the proximal tubule is also the primary location for secretion of compounds into the urine. These features offer attractive opportunities for the active uptake of drug carrier systems, as will be discussed shortly.

2.2. Physiological barriers at the apical and basolateral side of proximal tubular cells

In order to target its cargo to the proximal tubule, a drug carrier needs to get access to this cell type, either at the basolateral or the apical side. Whether or not a carrier system is able to reach the target cells depends on the anatomical and physiological environment of the nephron. The following paragraphs describe the barriers that need to be passed before reaching the proximal tubular cells, and which factors can limit the penetration of carriers into the renal tissue (**Figure 2**).

Barriers encountered at the basolateral side of the proximal tubular cells are the capillary endothelial cell layer of the peritubular capillaries and, after passage across the vascular wall, the tubulointerstitium between the capillaries and the tubular cells (58, 59) (**Figure 2B**). As reported by Satchell *et al.*, the renal peritubular capillaries contain endothelial fenestrations, with a diameter of around 60-70 nm (60). These fenestrations are closed by a diaphragm of approximately 3-5 nm thickness composed of radial fibrils which interweave into a central knob (60, 61). Although the maximum size of particles that can penetrate between the fibrils is not exactly known, the pore size seems to be around 5.0-5.5 nm (62, 63). Due to the fact that the fenestrae contain negatively charged heparin sulfate, positively charged macromolecules and particles will be transported more easily than negatively charged drug carriers (60). The next barrier that lies between the endothelium and the basal side of the proximal tubuli is the tubulointerstitium. In here, fibroblasts and cells of the immune system like dendritic cells reside, surrounded by an extracellular matrix consisting of proteoglycans, glycoproteins, fibrils and interstitial fluid (58, 64).

In order to access the apical side of the tubular cell, *i.e.* from the tubulary lumen, a carrier system needs to be filtered through the glomerulus. Glomerular filtration of compounds involves several barriers, as the carrier needs to pass consecutively the endothelial layer, the glomerular basement membrane (GBM) and the podocyte foot processes (65) (**Figure 2A**). Like the renal peritubular capillaries at the basolateral side of the proximal tubuli, the endothelium of the glomerulus also contains fenestrations. These fenestrations have a larger diameter of approximately 70-100 nm (65, 66). Moreover, the endothelial fenestrations in the glomerulus are not closed by diaphragms, enabling larger molecules to cross the glomerular endothelium relatively easily (60). The next barrier, the GBM, is the main filtration barrier of the glomerulus. The GBM is composed of the

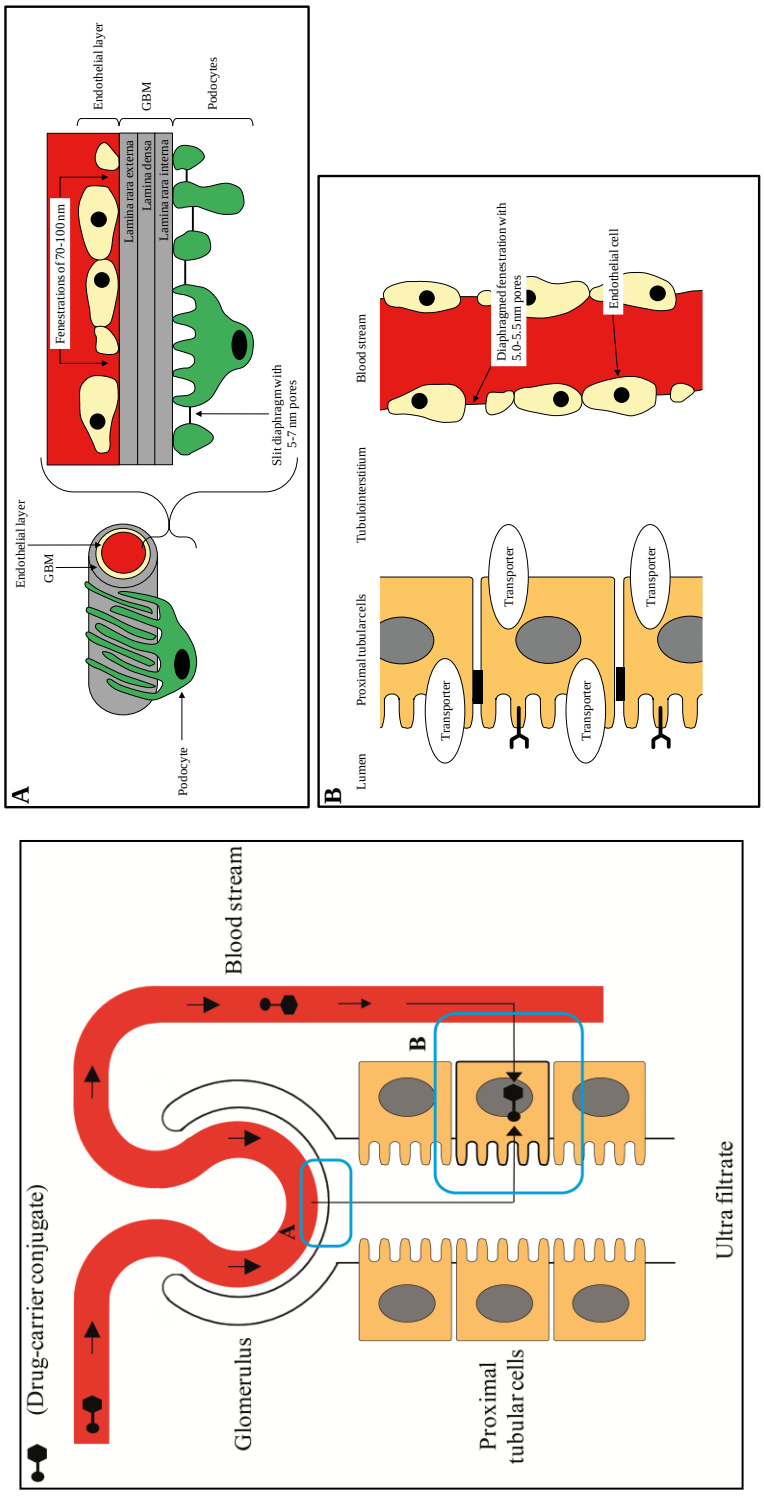

Figure 2. Anatomical barriers between the circulation and the proximal tubular cell. A) Glomerular filtration barriers. Drug delivery systems can cross the glomerular endothelium via its fenestrae. Passage into the tubular lumen requires diffusion across the basement membrane and subsequent filtration through the slit diaphragm of the podocytes. B) Basolateral barriers. The basolateral side of the proximal tubular cells can be reached after penetration through diaphragmed fenestrae in the endothelial cell layer of the peritubular capillary and passive diffusion through the tubulointerstitium.

lamina rara externa, the lamina densa and the lamina rara interna. The presence of negatively charged sulfated glycosaminoglycans in the lamina rara externa and lamina rara interna favours the passage of positively charged carrier systems across the GBM, as compared to negatively charged carriers (67-70). The last barrier of the glomerulus consists of the epithelial podocytes, which form a stabile network around the GBM by foot processes that are interconnected by slit diaphragms (65, 71). These slit diaphragms determine the upper size limit of macromolecules and particles for glomerular filtration (65, 72). Under normal physiological conditions, particles with a hydrodynamic diameter up to 5-7 nm can be filtered through the glomerulus and reach the apical side of the proximal tubular cells (73-75).

2.3. Uptake of drug-carrier conjugates by proximal tubular cells

Although the glomerular filtration of compounds may be comparable to the extravasation of macromolecules in leaky tumour vessels, the subsequent uptake of compounds in the proximal tubular cells is a highly active process. Proximal tubular cells contain different receptors and transporters that can be exploited for the active targeting of drugs. Although appealing at a first glance, it is not efficient to use a transporter for this purpose. First of all, these transporters are primarily involved in the uptake of small endogenous molecules, such as glucose, peptides and neurotransmitters, but also xenobiotics such as small molecule drugs (76-81). It is highly questionable whether such membrane proteins will accept larger drug-carrier conjugates as substrates for transport. Another disadvantage is that the intracellularly accumulated substrates may be excreted again from the cells into the urine or into the renal interstitium, by either the same transporter or via a different transporter expressed in the tubular cell membrane. As a consequence, the residence time of the transported compounds within the proximal tubular cell is limited. Lastly, many transporters expressed in the kidney are also expressed in other organs, and therefore will not be proper targets for renal-specific uptake of the delivered compound (79, 82). Drug delivery into the proximal tubular cells via receptor-mediated endocytosis therefore seems a more attractive approach. Renal proximal tubular cells contain different internalizing receptors, which are able to internalize small molecules as well as macromolecules such as proteins that are filtered into the urine. Since these receptors, however, are solely localized on the apical membranes of the tubular cells (83-85), targeting of drugs to the luminal side of the tubular cells via carriers that bind these internalizing receptors is the most straightforward strategy to obtain efficient uptake of the drug.

Drug modification with alkylglycosides has been investigated as a strategy to deliver drugs into the tubular cells via the basolateral membrane (86, 87). Alkylglycosylated low molecular weight peptides were shown to be rapidly taken up in the proximal tubular cells, *i.e.* within 5 minutes after intravenous administration in rats. However, the intracellular handling of these peptide derivatives after 5 minutes as well as their uptake mechanism is not known (86, 87). At the moment no receptor on the basolateral membrane of the proximal tubular cells has been elucidated responsible for the specific uptake of sugar modified compounds and uptake of alkyl glycosylated peptides via glucose transporters seems to be most likely. If alkylglycosylated drugs are taken up via transporters, research needs to be done to investigate if they are not excreted from the cells before the drug can be released. The tubular cells are known to express several glucose transporters at the apical (SGLT1-3) and basolateral (GLUT1, -2 and 5) membrane that can excrete glucose from the cell into the tubular lumen or tubulointerstitium (88, 89).

2.4. Receptor-mediated endocytosis

Two well studied internalizing receptors expressed on the apical membrane of proximal tubular cells are megalin and cubilin (83, 90-92). The megalin receptor is a protein of approximately 600 kDa that consists of a large extracellular domain, a hydrophobic transmembrane segment and a small intracellular domain which triggers the endocytic trafficking of ligands. In contrast to megalin, cubilin (~ 460 kDa) only consists of an extracellular domain, which is attached to the plasma membrane via the membrane-associated domain. Interactions with colocalized megalin stimulate the co-internalization of cubilin and megalin. Receptor-mediated endocytosis via megalin and cubilin starts with the internalization of the ligand–receptor complex in clathrin-coated vesicles. Via these coated vesicles the ligand–receptor complexes end up in the endosomes and subsequently in the lysosomal compartment of the cell. The low pH within the late endosomes and lysosomes allows the release of the ligand from the receptor and the return of megalin and cubilin to the apical membrane (92-94). Megalin and cubilin are most abundant in the upper part of the proximal tubule, in the so-called S1 and S2 segments (95). Although these receptors have a broad substrate specificity, their interaction with ligands is specific and shows typical ligand-receptor kinetics, as has been demonstrated by Biacore receptor interaction studies (96). Examples of ligands for megalin/ cubilin are albumin, receptor-associated protein (RAP), lysozyme and cytochrome c (83, 90-92).

Other internalizing receptors expressed on the apical membrane of proximal tubular cells are the ~ 40 kDa folate receptors (FRs). Of the four isoforms of the folate receptor identified in humans, only the membrane-associated folate receptors FRα and FRβ have been detected in the proximal tubular cells (84, 85). The main function of the renally expressed folate receptors is the reabsorption of folate from the tubular lumen after glomerular filtration of this vitamin. Besides FRs, also the reduced folate carrier (RFC) at the basolateral side of the proximal tubular cells is involved in the vitamin transport (97-99). RFC selectively transports the reduced form of folic acid, in contrast to FRs which can transport both folic acid and folate-linked complexes (100). The major part of the folic acid that is taken up via the folate receptors at the apical membrane of the proximal tubular cells is transported into the lysosomes. However, part of the folic acid is transported to the basolateral membrane via transcytosis, offering possibilities to direct drugs to the basolateral side of the tubular cells (97). Furthermore, in tumour tissues the endocytic routing of folate conjugates was found to be dependent on the valency of the conjugates. Typically, multivalent folate carriers ended up in the lysosomal compartment, while monovalent folate conjugates were routed to a non-acidic intracellular compartment (101). Whether or not the same applies for the renal handling of folate conjugates is not known. Folate receptors are overexpressed in multiple malignant tissues and have been employed for the tumour-targeted delivery of anticancer drugs (100, 102-104). Besides in the kidneys, FRα and FRβ are mainly expressed in the choroid plexus, placenta, lungs and intestines (100, 104, 105).

Although the expression of the above discussed receptors is not limited to the kidneys, they are attractive for renal drug targeting approaches. This can be explained by the preferential expression of megalin, cubilin and the FRs on the microvillar surface at the luminal side of epithelial cells. While the luminal side of the tubular epithelial cells in the kidneys can be reached via the blood stream after glomerular filtration, the epithelial cells in other organs pose a barrier that prevents the possibility of macromolecular drug-carrier conjugates to reach the internalizing receptors at the luminal side (100).

3. Overview of carrier systems for proximal tubular cell targeting

As discussed in the previous section, the glomerular filtration barrier dictates that only carrier systems with a hydrodynamic diameter below 5-7 nm can reach the luminal surface of proximal tubular cells. This size limit excludes commonly used drug carrier systems like liposomes and antibodies. More appropriately, macromolecular carriers with a relatively low molecular weight have been applied as drug carriers for proximal tubular targeting. Only a limited number of carriers have been intentionally applied for renal drug targeting. We have discussed these carriers in the referred section of the review. Many more potential carriers for drug targeting to proximal tubular cells can be envisioned when one considers the common denominators of the discussed systems. We have broadened the scope of the review by also discussing such potential carriers, but have limited our selection to those carriers for which tubular uptake has been reported.

3.1. Protein- and peptide-based carrier systems

Low molecular weight proteins have been studied most extensively as renal carrier system for the intracellular delivery of therapeutic drugs into proximal tubular cells. Like for peptides, an important advantage of protein-based carrier systems is their *in vivo* biodegradability. The most popular renal carrier is lysozyme with a molecular weight of 14 kDa. Lysozyme is almost freely filtered in the urine and has a glomerular sieving coefficient of 0.8 (106). After filtration in the urine, lysozyme is reabsorbed by the proximal tubular cells via the megalin receptor (91, 92). Lysozyme has been employed for the delivery of various low molecular weight drugs, as will be discussed below. Biodistribution studies in rats showed a maximum accumulation within the proximal tubuli of approximately 20%, obtained in 30 minutes after intravenous administration of the drug-lysozyme conjugates. Hardly any accumulation was observed in other organs (34, 40, 107). To investigate the capability of lysozyme to enter the proximal tubular cells in advanced renal disease, the renal accumulation of radiolabeled lysozyme in healthy rats has been compared with its renal accumulation in the adriamycin model of advanced renal disease in rats (108). In this model, initial tubular damage develops into renal fibrosis over the course of six weeks, with massive proteinuria. The cumulative accumulation of lysozyme in the diseased animals was found to be 70% of the cumulative accumulation in healthy rats (108). Moreover, the reduced tubular reabsorption of lysozyme due to competition with filtered albumin or due to loss of megalin receptors will not result in unwanted accumulation of the conjugate in non-target tissues, since the protein (and drug-lysozyme conjugates) will be excreted into the urine. This elevated loss into the urine may be compensated by injection of a (slightly) elevated dose of the drug-lysozyme conjugate.

Schechter *et al.* investigated the use of streptavidin as a potential carrier for drug targeting to the kidneys (109). Streptavidin is a tetrameric protein purified from *Streptomyces avidinii*. In most cases proteolytic degradation during the purification procedure of the protein results in a truncated form with a molecular weight of about 58 kDa. While low kidney levels were observed with the intact native form of streptavidin, the truncated form of streptavidin showed remarkably higher kidney levels (109). *In vivo* biodistribution studies with truncated streptavidin in mice showed a maximum renal accumulation of approximately 70-80% of the administered dose per gram tissue at 24 hours after a single intravenous injection (109). Assuming a total kidney weight of approximately 300 mg for 10-12-week-old Balb/ c mice (110, 111), this means a

total accumulation of approximately 22% of the injected dose in both kidneys. Immunohistochemical studies have further demonstrated the renal accumulation of streptavidin in proximal tubular cells (109). Truncated streptavidin was also found to a minor extent within other organs, such as the liver and spleen (109).

Lysozyme and streptavidin are the only low molecular weight proteins that have been tested as renal carrier systems for drug delivery to proximal tubular cells. But the internalizing receptors megalin and cubilin have a broad substrate specificity and, hence, are involved in the tubular reabsorption of many other low molecular weight proteins (91). Therefore also other proteins or protein fragments may be used as renal carrier system, such as albumin fragments. Although albumin itself is hardly filtered in the kidney, it has affinity for the megalin- and cubilin receptor (90, 91). Vegt *et al*. demonstrated that albumin fragments of 3-50 kDa accumulated in rat kidneys to about approximately 15% of the injected dose per gram tissue at 20 hours after administration. Assuming that the weight of both kidneys in rats is 0.9% of the total body weight (112), this means a total accumulation in both kidneys of approximately 28% (113), which is comparable to the kidney accumulation of the above described low molecular weight proteins (40, 109).

Besides low molecular weight proteins, also peptides may be used as tubular cell-directed drug carriers. Examples of peptides of which renal accumulation has been described in literature are octreotide, gastrin, glucagon-like peptide-1 and bombesin, all peptides that are used for tumour radiotherapy (113, 114). Of these peptides, gastrin and glucagon-like peptide-1 are the most interesting, since approximately 25% of the injected activity of radiolabeled gastrin and 46% of the injected activity of radiolabeled glucagon-like peptide-1 was found in both kidneys at 24 hours after administration (114). In contrast, the renal uptake of bombesin and octreotide in rats was low. Studies in megalin knock-out mice confirmed the uptake of octreotide by proximal tubular cells via binding to the megalin receptor (114). The uptake mechanism of the other peptides in proximal tubular cells has not yet been elucidated.

3.2. Polymeric carrier systems

Different polymer systems have been described for renal drug targeting. One example concerns anionized derivatives of polyvinylpyrrolidone (PVP). Low molecular weight polyvinylpyrrolidone does not accumulate in the kidneys and is excreted in the urine (115, 116). However, *in vivo* studies in mice demonstrated that copolymers of *N*-vinylpyrrolidone with anionic monomers resulted in increased renal levels (115). Parameters that play a crucial role in the capability of anionized PVPs to accumulate in renal tubular cells are the type of anionic groups introduced in the PVP polymers, the comonomer content and the molecular weight of the final polymers. Higher renal levels were observed for carboxylated PVP, compared with sulfonated PVP (115). The highest renal accumulation was obtained with 20% carboxylated PVP with a molecular weight of approximately 10 kDa. Kodeira *et al*. found a maximal renal accumulation of 30% of the injected dose 3 hours after administration. They also demonstrated specific uptake of carboxylated PVP in the proximal tubuli of the kidneys (115). Although 30% accumulation is already very promising, an even higher renal accumulation was obtained with another PVP copolymer, namely poly(vinylpyrrolidone-co-dimethyl maleic acid) (PVD) (117). The highest renal levels were obtained with PVD with a molecular weight of 6-8 kDa, of which about 80% of the administered dose accumulated in the kidneys at 3 hours after administration (116). PVD has a long retention time in the kidneys, since still 60% of the administered dose could

be detected at 24 hours after injection (117). No toxicity was observed with the investigated anionized PVPs (115, 116). So far, PVD has been evaluated as a renal carrier for the protein drug superoxide dismutase (SOD). The therapeutic effects of PVD-SOD were investigated in mice with acute renal failure (ARF) and compared with therapeutic effects of native SOD. PVD-SOD stopped the progression of ARF and accelerated recovery of the disease, as demonstrated by the inhibitory effects on urinary markers of renal disease and serum creatinine levels (116).
Another polymer that has successfully been used for drug targeting to the proximal tubular cells is acetylated low molecular weight chitosan (LMWC) (118, 119). Chitosan is a well known biocompatible and biodegradable polymer (119, 120). Randomly 50% acetylated LMWCs with different molecular weights were investigated for their potential to deliver the glucocorticoid prednisolone to the tubular epithelial cells. The highest accumulation was observed for LMWC with a molecular weight of 19 kDa. Within 15 minutes after administration in mice, a maximum kidney accumulation of approximately 15% of the injected dose was observed. Compared to the low molecular weight proteins lysozyme and truncated streptavidin and carboxylated PVP, acetylated LMWC is cleared from the kidneys more rapidly. Besides, acetylated LMWC seemed to be less renal specific, since accumulation was also observed in the lungs and liver (118). Recently, Yuan *et al*. investigated the mechanism by which LMWC accumulates in the proximal tubular cells. The reduced renal levels of LMWC observed in megalin-shedding mice indicate a possible crucial role of the megalin receptor in the renal uptake of this polymer (119).
Several other polymers that have not specifically been investigated as potential renal carrier system may also be of use for this purpose, since their renal accumulation has been described in literature. An example of such a polymer is poly[*N*-(2-hydroxypropyl) methacrylamide] (pHPMA), well-known for its capability to deliver anticancer drugs to tumour tissues (121-123). HPMA (co)polymers contain a non-biodegradable backbone, but are frequently used because they are biocompatible, water-soluble and non-immunogenic (124). Kissel *et al*. compared the biodistribution of 26 kDa biotinylated pHPMA with the biodistribution of 27 kDa non-biotinylated pHPMA in tumour-bearing rats. Although in both cases the highest accumulation was observed in the spleen, liver and tumour, biotinylation of pHPMA resulted in a significant increase in kidney accumulation (125). At day 7 after the intravenous injection of both polymers, biotin-pHPMA showed a renal uptake in the proximal tubular cells of both kidneys of approximately 8.5% of the injected dose (*i.e.* 4.7% per gram tissue), while in case of pHPMA this percentage was only approximately 0.25% (*i.e.* 0.14% per gram tissue) (125). The influence of molecular weight and charge on the organ biodistribution of HPMA copolymers was studied by Mitra *et al*. (126). Neutral and negatively charged HPMA copolymers with average molecular weights of approximately 8 kDa, 23 kDa and 73 kDa were synthesized and administered to mice. The highest renal uptake was observed for the negatively charged HPMA copolymers. Although the neutral copolymers were also found to be taken up by the liver and spleen, no significant concentrations of the negatively charged copolymers were found in other organs. For both, the neutral and negatively charged HPMA copolymers, the 23 kDa copolymers gave the highest renal levels 24 hours after intravenous injection (126). Borgman *et al*. investigated the biodistribution of HPMA copolymer-(RGDfK)-(CHX-A"-DTPA) conjugates in mice bearing Lewis lung carcinoma tumours (RGDfK = Arg-Gly-Asp-D-Phe-Lys; CHX-A"-DTPA = *trans*-(*S*,*S*)-cyclohexane-1,2-diamine-*N,N,N',N",N"*-pentaacetic acid). CHX-A"-DTPA was incorporated to introduce negatively charged side groups in the conjugates. Conjugates with varying molecular

weights (43 kDa, 20 kDa and 10 kDa) and charge content were tested (122, 127). For all conjugates accumulation in the kidneys was found to be much higher than tumour accumulation. The highest renal accumulation was obtained with the more negatively charged 43 kDa conjugate. Approximately 40% of the injected dose accumulated in the kidneys at 24 hours after injection. Similar to biotinylated pHPMA, kidney accumulation of the 43 kDa conjugate lasted for days. This indicates a slow renal degradation of HPMA containing polymers (122, 127). Earlier studies with a 35 kDa HPMA copolymer-(RGDfK)-(CHX-A"-DTPA) conjugate, with a lower negative charge compared to the 43 kDa conjugate, showed lower kidney and higher tumour accumulation. This confirms that the presence of negatively charged side groups in HPMA copolymers plays a major role in their inclination to accumulate in the kidneys (122, 127). The mechanism by which HPMA copolymers are taken up by the proximal tubular cells has not yet been investigated.

Rypáček *et al*. studied the renal excretion and retention of other polymers, namely 11 kDa α,β-poly(*N*-2-hydroxyethyl)aspartamide (PHEA) and equally sized derivatives of PHEA, obtained by derivatization of approximately 20% of the 2-hydroxyethyl side groups by side chains with different physicochemical properties (*i.e.* aliphatic *n*-butylamine groups, phenolic groups, cationic tertiary amine side chains or anionic carboxylic side chains) (128). Although studies with other polymers demonstrated higher renal levels of charged polymers, derivatization of 2-hydroxyethyl side groups with n-butylamine or phenolic residues resulted in the highest increase in kidney retention (12.5% and 37% of the administered dose in mice, respectively, compared with only 0.4% PHEA). Distribution studies showed that both conjugates mainly accumulated in the proximal tubular cells by tubular reabsorption and, thus, may be very efficient in the delivery of therapeutic agents to the proximal tubuli. The main drawback of these polymers is their poor biodegradability. Fifty-four days after intravenous administration of a high dose of the polymers, they are also observed in other parts of the nephron (128).

The highly-branched commercially available polyamidoamine (PAMAM) dendrimers and diaminobutane (DAB)-based dendrimers constitute another class of synthetic polymers that are taken up by the kidneys. PAMAM dendrimers have been used as contrast agents for magnetic resonance imaging (MRI) of the kidney (129-132). Although DAB-based dendrimers are used as liver MRI contrast agents and have been shown to accumulate in the liver, relatively high *in vivo* renal levels were found in studies performed by Kobayashi *et al.* Biodistribution studies in mice with different gadolinium (Gd (III)) radiolabeled DAB dendrimers showed that approximately 60-90% of the injected dose was retained within the kidneys per gram tissue 15 minutes after injection (130), corresponding with approximately 15-23% of the injected dose in both kidneys (111, 133). Even higher renal levels were obtained with the Gd (III) radiolabeled PAMAM dendrimers. In the same study the renal levels of generation-2, -3 and -4 (G2, G3 and G4) PAMAM dendrimers were found to be approximately 23%, 41% and 38% of the injected dose, respectively (*i.e.* 90%, 160% and 150% per gram tissue). Liver accumulation of these dendrimers was lower compared with the DAB dendrimers (130). The fact that coadministration of lysine (a competing ligand for internalizing receptors) as well as cisplatinum-induced damage of proximal tubular cells resulted in decreased renal levels of PAMAM-G4 dendrimers indicates that PAMAM dendrimers are taken up by the proximal tubuli (134, 135). *In vivo* studies with PAMAM-G5 dendrimer conjugates showed long renal residence times (*i.e.* up to 7 days) and the absence of acute or chronic toxicity (136).

3.3. Folate

In the drug delivery field folate is primarily known for its ability to target tumour cells (101, 137). The kidneys, however, also express several receptors for the transport of folate, which could be exploited for the targeting of drugs to proximal tubular cells. Mathias *et al.* evaluated the *in vivo* distribution of radiolabeled DTPA-folate conjugates in mice. The average accumulation of the investigated DTPA-folate conjugates in both kidneys was approximately 9% of the injected dose at 4 hours after intravenous administration (*i.e.* approximately 23% per gram tissue) (138). Preadministration of folic acid reduced the renal levels of the radiolabeled conjugates with approximately 90% (138). This observation, together with the rapid clearance of the DTPA-folate conjugates from FR-negative tissues, implicates the crucial role of folate receptors in the renal uptake of these conjugates (101). The same study showed that [^{99m}Tc]DTPA-folate was rapidly taken up by the kidneys, because the renal levels were already over 20% of the administered dose per gram tissue at 5 minutes post administration (138). Similar biodistribution studies in mice with [^{99m}Tc](CO)$_3$-DTPA-folate showed even higher renal levels of up to approximately 47% of the injected dose per gram tissue 4 hours after administration (139).

3.4. Antibody fragments

Since intact antibodies are not able to be filtered through the glomerulus, due to their high molecular weight of approximately 150 kDa, they cannot be used as carrier system for the delivery of therapeutic agents to the renal proximal tubuli (140). However, radiolabeled monoclonal antibody fragments investigated for cancer treatment have been shown to accumulate in renal tubuli (140-142). Although accumulation and retention of radiolabeled antibody fragments in the kidneys is an unwanted side effect of these anticancer therapeutics, the use of antibody fragments as renal carrier system may be promising. The advantage of using antibody fragments for the delivery of therapeutics into proximal tubular cells is that they can be directed against growth factor receptors involved in the disease process, such as the EGF receptor and TGF-β receptor which are localized on the basolateral as well as apical membranes of the proximal tubular cells (143, 144). Antibody-drug conjugates therefore can potentially display a dual inhibitory activity, first via blockade of the binding of natural ligands to the receptor, second via the delivered drug after internalization of the drug-antibody conjugate by the target cells.

4. Linkage technologies and drugs applied for renally targeted conjugates

For the preparation of drug-carrier conjugates the commonly applied approach is to couple the drug covalently to side chain groups of the carrier, either by direct linkage or via a linker. The characteristics of the bond between the drug and carrier system greatly influence the *in vivo* behaviour of the drug-carrier conjugate. The conjugate needs to be stable in the circulation to prevent premature loss of the free drug, *i.e.* before the carrier has been accumulated in the intended target cells. But after its accumulation, quantitative release of the drug from the carrier and regeneration of the parent drug is desired. Frequently, coupling of the drug to the carrier inactivates the drug due to modification of the drug's pharmacophore. Secondly, most drug-carrier conjugates end up within lysosomes via receptor-mediated endocytosis, which is often not the proper cellular compartment for the drug's activity. Since lysosomal membranes do not

allow further transport of macromolecules to the cytosol of the cell, release of the drug or at least its conversion to a cell-permeable metabolite is a prerequisite for successful delivery of the drug to its final pharmacological target (145, 146).

Among the linkages that may be used for the bioreversible coupling of drugs to a carrier are amide-, ester-, disulfide-, hydrazone-, carbonate-, carbamate- and coordinative bonds. Due to the high hydrolytic stability of amide bonds (145, 147, 148), the degradation of this type of linkage is dependent on the presence of hydrolytic enzymes at the target site. Lysosomes contain many proteases (*e.g.* endo- and exopeptidases) that can be exploited for this purpose (149). Lysosomal hydrolysis of the less stable ester-, carbonate- and carbamate bonds may occur either enzymatically by esterases, or can be catalyzed by the low pH (*i.e.* pH 4-5) within the lysosomes (147, 150-152). In general, carbamates are more stable than carbonates, which in turn are more hydrolytically stable than esters (145, 153). In the synthesis of drug-carrier conjugates hydrazone bonds are often used as pH sensitive linkers. Hydrazones are relative stable at physiological pH, but can be easily hydrolyzed in mild acidic environments (94). They are more sensitive for acid-catalyzed hydrolysis than ester bonds (147).

Other bioreversible linkages applied for the coupling of drugs to carrier systems are disulfide bonds (154). The intracellular concentration of gluthathione (GSH) is approximately 5 mM, favouring thiol-disulfide exchange with the coupled drug. Due to the low extracellular concentration of GSH (approximately 10 µM) disulfide bonds between drug and renal carrier are relatively stable in the circulation (94, 146).

Lastly, a relatively novel approach has been described, namely the linking of drugs to carriers via coordination chemistry. Platinum (II) can form metal-ligand coordination bonds with aromatic nitrogen atoms as an electron-rich donor group. Since these functional groups are present in many drug molecules, this type of coordination linker can be applied for the coupling of a variety of drug molecules without extensive derivatization of the drug. Coordination chemistry enables the linking of drugs that lack functionalities (*e.g.* hydroxyl, carboxylic acid or amine groups) normally used for conjugation reactions. This linker approach has been used for the preparation of drug-carrier conjugates directed to proximal tubular cells, as will be discussed below. An important characteristic of the coordinative linkage is its relative high stability despite its non-covalent nature, which enables the purification and further use of the conjugates without immediate dissociation of the conjugate into free drug and carrier. In fact, these conjugates showed a slow dissociation with a half life of several days upon administration in vivo and accumulation in the target organ (37, 40, 155).

Table 1 gives an overview of drug-carrier conjugates directed to proximal tubular cells, while **Figure 3** shows the structures of the discussed conjugates. The following paragraphs illustrate that a variety of drugs have been investigated, and that in some cases different linking approaches have been explored for the same drug.

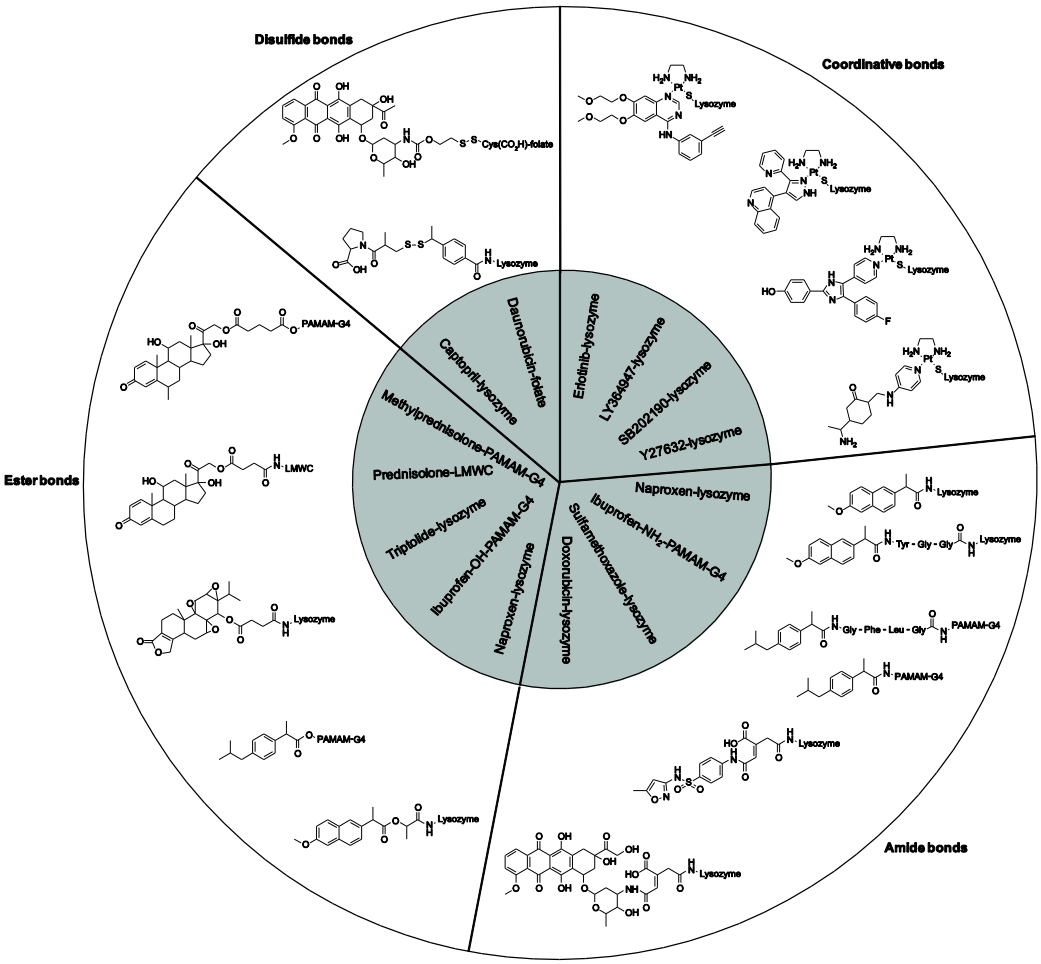

Figure 3. Chemical structures of the proximally targeted drugs and their linkage to the carrier.

4.1. Amide or ester bonds containing conjugates

One of the most extensively studied conjugates for renal drug targeting is naproxen-lysozyme. Several linking techniques have been explored for the preparation of naproxen-lysozyme conjugates, and both pharmacokinetics and efficacy of these products have been explored in animals (156-158). Initially, naproxen has been conjugated to lysozyme via direct linkage, *i.e.* via an amide bond between its carboxylic acid group and one of the lysine side chains of the proteinaceous carrier (158). It was however demonstrated that this type of naproxen-lysozyme conjugate was not enzymatically degraded into the parent drug naproxen, but yielded naproxen with one lysine residue attached to it as final metabolite. Apparently, the amide bond between the drug and the ε-amino group of lysine is not recognized as a natural peptide bond by endogenous peptidases. Fortunately, naproxen-lysine inhibited cyclooxygenase to the same extent as naproxen itself, meaning that naproxen-lysozyme was converted into an active

metabolite after its uptake in the kidney's proximal tubular cells. The *in vivo* activity of naproxen-lysozyme was evaluated in rats in which the renal prostaglandin system was activated by a low-sodium diet (159). Although naproxen-lysozyme showed a beneficial effect on prostaglandin E_2 levels, as reflected in PGE_2 excretion into the urine, the conjugate did not produce a clear effect on renal functional parameters (159).

Table 1. Drugs and linkers applied for the preparation of renally directed drug-carrier conjugates.

Drug	Conjugation to renal carrier	Drug coupling via	Reference
Naproxen	Direct coupling to lysozyme	Amide bond	*(158)*
	Coupling to lysozyme via the peptide linker tyr-gly-gly	Amide bond	*(156)*
	Coupling to lysozyme via L-lactic acid	Ester bond	
Ibuprofen	Direct coupling to NH_2-PAMAM-G4 dendrimer	Amide bond	*(160)*
	Coupling to NH_2-PAMAM-G4 dendrimer via the peptide linker gly-phe-leu-gly	Amide bond	
	Direct coupling to OH-PAMAM-G4 dendrimer	Ester bond	
Triptolide	Coupling to lysozyme via the succinate linker	Ester bond	*(107)*
Prednisolone	Coupling to 50% acetylated LMWC via the succinate linker	Ester bond	*(119)*
Methylprednisolone	Coupling to OH-PAMAM-G4 dendrimer via glutaric acid	Ester bond	*(161)*
Sulfamethoxazole	Coupling to lysozyme via *cis*-aconitic anhydride	Amide bond	*(164)*
Doxorubicin	Coupling to lysozyme via *cis*-aconitic anhydride	Amide bond	*(165)*
Captopril	Coupling to lysozyme via SMPT	Disulfide bond	*(169, 170)*
Daunorubicin	Coupling to folate via the self-immolitive disulfide-containing linker	Disulfide bond	*(172)*
SB202190	Coupling to lysozyme via the platinum (II)-based linker ULS™	Coordinative bond	*(37)*
LY364947	Coupling to lysozyme via the platinum (II)-based linker ULS™	Coordinative bond	*(34)*
Y27632	Coupling to lysozyme via the platinum (II)-based linker ULS™	Coordinative bond	*(40)*
Erlotinib	Coupling to lysozyme via the platinum (II)-based linker ULS™	Coordinative bond	*(35)*

To obtain a cleavable naproxen-lysozyme conjugate, peptide and ester linkers have been explored, with different success rates. Peptide-derivatives of naproxen did not yield enzymatically degradable conjugates, as was observed for either monopeptide linkers or even tripeptides linkers like leu-gly-gly or tyr-gly-gly (156). *In vitro* incubation of these conjugates with lysosomal enzymes yielded the naproxen-amino acid adduct as most prominent metabolite (156).

As an alternative approach for the preparation of fully cleavable naproxen-lysozyme conjugates, ester-linked derivatives were explored. Both lactic- and glycolic acid derivatives of naproxen were readily converted into the parent compound after incubation with lysosomal enzymes (156).

Other examples in which different linkages were compared for the coupling of a drug to a kidney-prone carrier are ibuprofen-PAMAM-G4 dendrimer conjugates. Kurtoglu *et al*. coupled this non-steroidal anti-inflammatory drug to either amino-terminated PAMAM dendrimers (resulting in amide-linked ibuprofen) or to hydroxyl-terminated PAMAM dendrimers (resulting in conjugates with ester-linked ibuprofen) (160). Steric hindrance of the bulky dendrimer core prevented the enzymatic release of ibuprofen from these conjugates. Insertion of a gly-phe-leu-gly tetrapeptide spacer between ibuprofen and the amino-terminated dendrimer avoided the steric hindrance, but degradation of this conjugate yielded free ibuprofen as well as ibuprofen with amino acids attached to it (160). These conjugates have only been evaluated *in vitro*, and it will be interesting to see whether future studies will indeed show preferential uptake in proximal tubular cells of the kidney, and renal-specific anti-inflammatory effects.

The homofunctional succinate linker has been used for the coupling of the anti-inflammatory drug triptolide to lysozyme and for the coupling of the corticosteroid prednisolone to 50% *N*-acetylated LMWC, both yielding ester-linked drug conjugates (107, 118). Similarly, glutaric acid was used as an ester-based linker for the coupling of methylprednisolone to hydroxyl-terminated PAMAM-G4 dendrimer (161). Khandare *et al*. used two methods for the synthesis of methylprenisolone-glutaric acid (GA)-PAMAM-G4 dendrimer conjugates, namely 1) coupling of methylprednisolone to GA-conjugated PAMAM-G4 dendrimer and 2) coupling of GA-conjugated methylprednisolone to PAMAM-G4 dendrimer (161). Although using equal molar ratios of drug to dendrimer in both syntheses, a higher drug payload was obtained with the second method. This could be explained by the fact that initial conjugation of GA to methylprednisolone resulted in a product with a higher reactivity compared with the drug itself, and that the GA spacer reduced the steric hindrance between coupled methylprednisolone groups (161).

Cis-aconitic anhydride (*cis*-Aco) is a homofunctional linker that has frequently been used for the synthesis of cancer directed doxorubicin-carrier conjugates (162, 163). The amide-bond that is formed with this type of linker is destabilized by anchimeric assistance of the neighbouring *cis*-carboxylic acid group, and hence already hydrolyses at lysosomal pH. *Cis*-Aco has been used in renal drug targeting for the conjugation of the low molecular weight drugs sulfamethoxazole and doxorubicin to lysozyme (164, 165). One of the drawbacks of *cis*-Aco is that the acid-sensitivity of the linker can get lost during the subsequent conjugation steps, either due to coupling of the carrier to the neighbouring carboxyl group instead of to the *trans*-carboxyl group, or due to *trans*-isomerisation of the linker. Alternative linkers have been developed in which the *trans*-carboxyl group has been replaced by a different functional group, which may then react via a different type of chemistry to the carrier (166-168). An example is the heterobifunctional *cis*-aconityl linker developed by Blättler *et al*. in which the *trans*-carboxyl group is replaced by a maleimidyl group that can react with thiol groups present in the carrier.

4.2. Disulfide-bond containing conjugates

SMPT (succinimidyloxycarbonyl-α-methyl-α-(2-pyridyldithio)toluene) is a disulfide based heterobifunctional linker that has been used for the coupling of the ACE inhibitor captopril to lysozyme (169, 170). The efficacy of captopril-lysozyme has been evaluated *in vivo* in rats with adriamycin-induced proteinuria fed with a high-sodium diet (108, 171). In contrast with the non-targeted free drug, which reduced the blood pressure without an effect on proteinuria, captopril-lysozyme reduced the proteinuria without systemic effects on the blood pressure (171). This study showed that captopril-lysozyme was still capable of achieving selective effects in the kidneys (171).

Disulfide bonds were also applied in a so-called self-immolative linker for folate targeted daunorubicin (172). Self-immolative linkers contain a trigger unit, or form a trigger unit upon conjugation with the carrier, which upon cleavage results in self-fragmentation of the linker and subsequent drug release (173-176). Satyam *et al.* developed a heterobifunctional self-immolative disulfide-containing linker for the synthesis of drug-folate conjugates. This linker is applicable for the conjugation of a broad range of therapeutics, *i.e.* drugs containing a primary- or secondary amino group via a carbamate bond and drugs containing a primary-, secondary- or phenolic hydroxyl group via a carbonate bond (172).

4.3. Platinum-coordinative linked conjugates

As mentioned above, drug-platinum coordination bonds display high stability as compared to other types of drug-metal coordination bonds, and this type of coordination bond has been exploited for the preparation of conjugates for renal drug targeting. Several anti-inflammatory or antifibrotic kinase inhibitors have been coupled to lysozyme via the so-called Universal Linkage System™ (ULS)™, such as the p38 MAPK inhibitor SB202190, the TGF-β receptor kinase inhibitor LY364947, the ROCK inhibitor Y27632 and the EGFR kinase inhibitor erlotinib (34, 35, 37, 40) (**Figure 4**). These kinase inhibitors have in common that they all contain aromatic nitrogens that can bind coordinatively to the platinum (II) atom in the linker. The final conjugation to lysozyme was achieved by coupling of ULS to methionine-residues introduced on the protein's surface. This novel linkage technology has several features that makes it different from other linking approaches (177). First, the reactivity of the linker with aromatic nitrogen groups creates new opportunities for synthesizing drug-carrier conjugates with drug molecules that cannot be linked easily with other strategies. Second, the release mechanism and kinetics are different, and typically yield conjugates with a slow-release profile, as will be discussed in the next section. Third, the use of platinum poses the obvious question of linker safety. Cisplatin is well-known for its toxicity to proximal tubular cells (178) and the ULS linker has great resemblance to this cytostatic drug. In this respect, the data obtained with one of the renally targeted conjugates, SB20190-ULS-lysozyme, are encouraging (37). Upon administration to rats, SB20190-ULS-lysozyme did not induce any sign of platinum-related toxicity, such as tubular cell apoptosis or body weight reduction, despite its efficient accumulation in the kidneys. A plausible explanation is that the platinum in these conjugates is already fully coordinated with rather stable ligands, and hence is less reactive towards DNA than cytostatic platinum compounds. Two representatives of this type of conjugates (LY364947-ULS-lysozyme and Y27632-ULS-lysozyme) have been evaluated in animal models of renal disease (34, 40). Both conjugates improved disease related parameters such as gene expression of fibrotic genes and influx of macrophages into the

renal interstitium. Several other conjugates are under investigation. The collective data of these studies will enable us to study the relative importance of specific pathways involved in renal fibrosis at a local renal level, rather than by systemic inhibition of the inflicted pathways.

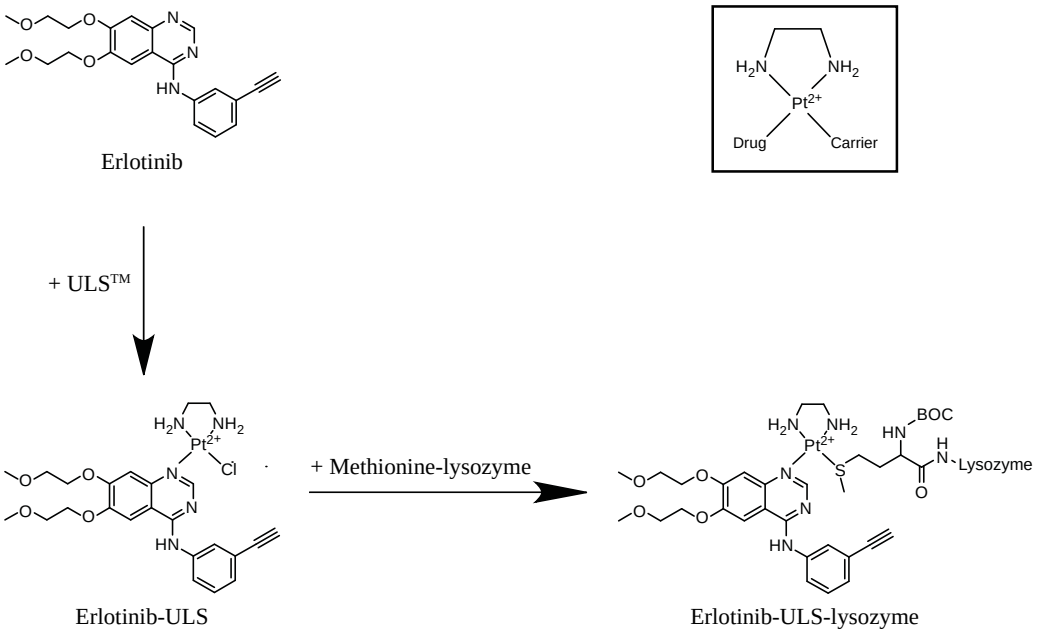

Figure 4. Synthesis scheme of erlotinib-ULS-lysozyme. The kinase inhibitor erlotinib was first coupled to the platinum-based linker ULS™. ULS formed a coordinative bond with the N^1 aromatic nitrogen of the quinazoline group of erlotinib. The erlotinib-ULS intermediate was subsequently reacted to lysozyme.

5. Cellular processing of targeted drugs by proximal tubular cells

Cell-specific drug targeting represents a promising strategy by which drugs can exert their therapeutic activity in a selective and safe manner. However, this approach remains challenging, because it relies on multiple aspects: the drug delivery system needs to distribute along the prospected route to the target tissue, it needs to be internalized by the designated target cells, and liberation of the therapeutic cargo from the carrier is required. This section will discuss the fate of delivered drugs once they have been accumulated into the proximal tubular cells. Both drug-related parameters and features of the carrier system are important at this stage of the targeted renal drug delivery process.

5.1. Lysosomal drug release into the cytosolic compartment of the proximal tubular cells

As the linker aspect of lysosomal drug release has already been addressed in the previous section, we will now only briefly address this topic. Obviously, the liberation of the drug from the carrier depends to a great extent on the nature of the drug-linker bond. The choice for a specific linkage should be made on chemical constraints of the drug and carrier system applied, but also pharmacokinetic considerations should be taken into account. Linker degradation rates

will greatly influence the final free drug levels that can be achieved in the targeted cells, as these depend on both the formation rate and the clearance rate of the active compound.
After the lysosomal release from their carrier systems, most drugs need to be transported across the lysosomal membrane into the cytosol, or even to other cellular compartments like the nucleus, to exert their effects. Transport of compounds across the lysosomal membrane may take place via passive diffusion (179). More research is needed to investigate the exact mechanisms by which drugs are able to cross the lysosomal membrane, and whether drug-specific lysosomal transporters are involved in this process. Although the exact mechanisms of lysosomal escape are unknown, indirect evidence exists that renally targeted drugs become active *in vivo*, and hence will have reached their pharmacological target. Examples hereof are the already discussed kinase inhibitor-lysozyme conjugates that have to escape from the lysosomal compartment in order to act on membrane-bound or cytosolic kinases (34, 37, 40).

5.2. Role of transporters in drug efflux from proximal tubular cells

After transport of the drug from the lysosomes into the cytosolic compartment, the intracellular residence time of the drug depends on the probability of the compound to be retained in the cells or, inversely, its capability to cross the cellular membrane of the targeted cells. Ideally, the active compound stays within the cell long enough and at sufficiently high concentrations to exert the desired effects. This can only be achieved when the drug is not immediately excreted from the target cell after reaching the cytosolic compartment.

Table 2. Localization of the drug transporters in proximal tubular cells and their primary transport direction.

	Localization in PTC	**Transport route**
Organic anion transporters (*79, 180, 181*)		
OAT1 and -3	Basolateral membrane	Blood → cell
OAT4	Apical membrane	Lumen → cell and cell → lumen
URAT1	Apical membrane	Lumen → cell
Organic anion transporting polypeptides (*79, 180*)		
OATP4C1	Basolateral membrane	Blood → cell
Multidrug resistance-associated protein (*79, 180-182*)		
MRP1, -5 and -6	Basolateral membrane	Cell → blood
MRP2 and -4	Apical mebrane	Cell → lumen
MDR1	Apical membrane	Cell → lumen
Organic cation transporters (*82, 183*)		
OCT1-3	Basolateral membrane	Blood → cell
Carnitine/organic cation transporters (*77, 81, 82*)		
OCTN1 and OCTN2	Apical membrane	Cell → lumen
MDR1/P-glycoprotein (*180, 184*)		
MDR1/ P-gp	Apical membrane	Cell → lumen
Multidrug and toxic compound extrusion transporters (*76, 82*)		
MATE1 and MATE2-K	Apical membrane	Cell → lumen
Peptide transporters (*77, 185*)		
PEPT1 and PEPT2	Apical membrane	Lumen → cell

As shown in **Table 2**, proximal tubular cells contain multiple transporters involved in the tubular reabsorption and secretion of small molecules. Many of these transporters are responsible for the transport of small molecule drugs from the tubular cells into the lumen and hence can play a role in the efflux of drugs from the target cells (79, 180, 181). Although it is not known whether these transporters play a role in the drug efflux of renally delivered drugs, this aspect should be seriously considered in the design of a drug-carrier conjugate, and potential substrates for drug efflux transporters should be avoided.

Conclusion

Drug targeting to the proximal tubular cells of the kidney is an emerging technology which can be of benefit in improving drug efficacy and safety. Within the kidney, the proximal tubular cell is an attractive target cell, because it is capable to efficiently accumulate drug carriers via receptor-mediated endocytosis. Herein, we have provided a comprehensive overview of the carriers that can be used for the intracellular delivery of drugs into the proximal tubular cells and the conjugation technologies that can be used for the coupling of drugs to these carriers. Both size and charge play crucial roles in the capability of a drug-carrier conjugate to reach the target cells. Eventually, the conjugates need to be small enough to be filtered in the glomerulus. Although the renal filtration of negatively charged carriers may be hampered by the charge-repulsion effect of the glomerular filtration barrier, negatively charged carrier systems should not be excluded as possible carriers. Carboxylated PVPs, for example, are negatively charged carriers with remarkable renal accumulation.

The linkage between the drug and carrier plays a crucial role in the *in vivo* efficacy of the drug. A proper balance between stability in the circulation and intrarenal drug release rate is required. New linker technologies render it possible to create conjugates with potent drugs that provide a continuous slow release of the drug, which may enable less frequent administration of the conjugate. However, the release rate should not be too slow to obtain therapeutic drug levels. Future studies should reveal whether such proximal tubulus-targeted therapies can be of benefit in the treatment of renal diseases such as tubulointerstitial fibrosis.

Acknowledgement

This work was made possible by a grant from the European Framework program FP6 (LSHB-CT-2007-036644).

References

1. J.A. Kellum, R. Bellomo and C. Ronco. Definition and classification of acute kidney injury. Nephron Clin Pract. 109:c182-187 (2008).
2. W. Van Biesen, R. Vanholder and N. Lameire. Defining acute renal failure: RIFLE and beyond. Clin J Am Soc Nephrol. 1:1314-1319 (2006).
3. A.S. Levey, K.U. Eckardt, Y. Tsukamoto, A. Levin, J. Coresh, J. Rossert, D. De Zeeuw, T.H. Hostetter, N. Lameire and G. Eknoyan. Definition and classification of chronic kidney disease: a position statement from Kidney Disease: Improving Global Outcomes (KDIGO). Kidney Int. 67:2089-2100 (2005).
4. B.O. Eriksen, J. Tomtum and O.C. Ingebretsen. Predictors of Declining Glomerular Filtration Rate in a Population-Based Chronic Kidney Disease Cohort. Nephron Clin Pract. 115:c41-c50 (2010).
5. E. Krol, B. Rutkowski, P. Czarniak, E. Kraszewska, S. Lizakowski, R. Szubert, S. Czekalski, W. Sulowicz and A. Wiecek. Early detection of chronic kidney disease: results of the PolNef study. Am J Nephrol. 29:264-273 (2009).
6. A. Meguid El Nahas and A.K. Bello. Chronic kidney disease: the global challenge. Lancet. 365:331-340 (2005).
7. Y. Liu. Renal fibrosis: new insights into the pathogenesis and therapeutics. Kidney Int. 69:213-217 (2006).
8. N.H. Uhlenhaut and M. Treier. Transcriptional regulators in kidney disease: gatekeepers of renal homeostasis. Trends in Genetics. 24:361-371 (2008).
9. G. Remuzzi, D. Cattaneo and N. Perico. The aggravating mechanisms of aldosterone on kidney fibrosis. J Am Soc Nephrol. 19:1459-1462 (2008).
10. M.S. Razzaque and T. Taguchi. Cellular and molecular events leading to renal tubulointerstitial fibrosis. Med Electron Microsc. 35:68-80 (2002).
11. A.A. Eddy. Molecular basis of renal fibrosis. Pediatr Nephrol. 15:290-301 (2000).
12. A.B. Fogo. Mechanisms of progression of chronic kidney disease. Pediatr Nephrol. 22:2011-2022 (2007).
13. A.A. Eddy. Serine proteases, inhibitors and receptors in renal fibrosis. Thromb Haemost. 101:656-664 (2009).
14. H.Y. Lan, W. Mu, N. Tomita, X.R. Huang, J.H. Li, H.J. Zhu, R. Morishita and R.J. Johnson. Inhibition of renal fibrosis by gene transfer of inducible Smad7 using ultrasound-microbubble system in rat UUO model. J Am Soc Nephrol. 14:1535-1548 (2003).
15. R. Misseri, R.C. Rink, D.R. Meldrum and K.K. Meldrum. Inflammatory mediators and growth factors in obstructive renal injury. J Surg Res. 119:149-159 (2004).
16. M.H. Branton and J.B. Kopp. TGF-beta and fibrosis. Microbes Infect. 1:1349-1365 (1999).
17. W.C. Burns, P. Kantharidis and M.C. Thomas. The role of tubular epithelial-mesenchymal transition in progressive kidney disease. Cells Tissues Organs. 185:222-231 (2007).
18. F.S. Shihab. Do we have a pill for renal fibrosis? Clin J Am Soc Nephrol. 2:876-878 (2007).
19. N.J. Laping. ALK5 inhibition in renal disease. Curr Opin Pharmacol. 3:204-208 (2003).
20. P. Fu, F. Liu, S. Su, W. Wang, X.R. Huang, M.L. Entman, R.J. Schwartz, L. Wei and H.Y. Lan. Signaling mechanism of renal fibrosis in unilateral ureteral obstructive kidney disease in ROCK1 knockout mice. J Am Soc Nephrol. 17:3105-3114 (2006).
21. P. Boor, K. Sebekova, T. Ostendorf and J. Floege. Treatment targets in renal fibrosis. Nephrol Dial Transplant. 22:3391-3407 (2007).
22. D. Ludewig, H. Kosmehl, M. Sommer, F.D. Bohmer and G. Stein. PDGF receptor kinase blocker AG1295 attenuates interstitial fibrosis in rat kidney after unilateral obstruction. Cell Tissue Res. 299:97-103 (2000).
23. T. Kisseleva and D.A. Brenner. Mechanisms of fibrogenesis. Exp Biol Med (Maywood). 233:109-122 (2008).
24. W.B. Melenhorst, G.M. Mulder, Q. Xi, J.G. Hoenderop, K. Kimura, S. Eguchi and H. van Goor. Epidermal growth factor receptor signaling in the kidney: key roles in physiology and disease. Hypertension. 52:987-993 (2008).
25. J.G. Gonzalez-Perez, L. Vale, S.C. Stearns and S. Wordsworth. Hemodialysis for end-stage renal disease: a cost-effectiveness analysis of treatment-options. Int J Technol Assess Health Care. 21:32-39 (2005).
26. J. Prakash, K. Poelstra, H. van Goor, F. Moolenaar, D.K.F. Meijer and R.J. Kok. Novel therapeutic targets for the treatment of tubulointerstitial fibrosis. Curr Signal Transduct Ther. 3:97-111 (2008).

27. L. Yu, N.A. Noble and W.A. Border. Therapeutic strategies to halt renal fibrosis. Curr Opin Pharmacol. 2:177-181 (2002).
28. E. Ripley. Complementary effects of angiotensin-converting enzyme inhibitors and angiotensin receptor blockers in slowing the progression of chronic kidney disease. Am Heart J. 157:S7-S16 (2009).
29. I. Guney, N.Y. Selcuk, L. Altintepe, H. Atalay, M.K. Basarali and S. Buyukbas. Antifibrotic effects of aldosterone receptor blocker (spironolactone) in patients with chronic kidney disease. Ren Fail. 31:779-784 (2009).
30. M.E. Cho and J.B. Kopp. Pirfenidone: an anti-fibrotic therapy for progressive kidney disease. Expert Opin Investig Drugs. 19:275-283 (2010).
31. M.E. Cho, D.C. Smith, M.H. Branton, S.R. Penzak and J.B. Kopp. Pirfenidone slows renal function decline in patients with focal segmental glomerulosclerosis. Clin J Am Soc Nephrol. 2:906-913 (2007).
32. Y.Y. Ng, T.P. Huang, W.C. Yang, Z.P. Chen, A.H. Yang, W. Mu, D.J. Nikolic-Paterson, R.C. Atkins and H.Y. Lan. Tubular epithelial-myofibroblast transdifferentiation in progressive tubulointerstitial fibrosis in 5/ 6 nephrectomized rats. Kidney Int. 54:864-876 (1998).
33. B. Rodriguez-Iturbe and G. Garcia Garcia. The Role of Tubulointerstitial Inflammation in the Progression of Chronic Renal Failure. Nephron Clin Pract. 116:c81-c88 (2010).
34. J. Prakash, M.H. de Borst, A.M. van Loenen-Weemaes, M. Lacombe, F. Opdam, H. van Goor, D.K. Meijer, F. Moolenaar, K. Poelstra and R.J. Kok. Cell-specific delivery of a transforming growth factor-beta type I receptor kinase inhibitor to proximal tubular cells for the treatment of renal fibrosis. Pharm Res. 25:2427-2439 (2008).
35. M.M. Fretz, M.E.M. Dolman, M. Lacombe, J. Prakash, T.Q. Nguyen, R. Goldschmeding, J. Pato, G. Storm, W.E. Hennink and R.J. Kok. Intervention in growth factor activated signaling pathways by renally targeted kinase inhibitors. J Control Release. 132:200-207 (2008).
36. F. Gellibert, A.C. de Gouville, J. Woolven, N. Mathews, V.L. Nguyen, C. Bertho-Ruault, A. Patikis, E.T. Grygielko, N.J. Laping and S. Huet. Discovery of 4-{4-[3-(pyridin-2-yl)-1H-pyrazol-4-yl]pyridin-2-yl}-N-(tetrahydro-2H- pyran-4-yl)benzamide (GW788388): a potent, selective, and orally active transforming growth factor-beta type I receptor inhibitor. J Med Chem. 49:2210-2221 (2006).
37. J. Prakash, M. Sandovici, V. Saluja, M. Lacombe, R.Q. Schaapveld, M.H. de Borst, H. van Goor, R.H. Henning, J.H. Proost, F. Moolenaar, G. Keri, D.K. Meijer, K. Poelstra and R.J. Kok. Intracellular delivery of the p38 mitogen-activated protein kinase inhibitor SB202190 [4-(4-fluorophenyl)-2-(4-hydroxyphenyl)-5-(4-pyridyl)1H-imidazole] in renal tubular cells: a novel strategy to treat renal fibrosis. J Pharmacol Exp Ther. 319:8-19 (2006).
38. M. Nishida, Y. Okumura, H. Sato and K. Hamaoka. Delayed inhibition of p38 mitogen-activated protein kinase ameliorates renal fibrosis in obstructive nephropathy. Nephrol Dial Transplant. 23:2520-2524 (2008).
39. C. Stambe, R.C. Atkins, G.H. Tesch, T. Masaki, G.F. Schreiner and D.J. Nikolic-Paterson. The role of p38alpha mitogen-activated protein kinase activation in renal fibrosis. J Am Soc Nephrol. 15:370-379 (2004).
40. J. Prakash, M.H. de Borst, M. Lacombe, F. Opdam, P.A. Klok, H. van Goor, D.K. Meijer, F. Moolenaar, K. Poelstra and R.J. Kok. Inhibition of renal rho kinase attenuates ischemia/ reperfusion-induced injury. J Am Soc Nephrol. 19:2086-2097 (2008).
41. S. Wang, M.C. Wilkes, E.B. Leof and R. Hirschberg. Imatinib mesylate blocks a non-Smad TGF-beta pathway and reduces renal fibrogenesis in vivo. Faseb J. 19:1-11 (2005).
42. G.H. Luo, Y.P. Lu, J. Song, L. Yang, Y.J. Shi and Y.P. Li. Inhibition of connective tissue growth factor by small interfering RNA prevents renal fibrosis in rats undergoing chronic allograft nephropathy. Transplant Proc. 40:2365-2369 (2008).
43. M. Hwang, H.J. Kim, H.J. Noh, Y.C. Chang, Y.M. Chae, K.H. Kim, J.P. Jeon, T.S. Lee, H.K. Oh, Y.S. Lee and K.K. Park. TGF-beta1 siRNA suppresses the tubulointerstitial fibrosis in the kidney of ureteral obstruction. Exp Mol Pathol. 81:48-54 (2006).
44. M. Murphy, N.G. Docherty, B. Griffin, J. Howlin, E. McArdle, R. McMahon, H. Schmid, M. Kretzler, A. Droguett, S. Mezzano, H.R. Brady, F. Furlong, C. Godson and F. Martin. IHG-1 amplifies TGF-beta1 signaling and is increased in renal fibrosis. J Am Soc Nephrol. 19:1672-1680 (2008).

45. Z. Xia, K. Abe, A. Furusu, M. Miyazaki, Y. Obata, Y. Tabata, T. Koji and S. Kohno. Suppression of renal tubulointerstitial fibrosis by small interfering RNA targeting heat shock protein 47. Am J Nephrol. 28:34-46 (2008).
46. T. Lammers, W.E. Hennink and G. Storm. Tumour-targeted nanomedicines: principles and practice. Br J Cancer. 99:392-397 (2008).
47. I. Brigger, C. Dubernet and P. Couvreur. Nanoparticles in cancer therapy and diagnosis. Adv Drug Deliv Rev. 54:631-651 (2002).
48. D. Peer, J.M. Karp, S. Hong, O.C. Farokhzad, R. Margalit and R. Langer. Nanocarriers as an emerging platform for cancer therapy. Nat Nanotechnol. 2:751-760 (2007).
49. O. Kaidanovich-Beilin and H. Eldar-Finkelman. Peptides targeting protein kinases: strategies and implications. Physiology (Bethesda). 21:411-418 (2006).
50. G. Loirand, P. Guerin and P. Pacaud. Rho kinases in cardiovascular physiology and pathophysiology. Circ Res. 98:322-334 (2006).
51. N. Wettschureck and S. Offermanns. Rho/ Rho-kinase mediated signaling in physiology and pathophysiology. J Mol Med. 80:629-638 (2002).
52. S.J. Harper and P. LoGrasso. Signalling for survival and death in neurones: the role of stress-activated kinases, JNK and p38. Cell Signal. 13:299-310 (2001).
53. C. Robert, J.C. Soria, A. Spatz, A. Le Cesne, D. Malka, P. Pautier, J. Wechsler, C. Lhomme, B. Escudier, V. Boige, J.P. Armand and T. Le Chevalier. Cutaneous side-effects of kinase inhibitors and blocking antibodies. Lancet Oncol. 6:491-500 (2005).
54. C.E. de Kogel and J.H. Schellens. Imatinib. Oncologist. 12:1390-1394 (2007).
55. T.F. Chu, M.A. Rupnick, R. Kerkela, S.M. Dallabrida, D. Zurakowski, L. Nguyen, K. Woulfe, E. Pravda, F. Cassiola, J. Desai, S. George, J.A. Morgan, D.M. Harris, N.S. Ismail, J.H. Chen, F.J. Schoen, A.D. Van den Abbeele, G.D. Demetri, T. Force and M.H. Chen. Cardiotoxicity associated with tyrosine kinase inhibitor sunitinib. Lancet. 370:2011-2019 (2007).
56. R. Kerkela, L. Grazette, R. Yacobi, C. Iliescu, R. Patten, C. Beahm, B. Walters, S. Shevtsov, S. Pesant, F.J. Clubb, A. Rosenzweig, R.N. Salomon, R.A. Van Etten, J. Alroy, J.B. Durand and T. Force. Cardiotoxicity of the cancer therapeutic agent imatinib mesylate. Nat Med. 12:908-916 (2006).
57. T.A. Stormark, K. Strommen, B.M. Iversen and K. Matre. Three-dimensional ultrasonography can detect the modulation of kidney volume in two-kidney, one-clip hypertensive rats. Ultrasound Med Biol. 33:1882-1888 (2007).
58. B. Kaissling, I. Hegyi, J. Loffing and M. Le Hir. Morphology of interstitial cells in the healthy kidney. Anat Embryol (Berl). 193:303-318 (1996).
59. K.V. Lemley and W. Kriz. Anatomy of the renal interstitium. Kidney Int. 39:370-381 (1991).
60. S.C. Satchell and F. Braet. Glomerular endothelial cell fenestrations: an integral component of the glomerular filtration barrier. Am J Physiol Renal Physiol. 296:F947-956 (2009).
61. R.V. Stan, M. Kubitza and G.E. Palade. PV-1 is a component of the fenestral and stomatal diaphragms in fenestrated endothelia. Proc Natl Acad Sci U S A. 96:13203-13207 (1999).
62. E.L. Bearer and L. Orci. Endothelial fenestral diaphragms: a quick-freeze, deep-etch study. J Cell Biol. 100:418-428 (1985).
63. B. Nico, E. Crivellato and D. Ribatti. The importance of electron microscopy in the study of capillary endothelial cells: an historical review. Endothelium. 14:257-264 (2007).
64. D. Alcorn, C. Maric and J. McCausland. Development of the renal interstitium. Pediatr Nephrol. 13:347-354 (1999).
65. S. Akilesh, T.B. Huber, H. Wu, G. Wang, B. Hartleben, J.B. Kopp, J.H. Miner, D.C. Roopenian, E.R. Unanue and A.S. Shaw. Podocytes use FcRn to clear IgG from the glomerular basement membrane. Proc Natl Acad Sci U S A. 105:967-972 (2008).
66. V. Levidiotis and D.A. Power. New insights into the molecular biology of the glomerular filtration barrier and associated disease. Nephrology (Carlton). 10:157-166 (2005).
67. M.J. Karnovsky. The ultrastructure of glomerular filtration. Annu Rev Med. 30:213-224 (1979).
68. E.J. Lewis and X. Xu. Abnormal glomerular permeability characteristics in diabetic nephropathy: implications for the therapeutic use of low-molecular weight heparin. Diabetes Care. 31 Suppl 2:S202-207 (2008).
69. S.R. Batsford, R. Rohrbach and A. Vogt. Size restriction in the glomerular capillary wall: importance of lamina densa. Kidney Int. 31:710-717 (1987).
70. K. Tryggvason. Unraveling the mechanisms of glomerular ultrafiltration: nephrin, a key component of the slit diaphragm. J Am Soc Nephrol. 10:2440-2445 (1999).

71. H. Pavenstadt. Roles of the podocyte in glomerular function. Am J Physiol Renal Physiol. 278:F173-179 (2000).
72. J. Reiser, W. Kriz, M. Kretzler and P. Mundel. The glomerular slit diaphragm is a modified adherens junction. J Am Soc Nephrol. 11:1-8 (2000).
73. M.L. Schipper, G. Iyer, A.L. Koh, Z. Cheng, Y. Ebenstein, A. Aharoni, S. Keren, L.A. Bentolila, J. Li, J. Rao, X. Chen, U. Banin, A.M. Wu, R. Sinclair, S. Weiss and S.S. Gambhir. Particle size, surface coating, and PEGylation influence the biodistribution of quantum dots in living mice. Small. 5:126-134 (2009).
74. Y. Takakura, R. Mahato, M. Nishikawa and M. Hashida. Control of pharmacokinetic profiles of drug-macromolecule conjugates. Adv Drug Deliv Rev. 19:377-399 (1996).
75. J.C. Atherton. Renal blood flow, glomerular filtration and plasma clearance. Anaesthesia & Intensive Care Medicine. 10:271-275 (2009).
76. T. Terada and K. Inui. Physiological and pharmacokinetic roles of H+/ organic cation antiporters (MATE/ SLC47A). Biochem Pharmacol. 75:1689-1696 (2008).
77. W. Lee and R.B. Kim. Transporters and renal drug elimination. Annu Rev Pharmacol Toxicol. 44:137-166 (2004).
78. B. Hagenbuch. Drug uptake systems in liver and kidney: a historic perspective. Clin Pharmacol Ther. 87:39-47 (2010).
79. A.A. El-Sheikh, R. Masereeuw and F.G. Russel. Mechanisms of renal anionic drug transport. Eur J Pharmacol. 585:245-255 (2008).
80. M.J. Dresser, M.K. Leabman and K.M. Giacomini. Transporters involved in the elimination of drugs in the kidney: organic anion transporters and organic cation transporters. J Pharm Sci. 90:397-421 (2001).
81. G. Ciarimboli. Organic cation transporters. Xenobiotica. 38:936-971 (2008).
82. H. Koepsell, K. Lips and C. Volk. Polyspecific organic cation transporters: structure, function, physiological roles, and biopharmaceutical implications. Pharm Res. 24:1227-1251 (2007).
83. A. Saito, H. Sato, N. Iino and T. Takeda. Molecular mechanisms of receptor-mediated endocytosis in the renal proximal tubular epithelium. J Biomed Biotechnol:403272 (2010).
84. H. Birn, O. Spiegelstein, E.I. Christensen and R.H. Finnell. Renal tubular reabsorption of folate mediated by folate binding protein 1. J Am Soc Nephrol. 16:608-615 (2005).
85. H. Birn. The kidney in vitamin B12 and folate homeostasis: characterization of receptors for tubular uptake of vitamins and carrier proteins. Am J Physiol Renal Physiol. 291:F22-36 (2006).
86. K. Suzuki, H. Susaki, S. Okuno and Y. Sugiyama. Renal drug targeting using a vector "alkylglycoside". J Pharmacol Exp Ther. 288:57-64 (1999).
87. K. Suzuki, H. Susaki, S. Okuno, H. Yamada, H.K. Watanabe and Y. Sugiyama. Specific renal delivery of sugar-modified low-molecular-weight peptides. J Pharmacol Exp Ther. 288:888-897 (1999).
88. Y.J. Lee, Y.J. Lee and H.J. Han. Regulatory mechanisms of Na(+)/ glucose cotransporters in renal proximal tubule cells. Kidney Int Suppl:S27-35 (2007).
89. I.S. Wood and P. Trayhurn. Glucose transporters (GLUT and SGLT): expanded families of sugar transport proteins. Br J Nutr. 89:3-9 (2003).
90. S.K. Moestrup and P.J. Verroust. Megalin- and cubilin-mediated endocytosis of protein-bound vitamins, lipids, and hormones in polarized epithelia. Annu Rev Nutr. 21:407-428 (2001).
91. E.I. Christensen, P.J. Verroust and R. Nielsen. Receptor-mediated endocytosis in renal proximal tubule. Pflugers Arch. 458:1039-1048 (2009).
92. E.I. Christensen and H. Birn. Megalin and cubilin: multifunctional endocytic receptors. Nat Rev Mol Cell Biol. 3:256-266 (2002).
93. P.J. Verroust and E.I. Christensen. Megalin and cubilin--the story of two multipurpose receptors unfolds. Nephrol Dial Transplant. 17:1867-1871 (2002).
94. K.R. West and S. Otto. Reversible covalent chemistry in drug delivery. Curr Drug Discov Technol. 2:123-160 (2005).
95. C. Lebeau, F.D. Debelle, V.M. Arlt, A. Pozdzik, E.G. De Prez, D.H. Phillips, M.M. Deschodt-Lanckman, J.L. Vanherweghem and J.L. Nortier. Early proximal tubule injury in experimental aristolochic acid nephropathy: functional and histological studies. Nephrol Dial Transplant. 20:2321-2332 (2005).

96. J.R. Leheste, B. Rolinski, H. Vorum, J. Hilpert, A. Nykjaer, C. Jacobsen, P. Aucouturier, J.O. Moskaug, A. Otto, E.I. Christensen and T.E. Willnow. Megalin knockout mice as an animal model of low molecular weight proteinuria. Am J Pathol. 155:1361-1370 (1999).
97. R.M. Sandoval, M.D. Kennedy, P.S. Low and B.A. Molitoris. Uptake and trafficking of fluorescent conjugates of folic acid in intact kidney determined using intravital two-photon microscopy. Am J Physiol Cell Physiol. 287:C517-526 (2004).
98. A. Hamid and J. Kaur. Decreased expression of transporters reduces folate uptake across renal absorptive surfaces in experimental alcoholism. J Membr Biol. 220:69-77 (2007).
99. J.F. Collins. Novel insights into intestinal and renal folate transport. Focus on "Apical membrane targeting and trafficking of the human proton-coupled folate transporter in polarized epithelia". Am J Physiol Cell Physiol. 294:C381-382 (2008).
100. A.R. Hilgenbrink and P.S. Low. Folate receptor-mediated drug targeting: from therapeutics to diagnostics. J Pharm Sci. 94:2135-2146 (2005).
101. P.S. Low and S.A. Kularatne. Folate-targeted therapeutic and imaging agents for cancer. Curr Opin Chem Biol. 13:256-262 (2009).
102. J. Sudimack and R.J. Lee. Targeted drug delivery via the folate receptor. Adv Drug Deliv Rev. 41:147-162 (2000).
103. Y. Lu and P.S. Low. Folate-mediated delivery of macromolecular anticancer therapeutic agents. Adv Drug Deliv Rev. 54:675-693 (2002).
104. M.D. Salazar and M. Ratnam. The folate receptor: what does it promise in tissue-targeted therapeutics? Cancer Metastasis Rev. 26:141-152 (2007).
105. S. Sabharanjak and S. Mayor. Folate receptor endocytosis and trafficking. Adv Drug Deliv Rev. 56:1099-1109 (2004).
106. C. Cojocel and K. Baumann. Renal handling of endogenous lysozyme in the rat. Ren Physiol. 6:258-265 (1983).
107. Z. Zhang, Q. Zheng, J. Han, G. Gao, J. Liu, T. Gong, Z. Gu, Y. Huang, X. Sun and Q. He. The targeting of 14-succinate triptolide-lysozyme conjugate to proximal renal tubular epithelial cells. Biomaterials. 30:1372-1381 (2009).
108. J. Prakash, A.M. van Loenen-Weemaes, M. Haas, J.H. Proost, D.K. Meijer, F. Moolenaar, K. Poelstra and R.J. Kok. Renal-selective delivery and angiotensin-converting enzyme inhibition by subcutaneously administered captopril-lysozyme. Drug Metab Dispos. 33:683-688 (2005).
109. B. Schechter, R. Arnon, C. Colas, T. Burakova and M. Wilchek. Renal accumulation of streptavidin: potential use for targeted therapy to the kidney. Kidney Int. 47:1327-1335 (1995).
110. K. Rudolphi, N. Gerwin, N. Verzijl, P. van der Kraan and W. van den Berg. Pralnacasan, an inhibitor of interleukin-1beta converting enzyme, reduces joint damage in two murine models of osteoarthritis. Osteoarthritis Cartilage. 11:738-746 (2003).
111. V.M. Vasandani, Y.N. Wu, S.M. Mikulski, R.J. Youle and C. Sung. Molecular determinants in the plasma clearance and tissue distribution of ribonucleases of the ribonuclease A superfamily. Cancer Res. 56:4180-4186 (1996).
112. E.S.R. de Cassia da Silveira and M. de Oliveira Guerra. Reproductive toxicity of lapachol in adult male Wistar rats submitted to short-term treatment. Phytother Res. 21:658-662 (2007).
113. E. Vegt, J.E. van Eerd, A. Eek, W.J. Oyen, J.F. Wetzels, M. de Jong, F.G. Russel, R. Masereeuw, M. Gotthardt and O.C. Boerman. Reducing renal uptake of radiolabeled peptides using albumin fragments. J Nucl Med. 49:1506-1511 (2008).
114. M. Gotthardt, J. van Eerd-Vismale, W.J. Oyen, M. de Jong, H. Zhang, E. Rolleman, H.R. Maecke, M. Behe and O. Boerman. Indication for different mechanisms of kidney uptake of radiolabeled peptides. J Nucl Med. 48:596-601 (2007).
115. H. Kodaira, Y. Tsutsumi, Y. Yoshioka, H. Kamada, Y. Kaneda, Y. Yamamoto, S. Tsunoda, T. Okamoto, Y. Mukai, H. Shibata, S. Nakagawa and T. Mayumi. The targeting of anionized polyvinylpyrrolidone to the renal system. Biomaterials. 25:4309-4315 (2004).
116. H. Kamada, Y. Tsutsumi, K. Sato-Kamada, Y. Yamamoto, Y. Yoshioka, T. Okamoto, S. Nakagawa, S. Nagata and T. Mayumi. Synthesis of a poly(vinylpyrrolidone-co-dimethyl maleic anhydride) co-polymer and its application for renal drug targeting. Nat Biotechnol. 21:399-404 (2003).
117. Y. Yamamoto, Y. Tsutsumi, Y. Yoshioka, H. Kamada, K. Sato-Kamada, T. Okamoto, Y. Mukai, H. Shibata, S. Nakagawa and T. Mayumi. Poly(vinylpyrrolidone-co-dimethyl maleic acid) as a novel renal targeting carrier. J Control Release. 95:229-237 (2004).

118. Z.X. Yuan, X. Sun, T. Gong, H. Ding, Y. Fu and Z.R. Zhang. Randomly 50% N-acetylated low molecular weight chitosan as a novel renal targeting carrier. J Drug Target. 15:269-278 (2007).
119. Z.X. Yuan, Z.R. Zhang, D. Zhu, X. Sun, T. Gong, J. Liu and C.T. Luan. Specific renal uptake of randomly 50% N-acetylated low molecular weight chitosan. Mol Pharm. 6:305-314 (2009).
120. T. Kean and M. Thanou. Biodegradation, biodistribution and toxicity of chitosan. Adv Drug Deliv Rev. 62:3-11 (2010).
121. Y. Noguchi, J. Wu, R. Duncan, J. Strohalm, K. Ulbrich, T. Akaike and H. Maeda. Early phase tumor accumulation of macromolecules: a great difference in clearance rate between tumor and normal tissues. Jpn J Cancer Res. 89:307-314 (1998).
122. D.B. Pike and H. Ghandehari. HPMA copolymer-cyclic RGD conjugates for tumor targeting. Adv Drug Deliv Rev (2009).
123. M.P. Borgman, O. Aras, S. Geyser-Stoops, E.A. Sausville and H. Ghandehari. Biodistribution of HPMA copolymer-aminohexylgeldanamycin-RGDfK conjugates for prostate cancer drug delivery. Mol Pharm. 6:1836-1847 (2009).
124. Y. Wang, F. Ye, E.K. Jeong, Y. Sun, D.L. Parker and Z.R. Lu. Noninvasive visualization of pharmacokinetics, biodistribution and tumor targeting of poly[N-(2-hydroxypropyl)methacrylamide] in mice using contrast enhanced MRI. Pharm Res. 24:1208-1216 (2007).
125. M. Kissel, P. Peschke, V. Subr, K. Ulbrich, A.M. Strunz, R. Kuhnlein, J. Debus and E. Friedrich. Detection and cellular localisation of the synthetic soluble macromolecular drug carrier pHPMA. Eur J Nucl Med Mol Imaging. 29:1055-1062 (2002).
126. A. Mitra, A. Nan, H. Ghandehari, E. McNeill, J. Mulholland and B.R. Line. Technetium-99m-Labeled N-(2-hydroxypropyl) methacrylamide copolymers: synthesis, characterization, and in vivo biodistribution. Pharm Res. 21:1153-1159 (2004).
127. M.P. Borgman, T. Coleman, R.B. Kolhatkar, S. Geyser-Stoops, B.R. Line and H. Ghandehari. Tumor-targeted HPMA copolymer-(RGDfK)-(CHX-A''-DTPA) conjugates show increased kidney accumulation. J Control Release. 132:193-199 (2008).
128. F. Rypacek, J. Drobnik, V. Chmelar and J. Kalal. The renal excretion and retention of macromolecules: The chemical structure effect. Pflugers Arch. 392:211-217 (1982).
129. H. Kobayashi, N. Sato, S. Kawamoto, T. Saga, A. Hiraga, T. Ishimori, J. Konishi, K. Togashi and M.W. Brechbiel. Novel intravascular macromolecular MRI contrast agent with generation-4 polyamidoamine dendrimer core: accelerated renal excretion with coinjection of lysine. Magn Reson Med. 46:457-464 (2001).
130. H. Kobayashi, S. Kawamoto, S.K. Jo, H.L. Bryant, Jr., M.W. Brechbiel and R.A. Star. Macromolecular MRI contrast agents with small dendrimers: pharmacokinetic differences between sizes and cores. Bioconjug Chem. 14:388-394 (2003).
131. H. Kobayashi, N. Sato, T. Saga, Y. Nakamoto, T. Ishimori, S. Toyama, K. Togashi, J. Konishi and M.W. Brechbiel. Monoclonal antibody-dendrimer conjugates enable radiolabeling of antibody with markedly high specific activity with minimal loss of immunoreactivity. Eur J Nucl Med. 27:1334-1339 (2000).
132. J.D. Eichman, A.U. Bielinska, J.F. Kukowska-Latallo and J.R. Baker, Jr. The use of PAMAM dendrimers in the efficient transfer of genetic material into cells. Pharm Sci Technolo Today. 3:232-245 (2000).
133. T. Kotoh, D.K. Dhar, R. Masunaga, H. Tabara, M. Tachibana, H. Kubota, H. Kohno and N. Nagasue. Antiangiogenic therapy of human esophageal cancers with thalidomide in nude mice. Surgery. 125:536-544 (1999).
134. H. Kobayashi, S. Kawamoto, S.K. Jo, N. Sato, T. Saga, A. Hiraga, J. Konishi, S. Hu, K. Togashi, M.W. Brechbiel and R.A. Star. Renal tubular damage detected by dynamic micro-MRI with a dendrimer-based magnetic resonance contrast agent. Kidney Int. 61:1980-1985 (2002).
135. H. Kobayashi, S.K. Jo, S. Kawamoto, H. Yasuda, X. Hu, M.V. Knopp, M.W. Brechbiel, P.L. Choyke and R.A. Star. Polyamine dendrimer-based MRI contrast agents for functional kidney imaging to diagnose acute renal failure. J Magn Reson Imaging. 20:512-518 (2004).
136. J.F. Kukowska-Latallo, K.A. Candido, Z. Cao, S.S. Nigavekar, I.J. Majoros, T.P. Thomas, L.P. Balogh, M.K. Khan and J.R. Baker, Jr. Nanoparticle targeting of anticancer drug improves therapeutic response in animal model of human epithelial cancer. Cancer Res. 65:5317-5324 (2005).

137. E.Q. Song, Z.L. Zhang, Q.Y. Luo, W. Lu, Y.B. Shi and D.W. Pang. Tumor cell targeting using folate-conjugated fluorescent quantum dots and receptor-mediated endocytosis. Clin Chem. 55:955-963 (2009).
138. C.J. Mathias, D. Hubers, P.S. Low and M.A. Green. Synthesis of [(99m)Tc]DTPA-folate and its evaluation as a folate-receptor-targeted radiopharmaceutical. Bioconjug Chem. 11:253-257 (2000).
139. D.P. Trump, C.J. Mathias, Z. Yang, P.S. Low, M. Marmion and M.A. Green. Synthesis and evaluation of 99mTc(CO)(3)-DTPA-folate as a folate-receptor-targeted radiopharmaceutical. Nucl Med Biol. 29:569-573 (2002).
140. H. Akizawa, T. Uehara and Y. Arano. Renal uptake and metabolism of radiopharmaceuticals derived from peptides and proteins. Adv Drug Deliv Rev. 60:1319-1328 (2008).
141. J. Grunberg, I. Novak-Hofer, M. Honer, K. Zimmermann, K. Knogler, P. Blauenstein, S. Ametamey, H.R. Maecke and P.A. Schubiger. In vivo evaluation of 177Lu- and 67/ 64Cu-labeled recombinant fragments of antibody chCE7 for radioimmunotherapy and PET imaging of L1-CAM-positive tumors. Clin Cancer Res. 11:5112-5120 (2005).
142. T.M. Behr, W.S. Becker, R.M. Sharkey, M.E. Juweid, R.M. Dunn, H.J. Bair, F.G. Wolf and D.M. Goldenberg. Reduction of renal uptake of monoclonal antibody fragments by amino acid infusion. J Nucl Med. 37:829-833 (1996).
143. R.J. Baines and N.J. Brunskill. The molecular interactions between filtered proteins and proximal tubular cells in proteinuria. Nephron Exp Nephrol. 110:e67-71 (2008).
144. S.N. Wang, J. Lapage and R. Hirschberg. Glomerular ultrafiltration and apical tubular action of IGF-I, TGF-beta, and HGF in nephrotic syndrome. Kidney Int. 56:1247-1251 (1999).
145. L.Y. Qiu and Y.H. Bae. Polymer architecture and drug delivery. Pharm Res. 23:1-30 (2006).
146. G. Saito, J.A. Swanson and K.-D. Lee. Drug delivery strategy utilizing conjugation via reversible disulfide linkages: role and site of cellular reducing activities. Advanced Drug Delivery Reviews. 55:199-215 (2003).
147. Y.E. Kurtoglu, R.S. Navath, B. Wang, S. Kannan, R. Romero and R.M. Kannan. Poly(amidoamine) dendrimer-drug conjugates with disulfide linkages for intracellular drug delivery. Biomaterials. 30:2112-2121 (2009).
148. H. Soyez, E. Schacht and S. Vanderkerken. The crucial role of spacer groups in macromolecular prodrug design. Advanced Drug Delivery Reviews. 21:81-106 (1996).
149. P. Bohley and P.O. Seglen. Proteases and proteolysis in the lysosome. Experientia. 48:151-157 (1992).
150. H. Huang, C. Ma, M. Yang, C. Tang and H. Wang. Adrenomedullin impairs the profibrotic effects of transforming growth factor-beta1 through recruiting Smad6 protein in human renal tubular cells. Cell Physiol Biochem. 15:117-124 (2005).
151. M.A. Sogorb and E. Vilanova. Enzymes involved in the detoxification of organophosphorus, carbamate and pyrethroid insecticides through hydrolysis. Toxicol Lett. 128:215-228 (2002).
152. R. Duncan, M.J. Vicent, F. Greco and R.I. Nicholson. Polymer-drug conjugates: towards a novel approach for the treatment of endrocine-related cancer. Endocr Relat Cancer. 12 Suppl 1:S189-199 (2005).
153. E. Carvalho, A.P. Francisco, J. Iley and E. Rosa. Triazene drug metabolites. Part 17: Synthesis and plasma hydrolysis of acyloxymethyl carbamate derivatives of antitumour triazenes. Bioorg Med Chem. 8:1719-1725 (2000).
154. F. Meng, W.E. Hennink and Z. Zhong. Reduction-sensitive polymers and bioconjugates for biomedical applications. Biomaterials. 30:2180-2198 (2009).
155. M.E.M. Dolman, M.M. Fretz, G.J. Segers, M. Lacombe, J. Prakash, G. Storm, W.E. Hennink and R.J. Kok. Renal targeting of kinase inhibitors. Int J Pharm. 364:249-257 (2008).
156. E.J. Franssen, J. Koiter, C.A. Kuipers, A.P. Bruins, F. Moolenaar, D. de Zeeuw, W.H. Kruizinga, R.M. Kellogg and D.K. Meijer. Low molecular weight proteins as carriers for renal drug targeting. Preparation of drug-protein conjugates and drug-spacer derivatives and their catabolism in renal cortex homogenates and lysosomal lysates. J Med Chem. 35:1246-1259 (1992).
157. E.J. Franssen, F. Moolenaar, D. de Zeeuw and D.K. Meijer. Low molecular weight proteins as carriers for renal drug targeting: naproxen coupled to lysozyme via the spacer L-lactic acid. Pharm Res. 10:963-969 (1993).
158. M. Haas, A.C. Kluppel, E.S. Wartna, F. Moolenaar, D.K. Meijer, P.E. de Jong and D. de Zeeuw. Drug-targeting to the kidney: renal delivery and degradation of a naproxen-lysozyme conjugate in vivo. Kidney Int. 52:1693-1699 (1997).

159. M. Haas, F. Moolenaar, D.K. Meijer, P.E. de Jong and D. de Zeeuw. Renal targeting of a non-steroidal anti-inflammatory drug: effects on renal prostaglandin synthesis in the rat. Clin Sci (Lond). 95:603-609 (1998).
160. Y.E. Kurtoglu, M.K. Mishra, S. Kannan and R.M. Kannan. Drug release characteristics of PAMAM dendrimer-drug conjugates with different linkers. Int J Pharm. 384:189-194 (2010).
161. J. Khandare, P. Kolhe, O. Pillai, S. Kannan, M. Lieh-Lai and R.M. Kannan. Synthesis, cellular transport, and activity of polyamidoamine dendrimer-methylprednisolone conjugates. Bioconjug Chem. 16:330-337 (2005).
162. K. Ulbrich, T. Etrych, P. Chytil, M. Jelinkova and B. Rihova. HPMA copolymers with pH-controlled release of doxorubicin: in vitro cytotoxicity and in vivo antitumor activity. J Control Release. 87:33-47 (2003).
163. K. Ulbrich and V. Subr. Polymeric anticancer drugs with pH-controlled activation. Adv Drug Deliv Rev. 56:1023-1050 (2004).
164. E.J.F. Franssen, F. Moolenaar, D. de Zeeuw and D.K.F. Meijer. Renal specific delivery of sulfamethoxazole in the rat by coupling to the low molecular weight protein lysozyme via an acid-sensitive linker. International Journal of Pharmaceutics. 80:R15-R19 (1992).
165. M. Haas, F. Moolenaar, A. Elsinga, E.A. Van der Wouden, P.E. de Jong, D.K. Meijer and D. de Zeeuw. Targeting of doxorubicin to the urinary bladder of the rat shows increased cytotoxicity in the bladder urine combined with an absence of renal toxicity. J Drug Target. 10:81-89 (2002).
166. M.C. Garnett. Targeted drug conjugates: principles and progress. Adv Drug Deliv Rev. 53:171-216 (2001).
167. W.A. Blattler, B.S. Kuenzi, J.M. Lambert and P.D. Senter. New heterobifunctional protein cross-linking reagent that forms an acid-labile link. Biochemistry. 24:1517-1524 (1985).
168. G.D. McIntyre, C.F. Scott, J. Ritz, W.A. Blattler and J.M. Lambert. Preparation and characterization of interleukin-2-gelonin conjugates made using different crosslinking reagents. Bioconjugate Chemistry. 5:88-97 (1994).
169. R.J. Kok, F. Grijpstra, R.B. Walthuis, F. Moolenaar, D. de Zeeuw and D.K. Meijer. Specific delivery of captopril to the kidney with the prodrug captopril-lysozyme. J Pharmacol Exp Ther. 288:281-285 (1999).
170. R.J. Kok, R.F. Haverdings, F. Grijpstra, J. Koiter, F. Moolenaar, D. de Zeeuw and D.K. Meijer. Targeting of captopril to the kidney reduces renal angiotensin-converting enzyme activity without affecting systemic blood pressure. J Pharmacol Exp Ther. 301:1139-1143 (2002).
171. W.A. Windt, J. Prakash, R.J. Kok, F. Moolenaar, C.A. Kluppel, D. de Zeeuw, R.P. van Dokkum and R.H. Henning. Renal targeting of captopril using captopril-lysozyme conjugate enhances its antiproteinuric effect in adriamycin-induced nephrosis. J Renin Angiotensin Aldosterone Syst. 5:197-202 (2004).
172. A. Satyam. Design and synthesis of releasable folate-drug conjugates using a novel heterobifunctional disulfide-containing linker. Bioorg Med Chem Lett. 18:3196-3199 (2008).
173. Y. Meyer, J.-A. Richard, B. Delest, P. Noack, P.-Y. Renard and A. Romieu. A comparative study of the self-immolation of para-aminobenzylalcohol and hemithioaminal-based linkers in the context of protease-sensitive fluorogenic probes. Organic & Biomolecular Chemistry. 8:1777-1780 (2010).
174. I. Ojima. Guided molecular missiles for tumor-targeting chemotherapy--case studies using the second-generation taxoids as warheads. Acc Chem Res. 41:108-119 (2008).
175. A. Gopin, C. Rader and D. Shabat. New chemical adaptor unit designed to release a drug from a tumor targeting device by enzymatic triggering. Bioorg Med Chem. 12:1853-1858 (2004).
176. D. Shabat, R.J. Amir, A. Gopin, N. Pessah and M. Shamis. Chemical adaptor systems. Chemistry. 10:2626-2634 (2004).
177. K. Temming, M.M. Fretz and R.J. Kok. Organ- and cell-type specific delivery of kinase inhibitors: a novel approach in the development of targeted drugs. Curr Mol Pharmacol. 1:1-12 (2008).
178. D. Sheikh-Hamad, K. Timmins and Z. Jalali. Cisplatin-induced renal toxicity: possible reversal by N-acetylcysteine treatment. J Am Soc Nephrol. 8:1640-1644 (1997).
179. J.B. Lloyd. Lysosome membrane permeability: implications for drug delivery. Adv Drug Deliv Rev. 41:189-200 (2000).
180. M. Li, G.D. Anderson and J. Wang. Drug-drug interactions involving membrane transporters in the human kidney. Expert Opin Drug Metab Toxicol. 2:505-532 (2006).
181. T. Sekine, H. Miyazaki and H. Endou. Molecular physiology of renal organic anion transporters. Am J Physiol Renal Physiol. 290:F251-261 (2006).

182. M.V. Varma, B. Feng, R.S. Obach, M.D. Troutman, J. Chupka, H.R. Miller and A. El-Kattan. Physicochemical determinants of human renal clearance. J Med Chem. 52:4844-4852 (2009).
183. S.H. Wright. Role of organic cation transporters in the renal handling of therapeutic agents and xenobiotics. Toxicol Appl Pharmacol. 204:309-319 (2005).
184. V. Launay-Vacher, H. Izzedine, S. Karie, J.S. Hulot, A. Baumelou and G. Deray. Renal tubular drug transporters. Nephron Physiol. 103:p97-106 (2006).
185. I. Rubio-Aliaga and H. Daniel. Peptide transporters and their roles in physiological processes and drug disposition. Xenobiotica. 38:1022-1042 (2008).

Chapter 3

Intervention in growth factor activated signaling pathways by renally targeted kinase inhibitors

M.M. Fretz[1], M.E.M. Dolman[1], M. Lacombe[2], J. Prakash[3], T.Q. Nguyen[4], R. Goldschmeding[4], J. Pató[5], G. Storm[1], W.E. Hennink[1], and R.J. Kok[1]

[1] Department of Pharmaceutics, Utrecht Institute of Pharmaceutical Sciences, Utrecht University, Utrecht, The Netherlands

[2] KREATECH Biotechnology B.V., Amsterdam, The Netherlands

[3] Department of Pharmacokinetics and Drug Delivery, University Center for Pharmacy, University of Groningen, Groningen, The Netherlands

[4] Department of Pathology, University Medical Centre Utrecht, Utrecht, The Netherlands

[5] Vichem Chemie, Budapest, Hungary

Journal of Controlled Release 132:200-207 (2008)

Abstract

Cell-specific targeting to renal tubular cells is an interesting approach to enhance the accumulation of drugs in the kidney. Low molecular weight proteins are rapidly filtered and extensively accumulate in proximal tubular cells. We therefore have used lysozyme (LZM, 14 kDa) as a tubular cell-specific carrier for the delivery of kinase inhibitors. Two different kinase inhibitors (LY364947 and erlotinib, directed to either the TGF-β receptor kinase or the EGF receptor kinase) were individually conjugated to LZM via a novel platinum (II)-based linker (Universal Linkage System; ULS). The cellular handling and pharmacological efficacy of the conjugates were evaluated in cultured proximal tubular cells (HK-2 cells). Both conjugates were efficiently internalized via endocytosis. TGF-β or EGF activated HK-2 cells showed a strong activation of the studied kinases and the conjugates inhibited these events, as was demonstrated by Western blotting of phosphorylated downstream mediators and quantitative gene expression analysis. In conclusion, we have developed tubular cell specific kinase inhibitor-LZM conjugates via a novel linker strategy, which both showed to be effective *in vitro*. Future *in vivo* studies should show their potential for the treatment of renal diseases.

1. Introduction

Growth factors play an important role in inflammatory and fibrogenic processes. Transforming growth factor beta (TGF-β) is a key regulator of the formation of extracellular matrix (ECM) and differentiation of tubular epithelial cells into (myo)fibroblasts (1). Epidermal growth factor (EGF) modulates fibrotic responses and plays a role in dedifferentiation and redifferentiation of tubular epithelial cells (2). Activation of EGF receptors by TGF-α, another ligand for this class of receptors, has been associated with the formation of renal fibrotic lesions (3). Obviously, the above reported studies only illustrate the importance of the listed growth factors. Several other growth factors play a pivotal role in fibrotic responses (4), and additive or synergistic responses between different mediators have been reported (5). Kinase inhibitors have been approved clinically for cancer only, but preclinical studies demonstrate their potential benefit in the treatment of many other diseases, such as renal fibrosis (6). In this paper, we have used the kinase inhibitors erlotinib (Tarceva®), which is an inhibitor of the EGF receptor kinase and well-known for its anti-proliferative actions in cancer (7), and LY364947, an experimental inhibitor of the TGF-β receptor kinase, also known as activin-like kinase 5 (ALK5). **Figure 1** schematically depicts the pathways and inhibitors investigated in this study.

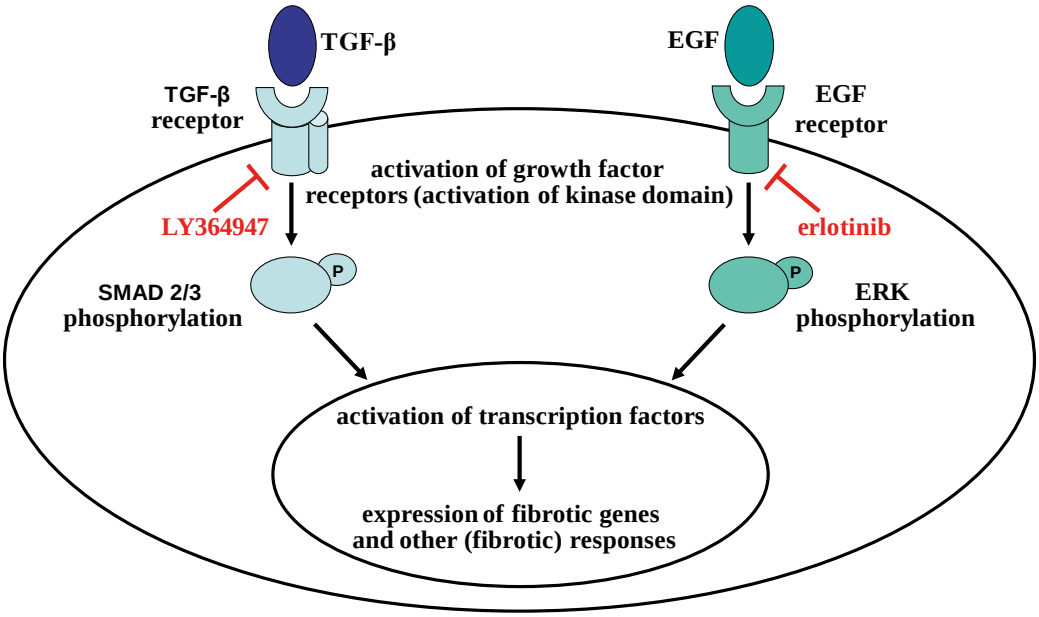

Figure 1. TGF-β and EGF mediated signal transduction pathways. Binding of TGF-β to the TGF-β receptor I leads to phosphorylation of Smad proteins which, when translocated to the nucleus, trigger the transcription of fibrosis related genes. LY364947 blocks the kinase domain of the TGF-β receptor I and thereby inhibits the downstream phosphorylation of Smads. EGF binds the EGF receptor which activates (among others) the extracellular-signal regulated kinase (ERK) pathway. The initial step in this cascade is the autophosphorylation of the EGF receptor, which is inhibited by erlotinib. Activation of both pathways ultimately results in (enhanced) transcription of inflammatory and profibrotic genes, like fibronectin, PAI-I, CTGF and procollagen 1α1.

Although kinase inhibitors are considered relatively safe therapeutics with a mild toxicity profile, their clinical use can result in a variety of adverse effects, as is becoming more and more evident from clinical studies (8). New and sometimes unexpected toxicities such as skin reactions and vascular toxicities occur in a dose-dependent manner, suggesting a direct relationship to the pharmacological activity of the compounds, *i.e.* the inhibition of the targeted kinase. Cell-specific drug targeting is a novel approach to improve the therapeutic profile of such compounds (9). Kinase inhibitors are lipophilic or amphiphilic compounds like most small molecule drugs, and will enter diseased and non-diseased cells alike. The targeted delivery of kinase inhibitors to a specific cell type will improve their therapeutic profile by preventing their entry into normal, non-target tissues, and will enhance their accumulation and hence their activity in the targeted cell type.

The cellular targeted conjugates we presently describe are composed of kinase inhibitors and the renal-specific carrier lysozyme. The low molecular weight protein lysozyme (14.3 kDa) is freely filtered from the circulation by the kidneys and efficiently reabsorbed by proximal tubular cells (10). Proteins are virtually absent in the finally excreted urine of healthy subjects, which illustrates the efficiency of this reabsorption process. Protein reabsorption by proximal tubular cells is mediated via the megalin receptor, one of the most abundantly expressed proteins in the renal cortex (11). Upon receptor-mediated endocytosis via clathrin-coated pits (12), reabsorbed proteins are degraded in the lysosomal compartment of proximal tubular cells. This will also be the fate of kinase inhibitor-lysozyme conjugates.

The kinase inhibitor-lysozyme conjugates with erlotinib and with LY364947 were prepared by linking the kinase inhibitors via a recently developed platinum (II)-based linker named the Universal Linkage System (ULS)™. This linker can form coordinate linkages with aromatic nitrogens in the kinase inhibitors, and can also react to methionine residues in the lysozyme carrier. We have characterized the conjugates and have studied their cellular handling by cultured proximal tubular cells (HK-2 cells). Lastly, we have studied the capability of erlotinib-ULS-lysozyme and LY364947-ULS-lysozyme to inhibit the responses to EGF and TGF in cultured proximal tubular cells.

2. Materials and methods

2.1. Materials

DRAQ5 nuclear dye was purchased from Biostatus (Shepshed, UK). Alexa568-phalloidin and goat anti-rabbit IgG antibody conjugated to Alexa488 were obtained from Invitrogen (Paisley, UK). Polyclonal rabbit anti-lysozyme IgG was obtained from Chemicon (Temecula, CA, USA). Antibodies for Western Blotting included rabbit anti-phospho-Smad2, rabbit anti-phospho-EGF receptor (Tyr1068), rabbit anti-β-actin and goat anti-rabbit IgG, HRP-linked antibodies (Cell Signaling Technology, Danvers, MA, USA). Human recombinant TGF-β1 and EGF were purchased from R&D Systems (Oxon, UK). The ALK5 inhibitor LY364947, (4-[3-(2-pyridinyl)-1H-pyrazol-4-yl]-quinoline, ALK5 Inhibitor I) was purchased from Calbiochem (Darmstadt, Germany). Erlotinib, *N*-(3-ethynylphenyl)-6,7-bis(2-methoxyethoxy)quinazolin-4-amine) was synthesized by Vichem Chemie (Budapest, Hungary). Chicken egg white lysozyme (LZM) was obtained from Sigma (St. Louis, USA). *N*-Boc-L-methionine *N*-hydroxysuccinimide and KSCN were purchased from Fluka (Buchs, Switserland). Sodium dithiocarbamate was obtained from Merck (Darmstadt, Germany).

2.2. Synthesis of kinase inhibitor-lysozyme conjugates

LY364947 was conjugated to lysozyme by platinum coordination chemistry as described before (13). In brief, the kinase inhibitor was reacted with an equimolar amount of the linker *cis*-Pt(ethylenediamine)nitrate-chloride (Universal Linkage System, ULS™, Kreatech, Amsterdam, The Netherlands) overnight at 37 °C. ^{195}Pt-NMR and mass spectrometry demonstrated complete conversion of the starting drug into the 1:1 molar drug-ULS adduct. LY364947-ULS was subsequently conjugated to lysozyme which had been derivatized with surface-exposed methionyl groups. Chicken egg-white lysozyme (LZM) was treated with a three-fold molar excess of *N*-Boc-L-methionine *N*-hydroxysuccinimide at pH 7.4 (PBS), extensively dialyzed and freeze-dried. Ion-spray mass spectrometry revealed an average of 3 introduced methionyl groups per protein. The final LY364947-ULS-LZM conjugate was prepared by reacting 4 molar equivalents of LY364947-ULS with methionine-LZM overnight at 37 °C in a 10 mM tricine/ nitrate pH 8.5 buffer. The resulting product was purified by dialysis against PBS at 4 °C and stored at -20 °C.

Mass spectrometry of LY364947-ULS: 562 $[M]^{1+}$; ^{195}Pt-NMR: -2554 ppm (N_3-Cl coordination at quinoline ring); -2504 ppm (N_3-Cl coordination at pyridine ring).

Erlotinib-ULS-lysozyme was prepared similarly as described above for LY364947, with minor modifications. Erlotinib-ULS was prepared by reacting erlotinib with a three-fold molar excess of ULS overnight at 65 °C. Completion of the reaction was followed by HPLC. Excess of ULS was precipitated by the addition of NaCl to a final concentration of 20 mM NaCl, which converted the non-reacted linker in the poorly soluble *cis*-Pt(ethylenediamine)dichloride. The product was stirred overnight, concentrated and redissolved in DMF. The precipitated linker was removed by filtration and the erlotinib-ULS adduct was stored at 4 °C. Mass spectrometry and ^{195}Pt-NMR confirmed the identity of the 1:1 adduct and the absence of free linker. Erlotinib-ULS was reacted at a 3:1 ratio to methionyl-LZM as described above.

Mass spectrometry of erlotinib-ULS: 684 $[M]^{1+}$; ^{195}Pt-NMR: -2548 ppm (N_3-Cl coordination at pyrimidine ring); -2319 ppm (N_3-O coordination, corresponding to the drug-ULS complex with water at remaining coordination site).

Both kinase inhibitor-LZM conjugates were characterized by protein content (BCA assay, Pierce), UV spectrometry and by HPLC. HPLC analyses were performed on a Waters liquid chromatograph (Waters, Milford, MA, USA) consisting of a 600 pump, an 717_{plus} autosampler and a 2996 photodiode array detector. A water:acetonitrile gradient containing 0.1% trifluoroacetic acid was used as mobile phase. LY364947-ULS-LZM was separated on a C18 Sunfire column (150 x 4.6 mm, 5 µm particle size, Waters) and erlotinib-ULS-LZM on a C4 Jupiter column (150 x 4.6 mm, 5 µm particle size, Phenomenex). Eluting peaks were detected at 320 nm (LY364947) or 346 nm (erlotinib).

Reversibility of the drug-ULS linkage was investigated by displacing the drug from the linker with known platinum ligands, as described before (13, 14). Overnight incubation with excess of either KSCN or sodium dithiocarbamate (both at 0.5 M in PBS) at 80 °C was used to displace the platinum-linked drug. Two volumes of acetonitrile were added to the samples to redissolve released drug and to simultaneously precipitate denaturated LZM. Samples were vortexed and centrifuged and stored at 4°C until further HPLC analysis as described above. Calibration curves of the free inhibitors were subjected to the same procedures as the conjugates.

2.3. Cell culture

The human kidney tubular cell line (HK-2) was obtained from ATCC (Manassas, USA). HK-2 cells were cultured in Dulbecco's modified Eagle's medium containing 3.7 g/ L sodium bicarbonate, 1 g/ L L-glucose and supplemented with 10% (v/ v) foetal calf serum (FCS), penicillin (100 IU/ mL), streptomycin (100 µg/ mL) and amphotericin B (0.25 µg/ mL) at 37 °C with 5% CO_2 in humidified air. All cell culture related materials were obtained from Gibco (Grand Island, NY, USA)

2.4. Binding and uptake of conjugates by cultured cells

Bound or internalized kinase inhibitor-LZM conjugates were visualized by anti-LZM immunofluorescence detection using confocal miscroscopy. HK-2 cells were seeded (1×10^4 cells/ well) onto 16-well chamber slides and allowed to adhere overnight. Culture medium was replaced by serum-free medium and cells were preincubated for another 24 h, after which wells were supplemented with the conjugates up to a final concentration of 10 µM. Cells were incubated for 4 h at either 4 °C or 37 °C.

Cells were washed with ice-cold PBS. After fixation (3.7% paraformaldehyde for 15 min at room temperature) cells were permeabilized with 0.1% Triton X-100 for 5 min at room temperature. Non specific binding sites were blocked by incubation with 5% (v/ v) FCS in PBS. Primary and secondary antibodies were diluted in 1% (v/ v) FCS, 0.05% Triton X-100 in PBS (primary antibody: rabbit anti-lysozyme, 1:500; secondary antibody: goat anti-rabbit IgG labeled with Alexa488, 1:200). To stain the nucleus and the cytoskeleton, cells were incubated with a solution containing DRAQ5 and Alexa568-phalloidin, respectively, for 15 min at room temperature. Cells were washed once and mounted with Fluorsave mounting medium. Confocal images were acquired on a Leica TCS-SP confocal laser scanning microscope equipped with a 488 nm Argon, a 568 nm Krypton and a 647 nm HeNe laser. Images were taken with a 40x oil immersion lens and processed with standard Leica software.

2.5. Effects of kinase inhibitor conjugates on cultured cells

HK-2 cells were seeded (2×10^5 cells/ well) onto 6-well plates and cultured overnight. Cells were serum deprived for 24 h. Kinase inhibitor-LZM conjugates (LY364947-ULS-LZM 10 µM; Erlotinib-ULS-LZM 10 µM, concentrations equivalent to the carrier concentration corresponding to 8 or 7 µM of the coupled kinase inhibitors) were added at the time of serum deprivation, *i.e.* 24 h before addition of growth factors, whereas equimolar doses of the free kinase inhibitors were added 30 min before growth factor stimulation (TGF-β1, 10 ng/ mL; EGF, 50 ng/ mL). Hereafter, cells were incubated at 37 °C for the indicated time periods (see below) and processed for Western Blotting or quantitative RT-PCR analysis. Statistical analyses were performed using Student's *T*-test with $p < 0.05$. For cell viability experiments, cells were incubated for another 24 h. Cell viability was determined using the XTT assay as previously described (15).

2.6. Western Blotting

Activation of the studied kinase pathways due to the added growth factors was detected by Western immunoblotting with phospho-specific antibodies recognizing phosphorylated key mediators in the TGF-β and EGF cascades. Ten or thirty minutes after treatment with EGF or TGF-β, respectively, the cells were lysed using RIPA buffer supplemented with protease and phosphatase inhibitors (all from Pierce, Rockford, IL, USA) on ice for 30 minutes. Protein concentrations were determined with a Pierce BCA protein assay (Pierce, Rockford, IL, USA) and equal amounts of protein were diluted in reducing sampling buffer and boiled for 5 minutes. The proteins were separated by SDS-polyacrylamide gel electrophoresis on NuPage Novex Bis-Tris precast gradient gels (4-12%) (Invitrogen, Breda, The Netherlands). The proteins were transferred on a nitrocellulose membrane using the iBlot dry blotting method (Invitrogen, Breda, The Netherlands). Blots were blocked with TBS-T (Tris Buffered Saline containing 0.1% (v/ v) Tween-20) with 5% (w/ v) milk powder for 1 hr at room temperature, and incubated with primary antibodies (1:1000 in TBS-T with 5% (w/ v) BSA) overnight at 4 °C. Blots were washed three times with TBS-T and incubated with HRP-labeled secondary antibody (1:2000 in blocking buffer) for 1 hr at room temperature. Proteins were visualized by a chemiluminescence-based detection reagent (Supersignal West Femto, Pierce, Rockford, IL, USA) and the protein bands were quantified on a Gel Doc Imaging system equipped with a XRS camera and Quantity One analysis software (Bio-Rad, Hercules, CA, USA). The membranes were stripped using Restore PLUS Western Blot Stripping Buffer (Pierce) and reprobed using anti-β-actin antibodies according to the above described method.

2.7. Determination of mRNA expression

Effects downstream of the activated kinase pathways were determined by quantitative RT-PCR gene expression analysis. Six hours after activation, cells were harvested using lysis buffer and total RNA was extracted with Qiagen RNeasy kit according to the manufactures protocol (Qiagen, Venlo, The Netherlands). cDNA was synthesized from 1 μg RNA using oligo-dT primers, hexamers (both from Promega) and Superscript RNaseH$^-$ Reverse Transcriptase (Gibco-BRL) for 1 hr at 42 °C.

Gene expression was assessed by quantitative real-time PCR using TaqMan Gene Expression with pre-designed probe and primers. Primers for procollagen type I alpha 1 (COL1A1; Hs00164004_m1), Fibronectin 1 (Hs00415006_m1), Connective tissue growth factor (CTGF; Hs00170014_m1), PAI-1 (SERPINE1; Hs00167155_m1) and GAPDH (Hs99999905_m1) were obtained from Applied Biosystems (Foster City, CA, USA). Expression of GAPDH was used as internal reference.

3. Results

3.1. Synthesis of kinase inhibitor-lysozyme conjugates

The structures of the kinase inhibitors and their conjugates with the renal carrier lysozyme are shown in **Figure 2**. For both erlotinib and LY364947, a 1:1 platinum-coordinated derivative was synthesized by reaction with the ULS linker, which was subsequently reacted to lysozyme modified with surface-exposed methionyl groups. The kinase inhibitor-ULS adducts were characterized by LC-MS and ^{195}Pt-NMR, and the final kinase inhibitor-lysozyme conjugates were characterized by UV-spectroscopy, protein content and HPLC (**Table 1**). HPLC analysis demonstrated negligible amounts of free drug and drug-ULS in the final products **(Figure 3**). Drug:LZM coupling ratio's were calculated from the drug content estimated by UV spectroscopy and the protein content of the conjugates.

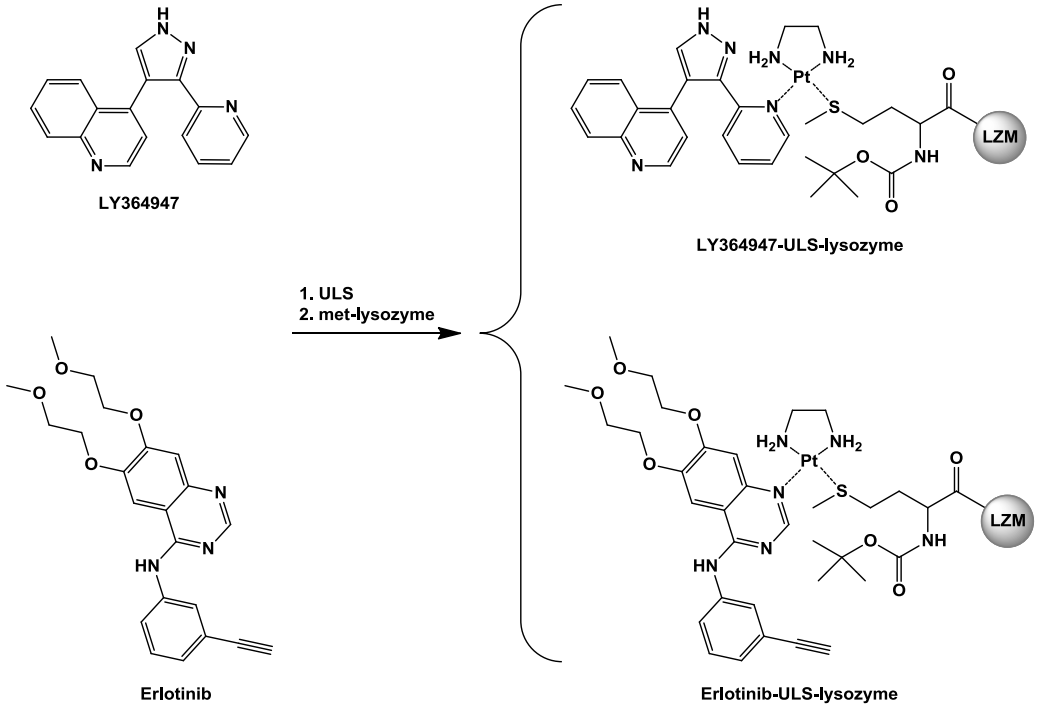

Figure 2. Synthesis scheme of LY364947-ULS-LZM and erlotinib-ULS-LZM. Kinase inhibitors were conjugated to LZM via the platinum (II)-based linker ULS, which formed a coordinative bond to one of the aromatic nitrogens in the drugs' structures. The drug-ULS intermediates were reacted to methionine modified LZM (met-lysozyme). Universal Linkage System is abbreviated as ULS.

Table 1. Characterization of drug-LZM conjugates.

Conjugate	synthesis ratio mole drug:mole LZM	Yield[a] (%)	Drug:carrier coupling ratio[b]	% conjugated drug[c]
Erlotinib-ULS-LZM	3:1	72%	0.7:1	97%
LY364947-ULS-LZM	4:1	76%	0.8:1	98%

[a] Based on the recovery of the carrier LZM after dialysis and subsequent filtration of the final product.

[b] Calculated from the protein content of the conjugate (BCA assay) and the estimated drug content by UV absorbance at 346 nm (erlotinib) and 320 nm (LY364947) at acidic pH (pH 2). Drug content was calculated versus a calibration curve of the free kinase inhibitors.

[c] As determined by peak area of the drug-LZM peak versus total peak area of conjugates, free inhibitors and inhibitor-ULS species in the HPLC chromatogram. Areas were recorded at the above mentioned drug specific wavelengths.

The release of kinase inhibitors from the conjugates was studied by competitive ligands such as KSCN and sodium dithiocarbamate, as been reported elsewhere (13, 14). These experiments showed that the bond between platinum-linker and bound kinase inhibitors was reversible. Drug release studies of the LY364947-ULS-LZM conjugate yielded a relatively drug content in the same range to the coupling degree as estimated by the UV absorbance of the intact non-degraded product. The amount of released drug now corresponded to a coupling ratio of 0.78:1 LY364947:LZM. On the other hand, erlotinib-ULS-LZM yielded relatively lower amounts of liberated drug, accounting for 48% less than the calculated amount of coupled drug. This discrepancy may relate to an altered UV-absorbance of erlotinib-ULS-LZM as compared to the free drug, although this could not be deduced from the spectra recorded by the photodiode array detector during HPLC analysis (**Figure 3B**).

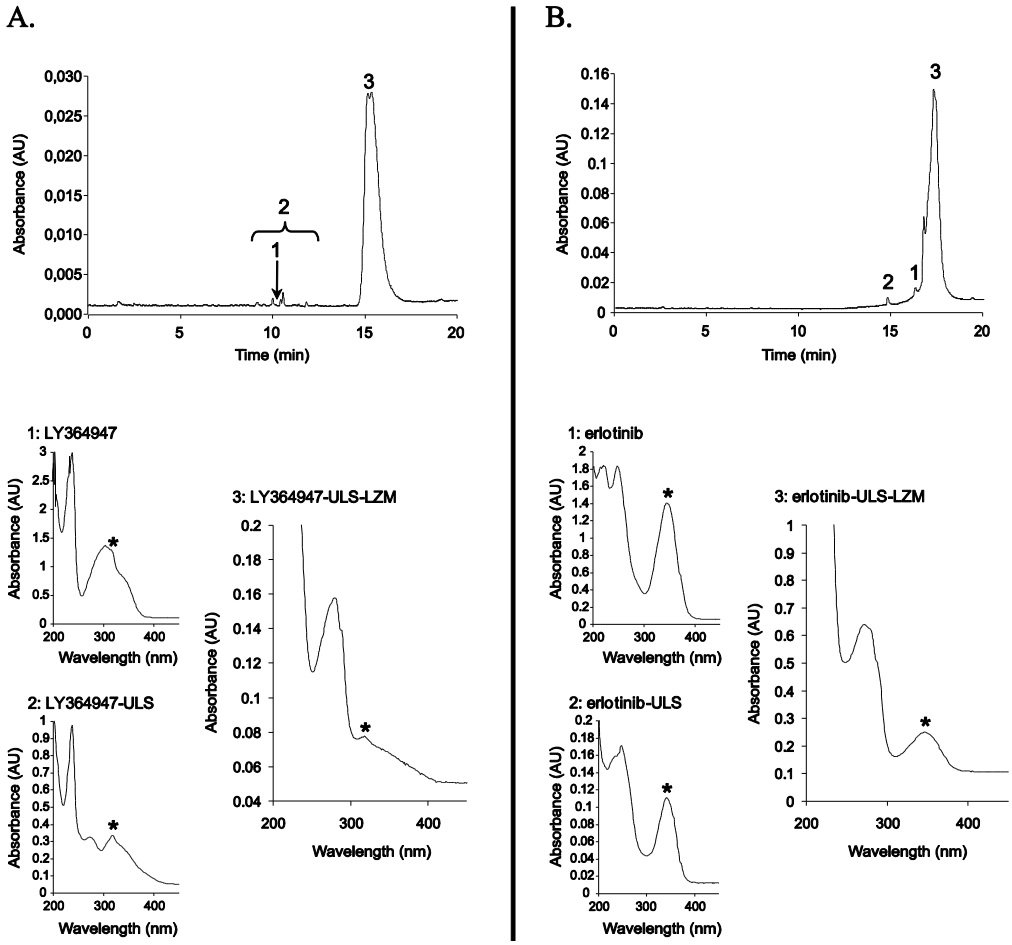

Figure 3. HPLC characterization of kinase inhibitor-LZM conjugates. (A) Separation of LY364947-ULS-LZM. Drug-containing peaks were monitored at 320 nm. Retention times of free LY364947 (1), LY364947-ULS (2) and LY364947-ULS-LZM (3) have been indicated. No free LY364947 was observed. Over 98% of the peak area was associated to the LY364947-ULS-LZM peak. Bottom panels show the absorbance spectra of the compounds (*:320 nm) Notice the differences in spectra between free drug and ULS-bound LY364947. (B) Separation of erlotinib-ULS-LZM. Drug-containing peaks were monitored at 346 nm. Retention times of free erlotinib (1), erlotinib-ULS (2) and erlotinib-ULS-LZM (3) have been indicated. Over 97% of the peak area was associated to the erlotinib-ULS-LZM peak. Bottom panels show the absorbance spectra of the compounds (*:346 nm).

3.2. Cellular uptake of drug-LZM conjugates

An important aspect we now report on is the cellular handling of drug-LZM conjugates by renal tubular cells. Human kidney (HK-2) tubular cells were incubated with the conjugates for 4 hrs at 37 °C and 4 °C. After fixation and staining, images were taken using a confocal microscope. The images are shown in **Figure 4** and demonstrate the internalization of the conjugate by the cells and their accumulation in the lysosomal compartment, as can be appreciated from the

intracellular vesicular staining observed after incubation at 37 °C (**Figure 4**, upper two lanes). Both conjugates showed identical intracellular distribution of LZM indicating that the cellular internalization and processing of both conjugates occurs in a similar manner. Similar intracellular staining intensity was observed with conjugates at both concentrations of 5 µM and 20 µM (data not shown), suggesting that the receptor-mediated uptake is saturated at these conditions. Incubations at 4 °C (**Figure 4**, lower two lanes) showed only binding of conjugates to the surface of the cells, while internalization was absent, supporting that internalization occurs via endocytosis.

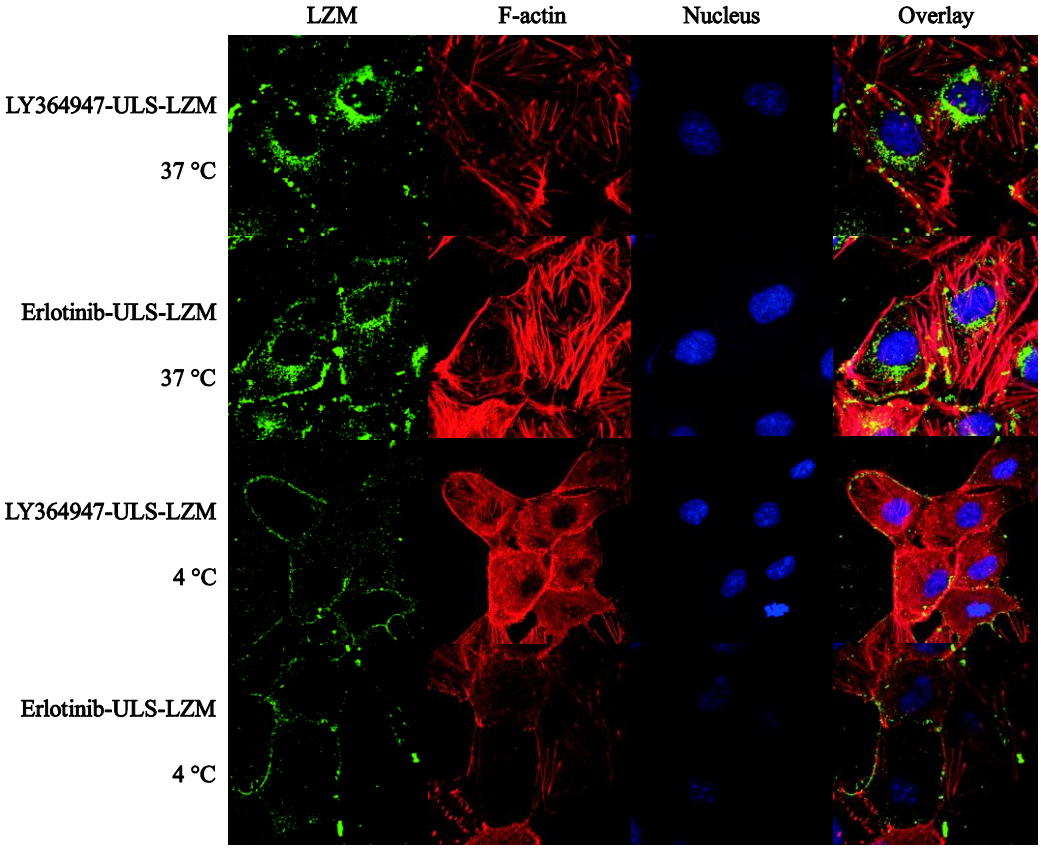

Figure 4. Cellular distribution of kinase inhibitor-LZM conjugates. HK-2 cells were incubated with kinase inhibitor-LZM conjugate (10 µM) in serum-free medium for 4 h at 4 or 37 °C. Fixed cells were stained with an antibody against lysozyme (green), Alexa568-phalloidin (F-actin; red) and DRAQ5 (nucleus; blue).

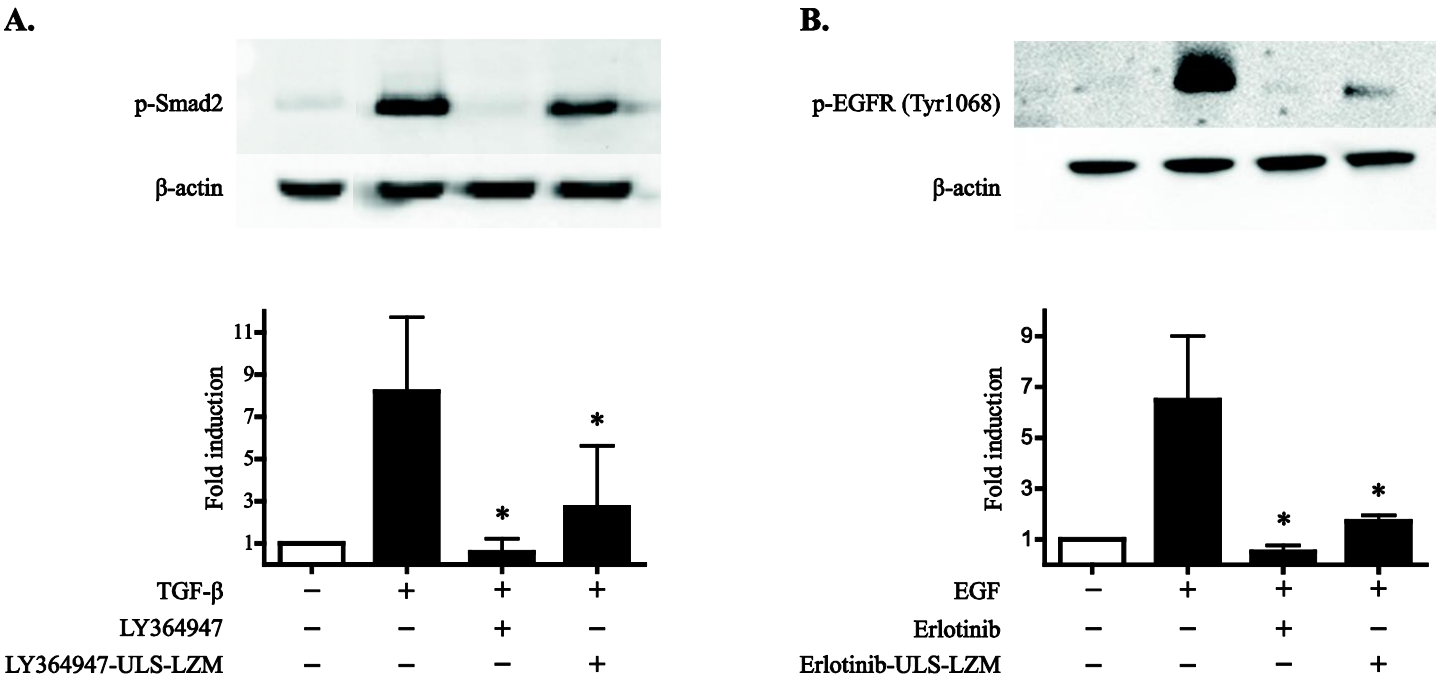

Figure 5. Inhibition of growth factor activated protein phosphorylation by kinase inhibitor-LZM conjugates. (A) HK-2 cells were stimulated with TGF-β for 30 min. LY364947-ULS-LZM was added at the time of serum deprivation, *i.e.* 24 h before addition of TGF-β, whereas an equimolar dose of free LY364947 was added 30 min before TGF-β stimulation. Total cell lysates were immunoblotted with antibodies specific for phosphorylated Smad2 (p-Smad2) and β-actin. (B) HK-2 cells were stimulated with EGF for 10 min. Erlotinib-ULS-LZM was added at the time of serum deprivation, *i.e.* 24 h before addition of EGF, whereas an equimolar dose of free erlotinib was added 30 min before EGF stimulation. Total cell lysates were immunoblotted with antibodies specific for phosphorylated EGF receptor at Tyrosine1068 (p-EGFR (Tyr1068)) and β-actin. Figures show in top panels a representative Western Blot and in bottom panels quantitative analysis based on densitometry as the ratio phosphorylated protein/ β-actin (mean ± stdev, n = 3, * $p < 0.05$ versus growth factor activated sample). Data are expressed as fold induction versus control cells.

3.3. Effects of kinase inhibitor conjugates on cultured cells

The effects of the kinase inhibitor-LZM conjugates were studied in the same renal tubular HK-2 cell line, by direct determination of the phosphorylation levels of the activated growth factor pathways and by gene expression analysis of reported fibrotic genes downstream of the signaling cascades. Kinase activation is a rapid and transient process and was studied at earlier time points after activation of the cells, while gene expression was studied at later time points.

Activation of the TGF-β pathway was investigated by Western Blot analysis with a phospho-specific antibody against phosphorylated Smad2, one of the downstream mediators of the TGF-β receptor kinase. Serum deprived HK-2 cells that had been stimulated with TGF-β1 for 30 minutes showed more than eight-fold elevated phospho-Smad2 levels (**Figure 5A**). Pre-incubation with the TGF-β receptor kinase inhibitor LY364947 (8 μM) completely inhibited the phosphorylation of Smad2, while pre-incubation with LY364947-ULS-LZM for 24 hours effectuated a clear reduction of approximately 70% in p-Smad2 levels.

A similar result was obtained when HK-2 cells were stimulated with EGF for 10 min. An over-6 fold activation of the EGF receptor kinase was demonstrated by phospho-staining of the Tyr1068 residue of the receptor (**Figure 5B**). This phosphorylation could be completely inhibited by pre-incubation with erlotinib (7 μM), while also erlotinib-ULS-LZM at the same drug concentration reduced the EGF receptor phosphorylation by 80%. From these results, we concluded that both conjugates effectively inhibited the activation of their targeted kinase pathways.

To further investigate the effect of the conjugated inhibitors in renal tubular cells, we studied their effects on the transcription of profibrotic genes. TGF-β1 stimulated the gene expression of three of the investigated genes, namely procollagen 1α1, CTGF and PAI-1. Treatment with free LY364947 or LY364947-ULS-LZM reduced the expression levels of those genes to basal or even lower levels (**Figure 6A**). TGF-β1 did not induce fibronectin gene expression, however pre-treatment with LY364947 and LY364947-ULS-LZM did reduce the expression of fibronectin below basal expression levels.

In contrast to the profound effects observed in the kinase activity assays, EGF did not induce elevated gene expression of procollagen 1α1, CTGF or fibronectin, nor did pre-treatment with erlotinib or erlotinib-ULS-LZM have pronounced inhibitory effects on the expression of those genes (**Figure 6B**). PAI-1 expression was slightly elevated after stimulation with EGF and this could be reduced by erlotinib to basal levels.

Cell viability experiments demonstrated that neither the conjugates nor free kinase inhibitors had apparent cytotoxic effects (data not shown).

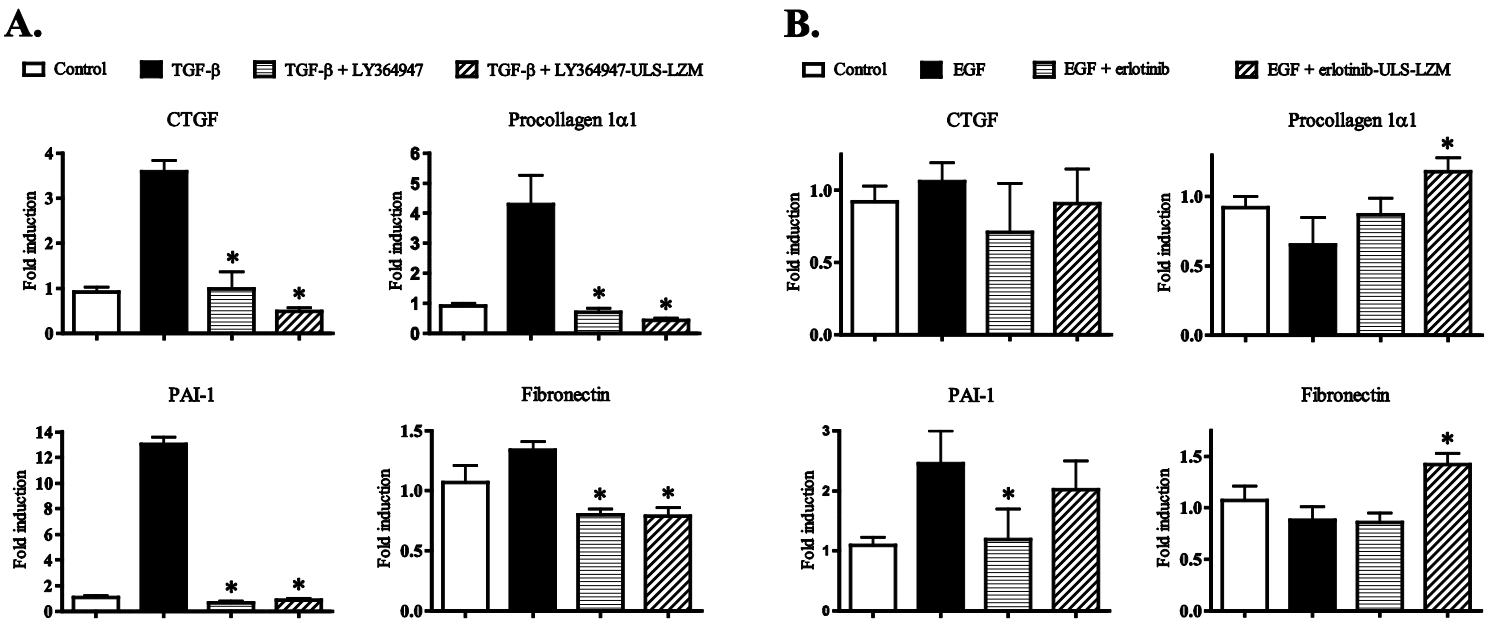

Figure 6. Effects of kinase inhibitor-LZM conjugates on growth factor induced expression of profibrotic genes. (A) HK-2 cells were stimulated with TGF-β for 6 h. LY364947-ULS-LZM was added at the time of serum deprivation, *i.e.* 24 h before addition of TGF-β, whereas an equimolar dose of free LY364947 was added 30 min before TGF-β stimulation. (B) HK-2 cells were stimulated with EGF for 6 hrs. Erlotinib-ULS-LZM was added at the time of serum deprivation, *i.e.* 24 h before addition of EGF, whereas an equimolar dose of free erlotinib was added 30 min before TGF- β stimulation. After treatment, mRNA was isolated and expression levels of procollagen 1α1, CTGF, fibronectin and PAI-1 were determined by quantitative RT-PCR. Expression of GAPDH was used as internal reference. Data are expressed as fold induction versus untreated controls (mean ± stdev, n = 3, $*p < 0.05$ versus growth factor activated sample).

Discussion

Kinase inhibitors are potent and selective drugs that, in principle, act on specified molecular targets. Their high specificity renders these agents attractive drug candidates for blockade of disease-activated pathways. Interference in the intracellular signaling lowers the eventual transcription of disease-related genes, and the progression or aggravation of the disease. Although quite different from a molecular or mechanistic point-of-view, the outcome of treatment with kinase inhibitors bears similarity to the activity of RNA-based silencing agents, which also specifically interfere in the transcription of genes and eventually lower the expression of specific proteins. Cell-specific delivery of RNA-interference is one of the most intensely studied topics in drug delivery nowadays. On one hand, this popularity can be attributed to the high promises of RNAi, on the other hand because the hydrophilic nature of nucleic acids necessitates a vector for their intracellular delivery. We now propose the cell-specific targeting of kinase inhibitors, which is an unexplored area within the drug delivery field so far.

Like most diseases, fibrosis is not regulated by a single growth factor. Its progression and severity is highly dependent on the interplay between different factors. Blocking the signaling pathways downstream of different growth factors therefore seems a rational approach. For this purpose, we developed conjugates with kinase inhibitors directed to different signaling pathways. In the future, this will enable studies in which we can block both or multiple pathways simultaneously, by combination of different cell-specific conjugates or by conjugation of multiple agents to a single carrier.

Two growth factors known to be upregulated in renal disease are EGF and TGF-β. They play a role in cell proliferation, migration, differentiation and extracellular matrix deposition (16, 17). Inhibition of the TGF-β signaling pathway significantly reduced renal fibrosis in different animal models of renal fibrosis (18, 19). Moreover, inhibition of EGF receptor signaling, either by erlotinib or another well known EGF receptor inhibitor, gefitinib, prevented expression of fibrotic markers and collagen deposition in either renal or lung models (20-22).

Previous studies in rats have shown the stability of this type of conjugates in the circulation and their intact accumulation in the designated target organ (13, 14, 23). We now confirmed this by uptake studies in cultured proximal tubular cells, which showed internalization of the conjugates by endocytosis. Furthermore, we demonstrated the pharmacological efficacy of the conjugates by virtue of their capability to inhibit the phosphorylation of downstream kinase substrates of the TGF-β or EGF pathway, as depicted in **Figure 1**. EGF rapidly induced the phosphorylation of the EGF receptor which was inhibited by either erlotinib or erlotinib-ULS-LZM. Similarly, LY364947-ULS-LZM and the free inhibitor effectively inhibited TGF-β induced phosphorylation of Smad2, a downstream mediator of the TGF-β receptor kinase. These results demonstrated that the kinase inhibitor-conjugates had been processed intracellularly to their active forms. Secondly, the efficacy of the conjugates was also assessed on the expression of profibrotic genes that, supposedly, are regulated via the investigated pathways (1, 24-26). LY364947-ULS-LZM conjugate potently reduced the TGF-β induced expression of three out four analyzed genes, to a similar extent as the free kinase inhibitor. Thus, although the LY364947-ULS-LZM conjugate acted less potently in the p-Smad2 assay than the free inhibitor, this difference was overcome in the gene-expression assay. The observed differences in activity between free drug and drug-LZM conjugate may furthermore relate to the differences in intracellular free drug concentration and

exposure times. Nevertheless, the present results clearly illustrate that LY364947-ULS-LZM has a similar activity to free LY364947 in the designated target cells.

Unexpectedly, stimulation of HK-2 cells with EGF resulted only in a slight increase of PAI-1 expression, while the expression of the other tested genes was largely unaffected. This is not in accordance with the high levels of EGF receptor phosphorylation in the same cell type, as shown in **Figure 5B**. This lack of activation by EGF also explains why both erlotinib and erlotinib-ULS-LZM hardly showed reductions in gene-expression levels. The regulation of the studied genes via EGF has been reported by others (24, 25), and we therefore expected a stimulating effect by this growth factor in our gene-expression assay. The profibrotic effect of EGF in renal tubular cells may, however, be mediated via other mechanisms not studied. Even when EGF by itself may not show impressive profibrotic activity, it may contribute to renal fibrosis via its interaction with TGF-β. Tian *et al.* showed the synergistic effect of EGF and TGF-β on the activation of the ERK signaling pathway. Furthermore, the combination of the two growth factors had a major effect on the production of matrix metalloproteinases, which are involved in cell migration (5). Docherty *et al.* showed that EGF was able to inhibit TGF-β induced apoptosis of HK-2 cells and enhanced the transformation of epithelial cells into fibroblasts (epithelial-mesenchymal transition, EMT) by TGF-β (24). Inhibition of either or both of these pathways by LY364947-ULS-LZM and/ or erlotinib-ULS-LZM will most likely reduce EMT.

The benefit of drug targeting will be most pronounced in the *in vivo* setting, in which the cellular targeted kinase inhibitor-LZM conjugates will accumulate in much higher amounts in the kidneys than freely administered kinase inhibitors (14). When tested in the unilateral ureteral obstruction rat model, which is characterized by increased TGF-β production, LY364947-ULS-LZM demonstrated superior effects over the equivalent dose of free kinase inhibitor (13). The presently reported data corroborate the efficacy of LY364947-ULS-LZM in cultured proximal tubular cells, and show the potential of similarly prepared conjugates with other kinase inhibitors. The applied platinum linker makes it feasible to prepare such conjugates with many different kinase inhibitors, making it feasible to intervene cell-specifically in disease-induced signaling cascades. Our studies show that the cellular activity of such products can be evaluated *in vitro* in HK-2 cells, since both endocytosis of the carrier and responsiveness to fibrotic growth factors are established. On the other hand, differences between read-out systems can confound the selection of active drug candidates, as was presently illustrated by the different effects of EGF and erlotinib in kinase activity assays and gene-expression studies. Proper validation of the cellular test system is therefore essential, and *in vivo* testing should be an integrate part of proof-of-concept studies. Our data suggest that these studies are best performed at the level of kinase activity assays, which is more closely related to the direct activity of kinase inhibitors. Nevertheless, such inhibitory data should also be corroborated by functional analyses downstream of the inhibited kinase, to account for the summative effects of continuous signaling inhibition in time and to warrant proper functional activity when tested *in vivo*.

Conclusion

With the Universal Linker System, we have prepared two different kinase inhibitor-lysozyme conjugates directed to different growth factor activated signaling pathways. Both conjugates are efficiently internalized by cultured proximal tubular cells and are effective in inhibiting growth factor induced phosphorylation events. These conjugates are interesting and promising tools to inhibit signaling pathways involved in renal disease, and may provide for a more organ and cell-type specific profile of kinase inhibiting drugs.

Acknowledgements

This work was made possible by a grant from the European Framework program FP6 (LSHB-CT-2007-036644). We thank Mies van Steenbergen and Dionne van der Giezen for technical assistance in chromatographic experiments and quantitative PCR experiments.

References

1. T.Q. Nguyen and R. Goldschmeding. Bone morphogenetic protein-7 and connective tissue growth factor: novel targets for treatment of renal fibrosis? Pharm Res. 25:2416-2426 (2008).
2. M.A. Hallman, S.G. Zhuang and R.G. Schnellmann. Regulation of dedifferentiation and redifferentiation in renal proximal tubular cells by the epidermal growth factor receptor. Journal of Pharmacology and Experimental Therapeutics. 325:520-528 (2008).
3. A. Lautrette, S. Li, R. Alili, S.W. Sunnarborg, M. Burtin, D.C. Lee, G. Friedlander and F. Terzi. Angiotensin II and EGF receptor cross-talk in chronic kidney diseases: a new therapeutic approach. Nat Med. 11:867-874 (2005).
4. J. Floege, F. Eitner and C.E. Alpers. A new look at platelet-derived growth factor in renal disease. J Am Soc Nephrol. 19:12-23 (2008).
5. Y.C. Tian, Y.C. Chen, C.T. Chang, C.C. Hung, M.S. Wu, A. Phillips and C.W. Yang. Epidermal growth factor and transforming growth factor-beta1 enhance HK-2 cell migration through a synergistic increase of matrix metalloproteinase and sustained activation of ERK signaling pathway. Exp Cell Res. 313:2367-2377 (2007).
6. J. Prakash, K. Poelstra, H. van Goor, F. Moolenaar, D.K.F. Meijer and R.J. Kok. Novel therapeutic targets for the treatment of tubulointerstitial fibrosis. Current Signal Transduction Therapy. 3:97-111 (2008).
7. M.A. Bareschino, C. Schettino, T. Troiani, E. Martinelli, F. Morgillo and F. Ciardiello. Erlotinib in cancer treatment. Ann Oncol. 18 Suppl 6:vi35-41 (2007).
8. C. Porta, C. Paglino, I. Imarisio and L. Bonomi. Uncovering Pandora's vase: the growing problem of new toxicities from novel anticancer agents. The case of sorafenib and sunitinib. Clinical and Experimental Medicine. 7:127-134 (2007).
9. K. Temming, M.M. Fretz and R.J. Kok. Organ- and Cell-Type Specific Delivery of Kinase Inhibitors: A Novel Approach in the Development of Targeted Drugs. Current Molecular Pharmacology 1:1-12 (2008).
10. M. Haas, F. Moolenaar, D.K. Meijer and D. de Zeeuw. Specific drug delivery to the kidney. Cardiovasc Drugs Ther. 16:489-496 (2002).
11. E.I. Christensen and J. Gburek. Protein reabsorption in renal proximal tubule-function and dysfunction in kidney pathophysiology. Pediatr Nephrol. 19:714-721 (2004).
12. N.S. Chung and K.M. Wasan. Potential role of the low-density lipoprotein receptor family as mediators of cellular drug uptake. Adv Drug Deliv Rev. 56:1315-1334 (2004).
13. J. Prakash, M.H. de Borst, A.M. van Loenen-Weemaes, M. Lacombe, F. Opdam, H. van Goor, D.K. Meijer, F. Moolenaar, K. Poelstra and R.J. Kok. Cell-specific delivery of a transforming growth factor-beta type I receptor kinase inhibitor to proximal tubular cells for the treatment of renal fibrosis. Pharm Res. 25:2427-2439 (2008).
14. J. Prakash, M. Sandovici, V. Saluja, M. Lacombe, R.Q.J. Schaapveld, M.H. de Borst, H. van Goor, R.H. Henning, J.H. Proost, F. Moolenaar, G. Keri, D.K.F. Meijer, K. Poelstra and R.J. Kok. Intracellular delivery of the p38 mitogen-activated protein kinase inhibitor SB202190 [4-(4-fluorophenyl)-2-(4-hydroxyphenyl)-5-(4-pyridyl)1H-imidazole] in renal tubular cells: A novel strategy to treat renal fibrosis. Journal of Pharmacology and Experimental Therapeutics. 319:8-19 (2006).
15. D.A. Scudiero, R.H. Shoemaker, K.D. Paull, A. Monks, S. Tierney, T.H. Nofziger, M.J. Currens, D. Seniff and M.R. Boyd. Evaluation of a soluble tetrazolium/ formazan assay for cell growth and drug sensitivity in culture using human and other tumor cell lines. Cancer Res. 48:4827-4833 (1988).
16. N. Sayed-Ahmed, N. Besbas, J. Mundy, E. Muchaneta-Kubara, G. Cope, C. Pearson and M. el Nahas. Upregulation of epidermal growth factor and its receptor in the kidneys of rats with streptozotocin-induced diabetes. Exp Nephrol. 4:330-339 (1996).
17. E.P. Bottinger and M. Bitzer. TGF-beta signaling in renal disease. J Am Soc Nephrol. 13:2600-2610 (2002).
18. M. Petersen, M. Thorikay, M. Deckers, M. van Dinther, E.T. Grygielko, F. Gellibert, A.C. de Gouville, S. Huet, P. ten Dijke and N.J. Laping. Oral administration of GW788388, an inhibitor of TGF-beta type I and II receptor kinases, decreases renal fibrosis. Kidney Int. 73:705-715 (2008).
19. E.T. Grygielko, W.M. Martin, C. Tweed, P. Thornton, J. Harling, D.P. Brooks and N.J. Laping. Inhibition of gene markers of fibrosis with a novel inhibitor of transforming growth factor-beta type I receptor kinase in puromycin-induced nephritis. J Pharmacol Exp Ther. 313:943-951 (2005).

20. H. Francois, S. Placier, M. Flamant, P.L. Tharaux, D. Chansel, J.C. Dussaule and C. Chatziantoniou. Prevention of renal vascular and glomerular fibrosis by epidermal growth factor receptor inhibition. Faseb J. 18:926-928 (2004).
21. M.V. Arcidiacono, T. Sato, D. Alvarez-Hernandez, J. Yang, M. Tokumoto, I. Gonzalez-Suarez, Y. Lu, Y. Tominaga, J. Cannata-Andia, E. Slatopolsky and A.S. Dusso. EGFR activation increases parathyroid hyperplasia and calcitriol resistance in kidney disease. J Am Soc Nephrol. 19:310-320 (2008).
22. W.D. Hardie, C. Davidson, M. Ikegami, G.D. Leikauf, T.D. Le Cras, A. Prestridge, J.A. Whitsett and T.R. Korfhagen. EGFR- tyrosine kinase inhibitors diminish transforming growth factor-alpha induced pulmonary fibrosis. Am J Physiol Lung Cell Mol Physiol (2008).
23. J. Prakash, M.H. de Borst, M. Lacombe, F. Opdam, P.A. Klok, H. van Goor, D.K. Meijer, F. Moolenaar, K. Poelstra and R.J. Kok. Inhibition of renal rho kinase attenuates ischemia/ reperfusion-induced injury. J Am Soc Nephrol. 19:2086-2097 (2008).
24. N.G. Docherty, O.E. O'Sullivan, D.A. Healy, M. Murphy, J. O'Neill A, J.M. Fitzpatrick and R.W. Watson. TGF-beta1-induced EMT can occur independently of its proapoptotic effects and is aided by EGF receptor activation. Am J Physiol Renal Physiol. 290:F1202-1212 (2006).
25. R. Samarakoon, S.P. Higgins, C.E. Higgins and P.J. Higgins. TGF-beta1-induced plasminogen activator inhibitor-1 expression in vascular smooth muscle cells requires pp60(c-src)/ EGFR(Y845) and Rho/ ROCK signaling. J Mol Cell Cardiol. 44:527-538 (2008).
26. R. Tan, W. He, X. Lin, L.P. Kiss and Y. Liu. Smad ubiquitination regulatory factor-2 in the fibrotic kidney: regulation, target specificity, and functional implication. Am J Physiol Renal Physiol. 294:F1076-1083 (2008).

Chapter 4

Imatinib-ULS-lysozyme: a proximal tubular cell-targeted conjugate of imatinib for the treatment of renal diseases

M.E.M. Dolman[1], K.M.A. van Dorenmalen[1], E.H.E. Pieters[1], M. Lacombe[2], J. Pató[3], G. Storm[1], W.E. Hennink[1], and R.J. Kok[1]

[1] Department of Pharmaceutics, Utrecht Institute of Pharmaceutical Sciences, Utrecht University, Utrecht, The Netherlands

[2] KREATECH Biotechnology B.V., Amsterdam, The Netherlands

[3] Vichem Chemie, Budapest, Hungary

Submitted for publication

Abstract

The anticancer drug imatinib is an inhibitor of the platelet-derived growth factor receptor (PDGFR) kinases, which are involved in the pathogenesis of fibrotic diseases. In the current study we investigated the delivery of imatinib to the proximal tubular cells of the kidneys and evaluated the potential antifibrotic effects of imatinib in tubulointerstitial fibrosis.

Coupling of imatinib to the low molecular weight protein lysozyme via the platinum (II)-based linker ULS yielded a 1:1 drug-carrier conjugate that rapidly accumulated in the proximal tubular cells upon intravenous and intraperitoneal administration. The bioavailability of intraperitoneally administered imatinib-ULS-lysozyme was 100%. Renal imatinib levels persisted for up to 3 days after a single injection of imatinib-ULS-lysozyme. Compared with an equal dose imatinib mesylate, imatinib-ULS-lysozyme resulted in a, respectively, 30- and 15-fold higher renal exposure of imatinib, for intravenous and intraperitoneal administration, respectively. Imatinib-ULS-lysozyme could not be detected in the heart, which is the organ at risk for side-effects of prolonged treatment with imatinib.

The efficacy of imatinib-ULS-lysozyme in the treatment of tubulointerstitial fibrosis was evaluated in the unilateral ureteral obstruction (UUO) model in mice. Three days UUO resulted in all signs of early fibrosis, *i.e.* an increased deposition of matrix and production of profibrotic factors. Although a moderately increased activity of PDGFR-β was observed, the profibrotic phenotype could not be inhibited with imatinib mesylate nor with imatinib-ULS-lysozyme. Further evaluation of imatinib mesylate and imatinib-ULS-lysozyme is therefore warranted in an animal model in which the activation of PDGFR-β is more pronounced.

1. Introduction

Kidney proximal tubular cells are capable of reabsorbing a variety of compounds from the urine. One of the most abundantly expressed receptors on proximal tubular cells is megalin, which is, in cooperation with the cubilin receptor, responsible for the reabsorption of proteins and the conservation of plasma protein-bound vitamins and trace elements (1, 2). We and others have exploited the megalin receptor for drug targeting to the proximal tubular cells (3). The megalin receptor is expressed on the luminal side of epithelial cells in different organs. Except for the kidneys, the epithelial cells in the other organs pose a barrier that prevents the transport of macromolecules to the luminal side and, therefore, to interact with the megalin receptor. In the kidneys, however, the luminal side of tubular epithelial cells can be reached by macromolecules (*e.g.* low molecular weight proteins) after glomerular filtration from the blood stream. The megalin receptor may therefore facilitate the receptor-mediated endocytosis of drug-carrier conjugates (4). Lysozyme is a low molecular weight protein that is freely filtered through the glomerulus and reabsorbed by the proximal tubular cells via megalin receptor-mediated endocytosis. In earlier studies lysozyme has successfully been used for the delivery of small molecule drugs into the proximal tubular cells (5-8). This does not only offer novel strategies to interfere in renal diseases in which the proximal tubular cells are involved, but also leads to a better understanding of their role in renal diseases.

Over the past years the number of patients that developed renal diseases increased remarkably (9). Progression of chronic renal diseases results in the development of renal fibrosis, characterized by glomerulosclerosis and tubulointerstitial fibrosis (10-12). In tubulointerstitial fibrosis injury of the proximal tubular cells results in the onset of multiple signaling cascades, initiating chronic inflammatory responses, epithelial-to-mesenchymal transition (EMT) of normal epithelial cells and the excessive production of an extracellular matrix (ECM). As a consequence of uncontrolled fibrogenesis, functional tissue is gradually replaced by scar tissue, eventually resulting in kidney failure (10-12). Currently no clinically available drugs are available that are able to halt or reverse tubulointerstitial fibrosis and the present treatment is focused on treating the underlying cause of the organ damage and slowing down the progression of the local fibrotic processes (12). For new treatments, it is important to focus on therapeutics that are able to reverse the disease processes or at least halt fibrogenesis, thereby preventing the ultimate need for interventions such as organ transplantation.

Kinase inhibitors are primarily known for their use in cancer treatment (13, 14), but are also promising drug candidates for the treatment of tubulointerstitial fibrosis because protein kinases play an essential role in the activated signaling cascades in proximal tubular cells (10, 15). One of the kinase inhibitors clinically available for the treatment of cancer and currently under investigation for the treatment of fibrotic diseases is the tyrosine kinase inhibitor imatinib. This drug inhibits the tyrosine kinase activity of the platelet-derived growth factor receptors PDGFR-α and PDGFR-β and Abelson tyrosine kinase (c-Abl) (16) and has been clinically approved for the treatment of Bcr-Abl-positive chronic myelogenous leukaemia and gastrointestinal stromal tumours (17). Activation of the tyrosine kinase c-Abl is mediated by the transforming growth factor-beta receptor (TGFR-β) kinases. Therefore imatinib is able to interfere in the PDGFR- as well as TGFR-β kinase mediated signaling pathways (16). PDGFR- and TGFR-β kinases play a role in embryogenesis and in wound healing and, in case of TGFR-β kinases, also in homeostasis, chemotaxis and cell cycle control (18-21). Both kinases for example have been reported to be

involved in the regeneration of proximal tubuli after acute ischemic renal injury (22). Overactivation of the PDGFR- and TGFR-β kinase pathways, however, has been shown to contribute to tubulointerstitial fibrosis (23-26). Activated PDGFR kinases exert their profibrotic effects by stimulating proliferation, migration and survival of myofibroblasts (10, 27), while elevated TGFR-β kinase activity stimulates the inflammatory responses as well as EMT and ECM (21, 25, 28). TGFR-β kinase induced fibrogenesis via Smad signaling has been the most extensively studied TGFR-β kinase mediated pathway (29), but TGFR-β mediated activation of c-Abl kinase seems to play an essential role in the synthesis of ECM proteins such as collagen and in fibroblast proliferation (17, 30, 31).

Imatinib has been investigated in preclinical studies for the treatment of fibrosis in different organs. Variable successes were obtained, depending on the diseased organ and the onset and duration of the treatment (31-39). Imatinib inhibited tubulointerstitial fibrosis in mice with unilateral ureteral obstruction (UUO) by inhibition of TGFR-β induced activation of c-Abl kinase (30, 38).

In the current study we investigated the delivery of imatinib to the proximal tubular cells of the kidneys, by means of the aforementioned technique of drug-lysozyme conjugates. At the moment it is not known which renal cell types are involved in the therapeutic responses to imatinib in the treatment of tubulointerstitial fibrosis. The use of a tubular cell-specific conjugate, that will specifically deliver its conjugated drug in the kidneys, will increase our knowledge on the importance of specific signaling cascades and cell types during the development of tubulointerstitial fibrosis. Furthermore, drug delivery systems that deposit their therapeutic cargo in the desired cell types can increase the efficacy and safety of the drug. Tyrosine kinase inhibitors are promising agents for the treatment of tubulointerstitial fibrosis, but are also associated with serious adverse reactions such as nausea, peripheral edema and skin rash but, more important, also cardiotoxicity (13, 16, 40).

For the targeting of imatinib to the proximal tubular cells the kinase inhibitor was conjugated to lysozyme via the platinum (II)-based Universal Linkage System™ (ULS)™ (5-7). Drug conjugation to a carrier protein via the ULS linker yields conjugates with a long residence time in the target cells and sustained release of the drug, as has been demonstrated for similar drug-carrier conjugates (7, 41). In the present study, we evaluated the *in vivo* pharmacokinetics of imatinib-ULS-lysozyme in healthy mice and evaluated the efficacy of imatinib and imatinib-ULS-lysozyme in the mouse UUO model of tubulointerstitial fibrosis.

2. Materials and methods

2.1. Materials and chemicals

Imatinib was obtained from Vichem Chemie (Budapest, Hungary). Imatinib mesylate was purchased from Sequoi Research Products (Pangbourne, United Kingdom). Lysozyme from hen egg white, potassium thiocyanate (KSCN), ethylenediaminetetraacetic acid (EDTA) and citric acid were purchased from Fluka (Zwijndrecht, The Netherlands). Acetonitrile (ACN) HPLC-S and *tert*-butyl methylether (TBME) were obtained from Biosolve (Valkenswaard, The Netherlands). Trifluoroacetic acid (TFA), protease XXIV, albumin from bovine serum (BSA), 4-hydroxybenzophenone, sodium azide, sodium citrate tribasic dehydrate, 3,3-diaminobenzidine (DAB) and hematoxylin solution (gill no. 2) were purchased from Sigma-Aldrich (Zwijndrecht,

The Netherlands). Rabbit anti-hen egg white lysozyme and Immobilon-P polyvinylidene fluoride (PVDF) Membrane (0.45 µm) were purchased from Millipore (Amsterdam Zuidoost, The Netherlands). Goat anti-mouse megalin (P-20), rabbit anti-mouse p-PDGFR-β and rabbit anti-mouse vimentin polyclonal antibodies were purchased from Santa Cruz (Heidelberg, Germany). Alexa Fluor® 488 donkey anti-rabbit, Alexa Fluor® 488 donkey anti-goat and Alexa Fluor® 647 donkey anti-rabbit secondary antibodies, TOPRO-3 iodide, NuPAGE® 4-12% Bis-Tris Gel and NuPAGE® MOPS SDS running buffer were purchased from Invitrogen (Breda, The Netherlands). The TaqMan® Universal PCR Master Mix, No AmpErase® UNG and The TagMan® Gene Expression Assays Mm00446973_m1, Mm00435860_m1, Mm00483888_m1, Mm01256734_m1 and Mm00441242_m1 for the detection of, respectively, TATA-binding protein (TBP), plasminogen activator inhibitor-1 (PAI-1), Collagen 1A2, fibronectin and monocyte chemotactic protein-1 (MCP-1) were purchased from Applied Biosystems (Nieuwerkerk aan den IJssel, The Netherlands). RIPA buffer, Halt™ Protease and Phosphatase Inhibitor Cocktail (100x) and 0.5 M EDTA solution (100x) were purchased from Thermo Scientific (Etten-Leur, The Netherlands). PageRuler™ Prestained Protein Ladder was purchased from Fermentas (Leon-Rot, Germany). 2-Amino-2-(hydroxymethyl)-1,3-propanediol (Tris) was purchased from Roche Diagnostics GmbH (Almere, The Netherlands). Glycine, hydrogen peroxidase 30% and disodium hydrogen phosphate dehydrate were purchased from Merck (Schiphol-Rijk, The Netherlands). Tween-20 was purchased from Acros Organics (Geel, Belgium). Rabbit anti-mouse β-actin polyclonal antibody and horseradish peroxidase (HRP)-conjugated goat anti-rabbit secondary antibody were purchased from Cell Signaling Technology (Leiden, The Netherlands). Rabbit anti-mouse α-SMA and rabbit anti-mouse collagen IV were purchased from Abcam (Cambridge, UK). BrightVision HRP-conjugated goat anti-rabbit secondary antibody was purchased from Immunologic (Duiven, The Netherlands).

2.2. Synthesis of imatinib-ULS-lysozyme

Imatinib was conjugated to lysozyme via the platinum (II)-based Universal Linkage System™ (ULS™; *cis*-[Pt(ethylenediamine)nitrate-chloride]), which was synthesized from *cis*-[Pt(ethylenediamine)dichloride as described elsewhere (42). Imatinib was first coupled to the ULS linker by incubation of 600 µmol ULS with 300 µmol imatinib in 73 mL DMF for 4 hours at 50 °C. After acidification of the solution to pH 4 with nitric acid the solvents were evaporated under reduced pressure at ambient temperature. Imatinib-ULS was redissolved in 6 mL DMF and purified by preparative high-performance liquid chromatography (HPLC). The HPLC system consisted of a ÄKTAexplorer instrument (GE Healthcare, The Netherlands) and a Phenomenex C18 column (250 x 21.2 mm, 10 µm particle size) (Phenomenex, The Netherlands). UNICORN 3.21 software was used for data recording. A gradient was used with eluent A consisting of TFA and eluent B of 50% (v/ v) TFA in methanol (B), pumped at 10 mL/ min. The amount of solvent B was increased from 0 to successively 50, 80 and 100% during 9, 35 and 5 minutes, respectively. The solvents were evaporated again under reduced pressure and the target species were redissolved in 1.2 mL DMF. Imatinib-ULS was analyzed with HPLC, ^{195}Pt-NMR and LC-MS. Lysozyme (10 mg/ mL in PBS) was reacted with a three times molar excess of BOC-L-methionine *N*-hydroxysuccinimide ester (50 mg/ mL in DMSO) for one hour at ambient temperature. The BOC-methionyl-modified lysozyme product was purified by dialysis against

water using a Spectra/ Por® 3 dialysis membrane with a molecular weight cut-off of 3,500. After lyophilization the final product was characterized by mass spectrometry. Lastly, imatinib-ULS was conjugated to BOC-methionyl-modified lysozyme by a overnight reaction of a three times molar excess of imatinib-ULS with methionine-modified lysozyme in 0.02 M tricine/ sodium nitrate buffer with pH 8.5 at 37 °C. The imatinib-ULS-lysozyme conjugate was purified by dialysis against water at 4 °C using a Slide-A-Lyzer dialysis cassette with a molecular weight cut-off of 10,000 (Pierce, Rockford, IL) and subsequently lyophilized.

2.3. Characterization of imatinib-ULS-lysozyme

A stock solution of imatinib-ULS-lysozyme in water was prepared in a final concentration of 8 mg/ mL and subsequently filtered. The lysozyme content in this solution was determined using the Micro BCA™ Protein Assay (Thermo Scientific; Etten-Leur, The Netherlands). To establish the amount of imatinib conjugated to lysozyme, the drug was released from the linker by competitive displacement with an excess of KSCN. In detail, the stock solution of imatinib-ULS-lysozyme was three times diluted in PBS. Calibration samples of imatinib mesylate in PBS were prepared in a concentration range of 3 – 600 µM. After the addition of 50 µL 1 M KSCN in PBS to 50 µL sample, the samples were incubated for 24 hours at 80 degrees. The samples were allowed to reach room temperature and mixed with 200 µL ACN with 0.1% TFA by vortex mixing and subsequent centrifugation for 4 minutes at 19,500 x g. Of the supernatants 50 µL was injected in a reversed phase HPLC system consisting of a Waters 2695 separations module, a Waters 2487 dual λ absorbance detector and a Waters SunFire™ C18 column (4.6 x 150 mm, 5 µm particle size) (Milford, USA). Empower 2 software was used for data recording. A gradient was used with eluent A consisting of 5% ACN/ 95% water/ 0.1% TFA (w/ w/ w) and eluent B consisting of ACN/ 0.1% TFA (w/ w). See **Table 1** for the details of the gradient. Imatinib mesylate was detected at 265 nm, the maximum wavelength of absorbance of the kinase inhibitor.

Table 1. HPLC gradient used for the detection of imatinib mesylate

Time (minutes)	Eluent A (%)	Eluent B (%)
0	100	0
25	20	80
26	0	100
33	0	100
34.5	100	0
Flow rate: 1 mL/ min		

2.4. Animals

In vivo experiments were performed in normal male C57Bl/ 6J mice obtained from Harlan (Zeist, The Netherlands). Mice with a body weight of 13-25 gram were ordered and used within four weeks after arrival. The mice were housed in cages in a 12 hours light and 12 hours dark cycle and given food and water *ad libitum*. Experimental protocols for pharmacokinetic and efficacy studies were approved by the animal ethics committee of the University of Utrecht, The Netherlands.

2.5. In vivo pharmacokinetics of imatinib-ULS-lysozyme and imatinib

Male mice were treated with a single intravenous injection of 20 mg/ kg imatinib-ULS-lysozyme (n = 10) or an equimolar dose imatinib (as mesylate) (n = 8) or with a single intraperitoneal injection of 20 mg/ kg imatinib-ULS-lysozyme (n = 8) or an equimolar dose imatinib (as mesylate) (n = 8). Animals were sacrificed at the indicated time points by a single intraperitoneal injection of 120-150 µL of a mixture of ketamine hydrochloride (47 mg/ mL), xylazine hydrochloride (8 mg/ mL) and atropine (0.07 mg/ mL). Blood samples were collected in K_2 EDTA prefilled blood tubes at one minute after administration of imatinib-ULS-lysozyme or imatinib mesylate and after sacrificing the mice. The blood samples were centrifuged two times at 5,500 x g for 15 minutes at 4 °C and subsequently stored at -80 °C till further analysis. For the evaluation of the biodistribution of imatinib-ULS-lysozyme, the kidneys, liver, spleen and heart were collected and processed as described below. Part of the kidneys, liver, spleen and heart was used for the preparation of 4% formaldehyde-fixed paraffin-embedded tissue sections for immunohistochemical analyses as described below. The remaining parts of the kidneys and heart were stored at -80 °C for the measurement of the amount of imatinib present in these organs. To investigate the presence of ULS-bound and released imatinib in the urine after injection of imatinib-ULS-lysozyme, the urine of one mouse treated with an intravenous injection of the conjugate was collected during the first 30 minutes after administration. Pharmacokinetic parameters were determined with non-linear curve-fitting of combined data sets of intravenously and intraperitoneally administered imatinib-ULS-lysozyme or imatinib mesylate.

2.6. Immunohistochemistry of paraffin-embedded sections

2.6.1. Uptake of imatinib-ULS-lysozyme in the proximal tubular cells of the kidneys

The colocalization of imatinib-ULS-lysozyme with proximal tubular cells was investigated by immunostaining of lysozyme and the megalin receptor. Paraffin-embedded kidney sections of 4 µm were deparaffinized in xylene and hydrated in a graded series of alcohol baths. Enzyme pretreatment of the dehydrated kidney sections was performed by boiling the kidney sections for 20 minutes in Tris/ EDTA buffer (containing 4.84 g/ L Tris and 372 mg/ L EDTA) with pH 9.0. After washing the kidney sections with PBS containing 0.05% tween-20 (further referred to as PBS/ 0.05T) they were incubated for 1 hour with goat anti-megalin primary antibody (1:50 in PBS with 1% BSA and 1% azide). The kidney sections were washed with PBS/ 0.05T and 30 minutes incubated with Alexa fluor 488 donkey anti-goat secondary antibody (1:50 in PBS with 1% BSA and 1% azide). After washing the kidney sections with PBS/ 0.05T the sections were incubated for 1 hour with rabbit anti-hen egg white lysozyme primary antibody (1:100 in PBS with 1% BSA and 1% azide), washed with PBS/ 0.05T and subsequently incubated for 30 minutes with Alexa fluor 647 donkey anti-rabbit secondary antibody (1:50 in PBS with 1% BSA and 1% azide). The stained kidney sections were washed with PBS/ 0.05T and mounted with vectashield mounting medium. All incubations were performed at room temperature and the kidney sections were protected from light from the moment they were incubated with the first secondary antibody. Stained sections were analyzed using confocal laser scanning microscopy (CLSM).

2.6.2. Distribution of imatinib-ULS-lysozyme to other tissues

Biodistribution of imatinib-ULS-lysozyme to the heart, liver and spleen was investigated by immunostaining of formaldehyde-fixed paraffin-embedded tissue sections for lysozyme and compared with the distribution of the conjugate to the kidneys. Paraffin-embedded tissue sections of 4 µm were deparaffinized in xylene and dehydrated in a graded series of alcohol baths. Enzyme pretreatment of the dehydrated tissue sections was performed for epitope retrieval by 5 minutes incubation of the sections with protease XXIV. After washing the tissue sections with PBS/ 0.05T they were incubated for 1 hour with rabbit anti-hen egg white lysozyme primary antibody (1:100 in PBS with 1% BSA and 1% azide). The sections were washed with PBS/ 0.05T and 30 minutes incubated with Alexa fluor 488 donkey anti-rabbit secondary antibody (1:50 in PBS with 1% BSA and 1% azide). After washing the kidney sections with PBS/ 0.05T nuclei were stained with TOPRO-3 iodide by incubation for 30 minutes. The stained sections were washed with PBS/ 0.05T and mounted with vectashield mounting medium. All incubations were performed at room temperature and the tissue sections were protected from light from the moment they were incubated with the secondary antibody. Stained sections were analyzed using CLSM.

2.7. Evaluation of the imatinib concentrations in plasma and tissues

2.7.1. Mice treated with a single injection of imatinib mesylate

The protocols used for the measurement of the imatinib concentrations in plasma and kidneys have been adjusted from a protocol developed by Oosterdorp *et al.* (43). Plasma imatinib levels were established according to the following protocol. Calibration samples were prepared in a concentration range of 100 ng/ mL – 5 µg/ mL by dilution of a 100 µg/ mL imatinib mesylate stock solution in PBS with human plasma. Plasma samples were analyzed undiluted. Before extraction 50 µL of a 50 µg/ mL 4-hydroxybenzophenone (used as internal standard) stock solution in methanol was mixed with 100 µL sample. Imatinib mesylate was extracted from plasma using TBME. To each sample 1 mL TBME was added after which the samples were mixed vigorously for 5 minutes and centrifuged for 5 minutes at 7,500 x g. The aqueous layer was frozen in liquid nitrogen and the organic TBME layer was collected. After repeating the extraction the two TBME fractions were mixed by vortexing and the TBME was evaporated in a Speed-Vac Plus SC210A (45 minutes at 45 °C). Samples were reconstituted in 100 µL 2/ 3 PBS and 1/ 3 ACN by successively 15 minutes sonication, 5 minutes vortexing and 3 minutes centrifugation at 21,000 x g. Supernatants were analyzed by HPLC with the same method used for the characterization of imatinib-ULS-lysozyme.

For the evaluation of the renal imatinib levels calibration samples were prepared in blank kidney homogenates of untreated mice. The samples and blank homogenates were prepared by homogenizing kidney tissue in 4% (w/ v) BSA in water with a polytron tissue homogenizer in a final concentration of 0.1 gram tissue/ mL. The resulting tissue homogenates were extracted and analyzed as described above for the plasma samples. Blank human plasma and kidney homogenate were used as control.

2.7.2. Mice treated with a single injection of imatinib-ULS-lysozyme

Total imatinib (reflecting the sum of imatinib species bound to ULS-(lysozyme) and carrier-released imatinib) and released imatinib levels were measured in plasma, kidneys and heart. The released imatinib concentrations in plasma and kidneys were measured using the same protocol as described for the mice treated with a single injection of imatinib mesylate. Adjustments were made for the analysis of the released imatinib levels in heart. Samples and blank heart homogenates were prepared by homogenizing heart tissue in 4% (w/ v) BSA in water in a final concentration of 50 mg tissue/ mL. Calibration samples were prepared in a concentration range of 50 ng/ mL - 2.5 µg/ mL. Instead of 100 µL sample 200 µL was used for extraction. After evaporation of the TBME the heart samples were also reconstituted in 100 µL 2/ 3 PBS and 1/ 3 ACN and analyzed by HPLC.

For the analysis of the total imatinib concentrations in plasma, kidneys and heart, samples were treated with KSCN to displace non-released imatinib from the platinum linker. To this end, after the addition of the internal standard (*i.e.* 4-hydroxybenzophenone), samples were incubated with an equivolume of 1 M KSCN in PBS for 24 hours at 80 °C. The resulting solutions were extracted and analyzed as described above. Plasma samples taken at 1 minute after administration were diluted three times with blank human plasma. Blank human plasma and blank kidney- and heart homogenates were used as control.

For the detection of imatinib-ULS-lysozyme in urine, the urine sample was diluted fifty times with PBS before analysis. For the detection of ULS-bound and carrier-released imatinib the same protocol has been used as described above.

2.8. In vivo efficacy of imatinib-ULS-lysozyme

2.8.1. Treatment of mice with unilateral ureteral obstruction (UUO)

The *in vivo* efficacy of imatinib-ULS-lysozyme was studied in the mouse UUO model. In this model ureteral obstruction of one of the kidneys results in a reduced renal blood flow and glomerular filtration rate, leading to interstitial inflammation, tubular dilatation and atrophy and tubulointerstitial fibrosis (44). Male mice were randomly divided into five groups: normal mice (n = 6), untreated UUO mice (n = 6) and UUO mice treated with either a single intravenous injection of 40 mg/ kg imatinib-ULS-lysozyme (corresponding with 2.2 µmol/ kg imatinib, n = 7), a single intravenous injection of 2.2 µmol/ kg imatinib mesylate (n = 7) or a daily intraperitoneal injection of 50 mg/ kg (= 84.8 µmol/ kg) imatinib mesylate (n = 7). The high imatinib mesylate doses used in the last group were based on the initial doses used by Wang *et al.* in their study of the antifibrotic effects of imatinib mesylate in the same disease model in rats (30). Because a normal urinary flow is essential for the transport of imatinib-ULS-lysozyme to the apical side of the proximal tubular cells of the kidneys, the intravenous injections of imatinib-ULS-lysozyme and imatinib mesylate and the first intraperitoneal injection of imatinib mesylate were administered one hour prior to induction of UUO. The second and third intraperitoneal injections of 50 mg/ kg imatinib mesylate were administered at 24 and 48 hours, respectively, after induction of UUO.

Before surgery mice received a single subcutaneous injection of the non-steroidal anti-inflammatory drug carprofen (5 mg/ kg) to relief the pain afterwards. Under isoflurane anesthesia (3% in 100% O_2; 1 L/ min) the ureter of the left kidney was ligated at two places with 5-0 silk. Pain treatment was continued after surgery by a second and third subcutaneous injection

of carprofen at 24 and 48 hours, respectively. Mice were sacrificed after three days UUO and the obstructed kidneys were taken out and used for the evaluation of the antifibrotic activity of imatinib-ULS-lysozyme. A representative section of the kidney containing both cortex and medulla was used for the preparation of 4% formaldehyde-fixed paraffin-embedded tissue sections for immunostaining and the remaining was stored at -80 °C for quantitative reverse transcription-polymerase chain reactions (qRT-PCR) and western blot analysis.

2.8.2. Western blot analysis of activated PDGFR (p-PDGFR)

Cortex homogenates were prepared by homogenizing a small part of the cortex in 400 µL RIPA buffer supplemented with protease- and phosphatase inhibitors and EDTA. The protein content of the samples was measured with the Micro BCA™ Protein Assay Kit. To an aliquot of the samples corresponding with 50 µg protein, 7 µL 4x sodium dodecyl sulfate (SDS)-containing loading buffer was added. The total volume was adjusted to 30 µL by the addition of demineralized water. After shortly vortexing and centrifugation of the samples in an eppendorf table centrifuge the samples were heated for 7 minutes at 95 °C. The samples were shortly centrifuged again and loaded onto a precast 4-12% Bis-Tris gel. Protein separation was performed in MOPS SDS running buffer using an initial voltage of 120 V for the first 20 minutes and 170 V for the remaining run time. The proteins were transferred onto a PVDF membrane by wet blotting, using a transfer buffer consisting of 25 mM Tris, 192 mM glycine and 10% methanol (v/ v) and a voltage of 100 V for 1 hour. PVDF membranes were split in two parts: the membranes containing the proteins with a molecular size > 100 kDa were used for the detection of p-PDGFR-β and the membranes containing the proteins with a molecular size < 100 kDa for the detection of the household gene β-actin. Membranes were blocked for 1 hour at room temperature in blocking buffer consisting of 5% nonfat dry milk in Tris buffered saline (TBS; 20 mM Tris and 8 g/ L NaCl in demineralized water, pH 7.6) with 0.1% (v/ v) Tween-20 (TBS with 0.1% (v/ v) Tween-20 will be further referred to as TBS/ T). After washing the membranes with TBS/ T the membranes were incubated overnight at 4 °C with the primary antibodies (*i.e.* rabbit anti-mouse p-PDGFR-β (Tyr 740) (1:200) or rabbit anti-mouse β-actin (1:1000) polyclonal antibody) in TBS/ T with 5% (w/ v) BSA. The membranes were washed again and incubated for 1 hour at room temperature with HRP-conjugated goat anti-rabbit secondary antibody (1:1000 in TBS/ T with 5% (w/ v) nonfat dry milk). After washing the membranes the SuperSignal® West Femto Maximum Sensitivity Substrate Kit (Thermo Scientific, Etten-Leur, The Netherlands) was used for the detection of p-PDGFR-β and β-actin.

2.8.3. mRNA expression of profibrotic factors

The inhibitory effects of imatinib-ULS-lysozyme on the mRNA expression of collagen 1A2, PAI-1, fibronectin and MCP-1 in the whole kidneys and the cortex have been analyzed by qRT-PCR. Total RNA was isolated from > 1.8 mg tissue using the RNeasy KIT from QIAGEN (Venlo, The Netherlands). The RNA content in the samples was measured by UV-detection with the nanodrop (NanoDrop, Wilmington, Delaware, United States). After RNA extraction 300 ng RNA was used for the synthesis of cDNA. For the synthesis of cDNA the RevertAid™ Premium First Strand cDNA Synthesis Kit (Fermentas, Sankt Leon-Rot, Germany) was used. The obtained cDNA samples were diluted ten times with MilliQ water before use. For the qRT-PCR analyses

each sample consisted of 2.5 µL ten times diluted cDNA, 0.625 µL TagMan® Gene Expression Assay, 6.25 µL TaqMan® Universal PCR Master Mix and 3.125 µL MilliQ water. The analysis were performed using the Applied Biosystems ABI PRISM® 7900HT Sequence Detection System (Nieuwerkerk aan den IJssel, The Netherlands). Sequence Detection System Software v2.2 was used for data analysis. Between the different steps the samples were stored at -80 °C. Statistical analysis of the results was performed using one-way analysis of variance (ANOVA), with $p < 0.05$ as the minimal level of significance.

2.8.4. Immunostaining of profibrotic factors

Paraffin-embedded kidney sections were immunostained for α-SMA, collagen IV and vimentin. Sections of 3 µm were deparaffinized in xylene and hydrated in a graded series of alcohol baths. To inactivate the endogenous peroxidase activity the kidney sections were incubated for 15 minutes in blocking buffer, prepared by the addition of 1 part hydrogen peroxide 30% to 19 parts of a solution containing 8.32 g/ L citric acid, 21.52 g/ L disodium hydrogen phosphate dehydrate and 2 g/ L sodium azide (pH 5.8). The coupes were washed with demineralized water and boiled for 15 minutes in 10 mM citrate buffer with pH 6.0 (*i.e.* for collagen IV and vimentin) or Tris/ EDTA buffer (containing 4.84 g/ L Tris and 372 mg/ L EDTA) with pH 9.0 (*i.e.* for α-SMA) for epitope retrieval. After reaching room temperature, the kidney sections were washed with PBS/ 0.05T and incubated for 1 hour at room temperature with the primary antibody. Primary antibodies were diluted in PBS with 1% (w/ v) BSA; rabbit anti-mouse α-SMA 1:400, rabbit anti-mouse collagen IV 1:400 and rabbit anti-mouse vimentin 1:200. The kidney sections were washed with PBS/ 0.05T and incubated for 30 minutes at room temperature with undiluted HRP-conjugated brightvision goat anti-rabbit secondary antibody. Kidney sections were washed with PBS and incubated for ten minutes with DAB in the presence of hydrogen peroxide (H_2O_2). To 1 mL 6 g/ L DAB in demineralized water 9 mL phosphate/ citrate buffer, pH 9.0, and 10 µL hydrogen peroxide 30% were added. Nuclei were stained by successively washing the kidney sections with demineralized water, placing them in undiluted hematoxylin solution for 10-15 seconds and rinsing them with normal tap water for at least ten minutes. The kidney sections were dehydrated in a graded series of alcohol baths and xylene and mounted with DePeX in xylene (3 to 1 ratio). Stained sections were analyzed using light microscopy.

3. Results

3.1. Synthesis and characterization of imatinib-ULS-lysozyme

Coupling of imatinib to the ULS linker yielded imatinib-ULS complexes consisting for 91% of the desired imatinib-ULS 1:1 adduct and for 7% of the imatinib-ULS-imatinib adduct, as confirmed by HPLC and LC-MS analysis. ^{195}Pt-NMR analysis demonstrated the coupling of the platinum linker to the pyridine nitrogen atom.

The ULS linker readily reacts with methionine residues in proteins, but the methionine residues of lysozyme (two per molecule (45)) are buried in the core of the protein and therefore not accessible for the conjugation reaction. We therefore introduced surface-exposed methionine residues onto lysozyme, by reacting lysine residues with BOC-L-methionine *N*-hydroxysuccinimide ester. Analysis by MALDI-TOF mass spectrometry confirmed the formation of BOC-methionine-lysozyme species with respectively one, two, three and four methionine

residues attached to it. Lastly, imatinib-ULS was conjugated to methionine-modified lysozyme in a final drug to lysozyme ratio of 0.8 to 1, as confirmed by HPLC- and protein analysis (see **Figure 1** for the reaction scheme of imatinib-ULS-lysozyme).

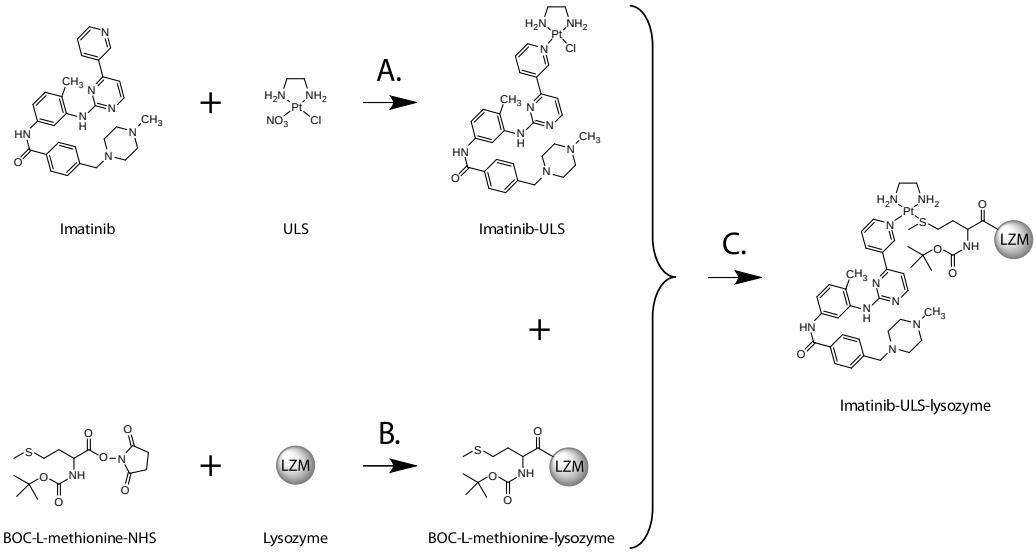

Figure 1. Reaction scheme for the synthesis of imatinib-ULS-lysozyme.

3.2. In vivo pharmacokinetics of imatinib-ULS-lysozyme

3.2.1. Internalization into renal proximal tubular cells

In the current study we aimed to deliver imatinib to the proximal tubular cells of the kidneys by conjugation to the renal carrier protein lysozyme. As stated before, lysozyme easily reaches and enters the target cells after glomerular filtration and subsequent internalization by the megalin receptor. Modification of the hydrophilic, cationic surface of lysozyme with methionine residues, the hydrophobic kinase inhibitor imatinib and the positively charged platinum linker might, however, have influenced the *in vivo* behaviour of lysozyme. We therefore investigated the pharmacokinetics of imatinib-ULS-lysozyme following intravenous administration in mice. We furthermore studied the fate of imatinib-ULS-lysozyme after intraperitoneal administration, to assess the extent and rate of absorption of the macromolecular conjugate.

As a first read-out of the renal uptake of imatinib-ULS-lysozyme in the kidneys and, more specifically, in the targeted cell type, we studied the colocalization of lysozyme with the internalizing megalin receptor on the apical membrane of the proximal tubular cells. For the lysozyme staining, an antibody was used that did not cross-react with mouse lysozyme, enabling us to study the renal accumulation of imatinib-ULS-lysozyme without interference of endogenous lysozyme. Results are shown in **Figure 2A** and **B**.

Figure 2A shows that imatinib-ULS-lysozyme was rapidly taken up by the proximal tubular cells after intravenous administration. Imatinib-ULS-lysozyme was already detectable inside the proximal tubular cells at ten minutes after intravenous administration. The internalization of imatinib-ULS-lysozyme was still ongoing at this time point, as indicated by the colocalization of

the renal carrier protein with the megalin receptor. At four hours after the intravenous injection of the conjugate, imatinib-ULS-lysozyme was intensively accumulated in the proximal tubular cells and primarily localized in vesicles. No colocalization of imatinib-ULS-lysozyme was observed at this time point, suggesting that the filtration of imatinib-ULS-lysozyme and subsequent binding to the cells had been completed. Lastly, at 24 hours after administration, lysozyme staining in the proximal tubular cells was absent, which confirmed the intracellular degradation of the renal carrier protein. As shown in **Figure 2B**, similar results were obtained for intraperitoneally injected imatinib-ULS-lysozyme. Also intraperitoneally administrated imatinib-ULS-lysozyme could be observed inside the proximal tubular cells at ten minutes after injection, although less intensively. A reasonable explanation for this is that intraperitoneally administered imatinib-ULS-lysozyme first needs to reach the blood stream from the peritoneal cavity. Uptake and degradation of the conjugate at 4 and 24 hours, respectively, after intraperitoneal injection were similar to intravenously administered imatinib-ULS-lysozyme.

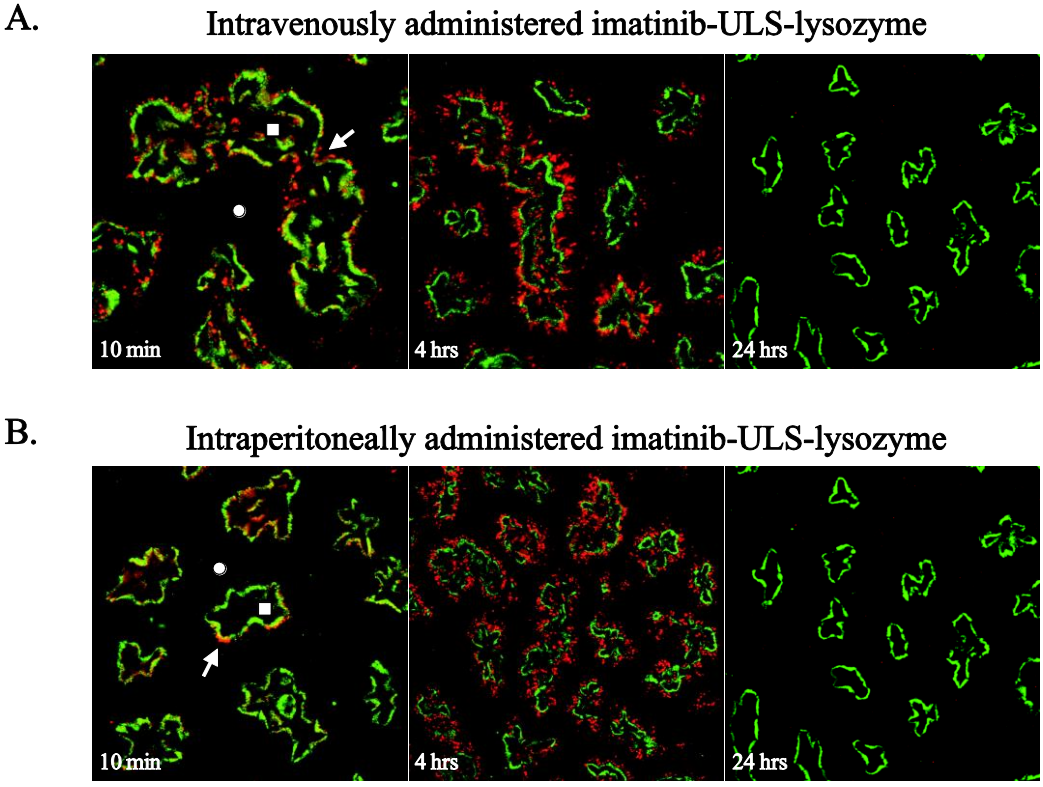

Figure 2. Colocalization of the renal carrier protein lysozyme and the internalizing megalin receptor on the proximal tubular cells of the kidneys after intravenous (A) and intraperitoneal (B) administration of a single dose of 20 mg/ kg imatinib-ULS-lysozyme. Formaldehyde-fixed paraffin-embedded kidney sections of 4 µm were immunostained for lysozyme (red colour) and megalin (green colour). The symbols in the figure represent the tubular lumen (□), the tubulointerstitial space (○) and the intracellular compartment of the proximal tubular cells (arrow).

3.2.2. Plasma disappearance of imatinib-ULS-lysozyme

The plasma disappearance of imatinib-ULS-lysozyme was evaluated by measuring the imatinib levels in the circulation (**Figure 3**). No released imatinib levels could be detected in the circulation after intravenous and intraperitoneal administration. Plasma disappearance curves of imatinib-ULS-lysozyme were fitted with a two compartment model. **Table 2** gives the pharmacokinetic parameters of the conjugate. Imatinib-ULS-lysozyme was rapidly eliminated from the circulation with an initial elimination half life of 12 minutes. But despite its rapid elimination, imatinib-ULS-lysozyme could be detected in the circulation for up to 24 hours after administration of the conjugate. This is in agreement with results obtained with earlier investigated kinase inhibitor-ULS-lysozyme conjugates with other kinase inhibitors (5-7). Upon intraperitoneal administration (**Figure 3B**) imatinib-ULS-lysozyme was rapidly absorbed from the peritoneal cavity (absorption half life of 29 minutes (**Table 2**)) and entered the circulation. The bioavailability of intraperitoneally injected imatinib-ULS-lysozyme was 100% as calculated from the plasma AUC.

Table 2. Pharmacokinetic parameters of imatinib-ULS-lysozyme derived from the plasma disappearance and renal accumulation curves after intravenous and intraperitoneal administration.

Pharmacokinetic parameter	Intravenous imatinib-ULS-lysozyme	Intraperitoneal imatinib-ULS-lysozyme
Plasma		
$(t_{1/2})_{absorption}$	-	29 min
$(t_{1/2})_{\alpha}$	12 min	
$(t_{1/2})_{\beta}$	18 h	
T_{max}	-	41 min
C_{max}	-	8.4%
Bioavailability	-	100%
Kidney		
$(t_{1/2})_{absorption}$	2.4 min	6.0 min
$(t_{1/2})_{elimination}$	48 h	67 h
T_{max}	24 min	58 min
C_{max}	5.6%	3.7%
$AUC_{0-\infty}$	368 h.%	360 h.%
Renal bioavailability		98%
Released imatinib in the kidney		
$AUC_{0-\infty}$	71 h.%	71 h.%

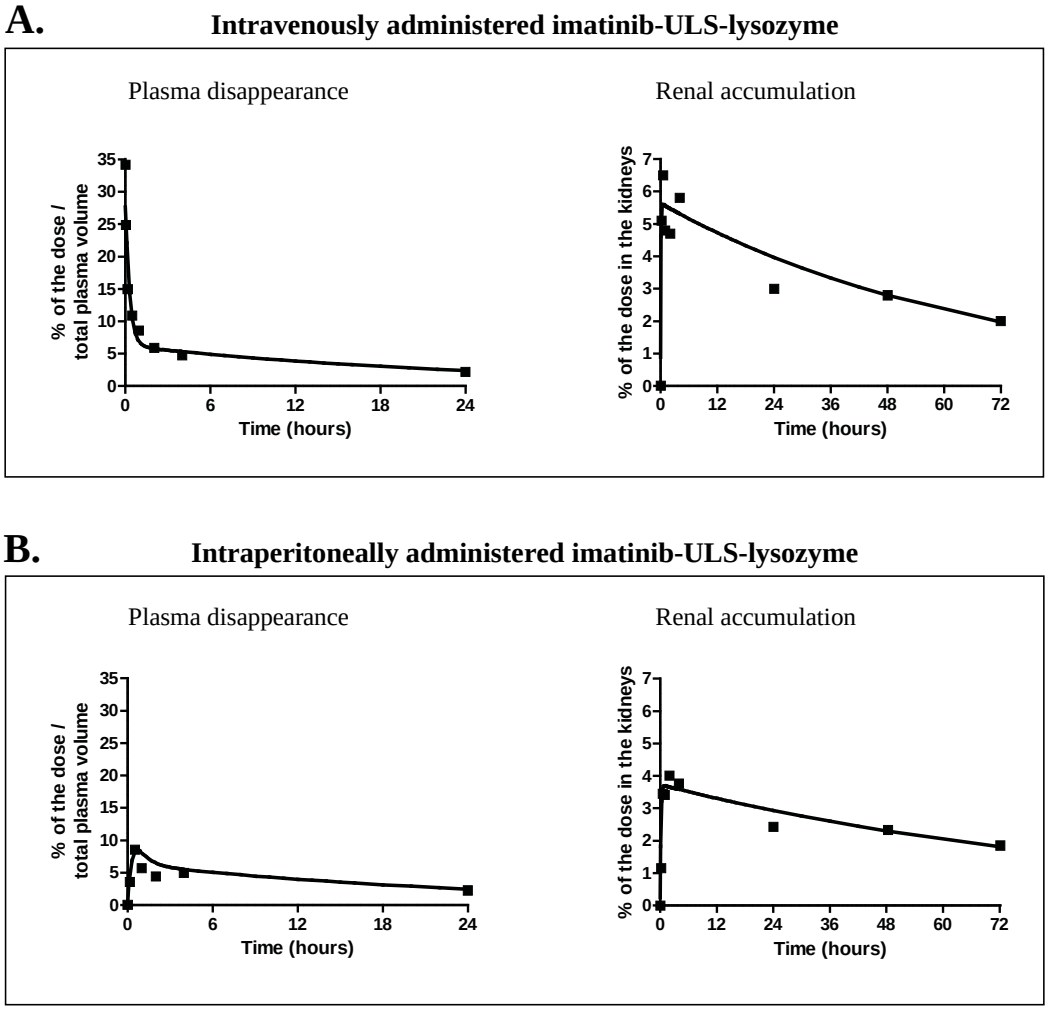

Figure 3. Plasma disappearance and renal accumulation of imatinib-ULS-lysozyme after intravenous (A) and intraperitoneal (B) administration in mice. Symbols represent the percentage of the imatinib-ULS-lysozyme dose at each time point. The calculation of the % of the dose in the total plasma volume was based on an average plasma volume of 0.05 mL/ g of mouse body weight (46). The continuous lines represent the data fitted to a two-compartment model.

3.2.3. Renal accumulation of imatinib-ULS-lysozyme

Total renal imatinib levels (**Figure 3**) were fitted with a two-compartment model and the pharmacokinetic parameters are summarized in **Table 2**. Intravenously administered imatinib-ULS-lysozyme was rapidly taken up from the circulation by the kidneys with a $(t_{1/2})_{absorption}$ of 2.4 minutes. A maximum renal level of 5.6% of the injected dose was observed within half-an-hour after intravenous administration. In accordance with the rapid appearance of imatinib-ULS-lysozyme in the circulation after intraperitoneal administration, the conjugate was rapidly taken

up by the kidneys. Intraperitoneally administered imatinib-ULS-lysozyme was taken up with a $(t_{1/2})_{absorption}$ of 6 minutes and the maximum renal level of 3.7% of the injected dose was reached within 1 hour after injection. These data confirmed the results of the immunohistochemical staining of imatinib-ULS-lysozyme in kidney sections. The renal bioavailability of intraperitoneally administered imatinib-ULS-lysozyme was almost 100%, as calculated from the renal AUC of both treatments. Imatinib-ULS-lysozyme was slowly eliminated from the kidneys, with a renal half-life of over 2 days (*i.e.* 48 h and 67 h for intravenously and intraperitoneally administered imatinib-ULS-lysozyme, respectively).

3.2.4. Intracellular release of imatinib

Figure 4 shows the released versus the total imatinib levels in the kidneys after intravenous and intraperitoneal administration of a single dose of imatinib-ULS-lysozyme. After intravenous as well as intraperitoneal administration, released imatinib was already detectable within ten minutes after injection of imatinib-ULS-lysozyme. A maximum renal level of released imatinib of 1.3% of the injected dose was obtained at 30 minutes after administration.

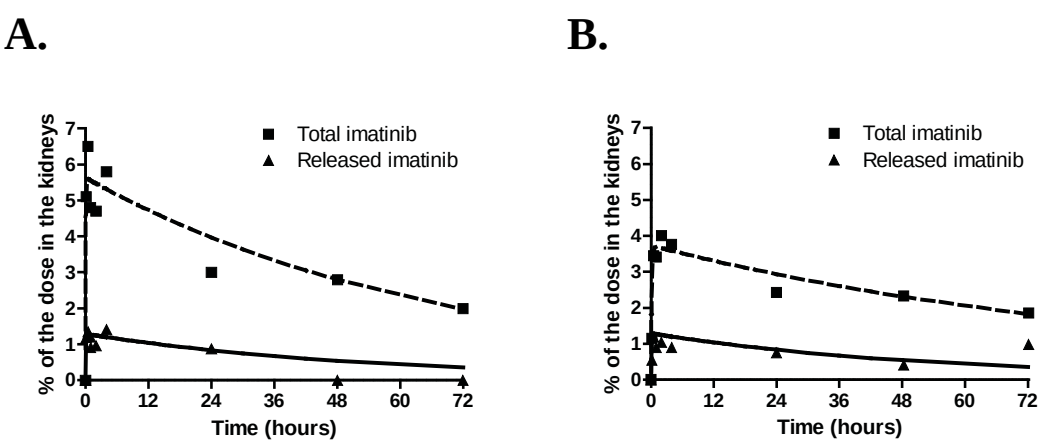

Figure 4. Total and released imatinib levels in the kidneys after administration of a single intravenous (A) and intraperitoneal (B) injection of imatinib-ULS-lysozyme mice. Symbols represent the percentage of the imatinib-ULS-lysozyme dose at each time point. The continuous lines represent the data fitted to a two-compartment model.

The released imatinib levels were compared with those obtained after administration of imatinib mesylate (**Figure 5**). **Table 3** shows the pharmacokinetic parameters of imatinib mesylate after intravenous and intraperitoneal administration, calculated by fitting the data to a two-compartment model. Imatinib mesylate was rapidly taken up by the kidneys with an absorption half live of 7.2 minutes and 8.4 minutes after intravenous and intraperitoneal administration, respectively. The renal exposure to imatinib (renal AUC) was approximately two times higher after intraperitoneal administration as compared with intravenous administration. This observation can be explained by the fact that intraperitoneally administered imatinib mesylate not only reaches the kidney via the circulation, but also via direct transport from the peritoneal

cavity to the kidneys. Although the peak concentrations after intravenous and intraperitoneal administration of imatinib mesylate (*i.e.* 3.7 and 7.8%, respectively) were higher compared to the released imatinib levels after administration of imatinib-ULS-lysozyme (*i.e.* 1.3%), imatinib mesylate was rapidly eliminated from the kidneys ($(t_{1/2})_{elimination}$: 12.0 and 9.0 minutes after intravenous and intraperitoneal administration, respectively). In contrast, imatinib-ULS-lysozyme provided sustained levels of imatinib. As a consequence, intravenous and intraperitoneal administration of imatinib-ULS-lysozyme resulted in a, respectively, 30 and 15 times higher renal exposure to active imatinib (renal AUC) as compared to imatinib mesylate.

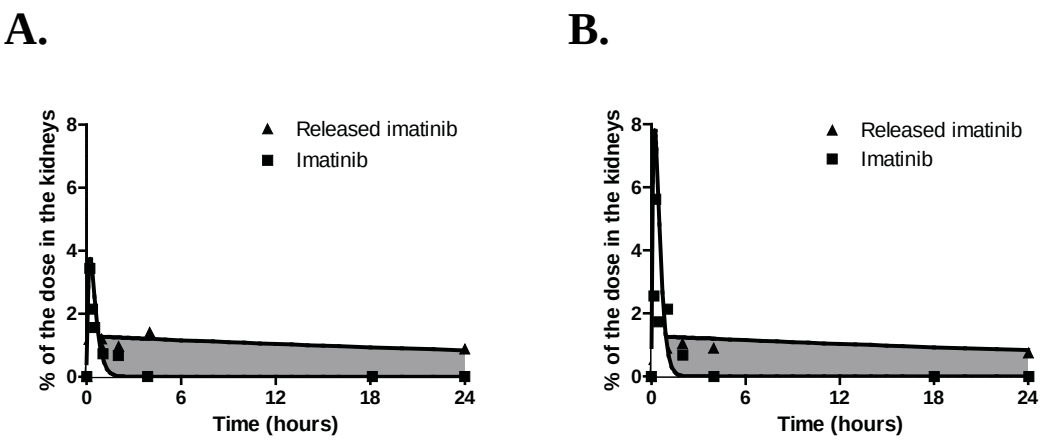

Figure 5. Imatinib levels in the kidneys after administration of imatinib-ULS-lysozyme and imatinib mesylate. Symbols represent the percentage of the dose at each time point. The continuous lines represent the data fitted to a two-compartment model. A = intravenous administration; B = intrapertitoneal administration.

Table 3. Pharmacokinetic parameters of imatinib mesylate derived from the plasma renal accumulation curves after intravenous and intraperitoneal administration.

Pharmacokinetic parameter	**Intravenous imatinib mesylate**	**Intraperitoneal imatinib mesylate**
$(t_{1/2})_{absorption}$	7.2 min	8.4 min
$(t_{1/2})_{elimination}$	12.0 min	9.0 min
T_{max}	14 min	13 min
C_{max}	3.7%	7.8%
$AUC_{0-\infty}$	2.4 h.% dose	4.6 h.% dose

3.2.5. Distribution of imatinib-ULS-lysozyme to other organs

Since the long term use of high doses imatinib is associated with cardiotoxicity (40) we evaluated the biodistribution of imatinib-ULS-lysozyme to the heart tissue. **Figure 6** shows the results of the anti-lysozyme staining of heart sections at two hours after intravenous (panel A) and intraperitoneal (panel B) administration of imatinib-ULS-lysozyme.

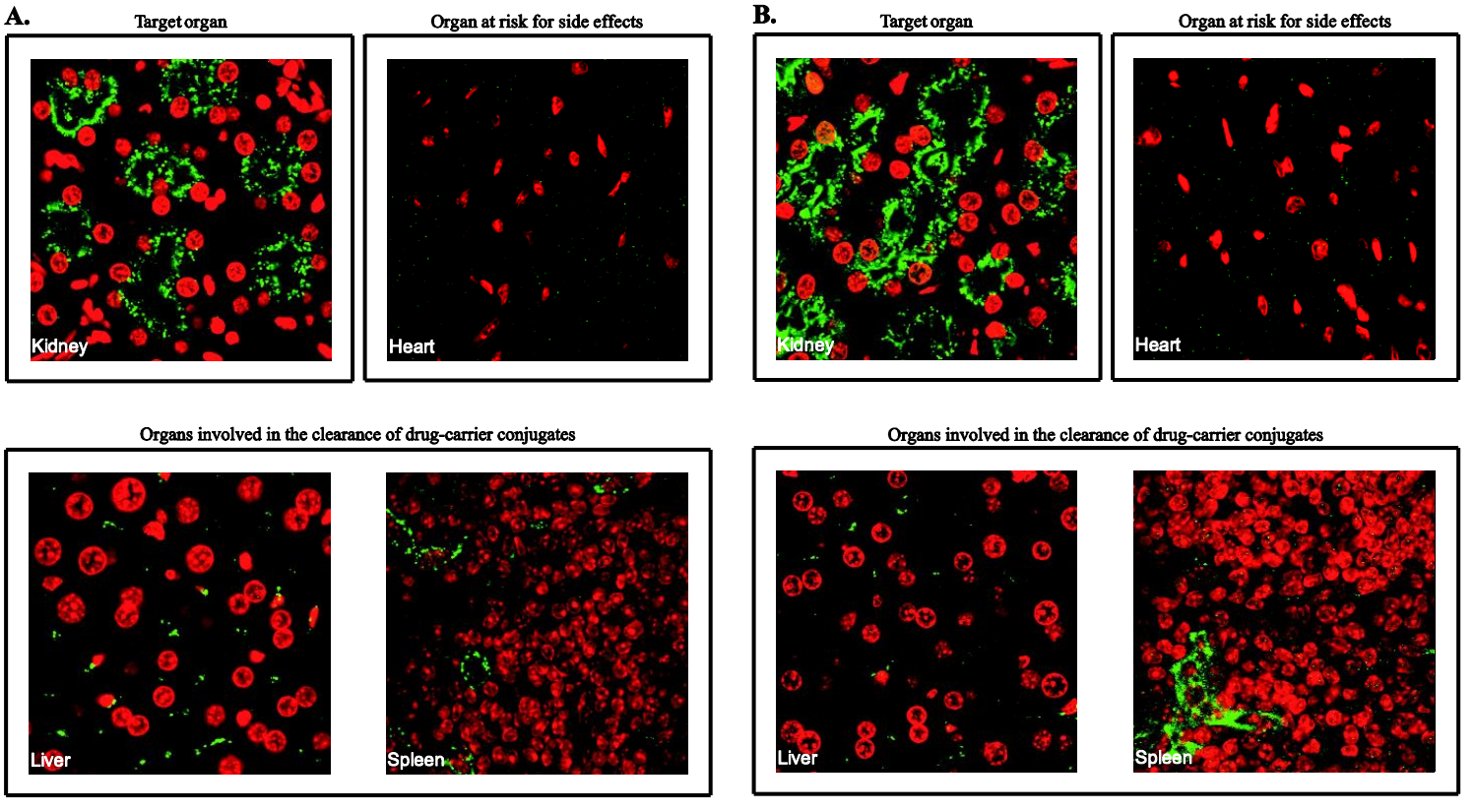

Figure 6. Organ distribution of imatinib-ULS-lysozyme two hours after a single intravenous (A) and intraperitoneal (B) injection of 20 mg/ kg in mice. Formaldehyde-fixed paraffin-embedded kidney-, heart-, liver-, and spleen sections of 3 µm were immunostained for lysozyme (green colour). Nuclei were stained with TOPRO-3 iodide (red colour). Sections were analyzed with CLSM.

No lysozyme could be detected in the heart after both routes of administration. These results were confirmed by the HPLC analysis of imatinib levels in the heart. Neither platinum-bound nor released imatinib was detected in heart tissue.

The potential uptake of imatinib-ULS-lysozyme in organs involved in the clearance of macromolecular drug conjugates, *i.e.* liver and spleen was also investigated. **Figure 6** shows that imatinib-ULS-lysozyme was primarily detected in the intercellular space of the liver and the vasculature of the spleen, but the levels were much less than in the kidneys. The excretion of imatinib in the urine collected during the first 30 minutes after intravenous administration of imatinib-ULS-lysozyme was measured. Imatinib could be detected in the urine within 30 minutes after the intravenous administration of imatinib-ULS-lysozyme. The majority of the imatinib present in the urine was present in its released form. As stated before, no released imatinib could be detected in the circulation after the administration of imatinib-ULS-lysozyme. This implicates that the free imatinib detected in the urine is excreted from the target cells into the urine.

3.3. In vivo efficacy of imatinib-ULS-lysozyme

3.3.1. Inhibitory effects of imatinib-ULS-lysozyme on p-PDGFR-β

The efficacy of imatinib-ULS-lysozyme was studied in the UUO model of tubulointerstitial fibrosis, after a single intravenous dose. Mice were subjected to three days of ureteral obstruction. The activation of PDGFR-β kinase was studied in mice with UUO by western blot analysis (**Figure 7A**). This figure shows that three days UUO resulted in a moderately increased activity of PDGFR-β kinase in the renal cortex, as demonstrated by the increased p-PDGFR-β levels. From **Figure 7B** it can be observed that no inhibitory effect was obtained with imatinib-ULS-lysozyme nor with the low and high doses imatinib mesylate.

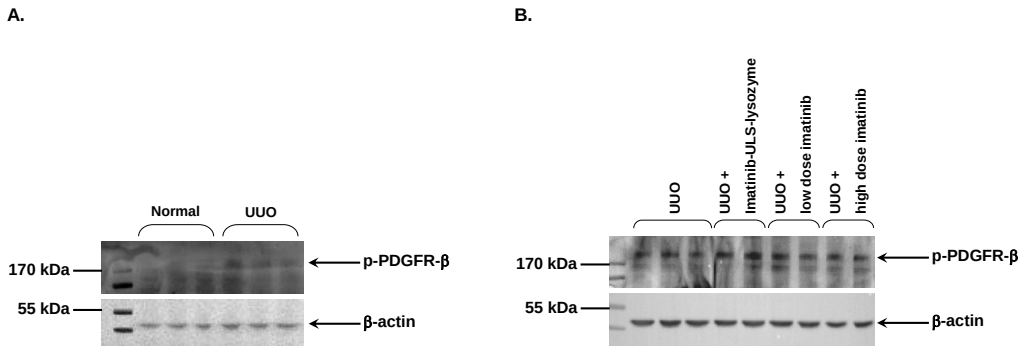

Figure 7. Western blot detection of p-PDGFR-β kinase in the renal cortex. Figure A displays the difference between normal mice and UUO mice. Figure B shows the effects of the therapeutic interventions on the elevated p-PDGFR-β levels in UUO mice. The expression of β-Actin was used as for normalization of expression levels.

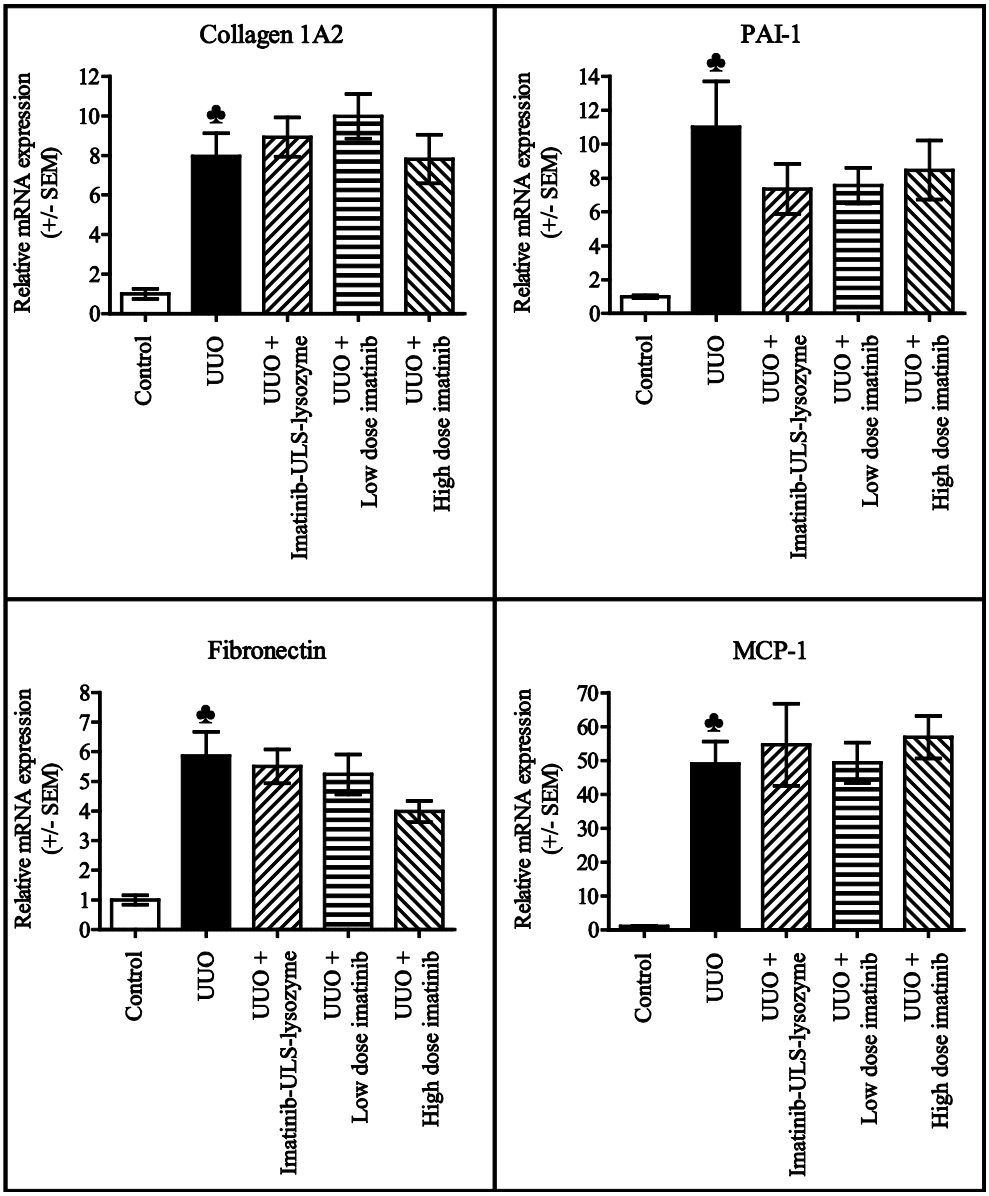

Figure 8. mRNA expression of collagen 1A2, PAI-1, fibronectin and MCP-1 in the kidneys of normal mice (n = 6), UUO mice (n = 6) and UUO mice treated with a single intravenous injection of 40 mg/ kg imatinib-ULS-lysozyme (corresponding with 2.2 µmol/ kg imatinib) (n = 7), a single intravenous injection of a low dose (*i.e.* 2.2 µmol/ kg) imatinib mesylate (n = 7) or daily intraperitoneal injections of a high dose (*i.e.* 50 mg/ kg or 84.8 µmol/ kg) imatinib mesylate (n = 7). mRNA levels were normalized to the household gene TBP. The normalized mRNA expression levels in the kidneys of non-treated and treated mice with UUO were related to the normalized mRNA expression levels in the kidneys of control mice (set at 1). Data represent the mean +/ - SEM. Statistical differences are indicated as ♣ ($p < 0.05$).

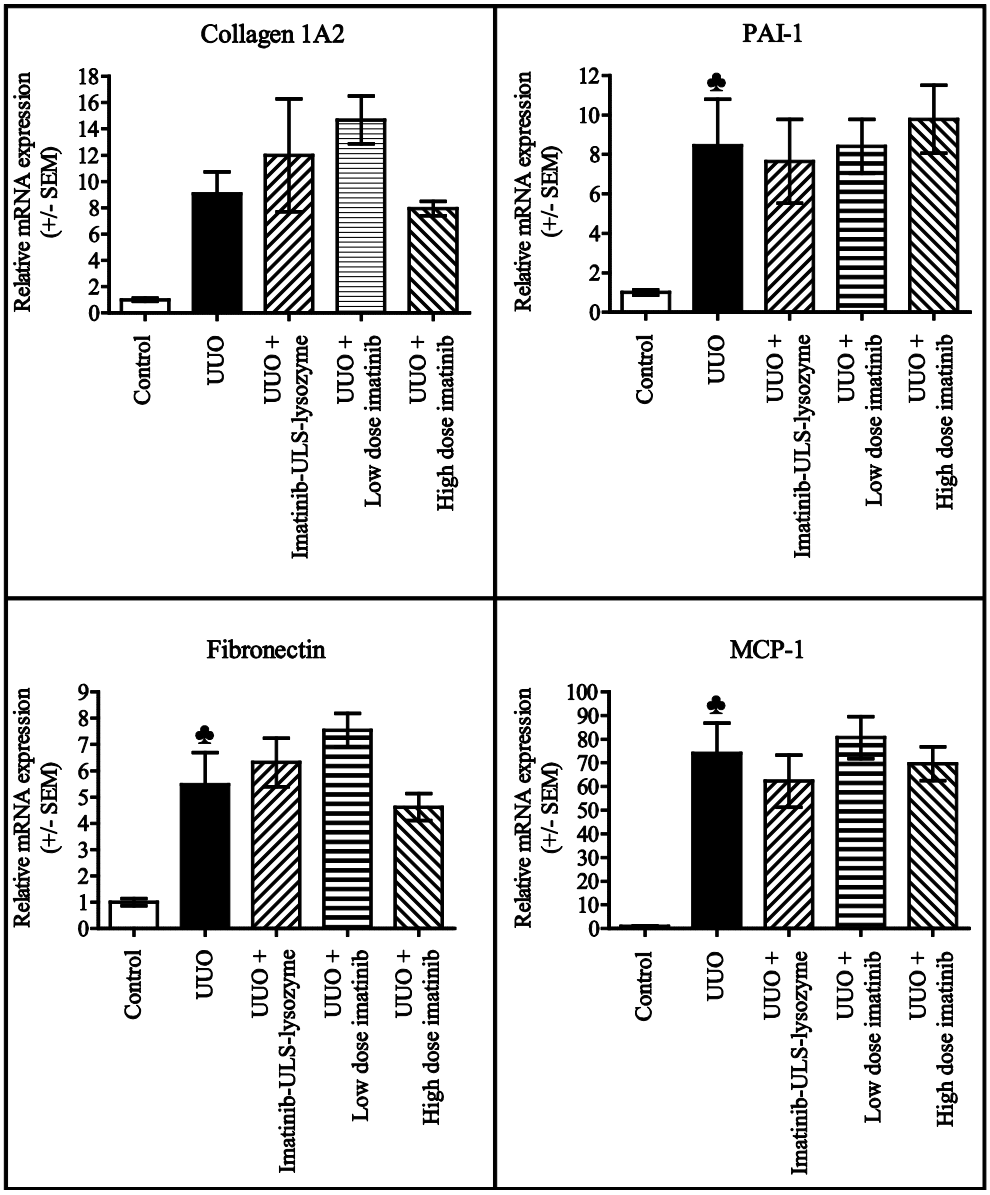

Figure 9. mRNA expression of collagen 1A2, PAI-1, fibronectin and MCP-1 in the renal cortex of normal mice (n = 6), UUO mice (n = 6) and UUO mice treated with a single intravenous injection of 40 mg/ kg imatinib-ULS-lysozyme (corresponding with 2.2 µmol/ kg imatinib) (n = 7), a single intravenous injection of a low dose (*i.e.* 2.2 µmol/ kg) imatinib mesylate (n = 7) or daily intraperitoneal injections of a high dose (*i.e.* 50 mg/ kg or 84.8 µmol/ kg) imatinib mesylate (n = 7). mRNA levels were normalized to the household gene TBP. The normalized mRNA expression levels in the kidneys of non-treated and treated mice with UUO were related to the normalized mRNA expression levels in the kidneys of control mice (set at 1). Data represent the mean +/ - SEM. Statistical differences are indicated as ♣ ($p < 0.05$).

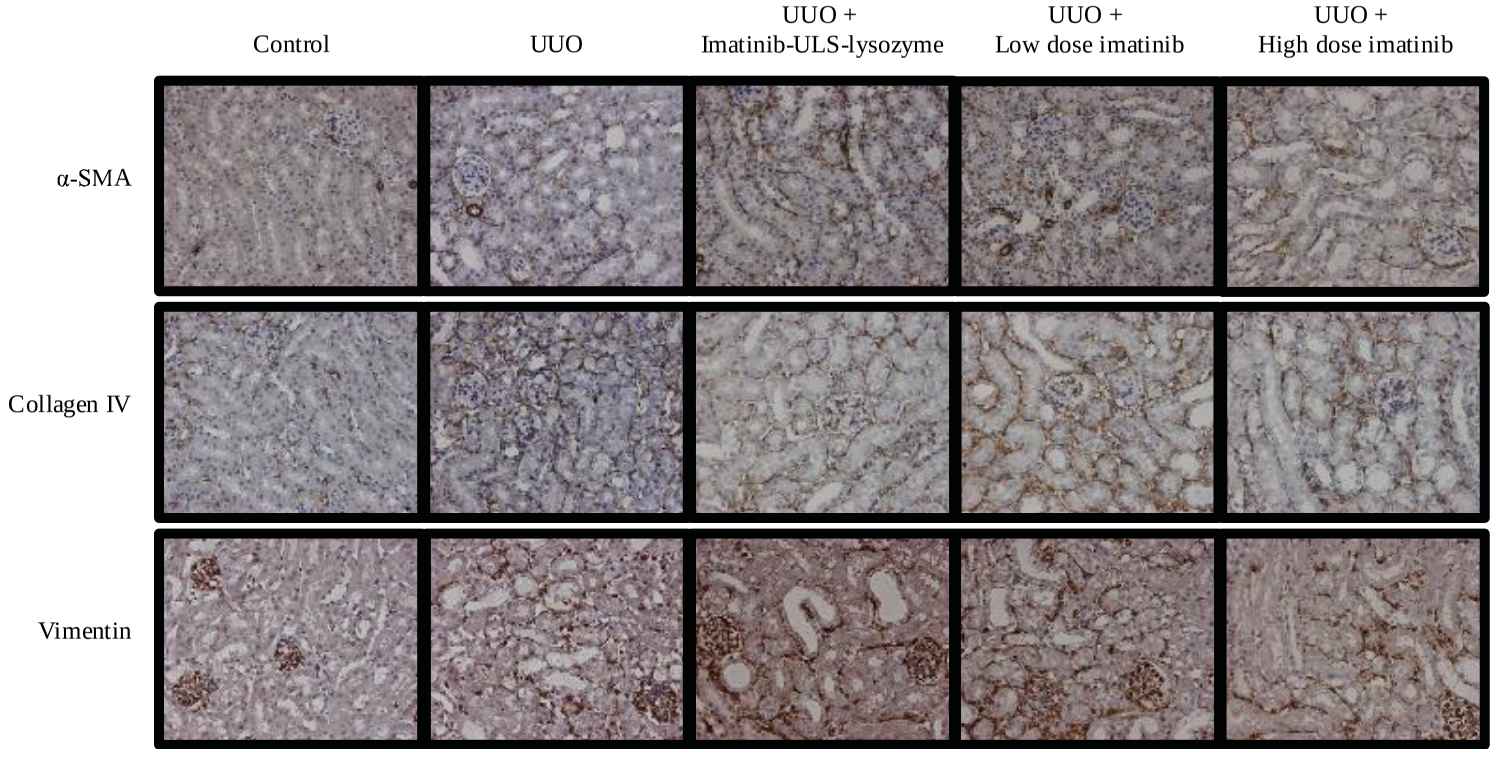

Figure 10. Representative microscopic images of paraffin-embedded kidney sections of control mice, UUO mice and UUO mice treated with a single intravenous injection of imatinib-ULS-lysozyme, a single intravenous injection of a low dose of imatinib (as mesylate) or daily intraperitoneal injections of a high dose of imatinib (as mesylate). Kidney sections were immunostained for α-SMA, collagen IV and vimentin (brown colour) and nuclei were counterstained with hematoxylin (blue colour). Magnification of the images: 20x.

3.3.2. Inhibitory effects of imatinib-ULS-lysozyme on downstream profibrotic factors

The inhibitory effects of imatinib-ULS-lysozyme on the mRNA expression of the profibrotic factors collagen 1A2, PAI-1, fibronectin and MCP-1 were analyzed by qRT-PCR. Collagen 1A2, PAI-1 and fibronectin are involved in the formation of ECM, while MCP-1 is involved in the inflammatory response in tubulointerstitial fibrosis (19, 28). The mRNA expression levels of collagen 1A2, PAI-1, fibronectin and MCP-1 were significantly elevated in the kidneys of mice with three days UUO (**Figure 8**). But no inhibitory effects were obtained with imatinib-ULS-lysozyme nor with the low and high dosage imatinib mesylate.

Since the proximal tubular cells are most abundant in the renal cortex, the gene expression levels of collagen 1A2, PAI-1, fibronectin and MCP-1 in the renal cortex were also evaluated (**Figure 9**). Similar elevations in expression levels of untreated UUO mice were found. Also in the renal cortex, however, no inhibition was observed for either imatinib-ULS-lysozyme or imatinib mesylate in low and high dosage.

Paraffin-embedded kidney sections were immunostained for α-SMA, collagen IV and vimentin. These profibrotic factors are involved in EMT (α-SMA and vimentin) and the formation of ECM (collagen IV and vimentin) (19, 47, 48). An increased deposition of α-SMA, collagen IV and vimentin was observed in the kidneys after three days UUO. But no inhibitory effects were obtained with imatinib-ULS-lysozyme nor with the low and high doses imatinib mesylate (**Figure 10**).

4. Discussion

Imatinib is an inhibitor of the PDGFR kinase and the TGFR-β mediated activation of c-Abl kinase. Although activated PDGFR- and c-Abl kinases are involved in the development of fibrotic diseases, variable successes have been obtained with imatinib in the treatment of fibrotic diseases. We investigated the delivery of imatinib using a water soluble macromolecular conjugate of this drug (imatinib-ULS-lysozyme). This conjugate is directed to the proximal tubular cells of the kidneys. We used this technique to investigate the role of this cell type in the antifibrotic effects of imatinib in the treatment of tubulointerstitial fibrosis.

In earlier studies, the imatinib derivative PAP19 has successfully been delivered to the hepatic stellate cells (HSC) of the liver by conjugation to the HSC-specific carrier mannose-6-phosphate modified human serum albumin (M6PHSA) (41). We now conjugated imatinib to the carrier protein lysozyme using the same platinum linker (*i.e.* ULS) as has been used in the PAP19-M6PHSA conjugate. An important characteristic of drug-ULS-carrier conjugates is the long residence time of the drug-ULS metabolites within the target cells and the sustained release of the drug (7, 41). Imatinib-ULS-lysozyme rapidly accumulated in the kidneys after intravenous as well as intraperitoneal administration. The time course of internalization of imatinib-ULS-lysozyme by the proximal tubular cells was followed by detection of the colocalization of the renal carrier lysozyme and the megalin receptor on the apical membrane of the target cells. Imatinib-ULS-lysozyme could be detected inside the proximal tubular cells within ten minutes after both intravenous and intraperitoneal injection. This means that, in accordance with our observations, imatinib-ULS-lysozyme was able to rapidly reach the blood stream from the peritoneal cavity, which can be explained by the size-independent transport of macromolecules from the peritoneal cavity into the bloodstream (49) and prevention of slower transport by the lymphatic system. As expected, the delivered kinase inhibitor resided within the target cells for

at least three days, and may therefore provide a prolonged inhibition of the targeted signaling cascades.

In imatinib-ULS-lysozyme the platinum linker is coupled to the pyridine nitrogen of imatinib, which is part of the pharmacophore responsible for the PDGFR- and c-Abl kinase inhibitory activity (50, 51). The pyridine moiety binds to the adenine pocket of the target kinases, where the aromatic nitrogen acts as a hydrogen bond acceptor (52). Attachment of the platinum linker to the pyridine ring may hinder the binding of imatinib to the ATP-binding pocket of the target kinases, and thus may interfere with the inhibitory activity of imatinib. Intracellular release of imatinib from the platinum linker is, therefore, likely essential for the activity of imatinib-ULS-lysozyme. We therefore also measured the released imatinib levels in the kidneys. Compared with the intravenous and intraperitoneal administration of imatinib mesylate, a single intravenous and intraperitoneal injection of lysozyme-conjugated imatinib resulted in a, respectively, 30- and 15-fold higher renal exposure of active (*i.e.* released) imatinib.

We evaluated the efficacy of imatinib-ULS-lysozyme in the UUO model of tubulointerstitial fibrosis, since prior studies reported favourable effects of imatinib in this model (30, 38). Animals were treated with a single intravenous injection of the conjugate. In the current study, however, no efficacy was obtained with imatinib-ULS-lysozyme nor with the low and high doses imatinib mesylate. In the studies performed by Wang *et al.* the efficacy of imatinib was investigated in mice that had suffered from seven days ureteral obstruction. Treatment of the animals with daily intraperitoneal injections of 50 mg/ kg (days 1-2), 100 mg/ kg (days 3-4) and 150 mg/ kg (days 5-7) imatinib mesylate, resulted in a decreased deposition and/ or production of, among others, collagen IV, fibronectin and α-SMA (30). Although the mice in the current study were only subjected to three days ureteral obstruction, the kidneys of these animals also showed increased levels of collagen IV, fibronectin and α-SMA. Unexpectedly, daily treatment with 50 mg/ kg imatinib mesylate did not result in inhibitory effects. A possible explanation for the lack of efficacy in our study may be the duration of ureter obstruction. So far, PDGFR kinase inhibitors have only been investigated for their potency in the treatment of tubulointerstitial fibrosis in animals subjected to UUO for seven days up tot 21 days of UUO (30, 38, 53). We now only studied early fibrotic events in the kidneys, and it may be possible that the processes targeted by imatinib are not yet induced during three days of ureter obstruction. Among the cell types that express PDGFR-β kinase are fibroblasts and myofibroblasts (10, 24, 54). EMT of proximal tubular cells into myofibroblasts is an important source of the increased number of PDGFR-β kinase-positive myofibroblasts in the interstitium of animals with UUO-induced tubulointerstitial fibrosis (55, 56). Since EMT in the UUO model is not evident at 3 days after ureteral obstruction (47), the relatively low activation of PDGFR-β kinase might explain the lack of efficacy observed with the high dosage of imatinib. EMT is evident from day 7 after ureteral obstruction (47).

As discussed above, one of the major differences between our study and previous reports is the relative short duration of ureteral obstruction. Several technical aspects of the UUO model however limited us in treating the animals at a later stage of the disease. We now studied the disease process up to day 3, based on the renal release profile of imatinib-ULS-lysozyme after a single dose. Extension of the treatment period would require repeated dosing of the conjugate. For internalization of imatinib-ULS-lysozyme into the proximal tubular cells it, however, is essential that the conjugate is able to reach the megalin receptor at the apical membrane of the cells, and hence is filtered in the tubular lumen. Since in the UUO model the urinary flow is

blocked, the conjugate could only be administered once before ureteral obstruction. Thus, it still can be that imatinib-ULS-lysozyme is effective in the treatment of tubulointerstitial fibrosis when investigated in animals that are longer subjected to ureteral obstruction. Such studies however would require major changes in the model, such as a restoration of the urine flow by ureter transplantation.

Conclusion

Coupling of the kinase inhibitor imatinib to lysozyme via the platinum linker ULS yields a conjugate that specifically delivers the kinase inhibitor into the proximal tubular cells of the kidneys and avoids transport of imatinib to the heart. Imatinib-ULS-lysozyme can be administered intravenously as well as intraperitoneally and slowly releases the kinase inhibitor within the target cells. The development of this cell-specific conjugate offers the possibility to study the role of, among other targets, PDGFR- and c-Abl kinase in the proximal tubular cells in the pathogeneses of renal diseases. Although a moderately increased activity of PDGFR-β was observed in mice subjected to three days UUO, treatment neither with imatinib mesylate nor with imatinib-ULS-lysozyme could inhibit the profibrotic events. Further evaluation of imatinib mesylate and imatinib-ULS-lysozyme is warranted in an animal model for tubulointerstitial fibrosis in which the activation of PDGFR-β is more pronounced.

Acknowledgements

We would like to thank D.M. van der Giezen for her assistance in the animal efficacy study and immunohistochemical analyses. We also would like to thank W.W. Kassing – van der Ven for her assistance in the pharmacokinetics study and K. van der Ven for his assistance in the immunohistochemical analyses and J.W. Leeuwis and A. Dendooven for their assistance in the immunohistochemical and qRT-PCR analyses. This work was made possible by a grant from the European Framework program FP6 (LSHB-CT-2007-036644).

References

1. E.I. Christensen, P.J. Verroust and R. Nielsen. Receptor-mediated endocytosis in renal proximal tubule. Pflugers Arch. 458:1039-1048 (2009).
2. E.I. Christensen and H. Birn. Megalin and cubilin: synergistic endocytic receptors in renal proximal tubule. Am J Physiol Renal Physiol. 280:F562-573 (2001).
3. M.E.M. Dolman, S. Harmsen, G. Storm, W.E. Hennink and R.J. Kok. Drug targeting to the kidney: Advances in the active targeting of therapeutics to proximal tubular cells. Adv Drug Deliv Rev (2010).
4. P.J. Verroust, H. Birn, R. Nielsen, R. Kozyraki and E.I. Christensen. The tandem endocytic receptors megalin and cubilin are important proteins in renal pathology. Kidney Int. 62:745-756 (2002).
5. J. Prakash, M.H. de Borst, M. Lacombe, F. Opdam, P.A. Klok, H. van Goor, D.K. Meijer, F. Moolenaar, K. Poelstra and R.J. Kok. Inhibition of renal rho kinase attenuates ischemia/ reperfusion-induced injury. J Am Soc Nephrol. 19:2086-2097 (2008).
6. J. Prakash, M.H. de Borst, A.M. van Loenen-Weemaes, M. Lacombe, F. Opdam, H. van Goor, D.K. Meijer, F. Moolenaar, K. Poelstra and R.J. Kok. Cell-specific delivery of a transforming growth factor-beta type I receptor kinase inhibitor to proximal tubular cells for the treatment of renal fibrosis. Pharm Res. 25:2427-2439 (2008).
7. J. Prakash, M. Sandovici, V. Saluja, M. Lacombe, R.Q. Schaapveld, M.H. de Borst, H. van Goor, R.H. Henning, J.H. Proost, F. Moolenaar, G. Keri, D.K. Meijer, K. Poelstra and R.J. Kok. Intracellular delivery of the p38 mitogen-activated protein kinase inhibitor SB202190 [4-(4-fluorophenyl)-2-(4-hydroxyphenyl)-5-(4-pyridyl)1H-imidazole] in renal tubular cells: a novel strategy to treat renal fibrosis. J Pharmacol Exp Ther. 319:8-19 (2006).
8. Z. Zhang, Q. Zheng, J. Han, G. Gao, J. Liu, T. Gong, Z. Gu, Y. Huang, X. Sun and Q. He. The targeting of 14-succinate triptolide-lysozyme conjugate to proximal renal tubular epithelial cells. Biomaterials. 30:1372-1381 (2009).
9. L.O. Lerman and A.R. Chade. Angiogenesis in the kidney: a new therapeutic target? Curr Opin Nephrol Hypertens. 18:160-165 (2009).
10. P. Boor, T. Ostendorf and J. Floege. Renal fibrosis: novel insights into mechanisms and therapeutic targets. Nat Rev Nephrol. 6:643-656 (2010).
11. Y. Liu. Renal fibrosis: new insights into the pathogenesis and therapeutics. Kidney Int. 69:213-217 (2006).
12. M. Zeisberg and E.G. Neilson. Mechanisms of tubulointerstitial fibrosis. J Am Soc Nephrol. 21:1819-1834 (2010).
13. A. Arora and E.M. Scholar. Role of tyrosine kinase inhibitors in cancer therapy. J Pharmacol Exp Ther. 315:971-979 (2005).
14. S.K. Grant. Therapeutic protein kinase inhibitors. Cell Mol Life Sci. 66:1163-1177 (2009).
15. J. Rosenbloom, S.V. Castro and S.A. Jimenez. Narrative review: fibrotic diseases: cellular and molecular mechanisms and novel therapies. Ann Intern Med. 152:159-166 (2010).
16. M.L. Hensley and J.M. Ford. Imatinib treatment: specific issues related to safety, fertility, and pregnancy. Semin Hematol. 40:21-25 (2003).
17. J.H. Distler and O. Distler. Imatinib as a novel therapeutic approach for fibrotic disorders. Rheumatology (Oxford). 48:2-4 (2009).
18. Y. Dai. Platelet-derived growth factor receptor tyrosine kinase inhibitors: a review of the recent patent literature. Expert Opin Ther Pat. 20:885-897 (2010).
19. M.S. Razzaque and T. Taguchi. Cellular and molecular events leading to renal tubulointerstitial fibrosis. Med Electron Microsc. 35:68-80 (2002).
20. J. Andrae, R. Gallini and C. Betsholtz. Role of platelet-derived growth factors in physiology and medicine. Genes Dev. 22:1276-1312 (2008).
21. A. Leask and D.J. Abraham. TGF-beta signaling and the fibrotic response. FASEB J. 18:816-827 (2004).
22. M. Takikita-Suzuki, M. Haneda, M. Sasahara, M.K. Owada, T. Nakagawa, M. Isono, S. Takikita, D. Koya, K. Ogasawara and R. Kikkawa. Activation of Src kinase in platelet-derived growth factor-B-dependent tubular regeneration after acute ischemic renal injury. Am J Pathol. 163:277-286 (2003).
23. P. Boor, K. Sebekova, T. Ostendorf and J. Floege. Treatment targets in renal fibrosis. Nephrol Dial Transplant. 22:3391-3407 (2007).

24. J. Floege, F. Eitner and C.E. Alpers. A new look at platelet-derived growth factor in renal disease. J Am Soc Nephrol. 19:12-23 (2008).
25. E.P. Bottinger and M. Bitzer. TGF-beta signaling in renal disease. J Am Soc Nephrol. 13:2600-2610 (2002).
26. W.W. Tang, T.R. Ulich, D.L. Lacey, D.C. Hill, M. Qi, S.A. Kaufman, G.Y. Van, J.E. Tarpley and J.S. Yee. Platelet-derived growth factor-BB induces renal tubulointerstitial myofibroblast formation and tubulointerstitial fibrosis. Am J Pathol. 148:1169-1180 (1996).
27. M. Trojanowska. Role of PDGF in fibrotic diseases and systemic sclerosis. Rheumatology (Oxford). 47 Suppl 5:v2-4 (2008).
28. A.A. Eddy. Molecular basis of renal fibrosis. Pediatr Nephrol. 15:290-301 (2000).
29. S. Bhattacharyya, W. Ishida, M. Wu, M. Wilkes, Y. Mori, M. Hinchcliff, E. Leof and J. Varga. A non-Smad mechanism of fibroblast activation by transforming growth factor-beta via c-Abl and Egr-1: selective modulation by imatinib mesylate. Oncogene. 28:1285-1297 (2009).
30. S. Wang, M.C. Wilkes, E.B. Leof and R. Hirschberg. Imatinib mesylate blocks a non-Smad TGF-beta pathway and reduces renal fibrogenesis in vivo. Faseb J. 19:1-11 (2005).
31. C.E. Daniels, M.C. Wilkes, M. Edens, T.J. Kottom, S.J. Murphy, A.H. Limper and E.B. Leof. Imatinib mesylate inhibits the profibrogenic activity of TGF-beta and prevents bleomycin-mediated lung fibrosis. J Clin Invest. 114:1308-1316 (2004).
32. A. Abdollahi, M. Li, G. Ping, C. Plathow, S. Domhan, F. Kiessling, L.B. Lee, G. McMahon, H.J. Grone, K.E. Lipson and P.E. Huber. Inhibition of platelet-derived growth factor signaling attenuates pulmonary fibrosis. J Exp Med. 201:925-935 (2005).
33. A. Akhmetshina, P. Venalis, C. Dees, N. Busch, J. Zwerina, G. Schett, O. Distler and J.H. Distler. Treatment with imatinib prevents fibrosis in different preclinical models of systemic sclerosis and induces regression of established fibrosis. Arthritis Rheum. 60:219-224 (2009).
34. Y. Aono, Y. Nishioka, M. Inayama, M. Ugai, J. Kishi, H. Uehara, K. Izumi and S. Sone. Imatinib as a novel antifibrotic agent in bleomycin-induced pulmonary fibrosis in mice. Am J Respir Crit Care Med. 171:1279-1285 (2005).
35. C.E. Daniels, J.A. Lasky, A.H. Limper, K. Mieras, E. Gabor and D.R. Schroeder. Imatinib treatment for idiopathic pulmonary fibrosis: Randomized placebo-controlled trial results. Am J Respir Crit Care Med. 181:604-610 (2010).
36. M. Neef, M. Ledermann, H. Saegesser, V. Schneider, N. Widmer, L.A. Decosterd, B. Rochat and J. Reichen. Oral imatinib treatment reduces early fibrogenesis but does not prevent progression in the long term. J Hepatol. 44:167-175 (2006).
37. R. Vittal, H. Zhang, M.K. Han, B.B. Moore, J.C. Horowitz and V.J. Thannickal. Effects of the protein kinase inhibitor, imatinib mesylate, on epithelial/ mesenchymal phenotypes: implications for treatment of fibrotic diseases. J Pharmacol Exp Ther. 321:35-44 (2007).
38. S. Wang, M.C. Wilkes, E.B. Leof and R. Hirschberg. Noncanonical TGF-beta pathways, mTORC1 and Abl, in renal interstitial fibrogenesis. Am J Physiol Renal Physiol. 298:F142-149 (2010).
39. H. Yoshiji, R. Noguchi, S. Kuriyama, Y. Ikenaka, J. Yoshii, K. Yanase, T. Namisaki, M. Kitade, T. Masaki and H. Fukui. Imatinib mesylate (STI-571) attenuates liver fibrosis development in rats. Am J Physiol Gastrointest Liver Physiol. 288:G907-913 (2005).
40. R. Kerkela, L. Grazette, R. Yacobi, C. Iliescu, R. Patten, C. Beahm, B. Walters, S. Shevtsov, S. Pesant, F.J. Clubb, A. Rosenzweig, R.N. Salomon, R.A. Van Etten, J. Alroy, J.B. Durand and T. Force. Cardiotoxicity of the cancer therapeutic agent imatinib mesylate. Nat Med. 12:908-916 (2006).
41. T. Gonzalo, L. Beljaars, M. van de Bovenkamp, K. Temming, A.M. van Loenen, C. Reker-Smit, D.K. Meijer, M. Lacombe, F. Opdam, G. Keri, L. Orfi, K. Poelstra and R.J. Kok. Local inhibition of liver fibrosis by specific delivery of a platelet-derived growth factor kinase inhibitor to hepatic stellate cells. J Pharmacol Exp Ther. 321:856-865 (2007).
42. R.P. van Gijlswijk, E.G. Talman, I. Peekel, J. Bloem, M.A. van Velzen, R.J. Heetebrij and H.J. Tanke. Use of horseradish peroxidase- and fluorescein-modified cisplatin derivatives for simultaneous labeling of nucleic acids and proteins. Clin Chem. 48:1352-1359 (2002).
43. R.L. Oostendorp, J.H. Beijnen, J.H. Schellens and O. Tellingen. Determination of imatinib mesylate and its main metabolite (CGP74588) in human plasma and murine specimens by ion-pairing reversed-phase high-performance liquid chromatography. Biomed Chromatogr. 21:747-754 (2007).
44. H.-C. Yang, Y. Zuo and A.B. Fogo. Models of chronic kidney disease. Drug Discovery Today: Disease Models. 7:13-19 (2010).

45. J.G. Kiselar, S.D. Maleknia, M. Sullivan, K.M. Downard and M.R. Chance. Hydroxyl radical probe of protein surfaces using synchrotron X-ray radiolysis and mass spectrometry. Int J Radiat Biol. 78:101-114 (2002).
46. A. Rippe, C. Rippe, K. Sward and B. Rippe. Disproportionally low clearance of macromolecules from the plasma to the peritoneal cavity in a mouse model of peritoneal dialysis. Nephrol Dial Transplant. 22:88-95 (2007).
47. Y. Liu. Epithelial to mesenchymal transition in renal fibrogenesis: pathologic significance, molecular mechanism, and therapeutic intervention. J Am Soc Nephrol. 15:1-12 (2004).
48. D. Vansthertem, A. Gossiaux, A.E. Decleves, N. Caron, D. Nonclercq, A. Legrand and G. Toubeau. Expression of nestin, vimentin, and NCAM by renal interstitial cells after ischemic tubular injury. J Biomed Biotechnol. 2010:193259 (2010).
49. D.G. Struijk, R.T. Krediet, G.C. Koomen, E.W. Boeschoten, H.J. vd Reijden and L. Arisz. Indirect measurement of lymphatic absorption with inulin in continuous ambulatory peritoneal dialysis (CAPD) patients. Perit Dial Int. 10:141-145 (1990).
50. S. Mahboobi, A. Sellmer, A. Eswayah, S. Elz, A. Uecker and F.D. Bohmer. Inhibition of PDGFR tyrosine kinase activity by a series of novel N-(3-(4-(pyridin-3-yl)-1H-imidazol-2-ylamino)phenyl)amides: a SAR study on the bioisosterism of pyrimidine and imidazole. Eur J Med Chem. 43:1444-1453 (2008).
51. E. Weisberg, P. Manley, J. Mestan, S. Cowan-Jacob, A. Ray and J.D. Griffin. AMN107 (nilotinib): a novel and selective inhibitor of BCR-ABL. Br J Cancer. 94:1765-1769 (2006).
52. M.A. Seeliger, P. Ranjitkar, C. Kasap, Y. Shan, D.E. Shaw, N.P. Shah, J. Kuriyan and D.J. Maly. Equally potent inhibition of c-Src and Abl by compounds that recognize inactive kinase conformations. Cancer Res. 69:2384-2392 (2009).
53. D. Ludewig, H. Kosmehl, M. Sommer, F.D. Bohmer and G. Stein. PDGF receptor kinase blocker AG1295 attenuates interstitial fibrosis in rat kidney after unilateral obstruction. Cell Tissue Res. 299:97-103 (2000).
54. M. Kimura, M. Asano, K. Abe, M. Miyazaki, T. Suzuki and A. Hishida. Role of atrophic changes in proximal tubular cells in the peritubular deposition of type IV collagen in a rat renal ablation model. Nephrol Dial Transplant. 20:1559-1565 (2005).
55. H.Y. Lan. Tubular epithelial-myofibroblast transdifferentiation mechanisms in proximal tubule cells. Curr Opin Nephrol Hypertens. 12:25-29 (2003).
56. F. Strutz and G.A. Muller. Renal fibrosis and the origin of the renal fibroblast. Nephrol Dial Transplant. 21:3368-3370 (2006).

Chapter 5

Targeting of a platinum-bound sunitinib analogue to renal proximal tubular cells

M.E.M. Dolman[1], S. Harmsen[1], R.W. Sparidans[2], E.H.E. Pieters[1], M. Lacombe[3], B. Szokol[4], L. Őrfi[4], G. Kéri[4,5], G. Storm[1], W.E. Hennink[1] and R.J. Kok[1]

[1] Department of Pharmaceutics, Utrecht Institute of Pharmaceutical Sciences, Utrecht University, Utrecht, The Netherlands

[2] Faculty of Science, Department of Pharmaceutical Sciences, Division of Pharmacoepidemiology and Clinical Pharmacology, Utrecht University, Utrecht, The Netherlands

[3] KREATECH Biotechnology B.V., Amsterdam, The Netherlands

[4] Vichem Chemie, Budapest, Hungary

[5] Pathobiochemistry Research Group of Hungarian Academy of Sciences and Semmelweis University, Budapest, Hungary

Submitted for publication

Abstract

Purpose Activated kinases in proximal tubular cells play an important role in tubulointerstitial fibrosis. A platinum-bound sunitinib analogue was developed that can be conjugated to the low molecular weight protein lysozyme. We investigated whether this kidney-targeted conjugate is capable of attenuating early fibrogenic events in tubulointerstitial fibrosis.

Methods An analogue of sunitinib with a pyridyl sidechain (named 17864 from here on) was developed. This side chain group enabled the coupling of 17864 via the platinum (II)-based universal linkage system (ULS)™ to the kidney-directed carrier protein lysozyme. The pharmacological activity of 17864-ULS-lysozyme and its metabolites was evaluated in human kidney proximal tubular cells (HK-2). Its pharmacokinetics was studied in mice after a single intravenous dose. Potential antifibrotic effects of a single dose treatment were evaluated in mice that had undergone unilateral ureteral obstruction (UUO) for three days.

Results The multitargeted 17864-ULS-lysozyme conjugate and its 17864-ULS metabolites strongly inhibited tyrosine kinase activity in HK-2 cells. Upon intravenous injection, 17864-ULS-lysozyme rapidly accumulated in the kidneys and provided 17864-ULS levels for up to 3 days after a single dose. Based on renal AUC, 17864-ULS-lysozyme provided a 28-fold increase in renal exposure versus an equimolar dose of sunitinib malate. Mice that had suffered from ureter obstruction for three days showed signs of early fibrosis such as increased collagen deposition and activation of fibrotic markers but these were not inhibited by a single dose of 17864-ULS-lysozyme. Daily treatment of UUO mice with a high dose sunitinib (50 mg/ kg) resulted in antifibrotic effects, but induced drug-related toxicity. Mice treated with 17864-ULS-lysozyme showed no signs of toxic effects.

Conclusions We have developed a kidney-targeted sunitinib derivative that rapidly accumulates in proximal tubular cells. The developed conjugate provided sustained levels of the multikinase inhibitor in the kidneys which lasted for several days. Although a single dose of the conjugate did not inhibit early fibrotic responses, sunitinib in a high dose ressorted effects. These results suggest that 17864-ULS-lysozyme may be effective at higher or more prolonged treatment. We conclude that multikinase inhibitors like sunitinib can be of benefit in the treatment of fibrotic diseases, precluding that their safety can be improved by strategies as presented in this paper.

1. Introduction

Progression of untreated kidney diseases results in tubulointerstitial fibrosis, eventually leading to end-stage renal disease (ESRD) (1, 2). Activation of proximal tubular cells is an important step in the pathogenesis of tubulointerstitial fibrosis (3). Activated proximal tubular cells secrete chemotactic proteins that attract macrophages and other immune cells (4). Tubular cell activation furthermore leads to epithelial-to-mesenchymal transition (EMT) of proximal tubular epithelial cells and excessive production of extracellular matrix (ECM) components. As a result, normal tissue is replaced by scar tissue and the kidney function is decreased (1, 5, 6). Since currently applied drugs like angiotensin-converting enzyme inhibitors and angiotensin II receptor type 1 antagonists are only partially effective (7, 8), there is an urgent need for drugs that halt or even reverse the profibrotic processes.

Multiple signaling pathways are involved in the activation of tubular cells in tubulointerstitial fibrosis (1, 2). Simultaneous inhibition of these cascades by a multitargeted kinase inhibitor therefore seems an attractive strategy. Sunitinib is a commercially available multitargeted tyrosine kinase inhibitor approved for the treatment of metastatic renal-cell carcinoma and gastrointestinal stromal tumors and currently also under investigation for the treatment of other types of cancer (9-11). Compared with other kinase inhibitors, sunitinib interacts with high affinity (*i.e.* K_d < 100 nM) with a broad range of kinases (12) that include the platelet-derived growth factor receptors PDGFR-α and -β and the vascular endothelial growth factor receptors VEGFR1 and -2 (9, 10). Overactivation of the PDGFR kinase pathway has been associated with the development of renal fibrosis by stimulating the proliferation, migration and survival of myofibroblasts (13, 14). The VEGFR kinase pathway has also been linked to renal fibrosis, although less clear than the PDGFR kinase pathway (15, 16). To our knowledge it is not known whether or not the other targets of sunitinib are involved in the pathogenesis of renal fibrosis. Sunitinib has not yet been investigated for the treatment of renal fibrosis, but has successfully been used to treat liver fibrosis (17). We now propose to use a renally targeted sunitinib analogue as an antifibrotic treatment in kidney fibrosis.

One main concern when using a multitargeted kinase inhibitor for the treatment of renal fibrosis is the possible increased risk of side effects compared with more selective kinase inhibitors (18). Sunitinib has been associated with many side effects, including severe cutaneous toxicities and cardiotoxicity (11, 19-22). To avoid these side effects, targeted delivery of sunitinib to the target cells, *i.e.* the proximal tubular cells of the kidneys, is a comprehensive approach. In earlier studies, other kinase inhibitors already have successfully been delivered to the proximal tubular cells by conjugation to lysozyme (23-25), a low molecular weight protein (~ 14 kDa) is rapidly filtered through the glomeruli of the kidneys and subsequently taken up at the apical membrane of proximal tubular cells via megalin receptor-mediated internalization (26).

Sunitinib does not contain functional groups such as hydroxyl or primary amino groups that can be used for the coupling to lysozyme. We therefore designed a sunitinib-derivative that can be linked to lysozyme when coordinated to the platinum (II)-based Universal Linkage System™ (ULS)™. This platinum linker forms stable coordinative bonds with drugs that contain pyridyl groups or other types of aromatic nitrogens in their structure, and can be conjugated to thiol groups in proteinaceous carriers (27). One of the important properties of conjugates prepared with this type of platinum linker is their prolonged retention inside the designated cells, as was demonstrated in pharmacokinetic studies in rats. Upon intravenous administration, the ULS-

bound drug persisted in the designated cells for several days (25, 28). The therapeutic index of a drug may therefore be improved when the targeted drug is not only active after its release from the ULS linker, but also in the ULS-bound form. A more rapid onset of activity and higher intracellular active inhibitor levels can be obtained. In the current study we aimed to design a ULS-bound sunitinib analogue with retained activity and to deliver this ULS-bound analogue to the proximal tubular cells of the kidneys.

Sunitinib is a type I ATP-competitive kinase inhibitor that exerts its effects on target kinases by binding in and around the adenine region of the ATP-binding pocket (29). Structural binding studies of sunitinib have revealed that the oxindole moiety of sunitinib is localized deep in the ATP-binding pocket of the kinase, where it is bound to the adenine region via hydrophobic interactions, while the *N*-2-(diethylamino)ethylene moiety is exposed outwards (30, 31). We therefore hypothesized that an active ULS-bound sunitinib analogue could be obtained by replacement of the *N*-2-(diethylamino)ethylene moiety by a pyridyl side chain that can be coordinated to the platinum linker. **Figure 1** shows the chemical structure of the newly developed sunitinib derivative 17864.

In the current study we investigated the coupling of 17864-ULS to the renal carrier lysozyme, as well as the *in vitro* capability of platinum-bound 17864 to inhibit kinase activity. The *in vivo* accumulation of 17864-ULS-lysozyme in the kidneys was studied after intravenous administration to mice. Moreover, we investigated the antifibrotic effects of 17864-ULS-lysozyme in mice with unilateral ureteral obstruction (UUO)-induced tubulointerstitial fibrosis.

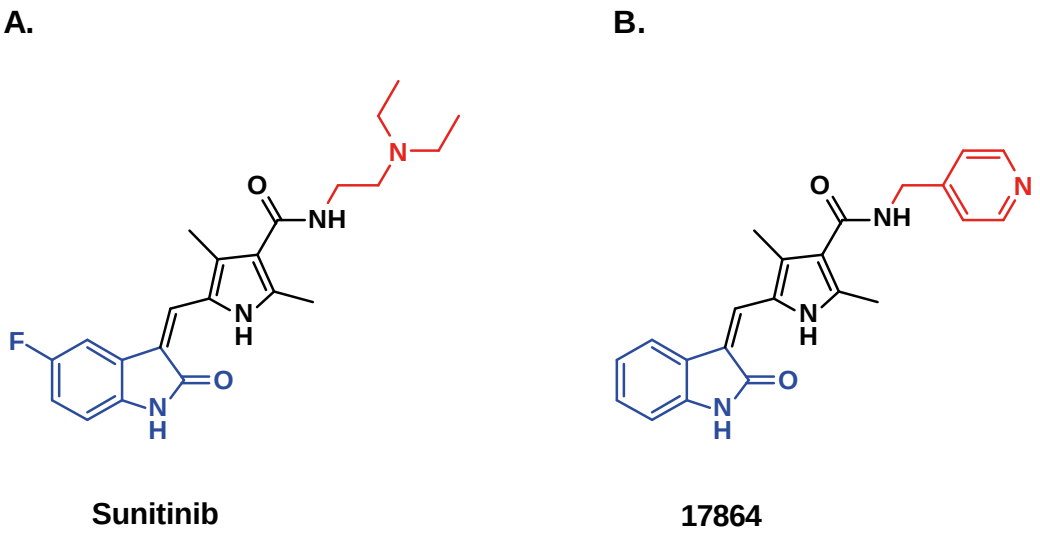

Figure 1. Structures of the multitargeted tyrosine kinase inhibitor sunitinib (A) and the ULS-linkable sunitinib derivative 17864 (B). The aliphatic *N*-2-(diethylamino)ethylene sidechain of sunitinib has been replaced by a *N*-4-methylpyridine (red colour). When binding to target kinases the oxindole moiety (blue colour) of the drug is located in the adenine region of the ATP-binding pocket, while the *N*-2-(diethylamino)ethylene moiety or *N*-4-methylpyridine are protruding outwards.

2. Materials and methods

2.1. Materials and chemicals

17864 was synthesized according to Sun *et al.* by Vichem Chemie (Budapest, Hungary) (32). Sunitinib malate was purchased from Sequoi Research Products (Pangbourne, United Kingdom). The Universal Linkage System (ULS)™ *cis*-[Pt(ethylenediamine)nitrate-chloride] was synthesized from *cis*-[Pt(ethylenediamine)dichloride as described elsewhere (33). Lysozyme from hen egg white, potassium thiocyanate (KSCN), ethylenediaminetetraacetic acid (EDTA) and citric acid were purchased from Fluka (Zwijndrecht, The Netherlands). Acetonitrile (ACN) HPLC-S and *tert*-butyl methylether (TBME) were obtained from Biosolve (Valkenswaard, The Netherlands). Trifluoroacetic acid (TFA), bovine serum albumin (BSA), 4-hydroxybenzophenone, sodium azide, sodium citrate tribasic dehydrate, 3,3-diaminobenzidine (DAB) and hematoxylin solution (gill no. 2) were purchased from Sigma-Aldrich (Zwijndrecht, The Netherlands). 2-Amino-2-(hydroxymethyl)-1,3-propanediol (Tris) was purchased from Roche Diagnostics GmbH (Almere, The Netherlands). Glycine, hydrogen peroxidase 30% and disodium hydrogen phosphate dehydrate were purchased from Merck (Schiphol-Rijk, The Netherlands). Tween-20 was purchased from Acros Organics (Geel, Belgium). The TaqMan® Universal PCR Master Mix, No AmpErase® UNG and The TagMan® Gene Expression Assays Mm00446973_m1, Mm00435860_m1, Mm00483888_m1, Mm01256734_m1 and Mm00441242_m1 for the detection of, respectively, TATA-binding protein (TBP), plasminogen activator inhibitor-1 (PAI-1), Collagen 1A2, fibronectin and monocyte chemotactic protein-1 (MCP-1) were purchased from Applied Biosystems (Nieuwerkerk aan den IJssel, The Netherlands). Mammalian Protein Extraction Reagent (M-PER), RIPA buffer, Halt™ Protease and Phosphatase Inhibitor Cocktail (100x) and 0.5 M EDTA solution (100x) were purchased from Thermo Scientific (Etten-Leur, The Netherlands). Immobilon-P polyvinylidene fluoride (PVDF) Membrane (0.45 µm) was purchased from Millipore (Amsterdam, The Netherlands). NuPAGE® 4-12% Bis-Tris Gel and NuPAGE® MOPS SDS running buffer were purchased from Invitrogen (Breda, The Netherlands). PageRuler™ Prestained Protein Ladder was purchased from Fermentas (Leon-Rot, Germany). Rabbit anti-mouse p-PDGFR-β and rabbit anti-mouse vimentin polyclonal antibodies were purchased from Santa Cruz (Heidelberg, Germany). Rabbit anti-mouse β-actin polyclonal antibody and horseradish peroxidase (HRP)-conjugated goat anti-rabbit secondary antibody were purchased from Cell Signaling Technology (Leiden, The Netherlands). Mouse anti-human phosphotyrosine [PY20] (HRP) monoclonal antibody, rabbit anti-mouse α-SMA and rabbit anti-mouse collagen IV were purchased from Abcam (Cambridge, UK). BrightVision HRP-conjugated goat anti-rabbit secondary antibody was purchased from Immunologic (Duiven, The Netherlands).

2.2. Synthesis of 17864-ULS-lysozyme

17864 was coupled to the platinum (II)-based linker ULS by incubating equimolar amounts (*i.e.* 107 µmol) of 17864 and ULS in DMF (9 mL) for 4 hours at 37 °C. To confirm the formation of the 17864-ULS 1:1 adduct the final product was analyzed with LC-MS and ^{195}Pt-NMR. For the coupling of 17864-ULS to lysozyme, the renal carrier protein needs to contain functional groups (*i.e.* aromatic nitrogens or thiol groups) that can be coordinated to the platinum linker. Since the thiol-containing methionine residues present in lysozyme are located in the core of the protein, thiol groups were introduced onto the protein's surface. Lysozyme (10 mg/ mL in PBS) was

reacted with a three times molar excess of BOC-L-methionine *N*-hydroxysuccinimide ester (50 mg/ mL in DMSO) for one hour at ambient temperature. Purification of the product was performed by dialysis against water using a Spectra/ Por® 3 dialysis membrane with a molecular weight cut-off of 3,500 Da. The methionine-lysozyme batch was lyophilized and stored at -20 °C untill further use. Characterization was performed by matrix-assisted laser desorption-ionization time-of-flight (MALDI-TOF) mass spectrometry. The final step in the synthesis of 17864-ULS-lysozyme was the conjugation of 17864-ULS to methionine-modified lysozyme. 17864-ULS was incubated in a three times molar excess with methionine-lysozyme in 0.02 M tricine/ sodium nitrate buffer pH 8.5, overnight at 37 °C. The obtained 17864-ULS-lysozyme conjugate was purified by dialysis against 10% DMSO in demineralized water, followed by extensive dialysis against demineralized water. The dialyses steps were performed at 4 °C using a Slide-A-Lyzer dialysis cassette with a molecular weight cut-off of 10,000 Da (Pierce, Rockford, IL). The purified conjugate was lyophilized and stored at -20 °C until further use.

2.3. Characterization of 17864-ULS-lysozyme

For the characterization of 17864-ULS-lysozyme an 8 mg/ mL stock solution in water was prepared and subsequently filtered through a 0.2 µm filter. The concentrations of 17864-ULS and lysozyme in this solution were measured to establish the drug/ carrier ratio in the final product. Lysozyme was measured using the Micro BCA™ Protein Assay Kit (Thermo Scientific; Etten-Leur, The Netherlands). For the analysis of the amount of 17864-ULS conjugated to lysozyme the drug was displaced from the linker with an excess of KSCN and the concentrations of liberated 17864 were determined with HPLC. Briefly, the stock solution was six times diluted in a mixture of 50% PBS, 50% ACN and 0.1% TFA containing a final concentration of 0.5 M KSCN. The samples were incubated for 24 hours at 80 °C. After reaching ambient temperature 200 µL ACN with 0.1% TFA was added to the samples. The samples were mixed by vortexing and centrifuged for 4 minutes at 19,500 x g. Of the supernatants 50 µL was injected in a reversed phase HPLC system consisting of a Waters 2695 separations module, a Waters 2487 dual λ absorbance detector and a Waters SunFire™ C18 column (4.6 x 150 mm, 5 µm particle size) (Milford, USA). Empower 2 software was used for data recording. The column- and sample temperature were maintained at 30 and 20 °C, respectively. A gradient was used with eluent A consisting of 5% ACN/ 95% water/ 0.1% TFA (w/ w/ w) and eluent B consisting of ACN/ 0.1% TFA (w/ w). The composition of the mobile phase was linearly changed from 100% eluent A to 20% eluent A and 80% eluent B in 25 minutes using a flow rate of 1 mL/ min. 17864 was detected at 431 nm.

2.4. In vitro activity

2.4.1. Cell culture

The immortalized human renal proximal tubule epithelial cell line (HK-2) (American Type Culture Collection, LGC Standards, Middlesex, UK) was cultured in Dulbecco's Modified Eagle's Medium (DMEM) containing 3.7 g/ L sodium bicarbonate, 1.0 g/ L glucose, supplemented with 10% (v/ v) fetal bovine serum, penicillin (100 U/ L), streptomycin (100 µg/ mL) and amphotericin B (0.25 µg/ mL) at 37 °C with 5% CO_2 in humidified air. All cell culture related media were obtained from PAA Laboratories GmbH (Pasching, Austria).

2.4.2. In vitro inhibition of tyrosine-residue activity after cellular uptake

The inhibitory effects of 17864-ULS-lysozyme on the phosphorylation of tyrosine kinases were studied after internalization in HK-2 cells seeded onto 96-well plates (1.5×10^4 cells/ well). Cells were serum-starved overnight and, subsequently, incubated with 10 μM 17864, 17864-ULS, methionine-modified lysozyme, 17864-ULS-lysozyme or sunitinib malate. After 24 hours, cells were washed thrice with PBS (PAA Laboratories GmbH) and lysed with M-PER containing protease- and phosphatase inhibitors. Protein concentrations were determined using the BCA protein determination assay (Thermo Fischer Scientific, Etten-Leur, The Netherlands). Phosphorylation of the tyrosine kinases was stimulated by 60 minutes incubation of the cell lysate with an equal volume of 10 μM ATP in Abl kinase assay buffer (consisting of 50 mM Tris–HCl [pH 7.5], 10 mM $MgCl_2$, 1 mM ethyleneglycoltetraacetic acid, 2 mM dithiothreitol (DTT), and 0.01% Brij-35) at 37 °C. The phosphorylation was terminated by adding reducing sample buffer (Invitrogen, Breda, the Netherlands) containing a final concentration of 40 mM DTT and 0.1% (w/ v) sodium dodecyl sulfate (SDS). Total protein (10 μg) was separated by SDS-polyacrylamide gel electrophoresis using a precast 4-12% Bis-Tris gel. Proteins were transferred onto a PVDF membrane by wet blotting. The transfer buffer consisted of 25 mM Tris, 192 mM glycine and 10% methanol (v/ v) and a transfer voltage was used of 100 V for 1 hour. After 1 hour blocking at room temperature with 3% (w/ v) BSA in Tris buffered saline (TBS) with 0.1% (v/ v) Tween-20 (TBS with 0.1% (v/ v) Tween-20 will be further referred to as TBS/ T), the membrane was incubated for 1 hour at room temperature with mouse anti-human phosphotyrosine [PY20] (HRP) monoclonal antibody (1:500) in 3% BSA in TBS/ T. The membrane was washed with TBS/ T and the proteins were visualized using the SuperSignal® West Femto Maximum Sensitivity Substrate Kit (Thermo Scientific, Etten-Leur, The Netherlands). The band density was determined on a Gel Doc XRS Imaging system with Quantity One analysis software (Bio-Rad, Hercules, CA, USA).

2.4.3. Activity of platinum-bound 17864

To demonstrate that the activity of 17864 is retained when coupled to the ULS linker we studied the inhibitory effects of 17864-ULS and 17864-ULS-lysozyme on the phosphorylation of tyrosine kinases in HK-2 cell lysate. In short, serum-starved HK-2 cells were lysed with M-PER containing protease- and phosphatase inhibitors. After measuring the protein content 0.1 mg/ mL HK-2 cell lysate was incubated with 2 μM 17864, 17864-ULS and 17864-ULS-lysozyme for 30 minutes at room temperature. For the phosphorylation of tyrosine kinases and the analysis of the inhibitory effects of the compounds the same protocol was used as described above for the investigation of the inhibitory effects after cellular internalization. Instead of 10 μM we used 1 μM ATP in Abl kinase assay buffer for the stimulation of the phosphorylation of tyrosine kinases.

2.5. Animals

All *in vivo* experiments were performed in normal male C57Bl/ 6J mice obtained from Harlan (Zeist, The Netherlands). Mice were ordered with a body weight of 13-25 gram and used for the animal experiments within four weeks after arrival. The mice were housed in cages in a 12 hours light and 12 hours dark cycle and given food and water *ad libitum*. Experimental protocols for

pharmacokinetic and efficacy studies were approved by the animal ethics committee of the Utrecht University, The Netherlands.

2.6. Pharmacokinetics of 17864-ULS-lysozyme

The pharmacokinetics of 17864-ULS-lysozyme were studied in male C57Bl/6J mice and compared with the pharmacokinetics of sunitinib malate. Mice received a single intravenous injection of either 17864-ULS-lysozyme (n = 17; 20 mg/kg) or an equimolar amount of sunitinib malate (n = 15). At one minute after administration of the compounds, a blood sample was taken via a cheek puncture. Animals were sacrificed at the indicated time points by an intraperitoneal injection of 120-150 µL of a mixture of ketamine hydrochloride (47 mg/mL), xylazine hydrochloride (8 mg/mL) and atropine (0.07 mg/mL). Blood samples were collected in K2 EDTA-prefilled blood tubes, two times centrifuged at 5,500 x g for 15 minutes at 4 °C and stored at -80 °C untill further analysis. Kidneys were removed and stored at -80 °C until further processing as described below. Plasma and renal drug levels were analyzed with Multifit pharmacokinetic software (Dr. Hans Proost, University of Groningen, The Netherlands). Curve-fitting with a two-compartment model was used to determine absorption- and elimination half lives, distribution volumes and area under the curves (AUCs). The calculation of the % of the dose in the total plasma volume was based on an average plasma volume of 0.05 ml/g of mouse body weight (34).

2.6.1. LC-MS/MS analysis of sunitinib

Plasma and renal sunitinib concentrations were measured according to the following protocol. Working solutions were prepared of 10 µg/mL sunitinib malate in PBS and of 50 µg/mL 4-hydroxybenzophenone (internal standard) in methanol. Calibration standards (10 ng/mL-1 µg/mL sunitinib malate in blank human plasma and 10-500 ng/mL in blank kidney homogenate) were prepared by dilution of the 10 µg/mL stock solution with the corresponding blank matrix. The plasma samples collected at 1 minute after administration of sunitinib malate were two times diluted with blank human plasma, other samples were processed undiluted. Blank kidney homogenate was prepared by homogenizing kidneys of non-treated C57Bl/6J mice in 4% (w/v) BSA in demineralized water with a polytron tissue homogenizer in a final concentration of 0.1 gram tissue/mL. The kidney homogenates of the mice injected with sunitinib malate were prepared in the same manner. Blank human plasma and kidney homogenate were used as negative control. To 100 µL sample 50 µL of the internal standard solution and 1 mL TBME were added. TBME was used for the extraction of the kinase inhibitor from biological matrices (*i.e.* plasma and kidney tissue). Samples were mixed vigorously for 15 minutes and centrifuged for 5 minutes at 7,500 x g. The aqueous layer was frozen in a bath of ethanol with dry ice and the TBME layer was collected. After repetition of the extraction procedure the samples were shortly vortexed and placed in a Speed-Vac Plus SC210A for 45 minutes at 45 °C to evaporate the TBME. The samples were reconstituted in 100 µL ACN containing 0.1% TFA by 15 minutes sonication and 15 minutes vortexing. After 3 minutes centrifugation at 21,000 x g supernatant was diluted 3 times with demineralized water before analysis with LC-MS/MS. The LC-MS/MS equipment and general MS/MS setting were reported previously by Sparidans *et al.* (35). Partial-loop injections (2 µl) were made on an Aquity UPLC® BEH C18 column (30 x 2.1 mm, d_p = 1.7 µm, Waters, Milford, USA) with the corresponding VanGuard pre-column (Waters, 5 x

2.1 mm, d_p = 1.7 µm). The column temperature was maintained at 40 ºC and the autosampler sample rack compartment was maintained at 4 ºC. The eluent comprised a mixture of two solvents: 0.1% (v/ v) formic acid in water (A) and methanol (B), pumped at 0.5 ml/ min. The amount of solvent B was increased from 20 to 60% during 2 minutes after injection, followed by flushing the column for 0.5 minute with 90% methanol and reconditioning the column at 20% methanol for 1.5 minute. The whole eluate was transferred into the electrospray ionization source, starting at 0.7 minute after injection by switching the MS inlet valve. The selected reaction monitoring mode was used with argon as the collision gas at 1.5 mTorr. Dwell times were 0.2 s for sunitinib and 0.1 s for the internal standard. The tube lens off set was 92 V for sunitinib and 100 V for the internal standard. Sunitinib was monitored at *m/z* 399.24→283.15 at -24 V collision energy; the internal standard at *m/z* 199.00→121.00 at -15 V.

2.6.2. LC-MS/MS analysis of 17864-ULS-lysozyme

Total 17864 (*i.e.* 17864-ULS-lysozyme + 17864-ULS + released 17864) and free 17864 (*i.e.* released 17864) levels were measured in plasma and kidney homogenate. Analyses were performed using the sunitinib malate protocol with minor modifications. For the analysis of the released 17864 levels in the circulation plasma samples were processed undiluted.

For the measurement of the total 17864 concentrations in plasma and kidneys samples were incubated with KSCN before extraction of the kinase inhibitor with TBME. To 100 µL sample and 50 µL of the internal standard solution 150 µL of 1 M KSCN in PBS was added. Samples were incubated at 80 °C for 24 hours. For the analysis of the total 17864 levels in the circulation at one minute after administration of 17864-ULS-lysozyme the plasma samples were three times diluted with blank human plasma.

For the 17864 LC-MS/ MS analysis the same equipment and column were used as for sunitinib, which some modifications to LC-MS/ MS conditions. The amount of solvent B was increased from 10 to 70% during 3 minutes after injection, followed by flushing the column for 0.5 minute with 70% methanol and reconditioning the column at 10% methanol for 1.5 minute. The whole eluate was transferred into the electrospray ionization source, starting at 0.8 minute after injection by switching the MS inlet valve, until 4 minutes after injection. The selected reaction monitoring mode was used with argon as the collision gas at 2.0 mTorr and 40 ms dwell times. 17864 was monitored at *m/z* 373.14→239.17 at -18 V collision energy and the tube lens off set was 108 V.

2.7. Antifibrotic effects of 17864-ULS-lysozyme in UUO-induced fibrosis

2.7.1. Treatment groups

The antifibrotic effects of 17864-ULS-lysozyme have been studied in mice with UUO-induced tubulointerstitial fibrosis. Surgically induced ureteral obstruction was performed according to the following protocol. Mice received a single subcutaneous injection of carprofen to relief the pain after surgery. Under isoflurane anesthesia (3% in 100% O_2; 1 L/ min) the ureter of the left kidney was ligated at two places with silk (5-0). Pain treatment after surgery was performed by additional subcutaneous injections of carprofen at 24 and 48 hours after surgery. Mice were sacrificed after three days ureteral obstruction by giving them an intraperitoneal injection of 120-

150 µL of a mixture of ketamine hydrochloride (47 mg/ mL), xylazine hydrochloride (8 mg/ mL) and atropine (0.07 mg/ mL).
Mice were randomly divided into two control groups (n = 6 per group) and three treatment groups (n = 7 per group). The first control group consisted of normal mice without UUO-induced tubulointerstitial fibrosis and the second control group of mice with UUO-induced tubulointerstitial fibrosis without treatment. In case of the treatment groups mice with UUO-induced renal fibrosis were treated with a single intravenous injection of 40 mg/ kg 17864-ULS-lysozyme (corresponding to 3.35 µmol/ kg or 1,250 µg/ kg 17864), a single intravenous injection of 3.35 µmol/ kg (1,785 µg/ kg) sunitinib malate or a daily intraperitoneal injection of 50 mg/ kg sunitinib malate.
The left (diseased) kidneys were used for the evaluation of the antifibrotic effects of 17864-ULS-lysozyme. A small part of the kidneys was used for the preparation of 4% formaldehyde-fixed paraffin-embedded tissue sections for immunostaining and the remaining was stored at -80 °C for western blot analysis and quantitative reverse transcription-polymerase chain reactions (qRT-PCR).

2.7.2. Western blot analysis

As stated in the introduction PDGFR-β belongs to one of the direct targets of sunitinib. In this study we investigated the activation of this receptor tyrosine kinase after three days ureteral obstruction and the inhibitory effects of the intrinsically active 17864-ULS-lysozyme conjugate on the activated PDGFR-β levels. Activated PDGFR-β was detected in the renal cortex by western blot analysis of phosphorylated PDGFR-β (p-PDGFR-β). Cortex homogenates were prepared by homogenizing a small part of the cortex in 400 µL RIPA buffer supplemented with protease- and phosphatase inhibitors and EDTA. After measuring the protein content of the samples with the Micro BCA™ Protein Assay Kit 7 µL 4x SDS-containing loading buffer was added to an aliquot of the samples corresponding with 50 µg protein. Demineralized water was added to adjust the total volume of the samples to 30 µL. After shortly vortexing, the samples were centrifuged in an eppendorf table centrifuge and subsequently heated for 7 minutes at 95 °C. The samples were shortly centrifuged again before loading onto a precast 4-12% Bis-Tris gel. Protein separation was performed in MOPS SDS running buffer using an initial voltage of 120 V for 20 minutes and 170 V for the remaining run time. Wet blotting was used to transfer the proteins onto a PVDF membrane. The transfer buffer consisted of 25 mM Tris, 192 mM glycine and 10% methanol (v/ v) and a transfer voltage was used of 100 V for 1 hour. After transferring the proteins onto a PVDF membrane, the membrane was split into two parts. The part containing the proteins with a molecular seize > 100 kDa was used for the detection of p-PDGFR-β and the membrane containing the proteins with a molecular seize < 100 kDa for the detection of β-actin. Membranes were blocked for 1 hour at room temperature in blocking buffer consisting of 5% nonfat dry milk in TBS/ T. After three times washing in TBS/ T for 5 minutes the membranes were incubated overnight at 4 °C with the primary antibodies (*i.e.* rabbit anti-mouse p-PDGFR-β (Tyr 740) (1:200) or rabbit anti-mouse β-actin (1:1000) polyclonal antibody) in TBS/ T with 5% (w/ v) BSA. The membranes were washed again and incubated for 1 hour at room temperature with HRP-conjugated goat anti-rabbit secondary antibody (1:1000 in TBS/ T with 5% (w/ v) nonfat dry milk). Washing the membranes was followed by the detection of p-PDGFR-β and β-actin using

the SuperSignal® West Femto Maximum Sensitivity Substrate Kit (Thermo Scientific, Etten-Leur, The Netherlands).

2.7.3. Determination of mRNA expression

The inhibitory effects of 17864-ULS-lysozyme on the mRNA expression of collagen 1A2, PAI-1, fibronectin and MCP-1 in the whole kidneys and the cortex have been analyzed by qRT-PCR. Total RNA was isolated from > 1.8 mg tissue using the RNeasy KIT from QIAGEN (Venlo, The Netherlands). The RNA content in the samples was measured by UV-detection with the nanodrop (NanoDrop, Wilmington, Delaware, United States). For all samples the ratio between the absorbance at 260 nm and 280 nm was higher than 1.8 indicating that the RNA samples were not contaminated with DNA. After RNA extraction 300 ng RNA was used for the synthesis of cDNA. For the synthesis of cDNA the RevertAid™ Premium First Strand cDNA Synthesis Kit of Fermentas (Sankt Leon-Rot, Germany) was used. The obtained cDNA samples were diluted ten times with MilliQ water before use. For the qRT-PCR analyses each sample consisted of 2.5 µL ten times diluted cDNA, 0.625 µL TagMan® Gene Expression Assay, 6.25 µL TaqMan® Universal PCR Master Mix and 3.125 µL MilliQ water. The analysis were performed using the Applied Biosystems ABI PRISM® 7900HT Sequence Detection System (Nieuwerkerk aan den IJssel, The Netherlands). Sequence Detection System Software v2.2 was used for data analysis. Statistical analysis of the results was performed using one-way analysis of variance (ANOVA), with $p < 0.05$ as the minimal level of significance.

2.7.4. Immunostaining of formaldehyde-fixed paraffin-embedded kidney sections

Paraffin-embedded kidney sections of 3 µm were immunostained for α-SMA, collagen IV and vimentin according to the following protocol. The paraffin-embedded kidney sections were deparaffinized in xylene and hydrated in a graded series of alcohol baths. To inactivate the endogenous peroxidase activity the kidney sections were incubated for 15 minutes in blocking buffer prepared by the addition of 1 part hydrogen peroxide 30% to 19 parts of a solution containing 8.32 g/ L citric acid, 21.52 g/ L disodium hydrogen phosphate dehydrate and 2 g/ L sodium azide (the pH of this solution has been adjusted to pH 5.8 with 1 N HCl). After washing the coupes with demineralized water enzyme pretreatment of the kidney sections was performed for epitope retrieval by boiling the kidney sections for 15 minutes in 10 mM citrate buffer with pH 6.0 (for collagen IV and vimentin) or Tris/ EDTA buffer (containing 4.84 g/ L Tris and 372 mg/ L EDTA) with pH 9.0 (for α-SMA). After reaching room temperature the kidney sections were washed twice with PBS/ 0.05T, before 1 hour incubation with the primary antibody at room temperature. All primary antibodies were diluted in PBS with 1% (w/ v) BSA; rabbit anti-mouse α-SMA 1:400, rabbit anti-mouse collagen IV 1:400 and rabbit anti-mouse vimentin 1:200. The kidney sections were washed with PBS/ 0.05T and incubated for 30 minutes at room temperature with undiluted HRP-conjugated brightvision goat anti-rabbit secondary antibody. Kidney sections were washed three times with PBS and incubated for ten minutes with DAB in the presence of hydrogen peroxide (H_2O_2). To 1 mL 6 g/ L DAB in demineralized water 9 mL phosphate/ citrate buffer, pH 9.0, and 10 µL hydrogen peroxide 30% were added. Nuclei were stained by washing the kidney sections three times with demineralized water, placing the sections 10-15 seconds in undiluted hematoxylin solution and rinsing them by holding them

under the running normal water tap for at least ten minutes. The kidney sections were dehydrated in a graded series of alcohol baths and xylene and mounted with DePeX in xylene (3 to 1 ratio). Stained sections were analyzed using light microscopy.

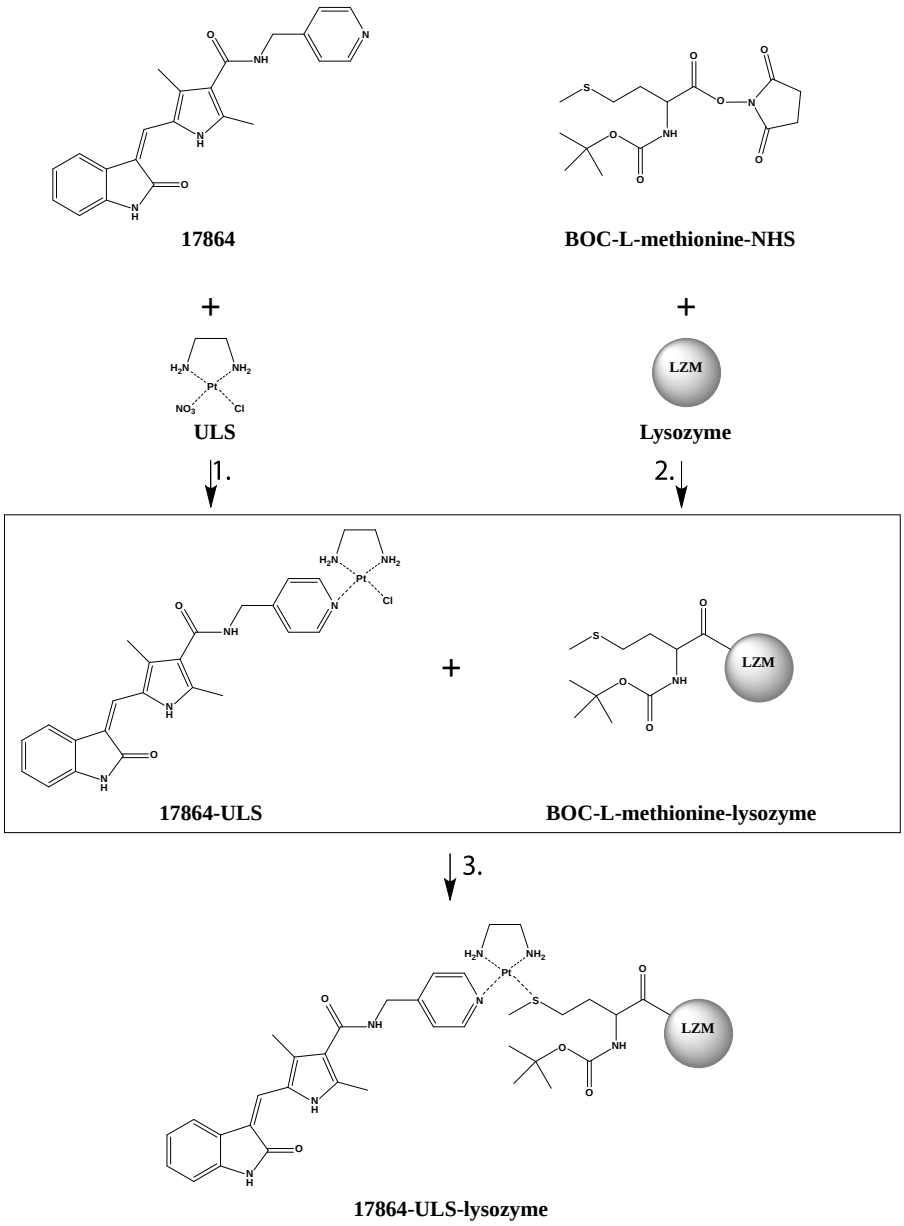

Figure 2. Synthesis scheme of 17864-ULS-lysozyme. The multitargeted kinase inhibitor 17864 was coupled to the ULS platinum linker (1). The carrier protein lysozyme was reacted with BOC-L-methionine *N*-hydroxysuccinimide to introduce thiol groups (2). Conjugation of 17864-ULS to methionine-modified lysozyme yielded the final renal-specific 17864-ULS-lysozyme conjugate (3).

3. Results

3.1. Synthesis and characterization of 17864-ULS-lysozyme

Figure 2 shows the reaction scheme followed for the preparation of 17864-ULS-lysozyme. The successful linkage of 17864 to the platinum (II)-based ULS linker was demonstrated by LC-MS analysis. ^{195}Pt-NMR analysis of 17864-ULS proved the formation of a coordinative bond between the platinum-atom of the linker and the aromatic nitrogen of the pyridine ring in the kinase inhibitor. The coupling reaction of 17864 to ULS yielded 80% of the desired 17864-ULS 1:1 adduct. Besides the 1:1 adduct the product also contained 14% of the dimeric adduct, *i.e.* $(17864)_2$-ULS. This type of drug-ULS-drug adduct cannot react with the renal carrier protein, and was removed from the 17864-ULS-lysozyme conjugate during the final dialysis step. Thiol groups were introduced on the surface of lysozyme by modification of the carrier protein with methionine residues. MALDI-TOF mass spectrometric analysis of the modified lysozyme demonstrated the attachment of 2-3 methionine residues per lysozyme molecule. In the last step of the synthesis 17864-ULS was conjugated to methionine-modified lysozyme. The molar 17864-ULS:lysozyme coupling ratio was established with HPLC and was found to be 1.2:1.

3.2. In vitro activity of 17864-ULS-lysozyme after uptake in HK-2 cells

We investigated the multikinase inhibitory effects of 17864-ULS-lysozyme after internalization and intracellular processing by HK-2 cells, by analyzing its potency to reduce the level of phosphorylation (= activation) of tyrosine kinases.

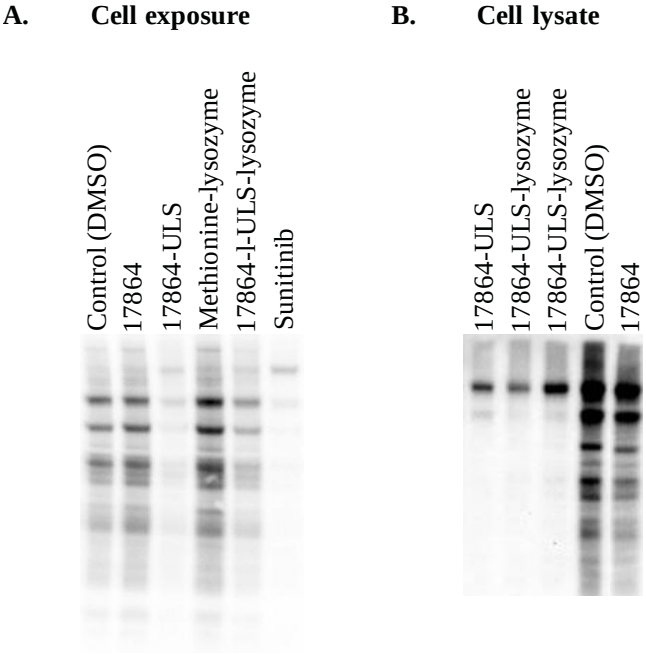

Figure 3. (A) HK-2 cells were incubated with 10 µM 17864, 17864-ULS, methionine-modified lysozyme, 17864-ULS-lysozyme and sunitinib and with 0.1% (v/ v) DMSO (control). After 24 hours incubation the cells were lysed and ATP was added to stimulate the phosphorylation of tyrosine kinases. Western blot analysis was performed to investigate the inhibitory effects of the compounds on the phosphorylation of tyrosine kinases. (B) Freshly prepared HK-2 cell lysates were spiked with 2 µM 17864, 17864-ULS and 17864-ULS-lysozyme (two batches) and with 0.1% (v/ v) DMSO (control). After 30 minutes incubation ATP was added to stimulate the phosphorylation of tyrosine kinases. Western blot analysis was performed to investigate the inhibitory effects of the compounds on the phosphorylation of tyrosine kinases.

Figure 3A shows the anti-phosphotyrosine western blot of HK-2 cells exposed to 10 µM of 17864, 17864-ULS, methionine-lysozyme, 17864-ULS-lysozyme and sunitinib malate, respectively. Both sunitinib and 17864-ULS-lysozyme strongly inhibited multiple kinases, as can be deduced from the strong reduction in tyrosine-phosphorylated proteins. The inhibitory effects of 17864-ULS were almost as strong as the inhibitory effects observed with sunitinib. Unexpectedly, unmodified 17864 did not reduce the phosphorylation of tyrosine kinases in this experimental set-up. We conducted an additional experiment, in which the compounds were spiked directly into the cell lysate. Differences in uptake and cytosolic delivery of the compounds were thereby avoided. Again, unmodified 17864 showed only a minor reduction in tyrosine phosphorylation, while a strong inhibition was observed with 2 µM of both 17864-ULS and 17864-ULS-lysozyme (**Figure 3B**).
The hypothesis that platinum-bound 17864 could still exert its effects was, therefore, confirmed. Linkage of 17864 to ULS or ULS-lysozyme even resulted in a stronger inhibitory effect of the kinase inhibitor.

3.3. Pharmacokinetics of 17864-ULS-lysozyme

The pharmacokinetics of 17864-ULS-lysozyme were investigated in mice and compared with the renal distribution of non-conjugated sunitinib. **Figure 4** shows the plasma disappearance curves of 17864-ULS-lysozyme and sunitinib after a single intravenous injection of the compounds. Pharmacokinetic parameters were calculated by fitting the data to a two-compartment model (**Table 1**). When comparing the plasma data of 17864-ULS-lysozyme and sunitinib, the most pronounced differences can be observed in the distribution volumes of the compounds. The initial volume of distribution (V_d) of sunitinib is over 15-fold higher than for 17864-ULS-lysozyme. A plausible explanation for the high V_d of sunitinib is its capability to penetrate easily into cells and tissues and its high protein binding in both plasma and tissues (10). In contrast, distribution of 17864-ULS-lysozyme will be restricted to the circulation and the extracellular fluids, as it cannot passively diffuse across membranes. The plasma elimination rate of 17864-ULS-lysozyme is in agreement with results obtained in earlier studies with other kinase inhibitor-ULS-lysozyme conjugates (23-25). Furthermore, no free 17864 could be detected in the circulation after administration of 17864-ULS-lysozyme.

Table 1. Pharmacokinetic parameters of 17864-ULS-lysozyme and sunitinib derived from the plasma disappearance curves after a single intravenous injection.

Pharmacokinetic parameter	17864-ULS-lysozyme	Sunitinib
Initial V_d	2.5 mL	44 mL
V_2	7.3 mL	87 mL
$(t_{1/2})_\alpha$	4 min	0.5 min
$(t_{1/2})_\beta$	3.3 h	25 min

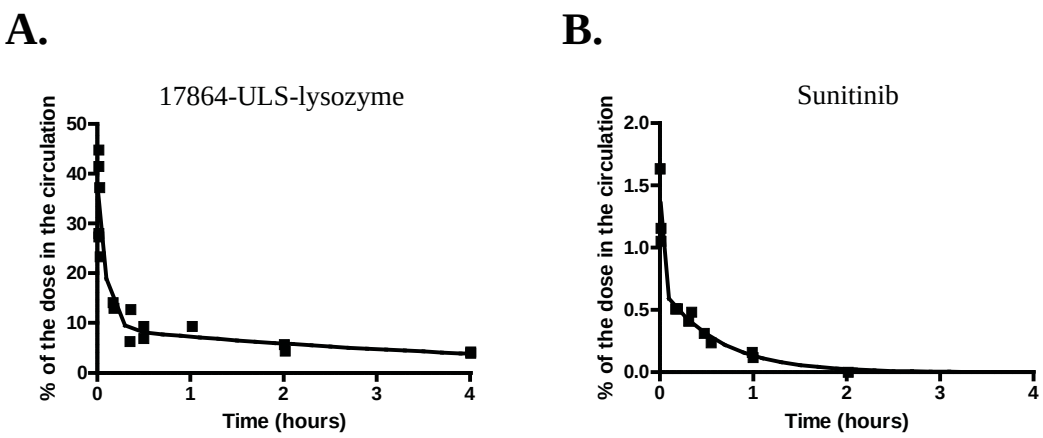

Figure 4. Plasma disappearance curves of 17864-ULS-lysozyme (A) and sunitinib (B) after a single intravenous injection in mice. Plasma concentrations were expressed as the % of the dose in the total circulation. The continuous lines represent the data fitted to a nonlinear multi-compartment model.

In addition to their plasma disappearance, we also analyzed the total renal kinase inhibitor levels after injection of 17864-ULS-lysozyme and sunitinib (**Figure 5A**). Data were fitted with a nonlinear two-compartment model and the pharmacokinetic parameters of the renal data are summarized in **Table 2**. Both 17864-ULS-lysozyme and sunitinib were rapidly taken up in the kidneys with short absorption half lives ($(t_{1/2})_{absorption}$). Maximum renal levels of 6.3% and 4.9% of the injected dose were reached within 30 minutes after administration of 17864-ULS-lysozyme and sunitinib, respectively. Comparing the renal residence time of 17864-ULS-lysozyme with the renal residence time of sunitinib, the renally targeted conjugate showed a drastically prolonged renal retention. The renal elimination half life $(t_{1/2})_{elimination}$ of sunitinib was 66 minutes, while 17864-ULS-lysozyme provided renal drug levels that lasted for several days and decayed with an elimination half life of 28 hours. Renal levels of 17864 were still detectable at the end of the experimental period, *i.e.* 3 days after administration of the conjugate. The drug exposure in the kidneys, as reflected in the renal AUC of the compounds, was increased 28-fold (261% dose*h versus 9.4% dose*h for 17864-ULS-lysozyme versus sunitinib, respectively). **Figure 5B** shows that more than 95% of the multitargeted kinase inhibitor 17864 detected in the kidneys was present in the more active ULS-bound form.

Table 2. Pharmacokinetic parameters of 17864-ULS-lysozyme and sunitinib derived from the renal accumulation curves after a single intravenous injection.

Pharmacokinetic parameter	17864-ULS-lysozyme	Sunitinib
$(t_{1/2})_{absorption}$	3 min	4 min
$(t_{1/2})_{elimination}$	28 h	66 min
C_{max} (% of the dose)	6.3%	4.9%
$AUC_{0-\infty}$	261 % dose*h	9.4 % dose*h

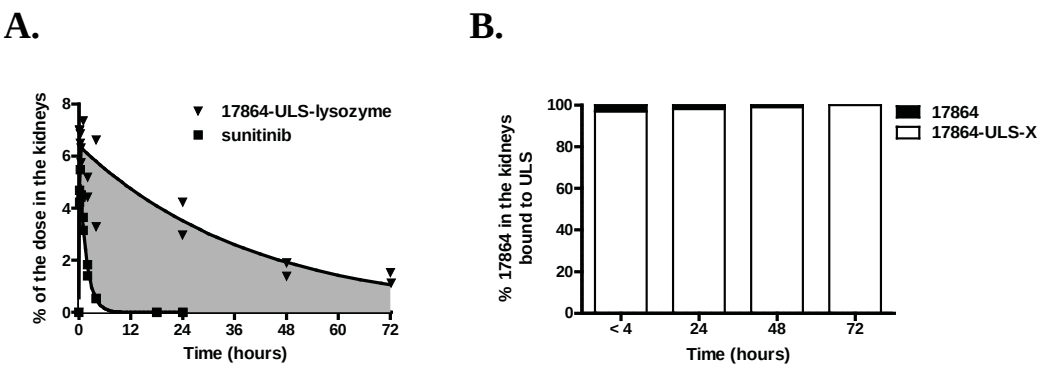

Figure 5. (A) Comparison of the total renal 17864 levels after a single intravenous injection of 17864-ULS-lysozyme and the renal sunitinib levels after a single intravenous injection of sunitinib malate. The increase in AUC obtained with 17864-ULS-lysozyme is highlighted in gray. The continuous lines represent the data fitted to a nonlinear two-compartment model. (B) Percentage of the total renal 17864 levels present in the more active 17864-ULS-X form. The average was taken of the mice sacrificed between 0 and 4 hours and sacrificed at 24, 48 and 72 hours, respectively.

3.4. Efficacy of 17864-ULS-lysozyme in renal fibrosis

3.4.1. Inhibitory effects on the activation of PDGFR-β

The antifibrotic effects of 17864-ULS-lysozyme were studied in mice with UUO-induced tubulointerstitial fibrosis and compared with the inhibitory effects obtained with a low dosage (*i.e.* a single dose equimolar to the conjugate) and a therapeutic dosage (*i.e.* daily 50 mg/ kg) of sunitinib malate. The therapeutic dosage was based on the normal dosage used in cancer treatment and was comparable with the dosage used for the investigation of the antifibrotic effects of sunitinib malate in the treatment of liver cirrhosis (*i.e.* daily 40 mg/ kg) (17, 36). Internalization of 17864-ULS-lysozyme by the renal proximal tubular cells is only possible when the conjugate is able to reach the megalin receptor on the apical membrane of the cells. In this model for tubulointerstitial fibrosis the urinary flow of the diseased kidney was disturbed, which negatively influenced the renal accumulation of 17864-ULS-lysozyme. Therefore, the intravenous injections of 17864-ULS-lysozyme and the low dose sunitinib malate and the first intraperitoneal injection of the high dose sunitinib malate were administered one hour prior to induction of UUO. The second and third intraperitoneal injections of 50 mg/ kg sunitinib malate were administered at 24 and 48 hours after UUO-induction, respectively.

In the group treated with the therapeutic dosage of sunitinib, three mice had to be withdrawn from the experiment after the second intraperitoneal injection (day two), due to drug-related systemic toxicity. No such adverse events were observed in the other groups.

As a first read-out of the fibrotic responses in the kidney after ureteral obstruction, we investigated the levels of activated PDGFR-β tyrosine kinase. Western blot analysis of the p-PDGFR-β levels in the renal cortex confirmed the slightly activation of PDGFR-β after three days of ureteral obstruction (**Figure 6A**). Daily treatment with a high dose sunitinib resulted in decreased p-PDGFR-β levels in the renal cortex, as compared with the non-treated mice with UUO-induced renal fibrosis. However, no inhibitory effects were observed for 17864-ULS-lysozyme and the low dose sunitinib (**Figure 6B)**.

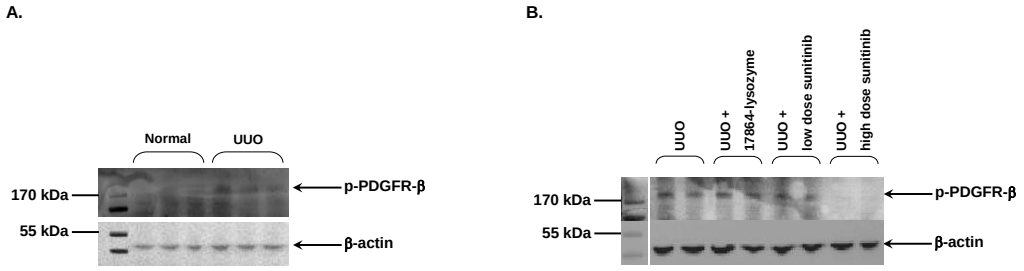

Figure 6. Western blot analysis of activated PDGFR-β (p-PDGFR-β) levels in the renal cortex. (A) Three days ureteral obstruction resulted in an increased activation of PDGFR-β tyrosine kinase. (B) Inhibitory effects were only obtained with daily intraperitoneal injections of 50 mg/ kg sunitinib malate.

3.4.2. mRNA expression of downstream profibrotic factors

As a more downstream read-out of profibrotic responses, we evaluated the renal mRNA expression levels of collagen 1A2, plasminogen activator inhibitor-1 (PAI-1), fibronectin and monocyte chemotactic protein-1 (MCP-1) in the kidneys. Collagen 1A2, PAI-1 and fibronectin are involved in ECM production, while MCP-1 contributes to inflammatory responses. Earlier performed experiments in animals with UUO-induced tubulointerstitial fibrosis have demonstrated the upregulation of these factors in this animal model (24, 37, 38). Indeed, the mRNA expression levels of collagen 1A2, PAI-1, fibronectin and MCP-1 in the kidneys were significantly elevated in mice with three days UUO compared with normal mice (**Figure 7**). No inhibitory effects on the elevated mRNA expression levels of the profibrotic genes, however, were obtained with 17864-ULS-lysozyme and the low dose sunitinib. Mice with UUO-induced tubulointerstitial fibrosis treated with a daily intraperitoneal injection of a high dose sunitinib had significant lower renal mRNA levels of collagen 1A2 and fibronectin.

Renal mRNA expression levels were also investigated in renal cortex homogenate, in addition to their analysis in total renal homogenate. These analyses provided similar trends in renal expression of the investigated genes (data not shown).

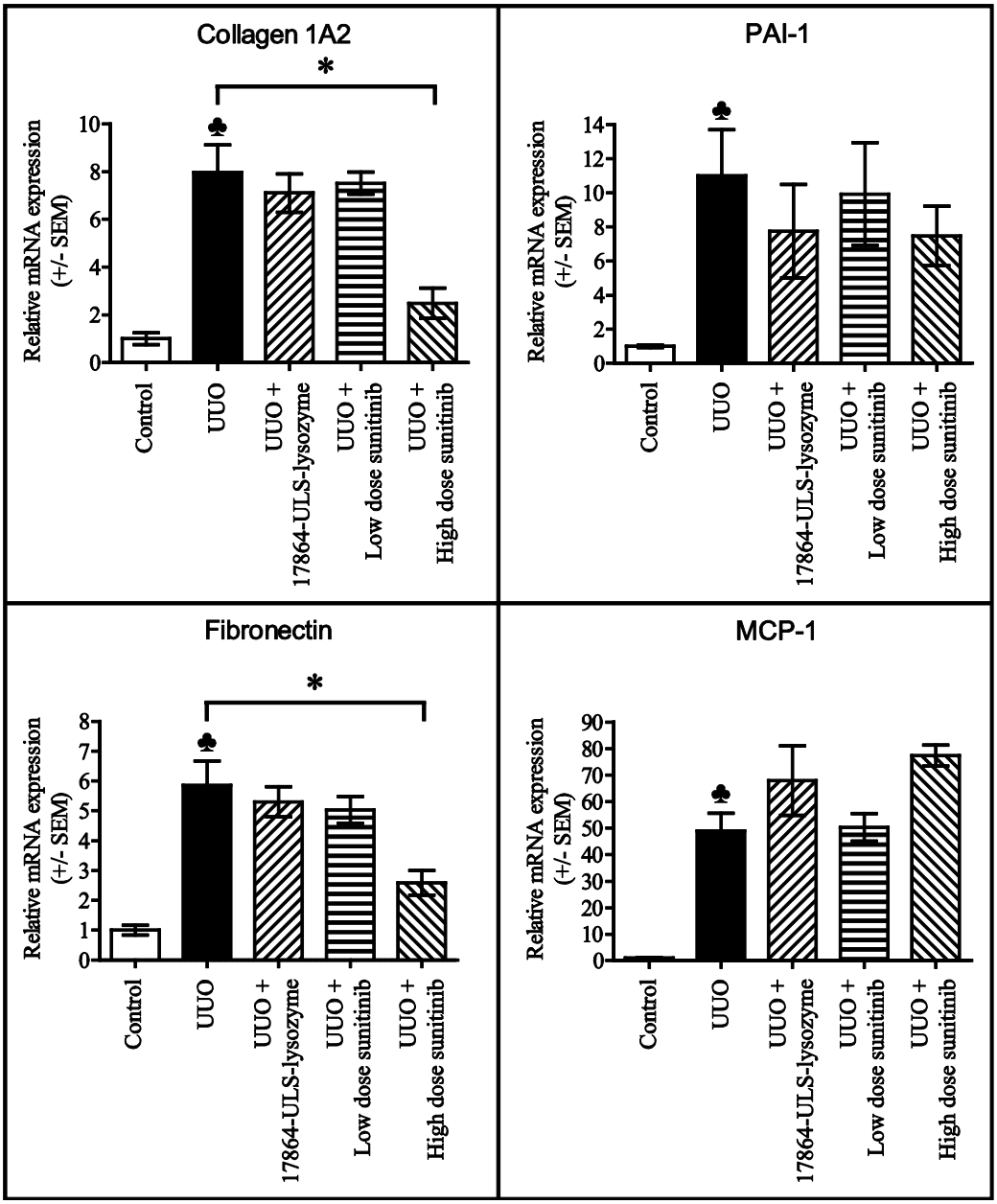

Figure 7. mRNA expression of collagen 1A2, PAI-1, fibronectin and MCP-1 in the kidneys. The mRNA levels were determined by qRT-PCR and normalized to the household gene TBP. The normalized mRNA expression levels in the kidneys of treated and non-treated mice with UUO were related to the normalized mRNA expression levels in the kidneys of control mice (set at 1). Data represent the mean +/ - SEM. Statistical differences between the non-treated mice with UUO and control mice are indicated as ♣ ($p < 0.05$). Statistical differences between the treated and non-treated mice with UUO are indicated as * ($p < 0.05$).

3.4.3. Immunohistochemistry of the renal cortex

Finally, we investigated the renal levels of α-SMA, collagen IV and vimentin in paraffin-embedded kidney sections by immunostaining (**Figure 8**). Daily treatment with 50 mg/ kg sunitinib malate seemed to decrease the deposition of vimentin in the kidneys, although these differences were not significant when quantified by morphometric analysis. Treatment with 17864-ULS-lysozyme and low dose sunitinib did not affect the elevated expression levels observed after ureter obstruction.

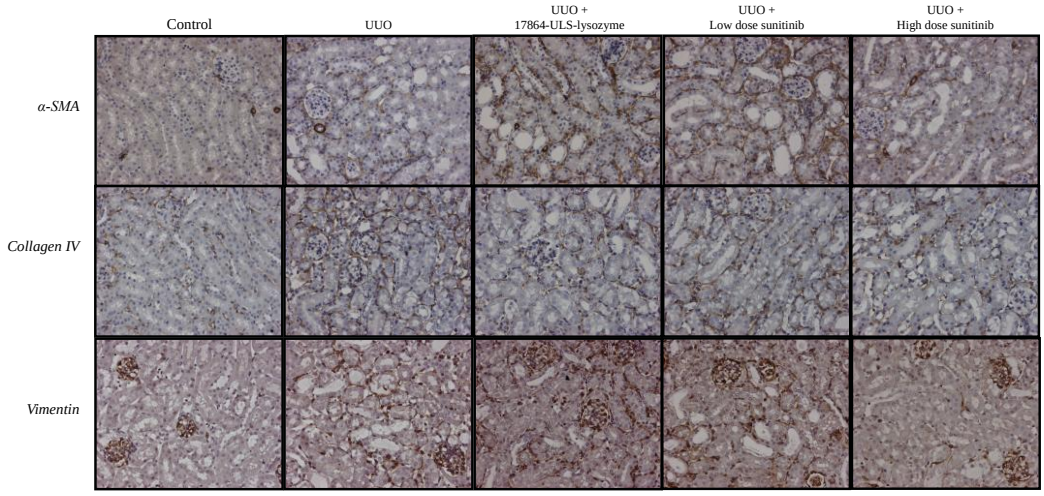

Figure 8. Representative microscopic images of paraffin-embedded kidney sections immunostained for α-SMA, collagen IV and vimentin. In the pathogenesis of renal fibrosis α-SMA is involved in EMT of normal epithelial cells into myofibroblasts, collagen IV in ECM production and vimentin in both processes. The magnification for all images was 20x.

4. Discussion

The pathogenesis of tubulointerstitial fibrosis is very complex and multiple kinase driven signaling cascades are involved. Treatment with a multitargeted kinase inhibitor might therefore be attractive. But due to their lower specificity, multitargeted kinase inhibitors are commonly associated with a broad range of side effects. In the current study we designed a platinum-bound sunitinib analogue (*i.e.* 17864-ULS) that could successfully be delivered to the kidneys by conjugation to the low molecular weight protein lysozyme. Such kidney-specific derivatives of sunitinib are expected not be internalized by non-target cells, and systemic side effects will therefore be avoided. We showed that coupling of the sunitinib analogue 17864 to the platinum linker ULS increased the activity of the multitargeted kinase inhibitor. The increase in activity was retained after conjugation of the 17864-ULS adduct to lysozyme.

Lysozyme is a prototypical carrier protein used for the delivery of drugs to the proximal tubular cells of the kidneys. Earlier studies have demonstrated that linkage of kinase inhibitors to lysozyme via the platinum (II)-based ULS linker yielded conjugates with a prolonged residence time in the designated cells and that the majority of the targeted drug was present in the ULS-bound form. The multitargeted kinase inhibitor sunitinib lacks functional groups that can be

coordinated to the platinum linker. We therefore developed a sunitinib derivative that could not only be coupled to the platinum linker, but also retained its activity in the ULS-bound form. The developed derivative 17864 is closely related to other sunitinib side-chain derivatives with comparable activity against PDGFR-β and VEGFR-2 (32). Our study confirmed that the activity of 17864 was retained when conjugated to the ULS linker or lysozyme (via ULS). Moreover, an even higher activity was observed with 17864-ULS adducts as compared with the parent drug. This observation is supported by other studies in which metal complexation of staurosporine-like kinase inhibitors resulted in stable scaffolds with an improved affinity for target kinases (39, 40).

In vivo, the multitargeted 17864-ULS-lysozyme conjugate was rapidly taken up by the kidneys and the renal exposure time of 17864 after a single intravenous injection of the conjugate in mice was longer than three days. A 28-fold increase in renal exposure of the kinase inhibitor was obtained versus an equimolar dose of sunitinib malate. Almost all 17864 detected in the kidneys was present in the platinum-bound form, which is the more active form. In contrast to 17864-ULS, which was retained in the kidneys, sunitinib was rapidly excreted from the kidneys. Sunitinib is a substrate of the broad spectrum efflux transporters P-glycoprotein (P-gp) and ATP-binding cassette sub-family G member 2 ABCG2, both expressed on the apical membrane of the proximal tubular cells (41, 42). It is reasonable to assume that slightly modified derivatives of sunitinib, such as 17864, also are substrates of these transporters. The sustained intracellular retention of 17864-ULS may, however, be explained by other differences between the administered compounds. Firstly, the platinum group of 17864-ULS is charged and the platinum complex thus will have a low tendency to diffuse across membranes. Furthermore, the structural features of the platinum adduct may make it a poor substrate for efflux transporters. Lastly, another feature that may be involved is the capability of 17864-ULS to bind to intracellular proteins or macromolecules, and such platinum adducts will not easily be excreted into the urine or into the renal interstitium.

The *in vivo* efficacy of 17864-ULS-lysozyme was tested in a mouse UUO model, which is a standard model for tubulointerstitial fibrosis (43). We however only studied mice that had suffered from three days ureteral obstruction, *i.e.* the early stages of renal fibrosis. The kidneys of these animals showed all signs of early fibrosis as indicated by the mild increase in PDGFR-β activation and increased deposition and production of profibrotic factors involved in inflammation, EMT and ECM. Daily treatment with a high dose sunitinib resulted in a reduction of some of the studied markers, indicating that this multitargeted kinase inhibitor may be beneficial for the treatment of renal fibrosis. The drug-related toxicity observed in this group, however, underscores the need for a more focused delivery of the drug to diseased tissues, as undertaken in this study. As anticipated, the single low sunitinib dose showed no therapeutic benefit. Our pharmacokinetic study showed that sunitinib was almost completely eliminated from the kidneys within twelve hours after administration, which explains the lack of efficacy at three days after administration. The absence of therapeutic responses following 17864-ULS-lysozyme treatment were, however, less expected since active 17864-ULS metabolites could still be detected in the kidneys at three days after injection. There may be several explanations for the observed lack of efficacy of 17864-ULS-lysozyme. First, the inhibitor levels reached within the target cells may have been too low. Treatment with a higher dose or repeated doses of 17864-ULS-lysozyme may overcome this problem. The dose used in the current study (*i.e.* 40 mg/ kg/ dose) was chosen based on the maximum solubility and injection volume of the

conjugate that can be tolerated by mice after intravenous injection without overloading the systemic circulation. Furthermore, the treatment of mice in this model with 17864-ULS-lysozyme was limited to a single dose, since the blockage of the ureter prevents the necessary transport of the conjugate to the apical side of the proximal tubular cells. Obviously, this situation is specific for the ureter obstruction model, and we will therefore investigate the multiple dosing of the conjugate in other renal models which will allow multiple dosing (25).

Another possible explanation for the lack of efficacy is that 17864-ULS does not escape easily from the lysosomal compartment, where it is accumulated after megalin receptor-mediated endocytosis. 17864-ULS-lysozyme will be enzymatically degraded within the lysosomes and 17864 will be slowly released from the platinum linker by competitive displacement of the drug by the relatively high intracellular concentrations of strong platinum ligands such as gluthathione and cysteine. When the charged 17864-ULS metabolites cannot diffuse readily over membranes, as discussed above, only the free 17864 can reach the cytosolic kinases or membrane bound receptor tyrosine kinases. If the 17864-ULS metabolites do not reach their pharmacological targets due to the lack of a proper transport mechanism allowing passage over the lysosomal membranes, this may explain the lack of antifibrotic effects observed with 17864-ULS-lysozyme.

Finally, another explanation for the lack of *in vivo* efficacy can be that 17864 should be targeted to other cell types besides proximal tubular cells to counteract fibrosis. Although the proximal tubular cells play a pivotal role in the pathogenesis of tubulointerstitial fibrosis, also the peritubular endothelial cells and interstitial fibroblasts are involved (1). Free distribution of sunitinib through the kidneys to these cell types might have contributed to the antifibrotic effects observed with the non-conjugated kinase inhibitor.

Conclusions

In the present study, a derivative of the multitargeted kinase inhibitor sunitinib was developed, *i.e.* 17864, that was conjugated to the renal carrier protein lysozyme via the platinum linker ULS. The resulting 17864-ULS-lysozyme conjugate and its 17864-ULS metabolites were active in a multikinase assay. Upon systemic administration in mice, 17864-ULS-lysozyme provided sustained levels of ULS-bound 17864 in the kidneys. We will evaluate the potential antifibrotic effects of this type of renally targered multikinase inhibitor conjugates in models of renal fibrosis that will allow frequent dosing of the conjugate, in order to provide intrarenal levels of a platinum-bound sunitinib analogue without the systemic side effects of non-cell specific multikinase inhibitors.

Acknowledgements

We would like to thank K.M.A. van Dorenmalen for her assistance in the animal experiments. We also would like to thank D.M. van der Giezen for her assistance in the animal efficacy study and immunohistochemical analyses and J.W. Leeuwis and A. Dendooven for their assistance in the immunohistochemical and qRT-PCR analyses. This work was made possible by a grant from the European Framework program FP6 (LSHB-CT-2007-036644).

References

1. M. Zeisberg and E.G. Neilson. Mechanisms of tubulointerstitial fibrosis. J Am Soc Nephrol. 21:1819-1834 (2010).
2. P. Boor, T. Ostendorf and J. Floege. Renal fibrosis: novel insights into mechanisms and therapeutic targets. Nat Rev Nephrol. 6:643-656 (2010).
3. S.A. Mezzano, M.A. Droguett, M.E. Burgos, L.G. Ardiles, C.A. Aros, I. Caorsi and J. Egido. Overexpression of chemokines, fibrogenic cytokines, and myofibroblasts in human membranous nephropathy. Kidney Int. 57:147-158 (2000).
4. K. Sean Eardley and P. Cockwell. Macrophages and progressive tubulointerstitial disease. Kidney Int. 68:437-455 (2005).
5. T.D. Hewitson. Renal tubulointerstitial fibrosis: common but never simple. Am J Physiol Renal Physiol. 296:F1239-1244 (2009).
6. M.E.M. Dolman, S. Harmsen, G. Storm, W.E. Hennink and R.J. Kok. Drug targeting to the kidney: Advances in the active targeting of therapeutics to proximal tubular cells. Adv Drug Deliv Rev. 62:1344-1357 (2010).
7. E. Ripley. Complementary effects of angiotensin-converting enzyme inhibitors and angiotensin receptor blockers in slowing the progression of chronic kidney disease. Am Heart J. 157:S7-S16 (2009).
8. L. Yu, N.A. Noble and W.A. Border. Therapeutic strategies to halt renal fibrosis. Curr Opin Pharmacol. 2:177-181 (2002).
9. L.F. Kontovinis, K.T. Papazisis, P. Touplikioti, C. Andreadis, D. Mouratidou and A.H. Kortsaris. Sunitinib treatment for patients with clear-cell metastatic renal cell carcinoma: clinical outcomes and plasma angiogenesis markers. BMC Cancer. 9:82 (2009).
10. M.P. Sablin, C. Dreyer, C. Colichi, M. Bouattour, C. Delbaldo, S. Faivre and E. Raymond. Benefits from pharmacological and pharmacokinetic properties of sunitinib for clinical development. Expert Opin Drug Metab Toxicol. 6:1005-1015 (2010).
11. W.J. Lee, J.L. Lee, S.E. Chang, M.W. Lee, Y.K. Kang, J.H. Choi, K.C. Moon and J.K. Koh. Cutaneous adverse effects in patients treated with the multitargeted kinase inhibitors sorafenib and sunitinib. Br J Dermatol. 161:1045-1051 (2009).
12. M.W. Karaman, S. Herrgard, D.K. Treiber, P. Gallant, C.E. Atteridge, B.T. Campbell, K.W. Chan, P. Ciceri, M.I. Davis, P.T. Edeen, R. Faraoni, M. Floyd, J.P. Hunt, D.J. Lockhart, Z.V. Milanov, M.J. Morrison, G. Pallares, H.K. Patel, S. Pritchard, L.M. Wodicka and P.P. Zarrinkar. A quantitative analysis of kinase inhibitor selectivity. Nat Biotechnol. 26:127-132 (2008).
13. J.C. Bonner. Regulation of PDGF and its receptors in fibrotic diseases. Cytokine Growth Factor Rev. 15:255-273 (2004).
14. M. Trojanowska. Role of PDGF in fibrotic diseases and systemic sclerosis. Rheumatology (Oxford). 47 Suppl 5:v2-4 (2008).
15. J. Kanellis, K. Paizis, A.J. Cox, S.A. Stacker, R.E. Gilbert, M.E. Cooper and D.A. Power. Renal ischemia-reperfusion increases endothelial VEGFR-2 without increasing VEGF or VEGFR-1 expression. Kidney Int. 61:1696-1706 (2002).
16. N.K. Malmstrom, E.A. Kallio, J.M. Rintala, A.I. Nykanen, A.K. Raisanen-Sokolowski, T. Paavonen, K.B. Lemstrom and P.K. Koskinen. Vascular endothelial growth factor in chronic rat allograft nephropathy. Transpl Immunol. 19:136-144 (2008).
17. S. Tugues, G. Fernandez-Varo, J. Munoz-Luque, J. Ros, V. Arroyo, J. Rodes, S.L. Friedman, P. Carmeliet, W. Jimenez and M. Morales-Ruiz. Antiangiogenic treatment with sunitinib ameliorates inflammatory infiltrate, fibrosis, and portal pressure in cirrhotic rats. Hepatology. 46:1919-1926 (2007).
18. T. Force, D.S. Krause and R.A. Van Etten. Molecular mechanisms of cardiotoxicity of tyrosine kinase inhibition. Nat Rev Cancer. 7:332-344 (2007).
19. D. Bovelli, G. Plataniotis and F. Roila. Cardiotoxicity of chemotherapeutic agents and radiotherapy-related heart disease: ESMO Clinical Practice Guidelines. Ann Oncol. 21 Suppl 5:v277-282 (2010).
20. G. Di Lorenzo, R. Autorino, G. Bruni, G. Carteni, E. Ricevuto, M. Tudini, C. Ficorella, C. Romano, M. Aieta, A. Giordano, M. Giuliano, A. Gonnella, C. De Nunzio, M. Rizzo, V. Montesarchio, M. Ewer and S. De Placido. Cardiovascular toxicity following sunitinib therapy in metastatic renal cell carcinoma: a multicenter analysis. Ann Oncol. 20:1535-1542 (2009).

21. N. Bhojani, C. Jeldres, J.J. Patard, P. Perrotte, N. Suardi, G. Hutterer, F. Patenaude, S. Oudard and P.I. Karakiewicz. Toxicities associated with the administration of sorafenib, sunitinib, and temsirolimus and their management in patients with metastatic renal cell carcinoma. Eur Urol. 53:917-930 (2008).
22. S.E. Rosenbaum, S. Wu, M.A. Newman, D.P. West, T. Kuzel and M.E. Lacouture. Dermatological reactions to the multitargeted tyrosine kinase inhibitor sunitinib. Support Care Cancer. 16:557-566 (2008).
23. J. Prakash, M.H. de Borst, M. Lacombe, F. Opdam, P.A. Klok, H. van Goor, D.K. Meijer, F. Moolenaar, K. Poelstra and R.J. Kok. Inhibition of renal rho kinase attenuates ischemia/ reperfusion-induced injury. J Am Soc Nephrol. 19:2086-2097 (2008).
24. J. Prakash, M.H. de Borst, A.M. van Loenen-Weemaes, M. Lacombe, F. Opdam, H. van Goor, D.K. Meijer, F. Moolenaar, K. Poelstra and R.J. Kok. Cell-specific delivery of a transforming growth factor-beta type I receptor kinase inhibitor to proximal tubular cells for the treatment of renal fibrosis. Pharm Res. 25:2427-2439 (2008).
25. J. Prakash, M. Sandovici, V. Saluja, M. Lacombe, R.Q. Schaapveld, M.H. de Borst, H. van Goor, R.H. Henning, J.H. Proost, F. Moolenaar, G. Keri, D.K. Meijer, K. Poelstra and R.J. Kok. Intracellular delivery of the p38 mitogen-activated protein kinase inhibitor SB202190 [4-(4-fluorophenyl)-2-(4-hydroxyphenyl)-5-(4-pyridyl)1H-imidazole] in renal tubular cells: a novel strategy to treat renal fibrosis. J Pharmacol Exp Ther. 319:8-19 (2006).
26. E.I. Christensen, P.J. Verroust and R. Nielsen. Receptor-mediated endocytosis in renal proximal tubule. Pflugers Arch. 458:1039-1048 (2009).
27. K. Temming, M.M. Fretz and R.J. Kok. Organ- and cell-type specific delivery of kinase inhibitors: a novel approach in the development of targeted drugs. Curr Mol Pharmacol. 1:1-12 (2008).
28. T. Gonzalo, L. Beljaars, M. van de Bovenkamp, K. Temming, A.M. van Loenen, C. Reker-Smit, D.K. Meijer, M. Lacombe, F. Opdam, G. Keri, L. Orfi, K. Poelstra and R.J. Kok. Local inhibition of liver fibrosis by specific delivery of a platelet-derived growth factor kinase inhibitor to hepatic stellate cells. J Pharmacol Exp Ther. 321:856-865 (2007).
29. Y. Liu and N.S. Gray. Rational design of inhibitors that bind to inactive kinase conformations. Nat Chem Biol. 2:358-364 (2006).
30. J.J. Liao. Molecular recognition of protein kinase binding pockets for design of potent and selective kinase inhibitors. J Med Chem. 50:409-424 (2007).
31. K.S. Gajiwala, J.C. Wu, J. Christensen, G.D. Deshmukh, W. Diehl, J.P. DiNitto, J.M. English, M.J. Greig, Y.A. He, S.L. Jacques, E.A. Lunney, M. McTigue, D. Molina, T. Quenzer, P.A. Wells, X. Yu, Y. Zhang, A. Zou, M.R. Emmett, A.G. Marshall, H.M. Zhang and G.D. Demetri. KIT kinase mutants show unique mechanisms of drug resistance to imatinib and sunitinib in gastrointestinal stromal tumor patients. Proc Natl Acad Sci U S A. 106:1542-1547 (2009).
32. L. Sun, C. Liang, S. Shirazian, Y. Zhou, T. Miller, J. Cui, J.Y. Fukuda, J.Y. Chu, A. Nematalla, X. Wang, H. Chen, A. Sistla, T.C. Luu, F. Tang, J. Wei and C. Tang. Discovery of 5-[5-fluoro-2-oxo-1,2-dihydroindol-(3Z)-ylidenemethyl]-2,4- dimethyl-1H-pyrrole-3-carboxylic acid (2-diethylaminoethyl)amide, a novel tyrosine kinase inhibitor targeting vascular endothelial and platelet-derived growth factor receptor tyrosine kinase. J Med Chem. 46:1116-1119 (2003).
33. R.P. van Gijlswijk, E.G. Talman, I. Peekel, J. Bloem, M.A. van Velzen, R.J. Heetebrij and H.J. Tanke. Use of horseradish peroxidase- and fluorescein-modified cisplatin derivatives for simultaneous labeling of nucleic acids and proteins. Clin Chem. 48:1352-1359 (2002).
34. A. Rippe, C. Rippe, K. Sward and B. Rippe. Disproportionally low clearance of macromolecules from the plasma to the peritoneal cavity in a mouse model of peritoneal dialysis. Nephrol Dial Transplant. 22:88-95 (2007).
35. R.W. Sparidans, D. Iusuf, A.H. Schinkel, J.H. Schellens and J.H. Beijnen. Liquid chromatography-tandem mass spectrometric assay for the light sensitive tyrosine kinase inhibitor axitinib in human plasma. J Chromatogr B Analyt Technol Biomed Life Sci. 877:4090-4096 (2009).
36. G.D. Demetri, A.T. van Oosterom, C.R. Garrett, M.E. Blackstein, M.H. Shah, J. Verweij, G. McArthur, I.R. Judson, M.C. Heinrich, J.A. Morgan, J. Desai, C.D. Fletcher, S. George, C.L. Bello, X. Huang, C.M. Baum and P.G. Casali. Efficacy and safety of sunitinib in patients with advanced gastrointestinal stromal tumour after failure of imatinib: a randomised controlled trial. Lancet. 368:1329-1338 (2006).

37. A.C. Chung, X.R. Huang, L. Zhou, R. Heuchel, K.N. Lai and H.Y. Lan. Disruption of the Smad7 gene promotes renal fibrosis and inflammation in unilateral ureteral obstruction (UUO) in mice. Nephrol Dial Transplant. 24:1443-1454 (2009).
38. S. Wang, M.C. Wilkes, E.B. Leof and R. Hirschberg. Imatinib mesylate blocks a non-Smad TGF-beta pathway and reduces renal fibrogenesis in vivo. Faseb J. 19:1-11 (2005).
39. A. Wilbuer, D.H. Vlecken, D.J. Schmitz, K. Kraling, K. Harms, C.P. Bagowski and E. Meggers. Iridium complex with antiangiogenic properties. Angew Chem Int Ed Engl. 49:3839-3842 (2010).
40. D.S. Williams, P.J. Carroll and E. Meggers. Platinum complex as a nanomolar protein kinase inhibitor. Inorg Chem. 46:2944-2946 (2007).
41. M. Huls, C.D. Brown, A.S. Windass, R. Sayer, J.J. van den Heuvel, S. Heemskerk, F.G. Russel and R. Masereeuw. The breast cancer resistance protein transporter ABCG2 is expressed in the human kidney proximal tubule apical membrane. Kidney Int. 73:220-225 (2008).
42. S. Shukla, R.W. Robey, S.E. Bates and S.V. Ambudkar. Sunitinib (Sutent, SU11248), a small-molecule receptor tyrosine kinase inhibitor, blocks function of the ATP-binding cassette (ABC) transporters P-glycoprotein (ABCB1) and ABCG2. Drug Metab Dispos. 37:359-365 (2009).
43. H.-C. Yang, Y. Zuo and A.B. Fogo. Models of chronic kidney disease. Drug Discovery Today: Disease Models. In Press, Corrected Proof: (2010).

Chapter 6

Development of a cell-selective and intrinsically active multikinase inhibitor bioconjugate

S. Harmsen[1], M.E.M. Dolman[1], Z. Nemes[1], M. Lacombe[2], B. Szokol[3], J. Pató[3], G. Kéri[3,4], L. Őrfi[3], G. Storm[1], W.E. Hennink[1] and R.J. Kok[1]

[1] Department of Pharmaceutics, Utrecht Institute of Pharmaceutical Sciences, Utrecht University, Utrecht, The Netherlands

[2] KREATECH Biotechnology B.V., Amsterdam, The Netherlands

[3] Vichem Chemie, Budapest, Hungary

[4] Pathobiochemistry Research Group of Hungarian Academy of Sciences and Semmelweis University, Budapest, Hungary

Bioconjugate Chemistry 22(4):540-545 (2011)

Abstract

Multikinase inhibitors are potent anticancer drugs that simultaneously intervene in multiple related signaling cascades, thus capable of blocking salvage pathways that may play a role in the development of drug resistance. Multikinase inhibitors are increasingly evaluated for other indications than cancer, but long-term safety risks dictated by off-organ toxicities of these agents may prevent their safe and effective use. Here, we describe a new approach in which platinum coordination chemistry is applied for the development of a cell-selective multikinase inhibitor bioconjugate. The platinum (II)-kinase inhibitor bioconjugate was designed to be active with the linker attached to the inhibitor and displayed improved activity by enhanced cell-specificity as well as enhanced intracellular retention thereby prolonging its pharmacological activity. In addition, the utilized platinum-based linkage technology potentiated the inhibitory activity of the multikinase inhibitor. These features in combination with carrier-mediated uptake in the target cells may revolutionize dosing regimens and safety profiles of (multi)kinase inhibitors.

1. Introduction

In recent years, kinase inhibitors have emerged as highly successful anticancer drugs. Initially designed to inhibit specific protein kinases such as BCR-ABL (*e.g.* imatinib), later multikinase inhibitors (*e.g.* sunitinib) were developed to concomitantly interrupt multiple distinct signaling pathways. Apart from cancer therapy, multikinase inhibitors are currently increasingly investigated for less life-threatening diseases as well, *i.e.* sunitinib has been shown to potently ameliorate liver cirrhosis (1) and chronic airway inflammation (2), while the related oxindole-based intedanib (BIBF-1120) shows potential in the treatment of idiopathic pulmonary fibrosis (3). A point of concern, however, is the safety profile of multikinase inhibitors (4). The most commonly reported multikinase inhibitor related toxicities include rash, diarrhea, nausea, while long-term toxicities include fatigue, hypothyroidism, and even cardiotoxicity (5, 6). Although these off-target toxicities are more acceptable in cancer therapy, they complicate long-term use of these agents in chronic, less life-threatening illnesses.

To address these safety issues, we developed a multikinase inhibitor-bioconjugate that accumulates in disease-inflicted organs in a target cell-selective manner by recognition of surface-exposed receptors that facilitate internalization. This approach permits lower drug dosages due to increased drug accumulation at the designated pathological tissue, while avoiding uptake in healthy tissues and, thus, decreases the risk of off-organ toxicities. Furthermore, the uptake into specific cell types within the targeted organ will greatly improve the specificity profile of such cellular targeted drugs. We have previously demonstrated that renal tubular cells can be targeted with drug-lysozyme conjugates (7). In the present study, we will use this type of drug-protein conjugates as platform technology for a new type of intrinsically active multikinase inhibitor-bioconjugates.

2. Materials and Methods

2.1. Materials and chemicals

All chemicals used in this study were of analytical grade or equivalent and obtained from Sigma Aldrich (Zwijndrecht, the Netherlands) and used without further purification unless otherwise stated. The multikinase inhibitor precursor (*Z*)-2,4-dimethyl-5-((2-oxoindolin-3-ylidene)methyl-1*H*-pyrrole-3-carboxylic acid was synthesized by Vichem Chemie (Budapest, Hungary). Universal Linkage System™ (monochloro-mononitrato(ethylenediamine)platinum (II)) was provided by Kreatech (Amsterdam, the Netherlands). HPLC grade acetonitrile (ACN), methanol (MeOH), isopropanol (IPA), formic acid (FA) and *N,N'*-dimethylformamide (DMF) which was dried over molecular sieve before use were purchased from Biosolve (Valkenswaard, the Netherlands). Products were characterized by ^{1}H/ ^{195}Pt NMR and LC-MS/ MS. ^{1}H/ ^{195}Pt NMR spectra were recorded on a Varian Gemini (300 MHz; 298 K; Varian Associates Inc., NMR Instruments, Palo Alto, CA) NMR spectrometer. The LC-MS/ MS equipment consisted of an Accela pump and autosampler and a TSQ Quantum Ultra quadrupole mass spectrometer with heated electrospray ionization (Thermo Fisher Scientific, San Jose, CA, USA). Data were recorded on and the system was controlled by a Dell Precision T3400 personal computer, equipped with the Thermo Fisher Xcalibur software (version 2.07). 5-µL injections were made on an Aquity UPLC® BEH C18 column (30 × 2.1 mm × 1.7 µm; Waters, Milford, USA) with the corresponding VanGuard pre-column (5 × 2.1 mm × 1.7 µm; Waters, Milford, USA). Column temperature was

maintained at 40 °C and the autosampler was maintained at 4 °C. A 20-90% gradient of solvent B over 2.5 min with a 0.5 mL/ min flow rate was used. Solvent A consisted of 0.1% (v/ v) formic acid in water and solvent B of methanol. The eluate was totally led into the electrospray probe, oriented at "+1" in the X-, at "1" in the Y- and at "C" in the Z-direction, from 0.7 min after injection. Electrospray (ESI+) settings were a 4000 V spray voltage, 350 °C capillary and vaporizer temperatures and a 1.0 mTorr argon collision pressure. The mass resolution was set at 0.7 full with at half height (unit resolution) for both separating quadrupoles.

2.2. Molecular modeling of an oxindole-based inhibitor in the ATP-binding pocket of c-KIT

YASARA (www.yasara.org; version 10.6.1) was used to evaluate how oxindole-based multikinase inhibitors generally bind to their targets. Therefore, protein structures co-crystallized with either sunitinib (3G0E) or intedanib (3C7Q) were downloaded from www.pdb.org and their orientation in the binding pocket of their target kinases was studied. YASARA was additionally used to generate a graphic representation of how compound **2** (see below) would bind to c-KIT by modification of the structure used in 3G0E.

*2.3. Synthesis of the multikinase inhibitor (compound **1**), multikinase inhibitor platinum complex (compound **2**) and drug-lysozyme conjugate (compound **3**)*

Compound 1

Compound **1** ((*Z*)-2,4-dimethyl-5-((2-oxoindolin-3-ylidene)methyl)-*N*-(pyridin-4-ylmethyl)-1*H*-pyrrole-3-carboxamide) was synthesized according to methods described by Sun *et al.* (8). In brief, (*Z*)-2,4-dimethyl-5-((2-oxoindolin-3-ylidene)methyl-1*H*-pyrrole-3-carboxylic acid (1.0 g, 3.5 mmol) was suspended in 40 mL dry DMF and 4-(aminomethyl)pyridine (0.38 g, 3.5 mmol), ethylene dichloride (EDC) (0.81 g, 4.2 mmol), *N*-hydroxybenzotriazole (HOBt) (0.57 g, 6.0 mmol) and triethylamine (0.74 mL, 5.3 mmol) were added to the suspension and stirred at 50 °C for 72 hours. The solvent was removed under reduced pressure and the residue was taken up with water and the product was filtered off yielding compound **1** (0.72 g, 54%). ^{1}H NMR (300 MHZ, DMF-d_7): δ (ppm): 10.87 (s, 1H, NH); 8.55 (d, 2H, 2CH, ^{3}J=4.2 Hz); 8.11 (t, 1H, NH); 7.85 (d, 1H, CH, ^{3}J=7.6 Hz); 7.79 (s, 1H, CH); 7.41 (d, 2H, 2CH, ^{3}J=5.0 Hz); 7.18 (t, 1H, CH, ^{3}J=7.6 Hz); 7.02 (t, 1H, CH, ^{3}J=7.6 Hz); 6.97 (d, 1H, CH); 4.60 (d, 2H, CH_2, ^{3}J=6.1); 2.56 (s, 3H, CH_3); 2.55 (s, 3H, CH_3). MS (ESI^+) calcd. for $C_{22}H_{20}N_4O_2H^+$ $[M+H]^+$ 373, detected 373.

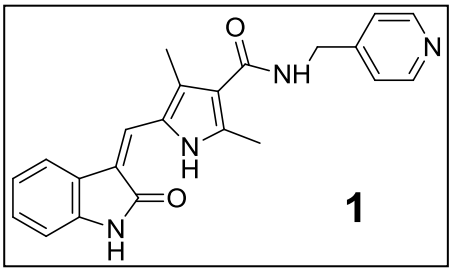

Time (minutes)	Eluent A (%)	Eluent B (%)
0	100	0
25	20	80
26	0	100
33	0	100
34.5	100	0

Table 1. HPLC gradient used for the detection of liberated **1**.

Compound 2

Compound **1** (15.0 mg, 40.3 μmol) was reacted with monochloro-mononitrato (ethylenediamine)platinum (II) (Universal Linkage System (ULS)™-nitrate; 14.2 mg, 40.3 μmol) in DMF for 2 hours at 37 °C to yield compound **2** (23.1 mg, 83.4%). ^{195}Pt NMR (300 MHz, DMF-d_7) -2492 ppm (N3PtCl). ^{1}H NMR (300 MHz, DMF-d_7): δ (ppm): 10.91 (s, 1H, NH); 8.80 (d, 2H, 2CH, ^{3}J=5.6 Hz); 8.23 (t, 1H, NH); 7.86 (d, 1H, CH); 7.81 (s, 1H, CH); 7.62 (d, 2H, 2CH, ^{3}J=6.2 Hz); 7.19 (t, 1H, CH, ^{3}J=7.7 Hz); 7.04 (t, 1H, CH, ^{3}J=7.4 Hz); 7.00 (d, 1H, CH); 6.31 (s, 2H, NH_2), 5.89 (s, 2H, NH_2); 4.69 (d, 2H, CH_2, ^{3}J=5.7 Hz); 2.58 (s, 3H, CH_3); 2.57 (s, 3H, CH_3); 1.56 (t, 2H, CH_2); 1.29 (s, 2H, CH_2).MS (ESI^+) calcd. for $C_{24}H_{28}N_6O_2HPtCl$ $[M+H]^+$ 663, detected 663 $[M+H]^+$.

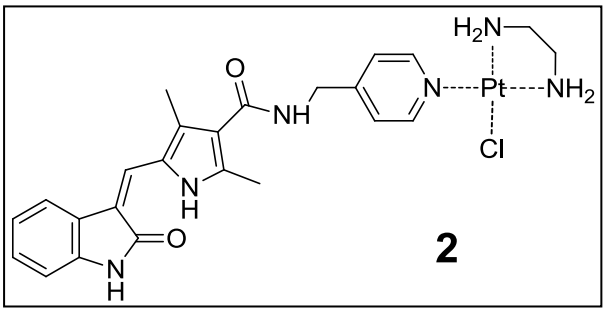

Compound 3

Methionylated lysozyme (LZM) was synthesized as previously described by Fretz *et al.* (9). Compound **2** (15.5 mg, 23.3 μmol) was reacted with methionylated LZM (112.1 mg, 7.8 μmol overnight in 0.02 M tricine/ sodium nitrate buffer (pH 8.5). The product was purified by dialysis (molecular weight cut-off 10,000 Da) against ultrapure water (MilliQ, Millipore, Bedford, MA, USA) and lyophilized. MS (ESI^+) calcd. for $C_{24}H_{28}N_6O_2HPt$-LZM $[M+H]^+$ 14930, detected 1493.0 $[M+H]^{10+}$ and 1357.2 $[M+H]^{11+}$ corresponding with 14930 $[M+H]^+$. Conjugation efficiency was determined as described previously (9). Liberated **1** was quantified in samples containing **3** incubated overnight at 80 °C in the presence of the strong platinum ligand thiocyanate (SCN; 0.5 M) thereby competitively displacing compound **1** from ULS by HPLC-photodiodearray (PDA) analysis at 431 nm. The HPLC system consisted of a Waters 717 autosampler, Waters 600 pumps and a Waters 2996 Photodiode Array Detector (Waters, Milford, USA). Data were recorded with Empower software (version2.0; Waters). 50-μL injections were made on SunFire™ C18 column (150 × 4.6mm × 5 μm; Waters). Gradient elution according to **Table 1** at 1 mL/ min was used with solvent A consisting of 5% ACN in water + 0.1% TFA (w/ w) and solvent B of 0.1% TFA (w/ w) in ACN.

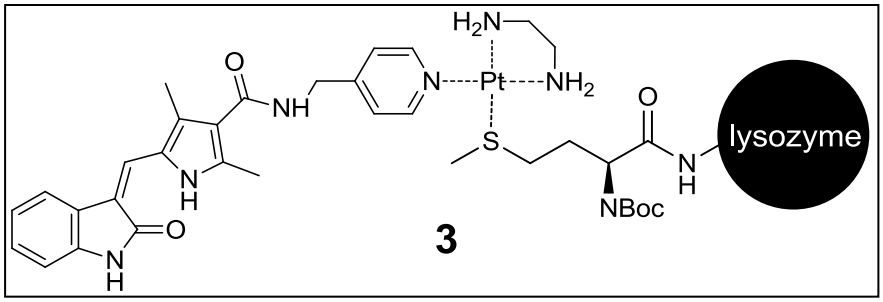

2.4. Determination of intrinsic activity

Cell lysate was prepared by lyzing serum-starved HK-2 cells using mammalian protein extraction reagent (M-PER) containing protease and phosphatase inhibitors (Thermo Fischer Scientific, Etten-Leur, the Netherlands). Protein concentrations were determined using the BCA protein determination assay (Thermo Fischer Scientific). HK-2 cell lysate (0.1 mg/ mL) was pre-incubated with equimolar amounts of **1**, **2** complex, or the **3** drug conjugate at room temperature for 30 minutes. Phosphorylation was initiated by adding 1 μM ATP in Abl kinase assay buffer (50 mM Tris–HCl [pH 7.5], 10 mM $MgCl_2$, 1 mM ethyleneglycoltetraacetic acid (EGTA), 2 mM dithiothreitol (DTT), and 0.01% Brij-35). The reaction mixture was incubated at 37 °C for 60 minutes. Phosphorylation was terminated by adding reducing sample buffer (Invitrogen, Breda, the Netherlands) containing a final concentration of 40 mM DTT and 0.1% (w/ v) SDS. Total protein (10 μg) was separated by SDS-polyacrylamide gel electrophoresis using NuPage novex 4-12% bis-tris gradient gels (Invitrogen, Breda, the Netherlands). Proteins were electroblotted onto Immobilon P polyvinylidenefluoride (PVDF) membranes (Millipore). After blocking (1 hour at room temperature) with 3% (w/ v) BSA in tris-buffered saline containing 0.1% (v/ v) Tween-20, the membranes were incubated for 1 hour at room temperature with a murine monoclonal anti-phosphotyrosine (pY) primary antibody (pY-20; 1:500; Abcam, Cambridge, UK) coupled to horse radish peroxidase (HRP). β-actin (1:10000; AC-15; Abcam, Cambridge, UK) was used as a loading control. The proteins were visualized by a chemiluminescence-based detection reagent (SuperSignal West Femto; Thermo Fischer Scientific, Etten-Leur, the Netherlands) and band density was determined on a Gel Doc XRS Imaging system with Quantity One analysis software (Bio-Rad, Hercules, CA, USA).

2.5. Cellular uptake and retention

2.5.1. Cell culture

The human kidney proximal tubular cell line HK-2 (ATCC, LGC Standards, Middlesex, UK) was cultured in Dulbecco's Modified Eagle's Medium (DMEM) containing 3.7 g/ L sodium bicarbonate, 1.0 g/ L glucose, supplemented with 10% (v/ v) fetal bovine serum, penicillin (100 U/ L), streptomycin (100 μg/ mL) and amphotericin B (0.25 μg/ mL) at 37 °C with 5% CO_2 in humidified air. All cell culture related media were obtained from PAA Laboratories GmbH (Pasching, Austria).

2.5.2. Cellular uptake

HK-2 cells (1.5×10^4 cells/ well) were seeded onto 96-well plates. Cells were serum-starved overnight before the uptake experiments were initiated. Cellular uptake was studied by incubating the HK-2 cells with **1** (10 μM) or **3** (10 μM) for different time intervals (t = 0, 1, 2, 3, 24, 48, 72 h) at 4 °C (only 1, 2, 3 h) or 37 °C. Uptake was determined by measuring the cellular optical density (OD) at 431 nm of **1** and 700 nm (reference wavelength) with a Versamax microplate reader (Molecular Devices, Sunnyvale, CA, USA). Values were normalized to the number of living cells (as determined with an Alamar Blue assay).

2.5.3. Cellular retention

Cellular retention was studied by incubating serum-starved HK-2 cells (1.5×10^4 cells/ well) with either 10 μM **1** or 10 μM **3**. After 24 h (indicated as t = 0 h), cells were washed thrice with phosphate buffered saline (PBS) and medium was replaced with blank serum-free DMEM medium every 24 hours. Cellular retention was determined by measuring the cellular $OD_{431/700}$ (normalized to the number of living cells (Alamar Blue).

2.6. Cellular activity

2.6.1. PamChip® peptide microarray

A microarray-based multiplex method with real-time detection was used to determine the inhibitory activity of **3** on the phosphorylation of peptide substrates that correspond with human proteins. In brief, HK-2 cell lysate (prepared from lysis with M-PER) spiked with **1** (2 μM) or **3** (2 μM) were incubated on a tyrosine kinase PamChip® microarray (PamGene International B.V., 's-Hertogenbosch, the Netherlands) with 10 μM ATP at 30 °C in a total volume of 25 μL. Just prior to the incubations, the PamChip was blocked with 2% (w/ v) BSA in water and washed three times with Abl kinase assay buffer. After application onto the array, the incubation mixture was pumped up and down through the array for 152 cycles at a rate of 2 cycles per minute. Peptide phosphorylation was detected with a monoclonal murine anti-phosphotyrosine primary antibody (pY-20) coupled to FITC. Images of each array were taken every fifth cycle. Data generated on PamChip peptide microarrays were analyzed with Bionavigator software (PamGene). The software quantifies signal intensity in each spot and its background, calculates signal minus background (10). The obtained data was ranked based on strongest pY inhibition compared to control.

2.6.2. IC_{50} determination

IC_{50} determinations of the compounds **1**, **2** and **3** against platelet-derived growth factor receptor (PDGFR)-β and c-KIT were performed by SignalChem (Richmond, Canada). In brief, protein kinase assays were performed in duplicate at room temperature for 30 min in a final volume of 25 μL containing ~10-20 nM recombinant kinase, peptide substrate (0.2 μg/ μL), 5 μM ^{33}P-ATP (0.04 μCi; PerkinElmer, Waltham, MA, USA), and the indicated compounds at concentrations ranging from 0.03 nM-1000 nM in kinase buffer. After the incubation period, the assay was terminated by spotting 10 μL of the reaction mixture onto Multiscreen phosphocellulose P81 plate. The Multiscreen phosphocellulose P81 plate was washed 3 times 15 minutes in a 1% phosphoric acid solution. The radioactivity on the P81 plate was counted in the presence of scintillation fluid in a Trilux scintillation counter.

2.6.3. In-cell western blotting

After incubation, cells were washed thrice with ice-cold PBS and were fixed with 3% (v/ v) formaldehyde (Sigma Aldrich) for 15 minutes. Cells were permeabilized by washing five times with 0.1% (v/ v) triton X-100 (Sigma Aldrich) in PBS for 5 minutes and blocked for 1 h with 3% (w/ v) BSA. After blocking, cells were incubated with a horseradish peroxidase coupled primary antibody raised against phosphorylated tyrosine residues (pY-20; Abcam, Cambridge, UK). After 1 h, cells were washed thrice with PBS and phosphorylation was visualized with a

chemiluminescence-based detection reagent (SuperSignal West Femto; Pierce, Rockford, IL, USA). The signal intensities were determined on a Gel Doc XRS Imaging system with Quantity One analysis software (Bio-Rad, Hercules, CA, USA).

3. Results and discussion

The linkage of the multikinase inhibitor to its carrier was achieved by the platinum (II)-based Universal Linkage System (ULS™; **Scheme 1**). This bioinorganic linker afforded a straightforward linking protocol and also ensured the formation of a conjugate that can be dissociated within cells by competitive displacement of the platinum ligands by endogenous thiols such as glutathione (GSH).

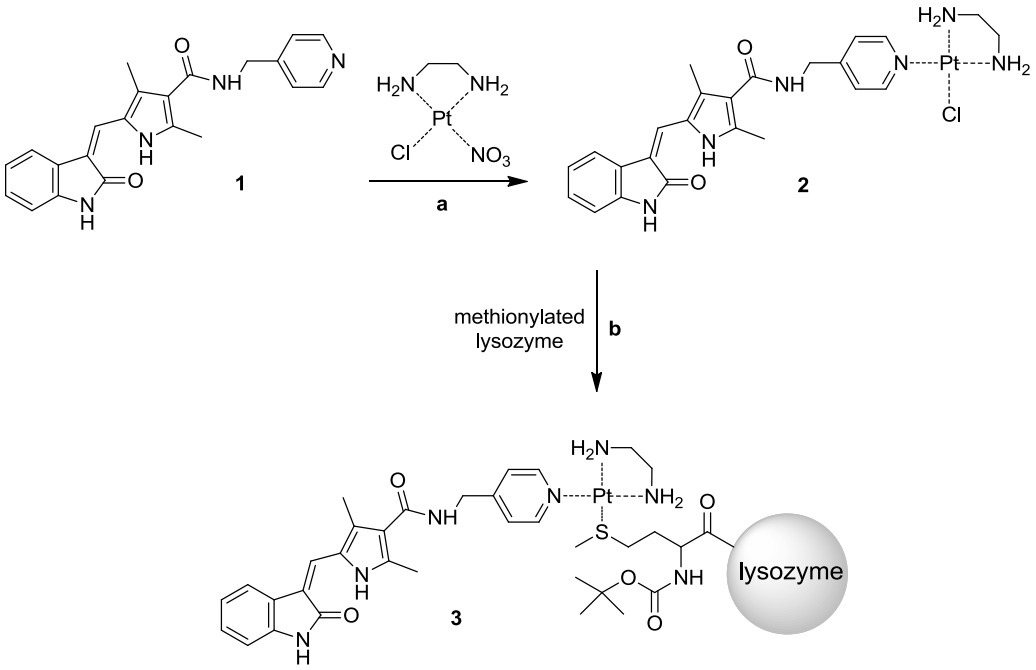

Scheme 1. Synthesis of a platinum-coordinated multikinase inhibitor-bioconjugate. The multikinase inhibitor **1** is complexed with monochloromononitrate-(ethylenediamine)platinum (II) (ULS)™ via binding to the pyridine nitrogen. The resulting drug-platinum complex **2** is conjugated to methionyl groups in lysozyme yielding **3**.

Since previous studies had demonstrated that drug-platinum conjugates linkages have a very long intracellular half-life after *in vivo* accumulation in target tissues, we now have designed a new class of kinase inhibitor-platinum adducts that can bind into the ATP-pocket of kinases when platinum is still bound to the parent drug. Such an approach infers that the ULS linker and the pending cell-specific carrier are conjugated to the multikinase inhibitor via a functional group that protrudes from the ATP-pocket. Therefore, we first investigated how oxindole-based multikinase inhibitors generally are oriented inside the active site of their target kinases. Analysis

of published protein structures co-crystallized with oxindole-based inhibitors revealed that the oxindole pharmacophore scaffold binds deeply within the ATP-binding pocket (11, 12) with the pyrrolylmethylidenyl and the pending side groups oriented towards the outside. Next, we synthesized an oxindole-based inhibitor **1** with a 4-(amidomethyl)pyridine side chain (8) that permitted complexation to the platinum (II)-based linker. As shown in **Figure 1**, the multikinase inhibitor **1** binds to the ATP-binding site of its target kinase, while leaving enough space to accommodate the platinum-based ULS linker and even a drug carrier at the X position, without directly disrupting inhibitor-kinase interactions. We therefore postulated that this type of inhibitor-platinum complexes could be used as intrinsically active, target cell-selective conjugates. Complexation of **1** with ULS (monochloro-mononitrate-(ethyl-enediamine)platinum (II)) for 4 h at 37 °C in the dark afforded complex **2** (84.0%). Finally, **2** was coupled to the prototypic drug-carrier protein lysozyme, which is a low-molecular weight protein that selectively accumulates in renal proximal tubular cells. The molar coupling ratio of **2** to LZM was determined to be 0.9:1.

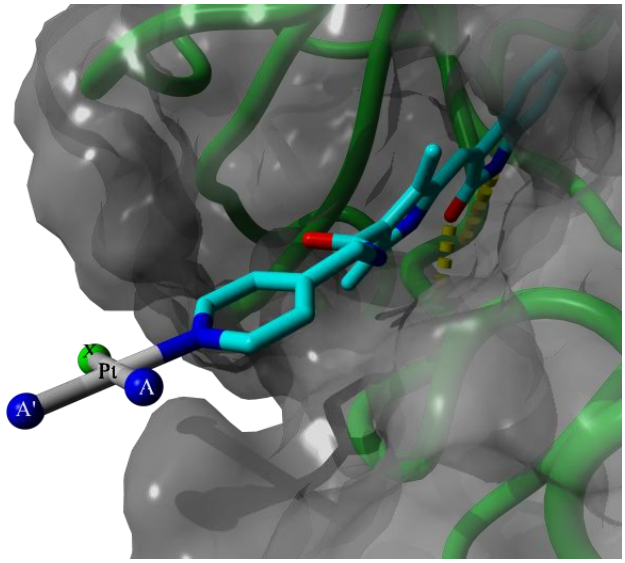

Figure 1. Illustration of the squareplanar multikinase inhibitor-platinum complex **2** (as depicted in **scheme 1**) bound to the ATP-binding pocket of the protein kinase c-KIT. The 4-(amidomethyl)pyridine is sticking outwards permitting binding to the platinum (II) atom and leaving enough space to accommodate a drug carrier at position X. Ethylene-diamine is complexed at position A and A'.

We evaluated whether platinum-coordination affected the pharmacological activity of **1**, by spiking freshly prepared human proximal tubular cell lysate with 2 μM concentrations of **1**, the intermediate complex **2** or conjugate **3**, and analyzing total tyrosine kinase phosphorylation in the lysate. Interestingly, **2** and **3** inhibited tyrosine phosphorylation more potently than **1** (**Figure 2**). As anticipated, these results demonstrate that the multikinase inhibitor-lysozyme conjugate is intrinsically active and, secondly, that the platinum (II)-based ULS positively contributes to the pharmacological activity of **1**, most likely through electrostatic interactions of the platinum (II)-scaffold with electron donating groups within the target protein(s).

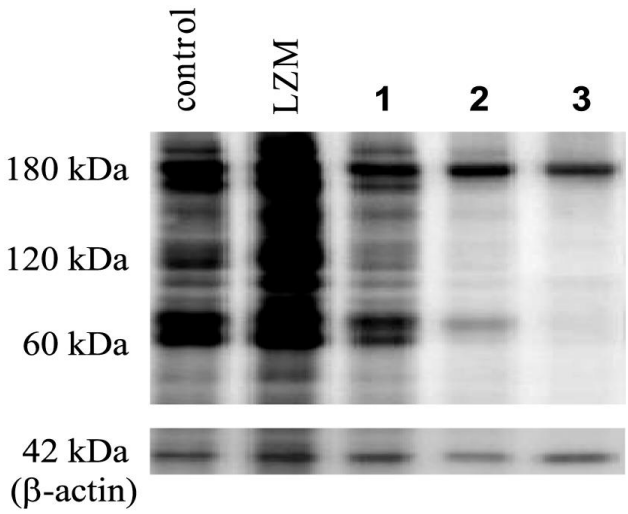

Figure 2. Pharmacologic activity of multikinase inhibitors. Cell lysate of immortalized proximal tubular cells (HK-2) was pre-incubated with equimolar amounts (2 μM) of **1**, **2**, **3**, unconjugated LZM or water (control) and activated with ATP. Phosphorylation was detected with an antibody raised against phosphorylated tyrosine residues (pY-20). While **1** showed only some inhibitory effects on total tyrosine phosphorylation, significant inhibitory effects were observed with **2** and **3**. β-actin was used as loading control.

Next, we investigated the capability of target cells to internalize **3**. Lysozyme is freely filtered through the glomerular barrier into the tubular lumen and is reabsorbed by proximal tubular cells via megalin- and cubilin receptor-mediated endocytosis (7). We studied drug uptake in immortalized human proximal tubular cells (HK-2), a cell line that can be used for *in vitro* testing of uptake of megalin-ligands (9). We exposed these cells to 10 μM of **1** or **3** for different time intervals and determined absolute intracellular drug accumulation.

Figure 3A. Cellular uptake of multikinase inhibitors in renal tubular cells. Uptake was determined by incubating HK-2 cells with 10 μM of **1** or **3** for different time intervals (pulse-time). Maximal uptake of cellular targeted complex **3** was set at 100%. Significance was determined for each time point versus t = 0 hours (*P < 0.05).

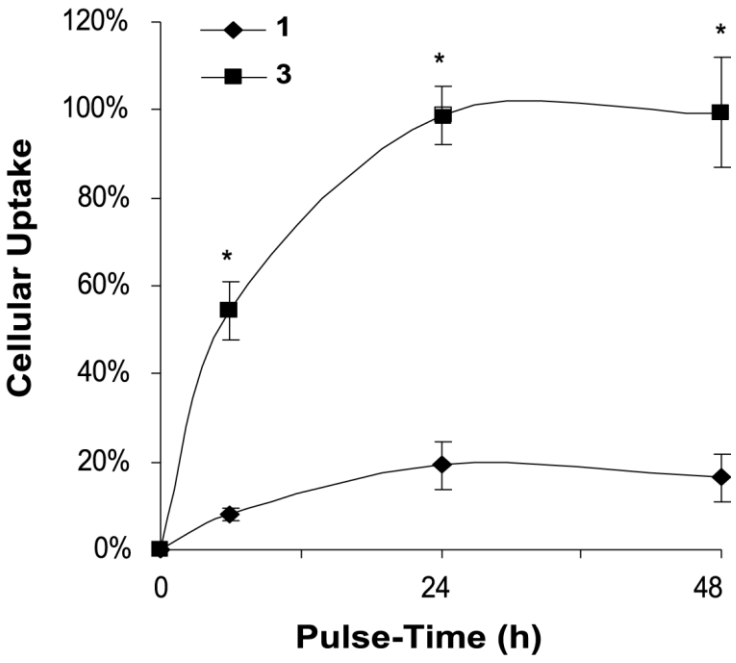

As shown in **Figure 3A**, the uptake of **3** reached a steady-state after 24 hours. Moreover, the intracellular drug accumulation in the cells treated with **3** was five times higher than in cells treated with **1**.

We additionally determined which intracellular kinases were affected by treatment with **1** and **3** by means of a flow-through tyrosine kinase peptide-array (10). We observed that **3** was more potent than **1** (**Figure 3B**). Interestingly, the most inhibited peptide-residues (**Table 2**) correspond with proteins that are either direct targets of similar oxindole-based kinase inhibitors sunitinib and indetanib (13-15) (vascular-endothelial growth factor receptor (VEGFR)-2, platelet-derived growth factor receptor (PDGFR)-β) or that lie downstream of these receptors (phosphoinositol-3-kinase (PI3K), paxillin, Ras p21 protein activator (RASA1), cyclin-dependent kinase (CDK)-2, and c-FES). These kinases play important roles in pathophysiological processes like angiogenesis, cell adhesion and migration; processes that underlie pathologies such as arteriosclerosis, rheumatoid arthritis and fibrosis.

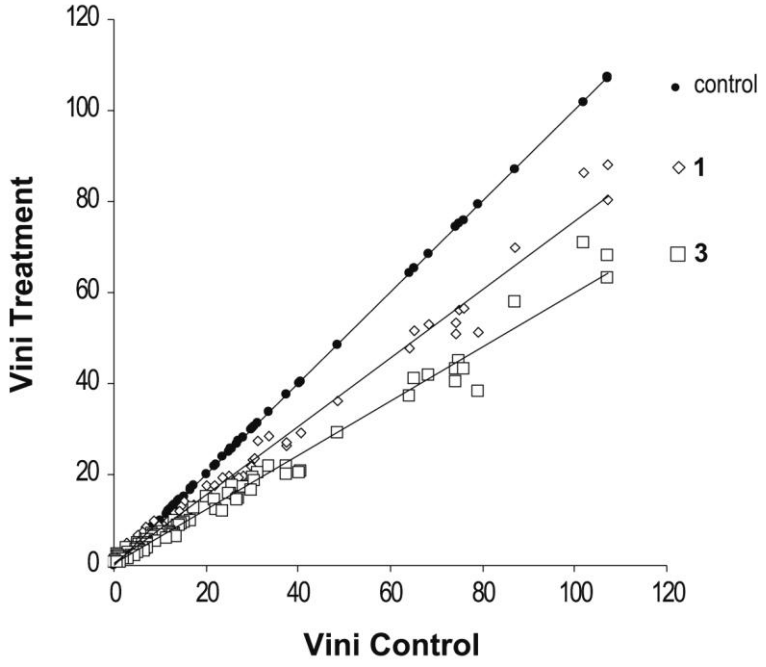

Figure 3B. Pharmacological profile of inhibitors in HK-2 cells. A flow-through tyrosine kinase peptide-array was used to determine the inhibitory activity of **1** and **3**. Peptide phosphorylation was detected in real-time with a monoclonal anti-phosphotyrosine antibody (pY-20) coupled to FITC. Data were expressed as Vini (initial linear rate of tyrosine residue phosphorylation) and ranked based on strongest pY inhibition compared to control. The slope of the plotted curves is a measure for pan-tyrosine pY inhibition (control slope = 1).

Table 2. Strongest inhibited tyrosine-peptide residues by **3** on the tyrosine kinase PamTyrChip® peptide-array.

	Protein (p-site)	*(Pathological) Function*
1	PI3K (p85 Y607)	cell motility/ proliferation
2	PDGFR-β (Y579/ 581)	cell proliferation, cell migration, differentiation
3	Paxillin (Y31/ 33)	focal adhesion, cell mobility and differentiation
4	Paxillin (Y118)	focal adhesion, cell mobility and differentiation
5	Pecam-1 (Y713)	endothelial marker (CD31)
6	EphrinA7 (Y608/ Y614)	often overexpressed in invasive tumours
7	c-FES (Y713)	cell migration
8	VEGFR-2 (Y996)	angiogenesis
9	CDK-2 (Y15/ 19)	cell cycling/ proliferation
10	RASA1 (Y460)	implicated in linking PDGFR signaling to RAS-GAP mitogenicity

To further evaluate whether platinum complexation or bioconjugation would affect the inhibitory activity of compound **1** towards its target kinases, we evaluated the inhibitory activity of **1**, **2** and **3** against recombinant PDGFR-β and c-KIT. As shown in **Figure 4** and **Table 3**, complexation of platinum with **1** did not affect the inhibitory activity of **1** against PDGFR-β and increased the inhibitory activity against c-KIT 3-fold. Interestingly, **1** and **2** were as potent as the clinically approved oxindole-based multikinase inhibitor sunitinib (**Table 3**). Conjugation to LZM slightly decreased the inhibitory activity towards both kinases, which might be due to steric hindrance of the relatively large LZM homing ligand. This part of the conjugate will be degraded into smaller peptide fragments upon internalization, and hence will not interfere with the kinase inhibitory activity of compound **2**.

Table 3. IC_{50} values for compound **1, 2, 3** and the reference compound sunitinib against c-KIT and PDGFR-β

	c-KIT IC_{50} (nM)	*PDGFR-β* IC_{50} (nM)
1	51	16
2	17	16
3	76	48
Sunitinib	23	14

To study the effect of drug conjugation on drug efflux, a pulse-chase experiment was conducted. HK-2 cells were exposed for 24 hours to **1** or **3** after which the cells were allowed to efflux in blank medium (chase time: t = 2, 24, 48 h). As shown in **Figure 5A**, cells treated with **1** rapidly cleared the drug (< 2 hours), while in the cells treated with **3**, the drug was still detectable after 48 hours. Due to its rapid intracellular turnover rate, it is expected that the lysozyme part of the drug-conjugate (**3**) is fully degraded within 48 hours. In addition, since **1** is rapidly cleared from the cell, we conclude that the oxindole inhibitor is still attached to platinum. In turn, complex **2** could be attached to degradation residues of the lysozyme such as methionine, but could also have competitively reacted with GSH or other strong electron donating group-rich molecules

such as thiol/ methionine-rich proteins, thereby creating an intracellular depot of **2'** (representing any metabolite of **2** that is formed by binding at the X-position) from which **1** is slowly released.

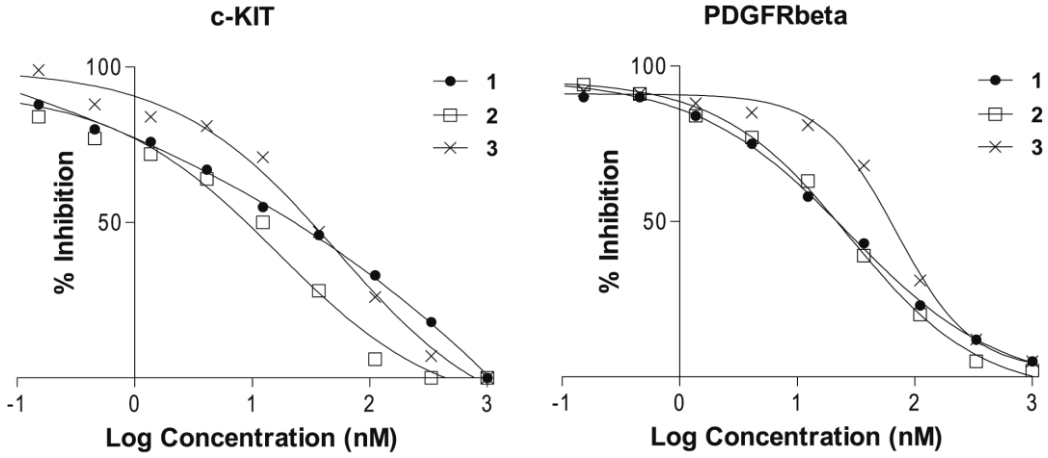

Figure 4. IC_{50} determinations of compound **1**, **2**, and **3** against recombinant c-KIT and PDGFR-β. Radiometric protein kinase assays were performed with the indicated compounds at various concentrations (0.03 – 1000 nM). Kinase inhibition was plotted as (%) of total kinase activity (control).

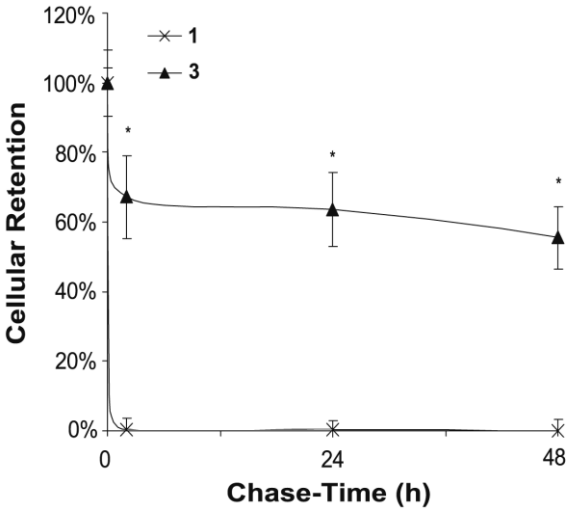

Figure 5A. The effect of platinum-based conjugation on cellular retention. Proximal tubular cells (HK-2 cells) were incubated for 24 hours (pulse-time) with equimolar amounts (10 μM) of **1** or **3** after which cells were allowed to efflux in blank medium for 0, 24, or 48 hours (chase-time). Values were normalized to the absolute **1** or **3** levels at t = 0 hours (100%) and expressed as % cellular retention. Significance of cellular retention was determined by comparing the intracellular concentration at different time points with the intracellular concentration at t = 0 hours (*P < 0.05).

To verify whether intracellular processing affects the pharmacological activity of **3**, the total tyrosine phosphorylation state was determined in the chased cells. **Figure 5B** shows that **1** significantly decreased the total endogenous phosphorylation status, but due to its rapid clearance, no significant decrease could be observed 24 and 48 hours after exposure. In contrast, treatment with equimolar amounts of **3** produced sustained inhibition on total endogenous tyrosine-residue phosphorylation of >10% for up to 48 hours confirming the presence of pharmacological active **2'** in the cells. These results demonstrate that complexation of **1** to platinum positively alters the efflux kinetics of this multikinase inhibitor without adversely affecting its pharmacological activity.

Taken together, the complexation of platinum to the oxindole-based multikinase inhibitor **1** did not affect its pharmacological activity, but additionally provided superior cellular kinetics compared to the free drug. Although the use of platinum as a linker would probably raise questions concerning safety, we have shown that drug-ULS complexes are by far less toxic than the prototypical platinum drug *cis*-diamine-dichloroplatinum (CDDP) (16, 17). Apart from platinum (18), several other transition metals such as ruthenium (19), osmium (20), iridium (21) and iron (22) have been complexed to kinase inhibitors without adversely affecting their pharmacological activity. However, a major difference between these compounds and the now reported platinum-complex is that platinum both served as a linker for attachment to a cell-selective carrier and as part of the pharmacophore of the multikinase inhibitor. Organometallic chemistry opens new opportunities in kinase inhibitor drug discovery, as well as in drug delivery research (23-25). One or more (kinase inhibiting) drugs can be bound to a transition metal center, while drug carriers such as antibodies, peptides or proteins, can be coordinated at another metal ligand-binding site. When properly designed, these complexes will provide intrinsically active site-selective drug-bioconjugates. This could reduce off-target toxicities and eventually enable the clinical use of drugs with currently unfavorable safety- or pharmacokinetic profiles.

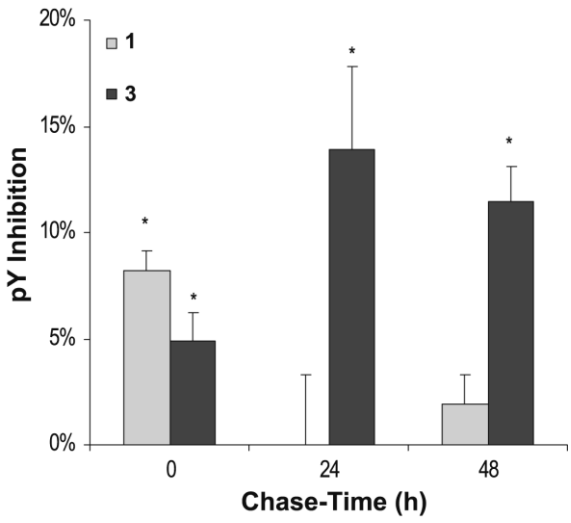

Figure 5B. The inhibitory effect of **1** and **3** on the intracellular phosphorylation of tyrosine residues (pY). HK-2 cells were exposed for 24 hours (pulse-time) with **1** (10 μM) or **3** (10 μM). After the pulse-time, the incubation medium was replaced with blank medium (t = 0). At t = 0, 24 and 48 hours (chase time) the endogenous pY state was determined by immunostaining of phosphorylated proteins with the anti-pY antibody pY-20. Total pY signal of treated cells was normalized to total pY signal of control cells and expressed as percentage pY inhibition (0% in control cells) (*P < 0.05).

Conclusions

We have developed an intrinsically active multikinase inhibitor-bioconjugate in which platinum not only enabled straightforward linkage, but also contributed to improved retention of the multikinase inhibitor in the target cells, thereby prolonging the pharmacological activity of the delivered compound. The developed cell-selective multikinase inhibitor-bioconjugate may eventually provide a safe and efficient way to administrate such agents in less life-threatening diseases without inducing dose-limiting off-organ toxicities.

Acknowledgements

This work was supported financially by the European Framework program FP6 (LSHB-CT-2007-036644). Dr. R.W. Sparidans, Dr. E.E. Moret and Dr. R. Ruijtenbeek are kindly acknowledged for performing the MS analyses and support with molecular modeling and kinase peptide array analyses, respectively.

References

1. S. Tugues, G. Fernandez-Varo, J. Munoz-Luque, J. Ros, V. Arroyo, J. Rodes, S.L. Friedman, P. Carmeliet, W. Jimenez and M. Morales-Ruiz. Antiangiogenic treatment with sunitinib ameliorates inflammatory infiltrate, fibrosis, and portal pressure in cirrhotic rats. Hepatology. 46:1919-1926 (2007).
2. M. Huang, X. Liu, Q. Du, X. Yao and K.S. Yin. Inhibitory effects of sunitinib on ovalbumin-induced chronic experimental asthma in mice. Chin Med J (Engl). 122:1061-1066 (2009).
3. S.A. Antoniu and M.R. Kolb. Intedanib, a triple kinase inhibitor of VEGFR, FGFR and PDGFR for the treatment of cancer and idiopathic pulmonary fibrosis. IDrugs. 13:332-345 (2010).
4. J.T. Hartmann, M. Haap, H.G. Kopp and H.P. Lipp. Tyrosine kinase inhibitors - a review on pharmacology, metabolism and side effects. Curr Drug Metab. 10:470-481 (2009).
5. S. George. Sunitinib, a multitargeted tyrosine kinase inhibitor, in the management of gastrointestinal stromal tumor. Curr Oncol Rep. 9:323-327 (2007).
6. M. Mego, M. Reckova, J. Obertova, Z. Sycova-Mila, K. Brozmanova and J. Mardiak. Increased cardiotoxicity of sorafenib in sunitinib-pretreated patients with metastatic renal cell carcinoma. Ann Oncol. 18:1906-1907 (2007).
7. M.E.M. Dolman, S. Harmsen, G. Storm, W.E. Hennink and R.J. Kok. Drug targeting to the kidney: Advances in the active targeting of therapeutics to proximal tubular cells. Adv Drug Deliv Rev. 62:1344-1357 (2010).
8. L. Sun, C. Liang, S. Shirazian, Y. Zhou, T. Miller, J. Cui, J.Y. Fukuda, J.Y. Chu, A. Nematalla, X. Wang, H. Chen, A. Sistla, T.C. Luu, F. Tang, J. Wei and C. Tang. Discovery of 5-[5-fluoro-2-oxo-1,2- dihydroindol-(3Z)-ylidenemethyl]-2,4- dimethyl-1H-pyrrole-3-carboxylic acid (2-diethylaminoethyl)amide, a novel tyrosine kinase inhibitor targeting vascular endothelial and platelet-derived growth factor receptor tyrosine kinase. J Med Chem. 46:1116-1119 (2003).
9. M.M. Fretz, M.E.M. Dolman, M. Lacombe, J. Prakash, T.Q. Nguyen, R. Goldschmeding, J. Pato, G. Storm, W.E. Hennink and R.J. Kok. Intervention in growth factor activated signaling pathways by renally targeted kinase inhibitors. J Control Release. 132:200-207 (2008).
10. R. Hilhorst, L. Houkes, A. van den Berg and R. Ruijtenbeek. Peptide microarrays for detailed, high-throughput substrate identification, kinetic characterization, and inhibition studies on protein kinase A. Anal Biochem. 387:150-161 (2009).
11. K.S. Gajiwala, J.C. Wu, J. Christensen, G.D. Deshmukh, W. Diehl, J.P. DiNitto, J.M. English, M.J. Greig, Y.A. He, S.L. Jacques, E.A. Lunney, M. McTigue, D. Molina, T. Quenzer, P.A. Wells, X. Yu, Y. Zhang, A. Zou, M.R. Emmett, A.G. Marshall, H.M. Zhang and G.D. Demetri. KIT kinase mutants show unique mechanisms of drug resistance to imatinib and sunitinib in gastrointestinal stromal tumor patients. Proc Natl Acad Sci U S A. 106:1542-1547 (2009).
12. M. Mohammadi, G. McMahon, L. Sun, C. Tang, P. Hirth, B.K. Yeh, S.R. Hubbard and J. Schlessinger. Structures of the tyrosine kinase domain of fibroblast growth factor receptor in complex with inhibitors. Science. 276:955-960 (1997).
13. F. Hilberg, G.J. Roth, M. Krssak, S. Kautschitsch, W. Sommergruber, U. Tontsch-Grunt, P. Garin-Chesa, G. Bader, A. Zoephel, J. Quant, A. Heckel and W.J. Rettig. BIBF 1120: triple angiokinase inhibitor with sustained receptor blockade and good antitumor efficacy. Cancer Res. 68:4774-4782 (2008).
14. A.D. Laird, P. Vajkoczy, L.K. Shawver, A. Thurnher, C. Liang, M. Mohammadi, J. Schlessinger, A. Ullrich, S.R. Hubbard, R.A. Blake, T.A. Fong, L.M. Strawn, L. Sun, C. Tang, R. Hawtin, F. Tang, N. Shenoy, K.P. Hirth, G. McMahon and Cherrington. SU6668

is a potent antiangiogenic and antitumor agent that induces regression of established tumors. Cancer Res. 60:4152-4160 (2000).

15. D.B. Mendel, A.D. Laird, X. Xin, S.G. Louie, J.G. Christensen, G. Li, R.E. Schreck, T.J. Abrams, T.J. Ngai, L.B. Lee, L.J. Murray, J. Carver, E. Chan, K.G. Moss, J.O. Haznedar, J. Sukbuntherng, R.A. Blake, L. Sun, C. Tang, T. Miller, S. Shirazian, G. McMahon and J.M. Cherrington. In vivo antitumor activity of SU11248, a novel tyrosine kinase inhibitor targeting vascular endothelial growth factor and platelet-derived growth factor receptors: determination of a pharmacokinetic/ pharmacodynamic relationship. Clin Cancer Res. 9:327-337 (2003).
16. M. Moreno, T. Gonzalo, R.J. Kok, P. Sancho-Bru, M. van Beuge, J. Swart, J. Prakash, K. Temming, C. Fondevila, L. Beljaars, M. Lacombe, P. van der Hoeven, V. Arroyo, K. Poelstra, D.A. Brenner, P. Gines and R. Bataller. Reduction of advanced liver fibrosis by short-term targeted delivery of an angiotensin receptor blocker to hepatic stellate cells in rats. Hepatology. 51:942-952 (2010).
17. J. Prakash, M. Sandovici, V. Saluja, M. Lacombe, R.Q. Schaapveld, M.H. de Borst, H. van Goor, R.H. Henning, J.H. Proost, F. Moolenaar, G. Keri, D.K. Meijer, K. Poelstra and R.J. Kok. Intracellular delivery of the p38 mitogen-activated protein kinase inhibitor SB202190 [4-(4-fluorophenyl)-2-(4-hydroxyphenyl)-5-(4-pyridyl)1H-imidazole] in renal tubular cells: a novel strategy to treat renal fibrosis. J Pharmacol Exp Ther. 319:8-19 (2006).
18. D.S. Williams, P.J. Carroll and E. Meggers. Platinum complex as a nanomolar protein kinase inhibitor. Inorg Chem. 46:2944-2946 (2007).
19. L. Zhang, P. Carroll and E. Meggers. Ruthenium complexes as protein kinase inhibitors. Org Lett. 6:521-523 (2004).
20. J. Maksimoska, D.S. Williams, G.E. Atilla-Gokcumen, K.S. Smalley, P.J. Carroll, R.D. Webster, P. Filippakopoulos, S. Knapp, M. Herlyn and E. Meggers. Similar biological activities of two isostructural ruthenium and osmium complexes. Chemistry. 14:4816-4822 (2008).
21. A. Wilbuer, D.H. Vlecken, D.J. Schmitz, K. Kraling, K. Harms, C.P. Bagowski and E. Meggers. Iridium complex with antiangiogenic properties. Angew Chem Int Ed Engl. 49:3839-3842 (2010).
22. J. Spencer, A.P. Mendham, A.K. Kotha, S.C. Richardson, E.A. Hillard, G. Jaouen, L. Male and M.B. Hursthouse. Structural and biological investigation of ferrocene-substituted 3-methylidene-1,3-dihydro-2H-indol-2-ones. Dalton Trans:918-921 (2009).
23. N. Chavain and C. Biot. Organometallic complexes: new tools for chemotherapy. Curr Med Chem. 17:2729-2745 (2010).
24. G. Gasser, I. Ott and N. Metzler-Nolte. Organometallic anticancer compounds. J Med Chem. 54:3-25 (2011).
25. E.A. Hillard and G. Jaouen. Bioorganometallics: future trends in drug discovery, analytical chemistry, and catalysis. Organometallics. 30:20-27 (2011).

Chapter 7

NH_2-PAMAM-G3 as carrier for the intracellular delivery of a sunitinib analogue into the proximal tubular cells of the kidneys

M.E.M. Dolman[1], K.M.A. van Dorenmalen[1], E.H.E. Pieters[1], R.W. Sparidans[2], M. Lacombe[3], B. Szokol[4], L. Őrfi[4], G. Kéri[4,5], N. Bovenschen[6], G. Storm[1], W.E. Hennink[1] and R.J. Kok[1]

[1] Department of Pharmaceutics, Utrecht Institute of Pharmaceutical Sciences, Utrecht University, Utrecht, The Netherlands

[2] Faculty of Science, Department of Pharmaceutical Sciences, Division of Pharmacoepidemiology and Clinical Pharmacology, Utrecht University, Utrecht, The Netherlands

[3] KREATECH Biotechnology B.V., Amsterdam, The Netherlands /
[4] Vichem Chemie, Budapest, Hungary

[5] Pathobiochemistry Research Group of Hungarian Academy of Sciences and Semmelweis University, Budapest, Hungary

[6] Department of Pathology, University Medical Center Utrecht, Utrecht, The Netherlands

Manuscript in preparation

Abstract

Amine-terminated poly(amidoamine) (NH_2-PAMAM) dendrimers are attractive carriers for drug delivery. They are frequently investigated for tumour targeting, but may also be promising carriers for drug targeting to other non–cancerous cell types. In the current study, we investigated whether generation-3 NH_2-PAMAM dendrimer (NH_2-PAMAM-G3) can be exploited as carrier for drug targeting to the proximal tubular cells of the kidneys. Activation of kinases in proximal tubular cells is one of the key processes contributing to the progression of tubulointerstitial fibrosis. An analogue of the multitargeted kinase inhibitor sunitinib has been developed, *i.e.* 17864, of which it can be expected that the activity is retained after coordination to the platinum (II)-based Universal Linkage System (ULS)^{TM}. To obtain a proximal tubular cell-specific agent, 17864-ULS was conjugated to NH_2-PAMAM-G3 (0.75 moles of 17864 per mole of NH_2-PAMAM-G3). The *in vitro* internalization of the conjugate into human kidney proximal tubular cells (HK-2 cells) and the capability to inhibit tyrosine kinase activity have been evaluated. *In vivo* accumulation of the conjugate in the kidneys was studied after systemic administration in mice.

Surface plasmon resonance receptor interaction studies showed that NH_2-PAMAM-G3 binds to megalin, one of the primary receptors involved in the reabsorption of filtered macromolecules by proximal tubular cells. The activity of 17864 was retained after coordination to the ULS linker alone or coupled to NH_2-PAMAM-G3, indicating that 17864-ULS-NH_2-PAMAM-G3 is pharmacological active and intracellular metabolism may yield active 17864-ULS adducts in addition to free 17864. It was further shown that 17864-ULS-NH_2-PAMAM-G3 was internalized by HK-2 cells. Upon intravenous administration of a single injection of 17864-ULS-NH_2-PAMAM-G3 in mice, the conjugate accumulated rapidly and efficiently in the kidneys, resulting in average intrarenal kinase inhibitor level of 13% of the injected dose at 1 hour after administration. High intrarenal kinase inhibitor levels persisted for several days (*i.e.* 15 and 14% of the injected dose at 1 and 3 days after intravenous administration, respectively). In conclusion, the results presented in this paper demonstrate that NH_2-PAMAM-G3 dendrimer can be used for drug targeting to the proximal tubular cells of the kidneys. One such drug-dendrimer conjugate, 17864-ULS-NH_2-PAMAM-G3, resulted in a sustained intrarenal depot of kinase inhibitor. Future studies will address the potential of this compound in halting the progression or even reverse chronic kidney disease.

1. Introduction

Dendrimers are hyperbranched synthetic polymers consisting of an initiator core, a branching interior layer of repeating units and a surface of equally reactive functional groups (1, 2).

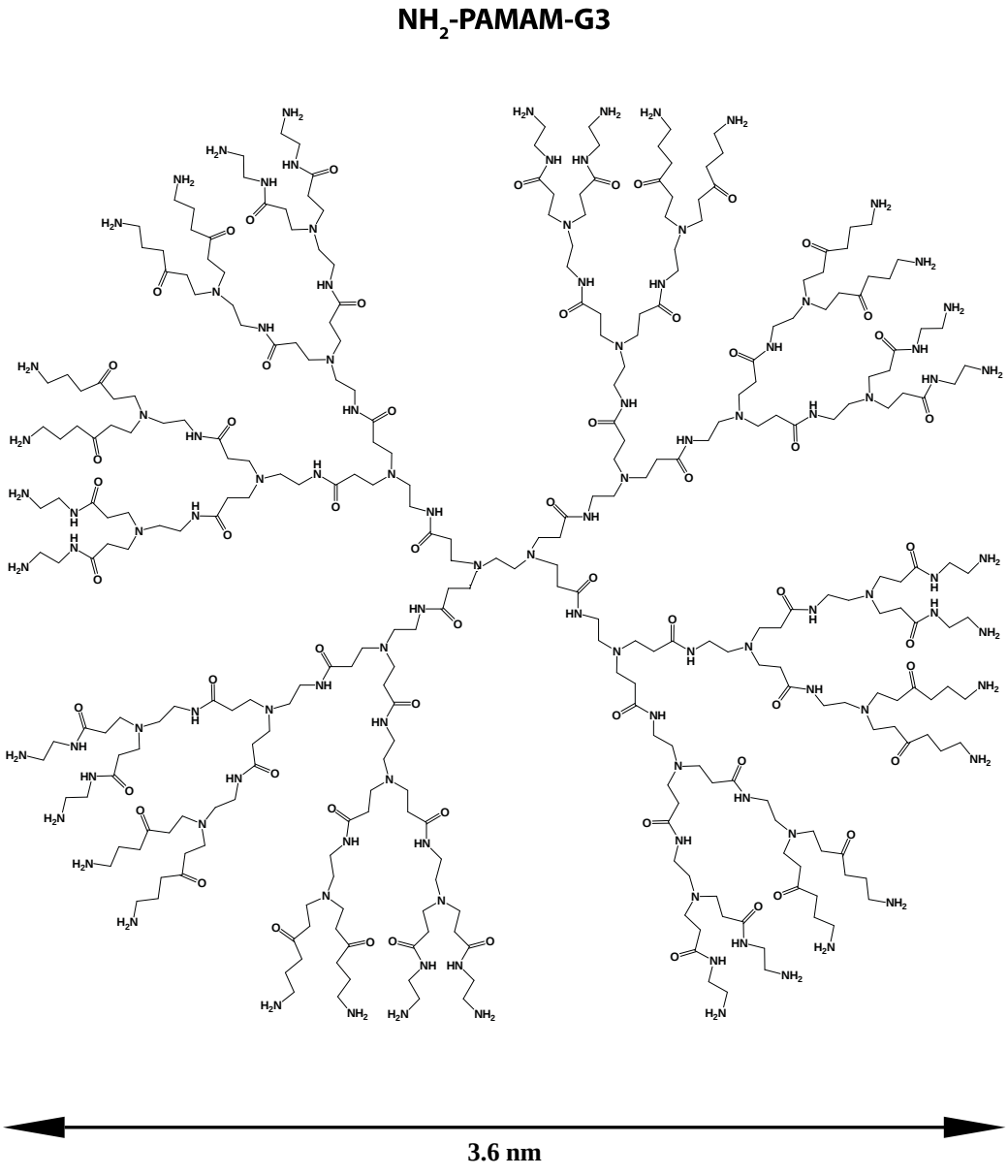

Figure 1. Chemical structure of generation-3 amine-terminated PAMAM dendrimer. The hyperbranched dendrimer with 32 functional amine groups and a molecular weight of 6909 Da is small enough for glomerular filtration.

They are considered promising carriers for the development of cell-specific macromolecular drug-carrier conjugates (1, 3, 4) because, in contrast with traditional polymers, the stepwise synthesis of dendritic carriers affords to accurately tailor size, molecular structure and the number of terminal functional groups. (1, 2, 4-8). Among the dendrimers that have successfully been investigated as carriers are the amine-terminated poly(amidoamine) (NH_2-PAMAM) dendrimers, which have been mainly applied for drug and gene delivery to solid tumours (4, 8-12). They have also been shown to accumulate in the proximal tubuli of the kidneys (13-15). The highest renal accumulation was observed for generation-3 NH_2-PAMAM dendrimer (NH_2-PAMAM-G3) (13), which contains 32 amine groups on its surface and is small enough (*i.e.* 3.6 nm) to reach the proximal tubular cells via glomerular filtration from the circulation (**Figure 1**) (1, 2). The exact mechanism by which NH_2-PAMAM dendrimers are taken up by the proximal tubular cells of the kidneys is not known, but macromolecular dendrimers are taken up via receptor- rather than transport-mediated internalization (16, 17). This is supported by the observation of Kobayashi *et al.* that co-administration of lysine, an inhibitor of megalin- and/ or cubilin receptor-mediated endocytosis, resulted in decreased levels of generation-4 NH_2-PAMAM dendrimer in the kidneys (15, 18, 19).

Tubulointerstitial fibrosis is a common characteristic of progressive kidney diseases and contributes to the development of end-stage renal disease (20, 21). Currently, however, no therapeutics are available that can halt further deterioration of kidney function (20, 22, 23). Because activated kinases in proximal tubular cells play a prominent role in the pathogenesis of tubulointerstitial fibrosis, these signaling proteins are attractive drug targets (24-29). Sunitinib is a multitargeted tyrosine kinase inhibitor that has successfully been investigated for the treatment of liver fibrosis (30) and may also be a drug candidate to treat tubulointerstitial fibrosis in chronic kidney diseases. However, its use is associated with severe cutaneous toxicities and cardiotoxicity (31, 32). Designing a sunitinib-PAMAM conjugate that provides sustained active kinase inhibitor levels within the proximal tubular cells of the kidneys and avoids toxic effects in other organs is therefore a rationale approach to improve the therapeutic index of the drug.

In earlier studies kinase inhibitors have successfully been conjugated to cell-specific carriers via the platinum (II)-based Universal Linkage System™ (ULS)™. *In vivo* biodistribution studies have shown that kinase inhibitor-ULS-carrier conjugates reside in the designated cells for several days and that the majority of the accumulated kinase inhibitor is present in the ULS-bound form (33-36). Because sunitinib cannot be coordinated to the ULS linker, we synthesized a sunitinib analogue, *i.e.* 17864, that has an extended pyridyl side chain. When the ATP-competitive kinase inhibitor sunitinib binds to its target kinases the oxindole moiety of sunitinib is localized deep in the ATP-binding pockets of the target kinases, while the *N*-2-(diethylamino)ethylene moiety is protruding outwards (37-39). We therefore hypothesized that replacement of the outwards protruding moiety by a *N*-4-methylpyridine that can be coordinated to the ULS linker would result in a multitargeted kinase inhibitor with retained activity when coordinated to ULS. **Figure 2** illustrates the binding of 17864-ULS to target kinases.

In the current study the capability of NH_2-PAMAM-G3 to bind to the internalizing megalin receptor was investigated in order to get more insight into the route by which this carrier is taken up by the proximal tubular cells. Furthermore, the conjugation of 17864-ULS to NH_2-PAMAM-G3 was studied as well as the *in vitro* activity and toxicity of 17864-ULS-NH_2-PAMAM-G3 in

proximal tubular cells. Finally, the *in vivo* renal accumulation of 17864-ULS-NH_2-PAMAM-G3 was studied upon systemic administration in mice.

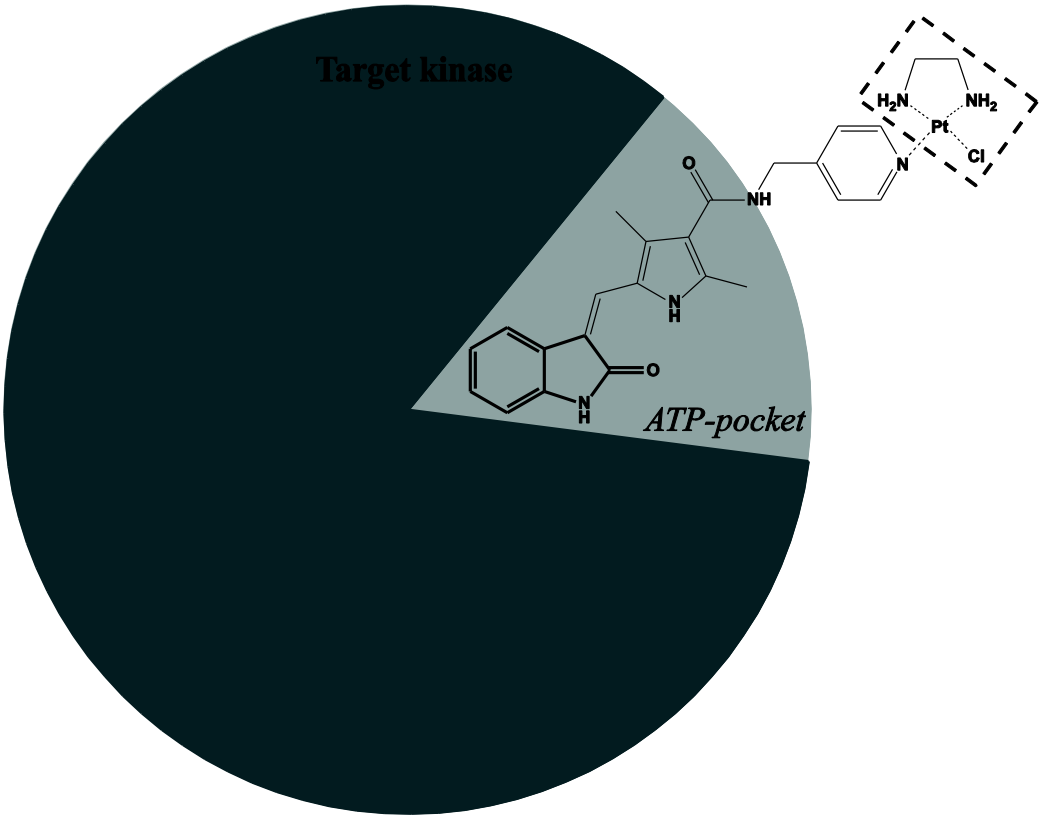

Figure 2. Illustration of the binding of 17864-ULS to target kinases. The oxindole moiety (bold structure) of 17864 is located in the adenine region of the ATP-binding pocket. Because the platinum linker ULS (dotted square) is bound to the outwards protruding *N*-4-methylpyridine, the multitargeted kinase inhibitor still fits in the ATP-binding pocket of target kinases.

2. Materials and methods

2.1. Materials and chemicals

The sunitinib analogue 17864 was synthesized according to Sun *et al.* by Vichem Chemie (Budapest, Hungary) (40). Sunitinib malate was purchased from Sequoi Research Products (Pangbourne, United Kingdom). The Universal Linkage System (ULS)™ cis-[Pt(ethylenediamine)nitrate-chloride] was synthesized from *cis*-[Pt(ethylenediamine)dichloride as described elsewhere (41). Purified megalin was kindly provided by Dr. S. Moestrup (University of Aarhus, Aarhus, Denmark). Acetonitrile (ACN) HPLC-S and *tert*-butyl methylether (TBME) were obtained from Biosolve (Valkenswaard, The Netherlands). Generation-3 PAMAM dendrimer (20 wt.% solution in methanol), trifluoroacetic acid (TFA), adenosine 5'-triphosphate disodium salt hydrate (ATP), bovine serum albumin (BSA) and 4-

hydroxybenzophenone were purchased from Sigma-Aldrich (Zwijndrecht, The Netherlands). Abl kinase assay buffer was purchased from New England Biolabs (Leusden, The Netherlands). Mammalian Protein Extraction Reagent (M-PER) and Halt™ Protease and Phosphatase Inhibitor Cocktail (100x) were purchased from Thermo Scientific (Etten-Leur, The Netherlands). Immobilon-P polyvinylidene fluoride (PVDF) Membrane (0.45 µm) was purchased from Millipore (Amsterdam, The Netherlands). NuPAGE® 4-12% Bis-Tris Gel and NuPAGE® MOPS SDS running buffer were purchased from Invitrogen (Breda, The Netherlands). PageRuler™ Prestained Protein Ladder was purchased from Fermentas (Leon-Rot, Germany). Mouse anti-human phosphotyrosine [PY20] (HRP) monoclonal antibody was purchased from Abcam (Cambridge, UK).

2.2. Surface Plasmon resonance

Binding of the carrier NH_2-PAMAM-G3 to the internalizing megalin receptor was studied on a BIAcore T100 instrument (GE Healthcare, Uppsala, Sweden). Megalin was immobilized on a series S CM5 sensor chip with a coating density of 20.7 fmol/ mm^2 (as has been calculated from the response units and the molecular weight of megalin, *i.e.* 600 kDa), according to the manufacturer's instructions. One control cell without immobilized megalin was routinely activated and blocked to subtract buffer refractive effects and as a control for unspecific binding. NH_2-PAMAM-G3 (1 µM in running buffer) was injected at a flow rate of 20 µL/ min at 25 °C, using a running buffer consisting of 20 mM HEPES [pH 7.4], 150 mM NaCl, 5 mM $CaCl_2$ and 0.005% Tween-20. The dendritic carrier was allowed to associate with the megalin receptor for 30 seconds and to dissociate for 1 minute. The sensor chip was regenerated with several pulses of a buffer consisting of 0.25 M EDTA [pH 8] and 0.5 M NaCl, at a flow rate of 20 µL/ min. Data were analyzed using BIAcore T100 Evaluation Software, version 2.0.3 (GE Healthcare).

2.3. Synthesis of 17864-ULS-NH_2-PAMAM-G3

The ULS-bound sunitinib analogue was synthesized by incubating 264.5 µmol 17864 and 248.5 µmol ULS in 22 mL DMF for 4 hours at 37 °C. To confirm the formation of the 17864-ULS 1:1 adduct the final product was analyzed with LC-MS and ^{195}Pt-NMR. In the next step 17864-ULS was conjugated to NH_2-PAMAM-G3. A three times molar excess of 17864-ULS (13.0 µmol) was incubated with NH_2-PAMAM-G3 (4.3 µmol) in 0.02 M tricine/ sodium nitrate buffer with pH 8.5 (13.5 mL), overnight at 50 °C. The obtained 17864-ULS-NH_2-PAMAM-G3 conjugate was purified by dialysis against demineralized water. The dialyses steps were performed at 4 °C using a Slide-A-Lyzer dialysis cassette with a molecular weight cut-off of 2,000 Da (Pierce, Rockford, IL). After filtration through a 0.2 µm filter the purified conjugate was lyophilized and stored at -20 °C until further use.

2.4. Characterization of 17864-ULS-NH_2-PAMAM-G3

For characterization of 17864-ULS-NH_2-PAMAM-G3 a 7.5 mg/ mL stock solution in demineralized water was prepared. Coupling of 17864-ULS to the functional amines of NH_2-PAMAM-G3 yields a conjugate in which the platinum (II) atom in the ULS linker is coordinated to four instead of three nitrogen atoms. The formation of a Pt-N_4 coordination was studied by

^{195}Pt-NMR. Two methods were used for the quantification of the 17864 concentration in the 17864-ULS-NH_2-PAMAM-G3 stock solution. First, the 17864 concentration was analyzed by UV analysis at the maximum wavelength of 17864-ULS, *i.e.* 422 nm. In the second method, the drug was displaced from the ULS linker with an excess of KSCN and the concentrations of liberated 17864 were determined by HPLC. Briefly, the stock solution was six times diluted in a mixture of 50% PBS, 50% ACN and 0.1% TFA containing a final concentration of 0.5 M KSCN. The samples were incubated for 24 hours at 80 °C. After reaching ambient temperature, 200 µL ACN with 0.1% TFA was added to the samples. The samples were mixed by vortexing and centrifuged for 4 minutes at 19,500 x g. Of the supernatants 50 µL was analyzed using a reversed phase HPLC system consisting of a Waters 2695 separations module, a Waters 2487 dual λ absorbance detector and a Waters SunFire™ C18 column (4.6 x 150 mm, 5 µm particle size) (Milford, USA). Empower 2 software was used for data recording. The column- and sample temperature were maintained at 30 and 20 °C, respectively. A gradient was used with eluent A consisting of 5% ACN/ 95% water/ 0.1% TFA (w/ w/ w) and eluent B consisting of ACN/ 0.1% TFA (w/ w). The composition of the mobile phase was linearly changed from 100% eluent A to 20% eluent A and 80% eluent B in 25 minutes using a flow rate of 1 mL/ min. 17864 was detected at its maximum wavelength, *i.e.* 431 nm. The NH_2-PAMAM-G3 concentration in the 17864-ULS-NH_2-PAMAM-G3 stock solution was calculated by subtracting the 17864-ULS concentration from the 17864-ULS-NH_2-PAMAM-G3 concentration in the stock solution. The conjugated amount of 17864 was calculated from the molar ratio between 17864 and NH_2-PAMAM-G3 in the stock solution.

2.5. In vitro activity and toxicity

2.5.1. Cell culture

The immortalized human renal proximal tubule epithelial cell line (HK-2) (American Type Culture Collection, LGC Standards, Middlesex, UK) was cultured in Dulbecco's Modified Eagle's Medium (DMEM) containing 3.7 g/ L sodium bicarbonate, 1.0 g/ L glucose, supplemented with 10% (v/ v) fetal bovine serum, penicillin (100 U/ L), streptomycin (100 µg/ mL) and amphotericin B (0.25 µg/ mL) at 37 °C with 5% CO_2 in humidified air. All cell culture related media were obtained from PAA Laboratories GmbH (Pasching, Austria).

2.5.2. In vitro activity of ULS-bound 17864

Serum-starved HK-2 cells were lysed with M-PER containing protease- and phosphatase inhibitors. The protein content was measured using the Micro BCA™ Protein Assay Kit (Prod #23235; Thermo Scientific; Etten-Leur, The Netherlands). Samples were prepared of 10 µM 17864, 17864-ULS, NH_2-PAMAM-G3, 17864-ULS-NH_2-PAMAM-G3 and sunitinib in demineralized water. Demineralized water was used as control. After addition of 20 µL sample to 20 µL HK-2 cell lysate (0.34 mg/ mL), samples were incubated for 30 minutes at room temperature. Phosphorylation of the tyrosine kinases was stimulated by 1 hour incubation of the samples with 40 µL 100 µM ATP in Abl kinase assay buffer (consisting of 50 mM Tris-HCl [pH 7.5], 10 mM $MgCl_2$, 1 mM ethyleneglycoltetraacetic acid, 2 mM dithiothreitol (DTT) and 0.01% Brei-35) at 37 °C. The phosphorylation was terminated by 5 minutes incubation at room temperature with 26 µL reducing sample buffer (Invitrogen, Breda, The Netherlands) containing a final concentration of 40 mM DTT and 0.1% (w/ v) sodium dodecyl sulfate (SDS). Protein (10 µL) was separated by

SDS-polyacrylamide gel electrophoresis using a precast 4-12% Bis-Tris gel and MOPS SDS running buffer. Proteins were transferred onto a PVDF membrane by wet blotting. The transfer buffer consisted of 25 mM Tris, 192 mM glycine and 10% methanol (v/ v) and a transfer voltage of 100 V was used for 1 hour. After 1 hour blocking at room temperature with 3% (w/ v) BSA in Tris buffered saline (TBS) with 0.1% (v/ v) Tween-20 (further referred to as 3% BSA in TBS/ T), the membrane was incubated overnight at 4 °C with mouse anti-human phosphotyrosine [PY20] monoclonal antibody (1:1000 in 3% BSA in TBS/ T). The membrane was washed with TBS/ T and the proteins were visualized using the SuperSignal® West Femto Maximum Sensitivity Substrate Kit (Thermo Scientific, Etten-Leur, The Netherlands). Band density was determined on a Gel Doc XRS Imaging system with Quantity One analysis software (Bio-Rad, Hercules, CA, USA).

2.5.3. In vitro inhibition of kinase activity after uptake in HK-2cells

HK-2 cells were seeded onto a 96-well plate (2×10^4 cells/ well) and serum-starved overnight. Cells were subsequently incubated with 10 µM 17864, 17864-ULS, NH_2-PAMAM-G3, 17864-ULS-NH_2-PAMAM-G3 and sunitinib in serum-free medium. After 24 hours incubation cells were washed thrice with PBS (PAA Laboratories GmbH, Cölbe, Germany) and lysed with M-PER containing protease- and phosphatase inhibitors. Protein contents were measured using the Micro BCA™ Protein Assay Kit (Prod #23235; Thermo Scientific; Etten-Leur, The Netherlands). For the phosphorylation of tyrosine kinases and the analysis of the inhibitory effects of the compounds the same protocol was used as described above for the inhibitory effects in HK-2 cell lysate. Instead of 100 µM ATP in Abl kinase assay buffer, the phosphorylation of tyrosine kinases was stimulated with 10 µM ATP in Abl kinase assay buffer. Samples containing 1µg total protein were separated by SDS-polyacrylamide gel electrophoresis.

2.5.4. In vitro cytotoxicity

HK-2 cells were seeded (8×10^3 cells/ well in a total volume of 100 µL complete medium) in 96-well plates 24 hours prior to addition of the samples. Cell were then incubated with 100 nM and 1 µM of 17864-ULS-NH_2-PAMAM-G3 and NH_2-PAMAM-G3 (both samples n = 6 for each concentration) for 24 hours under normal culture conditions. Untreated HK-2 cells (n = 12 for each concentration) were used as control. The cytotoxicity of the samples was established using the sulphorhodamine B (SRB) colorimetric assay (42). After incubation, HK-2 cells were fixed *in situ* by incubation with 50 µL/ well 12.5% (w/ v) trichloroacetic acid (TCA) in demineralized water for 1.5 hour at 4 °C. Supernatants were removed from the wells and the cells were washed four times with normal water and subsequently air-dried. Staining was performed by incubation of the cells with 100 µL/ well 0.4% (w/ v) SRB in 1% acetic acid in demineralized water for 15 minutes at room temperature, under shaking. The SRB solution was removed from the wells and the cells were washed four times with 1% (v/ v) acetic acid in demineralized water. After air-drying, cells were incubated with 200 µL/ well 10 mM Trizma® base in demineralized water for 15 minutes at room temperature, under shaking. The optical density was measured at 550 nm. Statistical analysis was performed using one-way analysis of variance (ANOVA), with $p < 0.05$ as the minimum level of significance.

2.6. Animals

In vivo experiments were performed in normal male C57Bl/ 6J mice obtained from Harlan (Zeist, The Netherlands). Mice with a body weight of 17-19 gram were ordered and used for the *in vivo* experiments within three weeks after arrival. The mice were housed in cages in a 12 hours light and 12 hours dark cycle and given food and water *ad libitum*. Experimental protocols for pharmacokinetic and efficacy studies were approved by the animal ethics committee of the University of Utrecht, The Netherlands.

2.7. In vivo renal accumulation of 17864-ULS-NH_2-PAMAM-G3

Mice received a single intravenous injection of 20 mg/ kg 17864-ULS-NH_2-PAMAM-G3 and were euthanized at 1 hour (n = 2), 24 hours (n = 3) and 72 hours (n = 3) after administration of the conjugate, by injection of a cocktail of ketamine hydrochloride (47 mg/ mL), xylazine hydrochloride (8 mg/ mL) and atropine (0.07 mg/ mL) (intraperitoneal 120-150 µl). Kidneys were removed and stored at -80 °C until further processing as described below.

2.7.1. LC-MS/MS analysis of 17864-ULS-NH_2-PAMAM-G3

Total 17864 levels (*i.e.* 17864-ULS-NH_2-PAMAM-G3 and the intracellular formed metabolites 17864-ULS and 17864) were measured in kidney homogenates. Kidney homogenates were prepared by homogenizing the kidneys in 4% (w/ v) BSA in demineralized water with a polytron tissue homogenizer in a final concentration of 0.1 gram tissue/ mL. Calibration standards (10 ng/ mL-1 µg/ mL 17864-ULS-NH_2-PAMAM-G3) were prepared in blank kidney homogenate. Blank kidney homogenate was used as negative control and 4-hydroxybenzophenone as internal standard. To 100 µL kidney homogenate 50 µL hydroxybenzophenone (50 µg/ mL in methanol) and 1 mL TBME (extraction agent) were added. Samples were incubated for 24 hours at 80 °C with an equivolume of 1 M KSCN in PBS to obtain free 17864. After incubation, samples were mixed vigorously for 15 minutes and centrifuged for 5 minutes at 7,500 x g. The aqueous layer was frozen in liquid nitrogen and the TBME layer was collected. After repetition of the extraction procedure the samples were shortly vortexed and placed in a Speed-Vac Plus SC210A for 45 minutes at 45 °C to evaporate the TBME. Samples were reconstituted in 100 µL ACN containing 0.1% TFA by 15 minutes sonication and 15 minutes vortexing. After 3 minutes centrifugation at 21,000 x g the supernatant was diluted 6 times with demineralized water before analysis with LC-MS/ MS. The LC-MS/ MS equipment and general MS/ MS setting were reported previously by Sparidans *et al.* (43). Partial-loop injections (2 µl) were made on an Aquity UPLC® BEH C18 column (30 x 2.1 mm, d_p = 1.7 µm, Waters, Milford, USA) with the corresponding VanGuard pre-column (Waters, 5 x 2.1 mm, d_p = 1.7 µm). The column temperature was maintained at 40 °C and the autosampler sample rack compartment was maintained at 4 °C. The eluent comprised a mixture of two solvents: 0.1% (v/ v) formic acid in water (A) and methanol (B), pumped at 0.5 ml/ min. The amount of solvent B was increased from 10 to 70% during 3 minutes after injection, followed by flushing the column for 0.5 minute with 70% methanol and reconditioning the column at 10% methanol for 1.5 minute. The whole eluate was transferred into the electrospray ionization source, starting at 0.8 minute after injection by switching the MS inlet valve, until 4 minutes after injection. The selected reaction monitoring mode was used with argon as the collision gas at 2.0 mTorr and 40 ms dwell times. Mass resolution was set at 0.7 full with at half

height (unit resolution) for both separating quadrupoles. The tube lens off set was 108 V for 17864 and 100 V for the internal standard. 17864 was monitored at *m/z* 373.14→239.17 at -18 V collision energy; the internal standard at *m/z* 199.00→121.00 at -15 V.

3. Results and discussion

3.1. Binding of NH_2-PAMAM-G3 to the internalizing megalin receptor

In the current study we investigated if NH_2-PAMAM-G3 binds to the megalin receptor by BIAcore receptor interaction studies. The surface plasmon resonance sensorgram in **Figure 3** shows that NH_2-PAMAM-G3 rapidly associated with the megalin receptor.

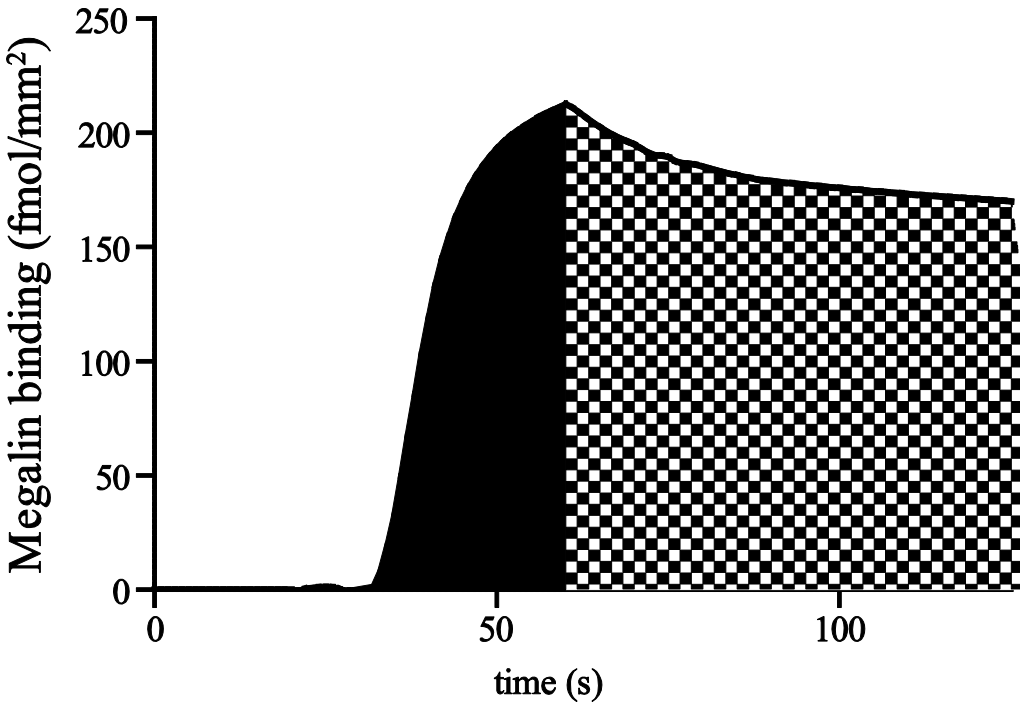

Figure 3. Surface plasmon resonance sensorgram of the binding of 1 µM NH_2-PAMAM-G3 to the megalin receptor. The association phase is depicted in black and the dissociation phase in black and white block print. Original response units (RU) were converted into fmol/ mm^2 using the equation 1000 RU = 1 ng protein/ mm^2 and the molecular weight of NH_2-PAMAM-G3 (*i.e.* 6909 Da). Signal was corrected for refractive effects and unspecific binding to the sensor chip.

From the slow dissociation of NH_2-PAMAM-G3 from the receptor it can be concluded that the interaction between the dendritic carrier and internalizing megalin receptor is strong. With an EDTA/ NaCl solution (which removes the calcium that is needed by megalin for ligand-bindig) 100% regeneration of the megalin-coated sensor chip was obtained. Altogether, the surface plasmon resonance study demonstrates that NH_2-PAMAM-G3 binds to megalin, which might

indicate that the dendritic carrier accumulates in the proximal tubular cells via megalin receptor-mediated endocytosis. This is corroborated by the earlier discussed observations by Kobayashi *et al*. that NH_2-PAMAM dendrimers accumulate in the renal cortex and that this can be inhibited by co-administration of an excess of the cationic amino acid lysine (15, 19).

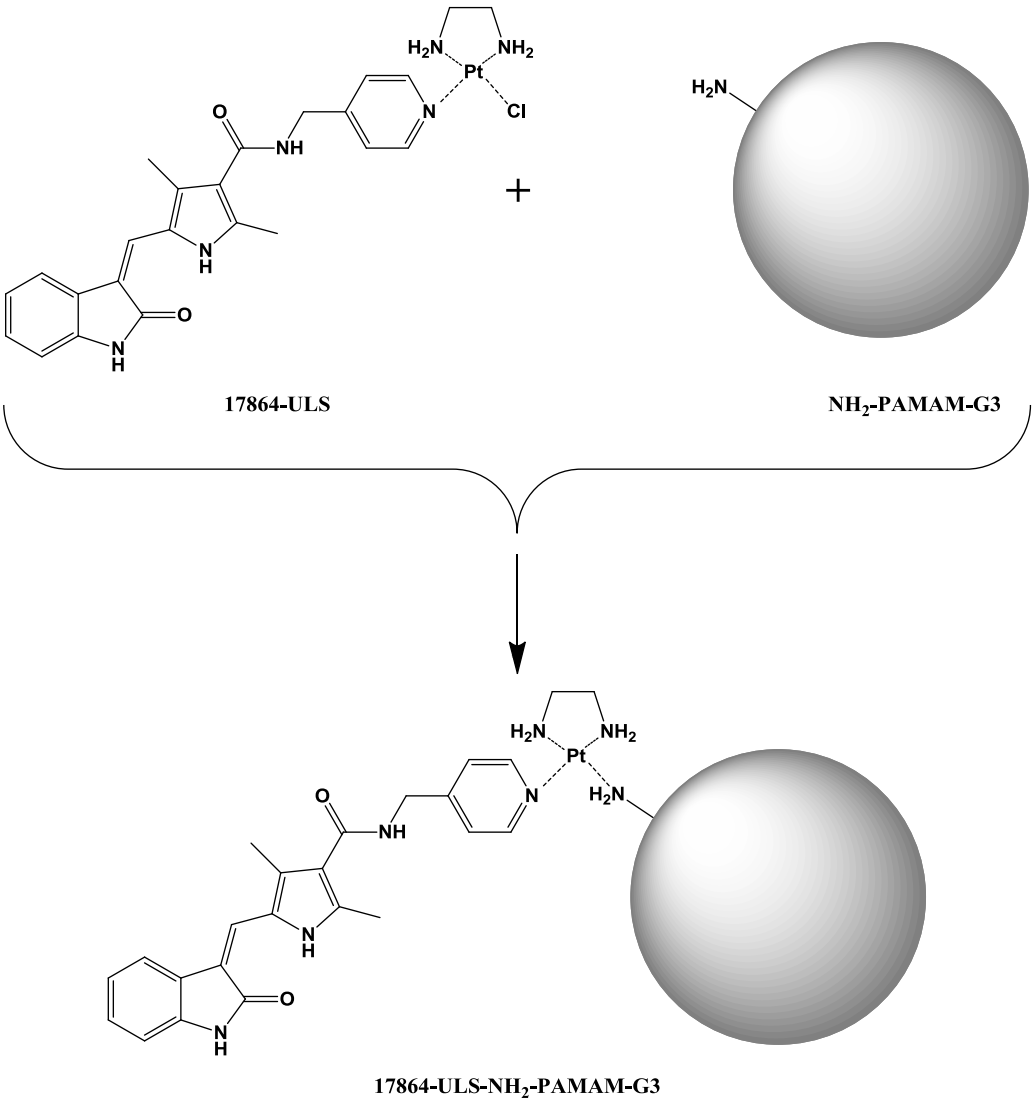

Figure 4. Conjugation of 17864-ULS to the terminal amine groups of the renal carrier NH_2-PAMAM-G3. Coordination of 17864-ULS to one of the 32 terminal amine groups of NH_2-PAMAM-G3 results in a Pt-N_4 coordination.

3.2. Synthesis and characterization of 17864-ULS-NH_2-PAMAM-G3

The successful synthesis of 17864-ULS was demonstrated by ^{195}Pt-NMR and LC-MS analysis. ^{195}Pt-NMR analysis of 17864-ULS showed a peak at -2493 ppm, characteristic for Pt-N_3 coordination (35), confirming the coupling of the ULS linker to one of the nitrogen atoms present in 17864. The fact that (*Z*)-3-(2,4-dimethyl-5-((2-oxoindolin-3-ylidene)methyl)-1*H*-pyrrol-3-yl)propanoic acid (*i.e.* the sunitinib analogue SU6668) cannot be coordinated to the ULS linker (data not shown), indicates that a coordinative bond is formed between the platinum atom of the linker and the pyridine nitrogen in 17864. **Figure 4** shows the coupling of 17864-ULS to NH_2-PAMAM-G3. The dendrimer yield after purification of 17864-ULS-NH_2-PAMAM-G3 was 100%. In case of dendritic carrier systems drug molecules can be complexed or conjugated to the terminal functional groups of the carrier and/or encapsulated in the void spaces of the dendrimer (5). To investigate the attachment of 17864-ULS to the terminal amine groups of NH_2-PAMAM-G3, the conjugate was analyzed by ^{195}Pt-NMR analysis which indeed showed one main peak at -2769 ppm, which is characteristic for Pt-N_4 coordination. Attachment of 17864-ULS to the terminal amine groups of NH_2-PAMAM-G3, rather than encapsulation in the void spaces, is in line with the expectations, because PAMAM dendrimers up to generation 3 have ellipsoidal shapes that lack void spaces that can be exploited for drug encapsulation (8). The molar 17864/ NH_2-PAMAM-G3 coupling ratio was established with UV and HPLC and was in both cases found to be 0.75:1.

3.3. Activity of ULS-bound 17864 in cell lysate

Figure 5 shows the anti-phosphotyrosine western blot of HK-2 cell lysate exposed to, respectively, 17864, 17864-ULS, 17864-ULS-NH_2-PAMAM-G3, 17864-ULS-NH_2-PAMAM-G3 and sunitinib.

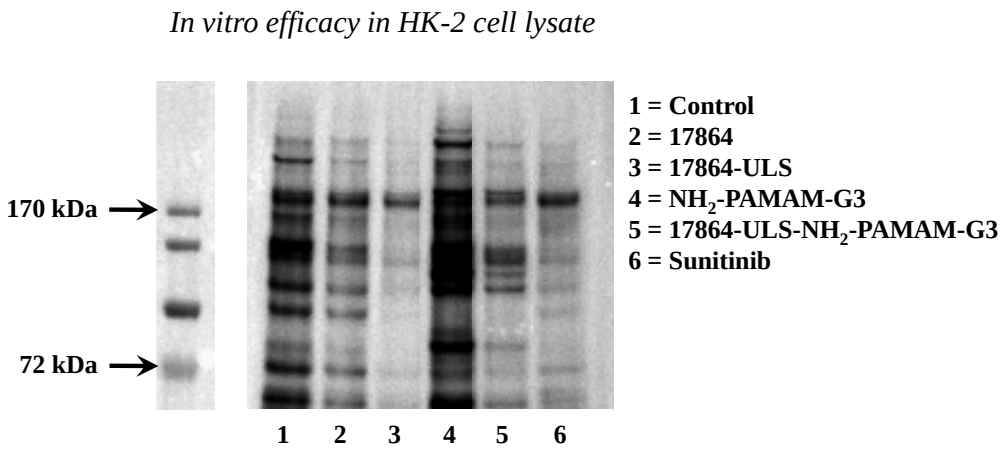

Figure 5. Representive anti-phosphotyrosine western blot of the inhibitory effects of 17864, 17864-ULS, 17864-ULS-NH_2-PAMAM-G3, 17864-ULS-NH_2-PAMAM-G3 and sunitinib on the phosphorylation of tyrosine kinases in HK-2 cell lysate. The novel sunitinib analogue 17864 remains active when coordinated to ULS or the dendritic carrier NH_2-PAMAM-G3 (via the ULS linker).

Sunitinib and 17864-ULS, both, strongly inhibited the phosphorylation of multiple tyrosine kinases, confirming the pharmacological activity of 17864-ULS. Surprisingly, the inhibitory effects observed for 17864-ULS were stronger as compared with 17864 which may be explained by participation of the ULS linker in the interaction of 17864-ULS with target kinases. Since prior studies with a different 17864-ULS-carrier conjugate demonstrated that degradation of this type of conjugate in proximal tubular cells primarily yields ULS-bound 17864 metabolites (chapter 5 of this thesis), the high kinase inhibitory activity of 17864-ULS may be advantageous in the treatment of tubulointerstitial fibrosis. **Figure 5** shows that the dendritic carrier alone did not inhibit tyrosine kinase activity while the intact conjugate, *i.e.* 17864-ULS-NH_2-PAMAM-G3, did inhibit the activation of tyrosine kinases. The lower activity of 17864-ULS-NH_2-PAMAM-G3 as compared with 17864-ULS can be explained by steric hindrance of the dendritic carrier. In conclusion, this experiment showed that intact 17864-ULS-NH_2-PAMAM-G3 is pharmacological active and that intracellular degradation of the conjugate may not only result into the active parent drug, *i.e.* 17864, but also in active 17864-ULS metabolites.

3.4. In vitro internalization and activity of 17864-ULS-NH_2-PAMAM-G3

The anti-tyrosine kinase activity of 17864-ULS-NH_2-PAMAM-G3 after internalization in HK-2 cells was studied. HK-2 cells were incubated with this conjugate as wells as with 17864, 17864-ULS, NH_2-PAMAM-G3 and sunitinib for 24 hours. **Figure 6** shows the inhibitory effects of the compounds on the phosphorylation of tyrosine kinases. The 17864-ULS-NH_2-PAMAM-G3 conjugate showed a similar degree of inhibition as the multitargeted kinase inhibitor sunitinib indicating that the conjugate can be internalized by the proximal tubular cells and that the internalized compound or its intracellularly generated metabolites (*i.e.* 17864 and/ or 17864-ULS adducts) are active. While 17864-ULS also inhibited tyrosine kinase activity after internalization in HK-2 cells, no inhibitory effects were observed for 17864. The lack of efficacy of 17864 can be explained by a less efficient uptake of the kinase inhibitor by the proximal tubular cells due to free diffusion across the cell membrane.

In vitro efficacy after cell uptake

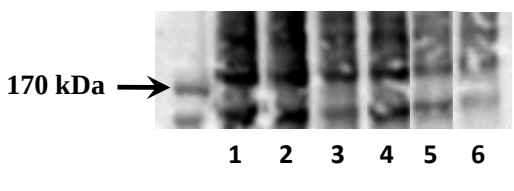

1 = Control
2 = 17864
3 = 17864-ULS
4 = NH_2-PAMAM-G3
5 = 17864-ULS-NH_2-PAMAM-G3
6 = Sunitinib

Figure 6. Anti-phosphotyrosine western blot of the inhibitory effects of 17864, 17864-ULS, NH_2-PAMAM-G3, 17864-ULS-NH_2-PAMAM-G3 and sunitinib on the tyrosine kinase activity after internalization by HK-2 cells. Equal protein amounts were loaded onto the gel.

3.5. In vitro cytotoxicity of 17864-ULS-NH_2-PAMAM-G3

Despite the increased interest in dendritic carrier systems, one concern is their potential toxicity (44). We evaluated the *in vitro* cytotoxic effects of 17864-ULS-NH_2-PAMAM-G3 on the proliferation of HK-2 cells. **Figure 7** shows the cell viability of HK-2 cells after 24 hours treatment with 100 nM and 1 µM 17864-ULS-NH_2-PAMAM-G3 and NH_2-PAMAM-G3. The cell viability was significantly reduced after 24 hours exposure of the cells to 1 µM NH_2-PAMAM-G3 (78% cell viability). In contrast, no significant toxicity was observed with 17864-ULS-NH_2-PAMAM-G3 in both concentrations. These results are in agreement with the observations of Jevrasesphant *et al.* (45) and Kolhatkar *et al.* (46) that derivatization of terminal amines with, for example, acetyl groups, lauroyl chains or polyethylene glycol resulted in a reduced cytotoxicity of different generation PAMAM dendrimers.

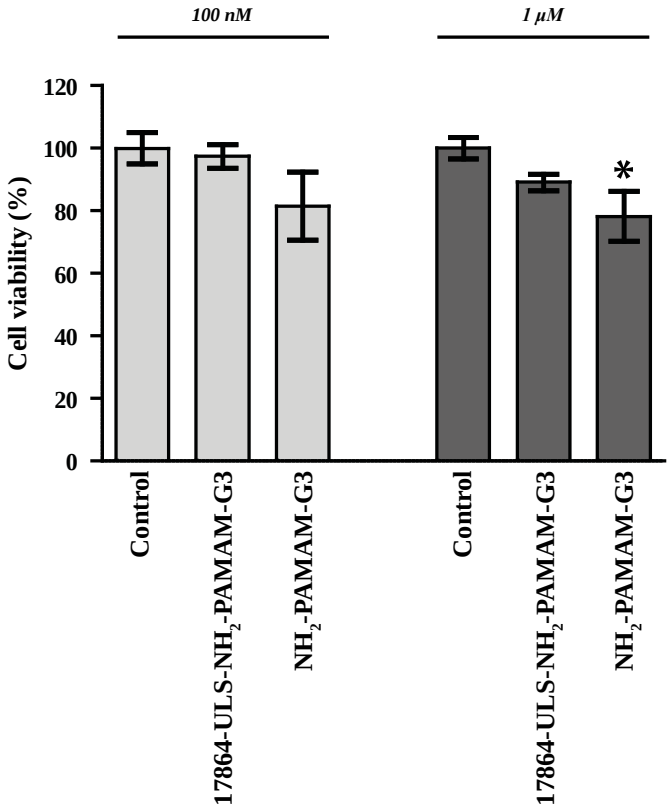

Figure 7. Cell viability of HK-2 cells after 24 hours incubation with 100 nM and 1 µM 17864-ULS-NH_2-ULS-PAMAM-G3 and NH_2-PAMAM-G3. Untreated HK-2 cells were used as control and set at 100%. Data represent the mean +/- SEM. Statistical significance versus controls is indicated as *($p < 0.05$).

3.6. Renal accumulation of 17864-ULS-NH_2-PAMAM-G3

The *in vivo* renal accumulation of 17864-ULS-NH_2-PAMAM-G3 was evaluated in mice. **Figure 8** shows the uptake in the kidneys after a single intravenous injection of the conjugate. 17864-ULS-NH_2-PAMAM-G3 rapidly accumulated in the kidneys, as was demonstrated by the high intrarenal levels (*i.e.* 13% of the injected dose) of the conjugate observed at 1 hour after administration. This result is in line with earlier studies in which radiolabeled NH_2-PAMAM-G3

and NH_2-PAMAM-G5 conjugates accumulated in the kidneys within 15 and 5 minutes after intravenous administration, respectively (13, 47).

The renal kinase inhibitor levels after administration of 17864-ULS-NH_2-PAMAM-G3 remained high for up to 3 days (*i.e.* 15 and 14% of the injected dose at 1 day and 3 days after administration, respectively). Biodistribution studies with radiolabeled NH_2-PAMAM dendrimers have shown that these macromolecules up to, at least, generation 5 are rapidly eliminated from the circulation via renal excretion (13, 47, 48). This can be easily explained by the small hydrodynamic diameter and compact structure of dendritic carriers (49). The hydrodynamic diameter of NH_2-PAMAM-G3 (*i.e.* 3.6 nm) is much lower than the cut-off size for glomerular filtration (*i.e.* < 5-7 nm) (22) and conjugation of one small molecule kinase inhibitor per molecule NH_2-PAMAM-G3 will therefore not limit the free glomerular filtration of 17864-ULS-NH_2-PAMAM-G3. This indicates that the almost equal kinase inhibitor levels observed in the kidneys at day 1 and 3 after administration of the conjugate are due to a long intrarenal residence time of 17864-ULS-NH_2-PAMAM-G3 and/ or its metabolites rather than due to continuous internalization from the tubular lumen. The sustained intrarenal drug levels after administration of 17864-ULS-NH_2-PAMAM-G3 are in line with the sustained radioactivity observed in the kidneys after administration of radiolabeled NH_2-PAMAM-G5 dendrimer conjugates (*i.e.* up to 7 days) (47).

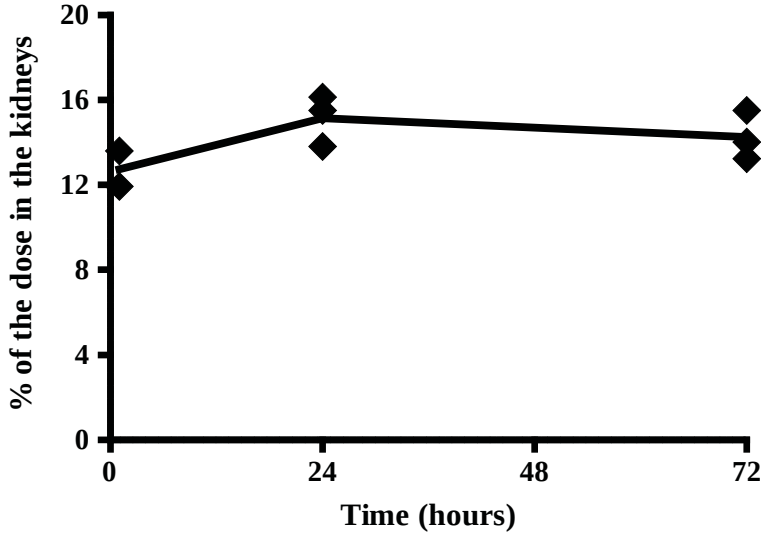

Figure 8. Renal accumulation of 17864-ULS-NH_2-PAMAM-G3 at 1 hour (n = 2), 24 hours (n = 3) and 72 hours (n = 3) post administration of an intravenous injection of 20 mg/ kg in mice.

In earlier studies we exploited the low molecular weight protein lysozyme as carrier system for the intracellular delivery of 17864 into the proximal tubular cells of the kidneys (chapter 5 of this thesis). Lysozyme is a well-known ligand of the megalin receptor, which is also small enough (*i.e.* 14 kDa) to be freely filtered through the glomerulus (50, 51). For the conjugation of 17864 to lysozyme, the same platinum (II)-based linker was used as for the conjugation to NH_2-PAMAM-

G3. Like 17864-ULS-NH_2-PAMAM-G3, 17864-ULS-lysozyme rapidly accumulated in the kidneys after intravenous administration in mice. Importantly, renal kinase inhibitor levels that are obtained in the present study with the dendritic carrier are approximately 2-fold higher than the renal drug levels obtained after administration of 17864-ULS-lysozyme. Another difference between the two conjugates is the intrarenal residence time of the kinase inhibitor. After administration of the lysozyme conjugate, renal drug levels decreased from approximately 6% of the injected dose at 30 minutes after administration to 1% of the injected dose at 3 days after administration. In contrast, renal drug levels after administration of 17864-ULS-NH_2-PAMAM-G3 remained persistently high at approximately 14-15%. The difference in renal residence time between 17864-ULS-lyozyme and 17864-ULS-NH_2-PAMAM-G3 can be explained by the difference in biodegradability. The proteinaous carrier lysozyme can be degraded enzymatically in the lysosomes, while the amide bonds in the synthetic NH_2-PAMAM-G3 dendrimer are not susceptible for either enzymatic or chemical degradation. The degradation rate of NH_2-PAMAM-G3 will therefore be slower than the degradation rate of lysozyme. Another explanation can be that the degradation of the platinum coordinative bonds is slower in the dendritic conjugate. While in 17864-ULS-lysozyme the platinum atom of the ULS linker is coordinated to methionyl residues, resulting in a platinum-thiol coordinative bond, the platinum atom in 17864-ULS-NH_2-PAMAM-G3 is coordinated to aliphatic nitrogens. Platinum (II) forms more stable coordination bonds with aliphatic nitrogens than with aliphatic thiols.

Kinase inhibitor-ULS-carrier conjugates that are internalized in the proximal tubular cells of the kidneys via megalin receptor-mediated endocytosis are routed to the lysosomal compartment of the cells. Since their target kinases are localized within the cytosolic compartment of the cells, lysosomal escape is a crucial step in the efficacy of the delivered kinase inhibitor. Although small molecules can cross the lysosomal membrane via passive diffusion or transporters (52), macromolecular drug-carrier conjugates are commonly not able to cross the lysosomal membrane. This may also be the case for 17864-ULS-NH_2-PAMAM-G3. Cationic PAMAM dendrimers have, however, successfully been applied in gene transfection, because they promote endo-lysosomal escape of the delivered gene (53). The capability of NH_2-PAMAM dendrimers to escape from the endo-lysosomal compartment of cells can, at least partly, be explained by the proton sponge theory. Due to the low pH within the endo-lysosomal compartment (*i.e.* pH 4-5), the protonation of terminal amines increases remarkably. This leads to the co-influx of protons and chloride ions, together with water to keep the endo-lysosomal environment iso-osmotic. Endosomal- and lysosomal membranes are disrupted as a consequence of the resulting swelling, allowing the escape of the dendritic carriers (54, 55). When this occurs with 17864-ULS-NH_2-PAMAM-G3, the conjugate will be able to reach its target kinases within the cytosolic compartment after receptor-mediated internalization in the proximal tubular cells. The escape efficiency of amine-terminated dendrimers increases with increased generation number and future studies may address this topic.

Conclusion

In the current study we developed a new type of drug-dendrimer conjugate for the intracellular delivery of a sunitinib analogue into the proximal tubular cells of the kidneys. A novel sunitinib analogue was developed, *i.e.* 17864, which was successfully conjugated to the terminal amines of NH_2-PAMAM-G3 via the platinum linker ULS. The pharmacological activity of 17864 was retained after coordination to the ULS linker alone or bound to NH_2-PAMAM-G3. We furthermore demonstrated the *in vitro* internalization of 17864-UlS-NH_2-PAMAM-G3 in human proximal tubular cells and the *in vivo* accumulation of 17864-ULS-NH_2-PAMAM-G3 in the kidneys. These results are encouraging for future studies focusing on the development of novel therapeutics for the treatment of renal diseases.

Acknowledgements

This work was made possible by a grant from the European Framework program FP6 (LSHB-CT-2007-036644).

References

1. B.K. Nanjwade, H.M. Bechra, G.K. Derkar, F.V. Manvi and V.K. Nanjwade. Dendrimers: emerging polymers for drug-delivery systems. Eur J Pharm Sci. 38:185-196 (2009).
2. H. Yang and W.J. Kao. Dendrimers for pharmaceutical and biomedical applications. J Biomater Sci Polym Ed. 17:3-19 (2006).
3. A. D'Emanuele and D. Attwood. Dendrimer-drug interactions. Adv Drug Deliv Rev. 57:2147-2162 (2005).
4. N.K. Jain and A. Asthana. Dendritic systems in drug delivery applications. Expert Opin Drug Deliv. 4:495-512 (2007).
5. N.K. Jain and U. Gupta. Application of dendrimer-drug complexation in the enhancement of drug solubility and bioavailability. Expert Opin Drug Metab Toxicol. 4:1035-1052 (2008).
6. C.C. Lee, J.A. MacKay, J.M. Frechet and F.C. Szoka. Designing dendrimers for biological applications. Nat Biotechnol. 23:1517-1526 (2005).
7. S. Svenson and D.A. Tomalia. Dendrimers in biomedical applications--reflections on the field. Adv Drug Deliv Rev. 57:2106-2129 (2005).
8. Y. Cheng, Z. Xu, M. Ma and T. Xu. Dendrimers as drug carriers: applications in different routes of drug administration. J Pharm Sci. 97:123-143 (2008).
9. E.R. Gillies and J.M. Frechet. Dendrimers and dendritic polymers in drug delivery. Drug Discov Today. 10:35-43 (2005).
10. I.J. Majoros, A. Myc, T. Thomas, C.B. Mehta and J.R. Baker, Jr. PAMAM dendrimer-based multifunctional conjugate for cancer therapy: synthesis, characterization, and functionality. Biomacromolecules. 7:572-579 (2006).
11. A.K. Patri, I.J. Majoros and J.R. Baker. Dendritic polymer macromolecular carriers for drug delivery. Curr Opin Chem Biol. 6:466-471 (2002).
12. A.V. Ambade, E.N. Savariar and S. Thayumanavan. Dendrimeric micelles for controlled drug release and targeted delivery. Mol Pharm. 2:264-272 (2005).
13. H. Kobayashi, S. Kawamoto, S.K. Jo, H.L. Bryant, Jr., M.W. Brechbiel and R.A. Star. Macromolecular MRI contrast agents with small dendrimers: pharmacokinetic differences between sizes and cores. Bioconjug Chem. 14:388-394 (2003).
14. H. Kobayashi, S.K. Jo, S. Kawamoto, H. Yasuda, X. Hu, M.V. Knopp, M.W. Brechbiel, P.L. Choyke and R.A. Star. Polyamine dendrimer-based MRI contrast agents for functional kidney imaging to diagnose acute renal failure. J Magn Reson Imaging. 20:512-518 (2004).
15. H. Kobayashi, S. Kawamoto, S.K. Jo, N. Sato, T. Saga, A. Hiraga, J. Konishi, S. Hu, K. Togashi, M.W. Brechbiel and R.A. Star. Renal tubular damage detected by dynamic micro-MRI with a dendrimer-based magnetic resonance contrast agent. Kidney Int. 61:1980-1985 (2002).
16. G. Ciarimboli. Organic cation transporters. Xenobiotica. 38:936-971 (2008).
17. B. Hagenbuch. Drug uptake systems in liver and kidney: a historic perspective. Clin Pharmacol Ther. 87:39-47 (2010).
18. K. Thelle, E.I. Christensen, H. Vorum, H. Orskov and H. Birn. Characterization of proteinuria and tubular protein uptake in a new model of oral L-lysine administration in rats. Kidney Int. 69:1333-1340 (2006).
19. H. Kobayashi, N. Sato, S. Kawamoto, T. Saga, A. Hiraga, T. Ishimori, J. Konishi, K. Togashi and M.W. Brechbiel. Novel intravascular macromolecular MRI contrast agent with generation-4 polyamidoamine dendrimer core: accelerated renal excretion with coinjection of lysine. Magn Reson Med. 46:457-464 (2001).
20. P. Boor, K. Sebekova, T. Ostendorf and J. Floege. Treatment targets in renal fibrosis. Nephrol Dial Transplant. 22:3391-3407 (2007).
21. H.Y. Lan. Tubular epithelial-myofibroblast transdifferentiation mechanisms in proximal tubule cells. Curr Opin Nephrol Hypertens. 12:25-29 (2003).
22. M.E.M. Dolman, S. Harmsen, G. Storm, W.E. Hennink and R.J. Kok. Drug targeting to the kidney: Advances in the active targeting of therapeutics to proximal tubular cells. Adv Drug Deliv Rev. 62:1344-1357 (2010).
23. J. Rosenbloom, S.V. Castro and S.A. Jimenez. Narrative review: fibrotic diseases: cellular and molecular mechanisms and novel therapies. Ann Intern Med. 152:159-166 (2010).
24. E. Healy and H.R. Brady. Role of tubule epithelial cells in the pathogenesis of tubulointerstitial fibrosis induced by glomerular disease. Curr Opin Nephrol Hypertens. 7:525-530 (1998).

25. H. Okada and R. Kalluri. Cellular and molecular pathways that lead to progression and regression of renal fibrogenesis. Curr Mol Med. 5:467-474 (2005).
26. M.H. de Borst, J. Prakash, M. Sandovici, P.A. Klok, I. Hamming, R.J. Kok, G. Navis and H. van Goor. c-Jun NH2-terminal kinase is crucially involved in renal tubulo-interstitial inflammation. J Pharmacol Exp Ther. 331:896-905 (2009).
27. D.C. Harris. Tubulointerstitial renal disease. Curr Opin Nephrol Hypertens. 10:303-313 (2001).
28. F.Y. Ma, M. Sachchithananthan, R.S. Flanc and D.J. Nikolic-Paterson. Mitogen activated protein kinases in renal fibrosis. Front Biosci (Schol Ed). 1:171-187 (2009).
29. M. Zeisberg, F. Strutz and G.A. Muller. Renal fibrosis: an update. Curr Opin Nephrol Hypertens. 10:315-320 (2001).
30. S. Tugues, G. Fernandez-Varo, J. Munoz-Luque, J. Ros, V. Arroyo, J. Rodes, S.L. Friedman, P. Carmeliet, W. Jimenez and M. Morales-Ruiz. Antiangiogenic treatment with sunitinib ameliorates inflammatory infiltrate, fibrosis, and portal pressure in cirrhotic rats. Hepatology. 46:1919-1926 (2007).
31. G. Di Lorenzo, R. Autorino, G. Bruni, G. Carteni, E. Ricevuto, M. Tudini, C. Ficorella, C. Romano, M. Aieta, A. Giordano, M. Giuliano, A. Gonnella, C. De Nunzio, M. Rizzo, V. Montesarchio, M. Ewer and S. De Placido. Cardiovascular toxicity following sunitinib therapy in metastatic renal cell carcinoma: a multicenter analysis. Ann Oncol. 20:1535-1542 (2009).
32. W.J. Lee, J.L. Lee, S.E. Chang, M.W. Lee, Y.K. Kang, J.H. Choi, K.C. Moon and J.K. Koh. Cutaneous adverse effects in patients treated with the multitargeted kinase inhibitors sorafenib and sunitinib. Br J Dermatol. 161:1045-1051 (2009).
33. T. Gonzalo, L. Beljaars, M. van de Bovenkamp, K. Temming, A.M. van Loenen, C. Reker-Smit, D.K. Meijer, M. Lacombe, F. Opdam, G. Keri, L. Orfi, K. Poelstra and R.J. Kok. Local inhibition of liver fibrosis by specific delivery of a platelet-derived growth factor kinase inhibitor to hepatic stellate cells. J Pharmacol Exp Ther. 321:856-865 (2007).
34. K. Temming, M.M. Fretz and R.J. Kok. Organ- and cell-type specific delivery of kinase inhibitors: a novel approach in the development of targeted drugs. Curr Mol Pharmacol. 1:1-12 (2008).
35. K. Temming, M. Lacombe, R.Q. Schaapveld, L. Orfi, G. Keri, K. Poelstra, G. Molema and R.J. Kok. Rational design of RGD-albumin conjugates for targeted delivery of the VEGF-R kinase inhibitor PTK787 to angiogenic endothelium. ChemMedChem. 1:1200-1203 (2006).
36. J. Prakash, M. Sandovici, V. Saluja, M. Lacombe, R.Q. Schaapveld, M.H. de Borst, H. van Goor, R.H. Henning, J.H. Proost, F. Moolenaar, G. Keri, D.K. Meijer, K. Poelstra and R.J. Kok. Intracellular delivery of the p38 mitogen-activated protein kinase inhibitor SB202190 [4-(4-fluorophenyl)-2-(4-hydroxyphenyl)-5-(4-pyridyl)1H-imidazole] in renal tubular cells: a novel strategy to treat renal fibrosis. J Pharmacol Exp Ther. 319:8-19 (2006).
37. K.S. Gajiwala, J.C. Wu, J. Christensen, G.D. Deshmukh, W. Diehl, J.P. DiNitto, J.M. English, M.J. Greig, Y.A. He, S.L. Jacques, E.A. Lunney, M. McTigue, D. Molina, T. Quenzer, P.A. Wells, X. Yu, Y. Zhang, A. Zou, M.R. Emmett, A.G. Marshall, H.M. Zhang and G.D. Demetri. KIT kinase mutants show unique mechanisms of drug resistance to imatinib and sunitinib in gastrointestinal stromal tumor patients. Proc Natl Acad Sci U S A. 106:1542-1547 (2009).
38. J.J. Liao. Molecular recognition of protein kinase binding pockets for design of potent and selective kinase inhibitors. J Med Chem. 50:409-424 (2007).
39. Y. Liu and N.S. Gray. Rational design of inhibitors that bind to inactive kinase conformations. Nat Chem Biol. 2:358-364 (2006).
40. L. Sun, C. Liang, S. Shirazian, Y. Zhou, T. Miller, J. Cui, J.Y. Fukuda, J.Y. Chu, A. Nematalla, X. Wang, H. Chen, A. Sistla, T.C. Luu, F. Tang, J. Wei and C. Tang. Discovery of 5-[5-fluoro-2-oxo-1,2-dihydroindol-(3Z)-ylidenemethyl]-2,4- dimethyl-1H-pyrrole-3-carboxylic acid (2-diethylaminoethyl)amide, a novel tyrosine kinase inhibitor targeting vascular endothelial and platelet-derived growth factor receptor tyrosine kinase. J Med Chem. 46:1116-1119 (2003).
41. R.P. van Gijlswijk, E.G. Talman, I. Peekel, J. Bloem, M.A. van Velzen, R.J. Heetebrij and H.J. Tanke. Use of horseradish peroxidase- and fluorescein-modified cisplatin derivatives for simultaneous labeling of nucleic acids and proteins. Clin Chem. 48:1352-1359 (2002).
42. K.T. Papazisis, G.D. Geromichalos, K.A. Dimitriadis and A.H. Kortsaris. Optimization of the sulforhodamine B colorimetric assay. J Immunol Methods. 208:151-158 (1997).
43. R.W. Sparidans, D. Iusuf, A.H. Schinkel, J.H. Schellens and J.H. Beijnen. Liquid chromatography-tandem mass spectrometric assay for the light sensitive tyrosine kinase inhibitor axitinib in human plasma. J Chromatogr B Analyt Technol Biomed Life Sci. 877:4090-4096 (2009).

44. R. Duncan and L. Izzo. Dendrimer biocompatibility and toxicity. Adv Drug Deliv Rev. 57:2215-2237 (2005).
45. R. Jevprasesphant, J. Penny, R. Jalal, D. Attwood, N.B. McKeown and A. D'Emanuele. The influence of surface modification on the cytotoxicity of PAMAM dendrimers. Int J Pharm. 252:263-266 (2003).
46. R.B. Kolhatkar, K.M. Kitchens, P.W. Swaan and H. Ghandehari. Surface acetylation of polyamidoamine (PAMAM) dendrimers decreases cytotoxicity while maintaining membrane permeability. Bioconjug Chem. 18:2054-2060 (2007).
47. J.F. Kukowska-Latallo, K.A. Candido, Z. Cao, S.S. Nigavekar, I.J. Majoros, T.P. Thomas, L.P. Balogh, M.K. Khan and J.R. Baker, Jr. Nanoparticle targeting of anticancer drug improves therapeutic response in animal model of human epithelial cancer. Cancer Res. 65:5317-5324 (2005).
48. M. Ogawa, C.A. Regino, B. Marcelino, M. Williams, N. Kosaka, L.H. Bryant, Jr., P.L. Choyke and H. Kobayashi. New nanosized biocompatible MR contrast agents based on lysine-dendri-graft macromolecules. Bioconjug Chem. 21:955-960 (2010).
49. W. Wijagkanalan, S. Kawakami and M. Hashida. Designing Dendrimers for Drug Delivery and Imaging: Pharmacokinetic Considerations. Pharm Res (2010).
50. E.I. Christensen and H. Birn. Megalin and cubilin: multifunctional endocytic receptors. Nat Rev Mol Cell Biol. 3:256-266 (2002).
51. E.I. Christensen, P.J. Verroust and R. Nielsen. Receptor-mediated endocytosis in renal proximal tubule. Pflugers Arch. 458:1039-1048 (2009).
52. J.B. Lloyd. Lysosome membrane permeability: implications for drug delivery. Adv Drug Deliv Rev. 41:189-200 (2000).
53. M. Neu, D. Fischer and T. Kissel. Recent advances in rational gene transfer vector design based on poly(ethylene imine) and its derivatives. J Gene Med. 7:992-1009 (2005).
54. A. Akinc, M. Thomas, A.M. Klibanov and R. Langer. Exploring polyethylenimine-mediated DNA transfection and the proton sponge hypothesis. J Gene Med. 7:657-663 (2005).
55. A. Kumar, V.K. Yellepeddi, G.E. Davies, K.B. Strychar and S. Palakurthi. Enhanced gene transfection efficiency by polyamidoamine (PAMAM) dendrimers modified with ornithine residues. Int J Pharm. 392:294-303 (2010).

Summarizing discussion

In the past decades, the worldwide number of patients with chronic kidney disease (CKD) has increased remarkably and it is expected that this increasing trend will continue during the coming years (1). At this moment, therapy is focused on the prevention of progressive CKD by treatment of the underlying causes, such as hypertension, diabetes and obesity. CKD is asymptomatic in the initial stage and is often diagnosed in a stage at which treatment of the underlying cause alone is not sufficient to stop loss of kidney function. As a consequence, CKD will gradually progress to end-stage renal disease (ESRD) and renal dialysis or kidney transplantation are then the only possibilities for patients to survive. Because of the lack of clinically available drugs that can halt the progression of CKD and the seriousness of the disease, there is a high need for novel drugs. This thesis focuses on the intracellular delivery of drugs into the proximal tubular cells of the kidneys. Tubulointerstitial fibrosis is one of the common hallmarks of progressive CKD and renal drug targeting to the proximal tubular cells can be of great value in the development of therapeutics that halt or reverse tubulointerstitial fibrosis.

Upon activation, proximal tubular cells induce inflammatory responses by secreting chemokines and other growth factors that attract or activate immune cells. Furthermore, epithelial-to-mesenchymal transition (EMT) of normal tubular epithelial cells into myofibroblasts and activation of fibroblasts induces the excessive production of extracellular matrix (ECM), eventually resulting in the formation of scar tissue and kidney function loss. These profibrotic processes are mediated by a complex intracellular network of signaling cascades, in which growth factor activated- and stress activated kinases play a crucial role. Kinase inhibitors acting at these processes are, therefore, promising candidates for the treatment of tubulointerstitial fibrosis. An important drawback of kinase inhibitors is, however, that their use is often associated with serious adverse reactions. Cellular targeting of kinase inhibitors to the proximal tubular cells is an attractive approach to enhance the drug concentration in the target cells and to avoid adverse reactions in other organs. Furthermore, drug delivery to the proximal tubular cells not only offers the possibility to improve the therapeutic indices of drugs that give severe side effects, but also to gain more insight into the signaling cascades that are responsible for the profibrotic actions of the proximal tubular cells in tubulointerstitial fibrosis. From a drug targeting point-of-view, proximal tubular cells are an attractive target site. They are capable of efficiently accumulating macromolecular drug conjugates via internalizing receptors on their luminal membranes. These receptors, among which the megalin receptor has been most exploited for drug targeting, can be reached relatively easily by macromolecular drug conjugates after glomerular filtration from the circulation.

Taken together, the aim of the current thesis was to develop kinase inhibitor-carrier conjugates for the cell-specific inhibition of the profibrotic events in proximal tubular cells that are involved in the progression of chronic kidney diseases. The ideal kinase inhibitor-carrier conjugate should not only be efficiently accumulated in the designated cell type, but also provide sustained intracellular active kinase inhibitor levels in a concentration that is high enough to obtain an effect. Besides, the intracellular formed active kinase inhibitor metabolites need to be able to reach the cytosolic compartment of the cells, where their target kinases are localized. Therefore, one needs to choose the right combination of carrier, linker and kinase inhibitor. But the choice for a specific combination not only depends on the desired pharmacokinetic behaviour of the

kinase inhibitor-carrier conjugate and the possible pharmacological response, but also on the physicochemical characteristics of the functional units (*i.e.* carrier, linker and kinase inhibitor). Detailed information about carrier systems that can be used for drug targeting to the proximal tubular cells and the linkage technologies that can be applied for drug coupling to these carrier systems is given in the reviews of **chapter 1 and 2**. The subsequent **chapters 3-7** report on the synthesis and *in vitro* and/ or *in vivo* evaluation of several kinase inhibitor-carrier conjugates with different carrier-linker-kinase inhibitor combinations.
Below the choice for a specific carrier, linker and kinase inhibitor will be discussed stepwise with the chapters of the present thesis as guiding principle. Furthermore, the *in vivo* evaluation of the antifibrotic effects of kinase inhibitor-lysozyme conjugates as well as their potential in other renal diseases will be discussed.

Carrier system: lysozyme versus PAMAM dendrimer

Most of the studies in this thesis have been performed with the low molecular weight protein lysozyme as proximal tubular cell-directed carrier. Lysozyme is almost freely filtered through the glomerulus and internalized by the proximal tubular cells via megalin receptor-mediated endocytosis. In **chapter 3** we studied the *in vitro* uptake and intracellular handling of two kinase inhibitor-lysozyme conjugates (*i.e.* LY364947-lysozyme and erlotinib-lysozyme) in proximal tubular cells. It was confirmed that kinase inhibitor-lysozyme conjugates are internalized via an active transport mechanism and accumulate in the lysosomal compartment of the proximal tubular cells. The next step was the investigation of the *in vivo* renal accumulation of kinase inhibitor-lysozyme conjugates. In **chapter 4 and 5** we studied the pharmacokinetics of two novel kinase inhibitor-lysozyme conjugates (*i.e.* imatinib-ULS-lysozyme and 17864-ULS-lysozyme, respectively) in mice. Both kinase inhibitor-lysozyme conjugates were rapidly taken up by the kidneys, with maximum renal levels of approximately 6% of the injected doses. For imatinib-ULS-lysozyme **(chapter 4)** we demonstrated that the conjugate specifically accumulated in the proximal tubular cells of the kidneys and that the renal carrier protein lysozyme is degraded within 24 hours after administration. Furthermore the possibility to administer kinase inhibitor-lysozyme conjugates intraperitoneally instead of intravenously was explored. For the investigation of the long term efficacy, animals need to be treated with repeated doses of the conjugate, in which case the frequent administration by intraperitoneal injection is more convenient for both researchers and animals. Intraperitoneally administered imatinib-ULS-lysozyme was rapidly absorbed from the peritoneal cavity into the circulation with a bioavailability of 100%. The renal exposure to imatinib-ULS-lysozyme was similar after intravenous and intraperitoneal administration. In earlier studies Prakash *et al.* studied the subcutaneous administration of captopril-lysozyme, directed to the angiotensin-converting enzyme (ACE). Captopril-lysozyme was absorbed from the subcutaneous injection site into the circulation and taken up in the kidneys. After subcutaneous administration captopril-lysozyme was more gradually taken up in the kidneys than after intravenous administration, but the maximum renal drug levels were similar after both administration routes. For at least the first 24 hours, the renal exposure to captopril-lysozyme was higher after subcutaneous administration as compared to intravenous administration (2). Combined, these results demonstrate that drug-lysozyme conjugates can be administered via different parenteral application routes.

As reviewed in **chapter 1 and 2** of this thesis, several other carrier systems can be used for the delivery of drugs to the proximal tubular cells. Lysozyme has some properties that make it an excellent carrier for kidney targeting. First of all, the pharmacokinetics of lysozyme and its uptake mechanism in the proximal tubular cells of the kidneys is known. Secondly, lysozyme is a natural substrate for lysosomal proteases that are able to break down the carrier protein into amino acids and/or peptide fragments. As a consequence, there will be no cumulative accumulation of the macromolecular carrier protein in the target cells after repeated administrations, thereby preventing intracellular toxicity on the long term. Lastly, lysozyme is freely available from commercial suppliers, affording the cost-effective preparation of drug-lysozyme conjugates. Other low molecular weight proteins and peptides that are taken up in proximal tubular cells via megalin-mediated endocytosis can also be used as carrier system for renal drug delivery, but their production is often costly or difficult.

But low molecular weight proteins such as lysozyme have also some disadvantages as drug carrier. So far, we have used henn-egg white lysozyme for the synthesis of drug-lysozyme conjugates. *In vivo* administration of such a non-autologous protein by repeated injections may, however, induce an immunological response. The alternative would be the use of recombinant human lysozyme, which can be produced nowadays in high quantity in transgenic mice. Although this will not prevent immunological responses in animal studies, recombinant human lysozyme would be advantageous in clinical studies. Moreover, proteins are sensitive for environmental conditions, such as temperature and solvents. During the synthesis of drug-carrier conjugates the product is commonly exposed to elevated temperatures and organic solvents, which can result in denaturation of the proteinaceous carrier and consequently there is a need for alternative carriers.

Carriers based on hydrophilic synthetic polymers form a good alternative for lysozyme, since they are commonly more resistant against extreme environmental circumstances and because the size and type and number of functional groups can be tailored. Moreover, different polymeric carrier systems have shown to more extensively accumulate in the kidneys than lysozyme. Among these systems are the amine-terminated poly(amidoamine) (PAMAM) dendrimers. These dendrimers contain a regularly hyperbranched three-dimensional structure and, in contrast with many linear synthetic polymers, they have a relatively low polydispersity. The presence of multiple, equally reactive, functional groups on their surface as well as their kidney accumulation make PAMAM dendrimers attractive for renal drug targeting. The possibility to use PAMAM dendrimers as carrier for the intracellular delivery of kinase inhibitors into the renal proximal tubular cells was explored in **chapter 7**. For this purpose, 17864-ULS was conjugated to generation-3 NH_2-PAMAM dendrimers (NH_2-PAMAM-G3). The *in vivo* renal accumulation of the resulting conjugate, *i.e.* 17864-ULS-NH_2-PAMAM-G3, was subsequently compared with that of 17864-ULS-lysozyme. Indeed, the highest renal drug levels were obtained with 17864-ULS-NH_2-PAMAM-G3 as compared to 17864-ULS-lysozyme. Besides, administration of 17864-ULS-NH_2-PAMAM-G3 resulted in more sustained active kinase inhibitor levels in the kidneys as compared with 17864-ULS-lysozyme. An explanation for the difference in renal elimination between 17864-ULS-lysozyme and 17864-ULS-NH_2-PAMAM-G3 is that 17864-ULS-NH_2-PAMAM-G3 can have a different susceptibility to agents that displace the drug from the dendrimer, due to steric hindrance and/or the more stable bond between 17864-ULS and the

dendritic carrier (as will be more extensively discussed below). A concern with respect to the NH_2-PAMAM dendrimers is their biodegradability. The hydrolytically stable amide bonds in NH_2-PAMAM dendrimers are not susceptible for enzymatic degradation and will therefore be degraded much more slowly as compared with the amide bonds present in proteinaceous carriers such as lysozyme.

Future perspectives

The high and sustained intrarenal kinase inhibitor levels obtained with the dendritic carrier NH_2-PAMAM-G3 are encouraging for future studies focusing on the development of proximal tubular cell-specific drug-carrier conjugates. In future studies, the in vivo toxicity as well as the capability of kinase inhibitor-NH_2-PAMAM-G3 conjugates to escape from the endo-lysosomal compartment need to be investigated. First, with respect to toxicity, the risk of toxicity depends on the positive charge of the conjugate. Possible toxicity can be tackled by derivatization of the cationic amine groups with neutral or negatively charged groups. Conjugation of ligands to the terminal amine groups may influence the affinity of the dendritic carrier for the internalizing receptor. Jevprasephant et al. demonstrated that it is not needed to modify all terminal amine groups to reduce toxicity, since conjugation of lauroyl chains to 6 out of the 32 amine groups in NH_2-PAMAM-G3 already resulted in a remarkable reduction in cytotoxicity (3). For our goal it would be more efficient to use a ligand of one of the internalizing receptors on proximal tubular cells to reduce the number of cationic amine groups. The proximal tubular cells express the internalizing receptors megalin and cubilin as well as the folate receptors α and β. Sing et al. directly conjugated folic acid to NH_2-PAMAM dendrimers (4). Kinase inhibitor-ULS-NH_2-PAMAM-G3 conjugates with folic acid molecules attached to the dendritic carrier may therefore be taken up by the proximal tubular cells of the kidneys via the folate receptors in addition to the megalin receptor.

As with respect to endolysosomal escape of kinase inhibitor-NH_2-PAMAM-G3 conjugates, NH_2-PAMAM dendrimers have shown to be able to escape from the endolysosomal compartments of cells depending on their generation number. Using this type of dendritic carrier offers therefore an attractive strategy to obtain a conjugate that can relatively easy distribute from the lysosomal into the cytosolic compartment after internalization by proximal tubular cells. An improved escape from the lysosomal compartment may be a further improvement in the drug-ULS-carrier conjugates described in this thesis.

Linkage technology: platinum (II)-based ULS linker versus direct linkage

Although the bond between a drug and carrier system only seems to be a simple “bridge”, also the applied linkage technology influences the *in vivo* behaviour of the drug-carrier conjugate. In the circulation, stability of the drug-carrier conjugate is required to prevent premature drug loss before internalization by the target cells. But after internalization, the drug-carrier conjugate needs to be converted into active metabolites that can be transported to their pharmacological targets. This not only depends on the biodegradability of the carrier, but also on the bioreversibility of the linker between the drug and carrier. The linkage technology that is used for the conjugation of a drug to a carrier is also determined by the physicochemical characteristics of the drug and carrier.

In this thesis the platinum (II)-coordinative Universal Linker System (ULS) is used for the coupling of kinase inhibitors to the renal carrier system (**Figure 1A**). The platinum (II) atom in the ULS linker forms metal-ligand coordination bonds with aromatic nitrogen atoms in the used

kinase inhibitors. In most of the drug-carrier conjugates, drugs are linked to, either carboxylic acid-, amine-, hydroxyl-, thiol- or keto groups. However, many kinase inhibitors that are interesting from a pharmacological point of view lack these functional groups. Instead, aromatic nitrogen groups are commonly present and can, in most cases, be used for direct conjugation to the ULS linker. Not all kinases are, however, successfully reacted with ULS. An example is the well-known multitargeted kinase inhibitor sunitinib (**Figure 1B**). Although sunitinib contains two nitrogen atoms in a ring structure, these do not coordinate with the platinum linker, which can be explained by the lack of a donor electron pair. As discussed in **chapter 5 and 6,** we therefore synthesized a sunitinib derivative (referred to as 17864) which has a pyridyl group suitable for subsequent conjugation to ULS (**Figure 1C**) and, eventually, to the renal carrier lysozyme. The pyridyl nitrogen can readily form a coordinative bond with the platinum atom in the ULS linker. In **chapter 7**, the ULS linker was coordinated to aliphatic amine groups in the dendritic carrier NH_2-PAMAM-G3. Like pyridyl nitrogens, aliphatic amine groups also have an electron pair available for the formation of a coordinative bond with the platinum atom in the linker. Introduction of a sulphide or thiol group in the drug or carrier is another strategy to obtain a compound that reacts with the ULS linker. For the coupling of the ULS linker to lysozyme, thioether groups were introduced on the protein's surface by modification of lysine residues with methionine residues. Compared to aromatic and aliphatic nitrogens, coordinative bonds between the ULS linker and sulphur-containing ligands are more easily formed which can be explained by the location of the electrons around the sulphur atom. The electrons participating in the binding to the ULS linker are moving in orbitals that are further away from the sulphur's nucleus and hence can more easily interact with the orbitals of the platinum (II) atom.

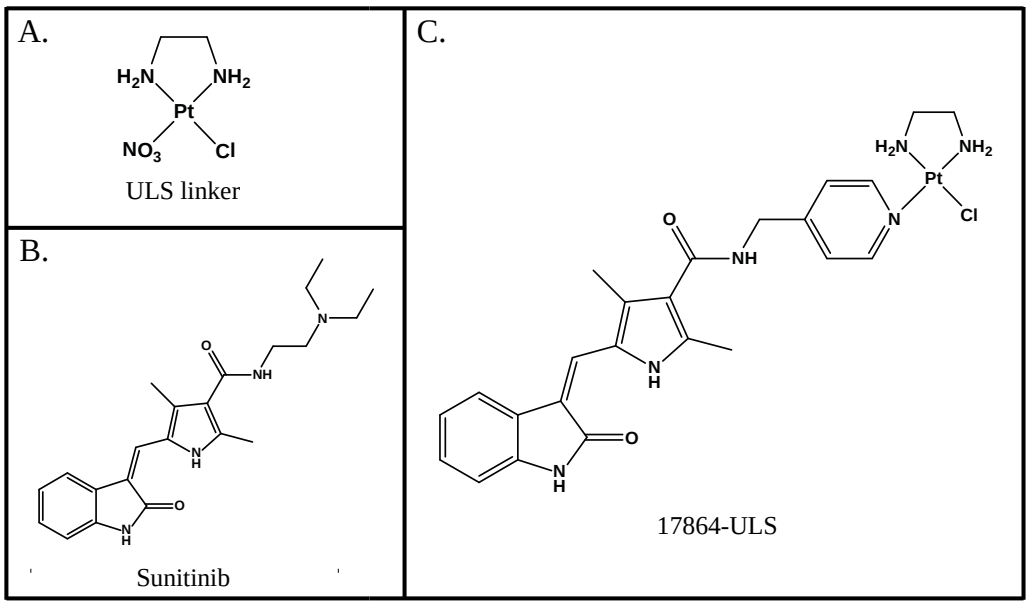

Figure 1. Chemical structures of the platinum (II)-based Universal Linker System (ULS) (A), the multitargeted kinase inhibitor sunitinib (B) and the novel sunitinib analogue 17864 coupled to ULS (C).

In the treatment of tubulointerstitial fibrosis a long residence time of the kinase inhibitor-carrier conjugate within the proximal tubular cells is advantageous, as long as the conjugate is converted into active kinase inhibitor levels that are sufficient to obtain a pharmacological effect. As shown in the **chapters 4, 5 and 7**, the now developed kinase inhibitor-ULS-carrier conjugates resided in the kidneys for at least three days. By analyzing renal drug levels via different pretreatment protocols, we could determine both free kinase inhibitor levels (released from the ULS linker) and ULS-bound kinase inhibitor levels. **Chapter 4 and 5** demonstrated that the majority of the delivered kinase inhibitor detected in the kidneys was present in the ULS-bound form, indicating that this type of product was efficiently retained in the cells. To exploit this, we developed a kinase inhibitor derivative (the earlier discussed sunitinib derivative 17864) that can be active in the ULS-bound form. The oxindole moiety of sunitinib binds deeply in the adenine region of the ATP-binding pocket of most of its target kinases, while the *N*-2-(diethylamino)ethylene moiety is protruding outwards. We therefore hypothesized that this class of kinase inhibitors could be linked to ULS in a manner that preserved their kinase inhibitor properties. In **chapter 6** we demonstrated by molecular modeling approaches that 17864 still fits in the binding pocket of target kinases when coupled to the platinum linker alone or bound to lysozyme and *in vitro* activity assays showed that the capability to inhibit tyrosine kinases was indeed retained. We showed that the activity of 17864 was not only retained after coupling to the ULS linker, but that an even enhanced activity was obtained. An improved fit of the platinum-bound kinase inhibitor in the ATP-binding pocket and/or participation of the linker in the interaction with target kinases can have contributed to the improved inhibitory activity. The observation that the enhanced activity of 17864-ULS was retained even after conjugation to lysozyme or NH_2-PAMAM-G3 suggests that the intracellular formed ULS-bound 17864 metabolites are active.

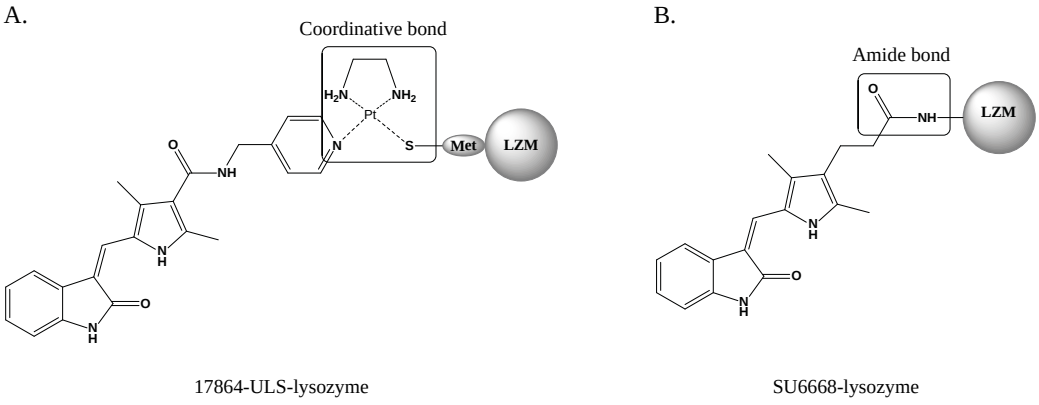

Figure 2. Chemical structures of 17864-ULS-lysozyme (A) and SU6668-lysozyme (B). The sunitinib analogue 17864 was conjugated to lysozyme via the platinum (II)-based ULS linker, while the sunitinib analogue SU6668 was directly conjugated to lysozyme via a classical amide bond.

Although primarily used in this thesis, it is not essential to use the ULS linker for the conjugation of kinase inhibitors to lysozyme. The sunitinib analogue SU6668 could be directly coupled to one of the primary amine groups of lysozyme via the carboxylic acid group of the kinase inhibitor

using 'classical' carbodiimide chemistry. **Figure 2** shows the different linkages formed in the two types of conjugates, *i.e.* 17864-ULS-lysozyme and SU6668-lysozyme. Drug-lysozyme conjugates with amide bonds are most likely not converted into the parent drug upon lysosomal degradation, but will eventually yield the drug with one or more amino acid residues attached to it (5). Direct linkage of a kinase inhibitor to lysozyme via an amide bond is therefore only useful when the attached amino acid residues do not block the activity of the kinase inhibitor. Lysosomal degradation of SU6668-lysozyme yielded SU6668-lysine as final product. In line with the data of 17864-ULS-lysozyme, we demonstrated that the activity of SU6668 was retained after conjugation to lysozyme, implicating that the in situ formed amino acid-bound SU6668 degradation products of the conjugate are active (**Figure 3**). However, the active 17864-ULS metabolites formed after administration of 17864-ULS-lysozyme retained longer within the proximal tubular cells than the active lysine-bound SU6668 metabolite formed after administration of SU6668-lysozyme.

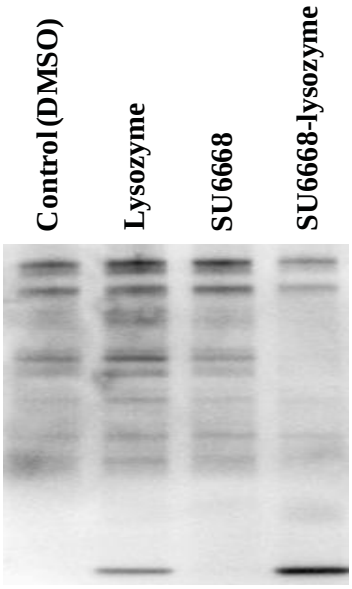

Figure 3. Freshly prepared lysates of immortalized human renal proximal tubular epithelial cells (HK-2) were spiked with 2 µM lysozyme, SU6668 and SU6668-lysozyme and with 0.1% (v/v) DMSO (control). After 30 minutes incubation ATP was added to stimulate the phosphorylation of tyrosine kinases. Western blot analysis was performed to investigate the inhibitory effects of the compounds on the phosphorylation of tyrosine kinases.

Using a platinum linker for the synthesis of kinase inhibitor-ULS-carrier conjugates raises the question if administration of these conjugates will result in platinum-induced toxicity, because platinum compounds such as cisplatin have been associated with severe nephrotoxicity (6, 7). In previous studies Prakash *et al.* showed that a single injection of SB202190-ULS-lysozyme (directed to p38 mitogen activated protein kinase (p38 MAPK) did not result in acute cytotoxic

effects, despite its efficient accumulation in the proximal tubular cells and the sustained levels of platinum compounds. A plausible explanation for the different behavior of "toxic" cisplatin and "non-toxic" drug-ULS-lysozyme conjugates is that the platinum atom in the ULS linker is fully coordinated with rather stable ligands. Cisplatin exerts is nephrotoxic effects in proximal tubular cells by the formation of intrastrand cross-links with two adjacent purines in DNA (8) and by coordination to thiol groups in proteins, resulting in cell apoptosis and necrosis (7, 9). In order to effectively kill cancer cells, cisplatin needs to reach relatively high intracellular levels (*i.e.* IC_{50} ~ 10 µM) (10). The relatively stable conjugates formed by drugs, ULS and the applied carriers are producing only very low levels of platinum metabolites that can react to other ligands. As such, acute toxicity of ULS is not observed.

Future perspectives

*The development of a kinase inhibitor-ULS-conjugate that is converted into active kinase inhibitor-ULS metabolites in addition to free kinase inhibitor is a major advancement. Future studies need to address the intracellular transport of kinase inhibitor-ULS metabolites from the lysosomal into the cytosolic compartment of the proximal tubular cells. For the treatment of tubulointerstitial fibrosis repeated doses of the kinase inhibitor-carrier conjugate are needed, which makes it important to investigate the long term toxicity of the ULS linker. Recently, an alternative platinum (II)-based linker has been developed, i.e. tridentate-ULS (**Figure 4**). Like the ULS linker, tridentate-ULS can form a stable coordinative bond with kinase inhibitors, but the aliphatic amine offers the possibility to use an alternative carrier system than the systems used in this thesis. Poly(vinylpyrrolidone-co-dimethyl maleic acid) (PVD), for example, accumulates more extensively in the kidneys than lysozyme and the NH_2-PAMAM-dendrimers (11, 12). Kinase inhibitor-ULS adducts cannot be coordinated to the linear polymer, while kinase inhibitor-tridentate-ULS adducts can be covalently attached to the carboxylic acid groups in PVD.*

Tridentate-ULS linker

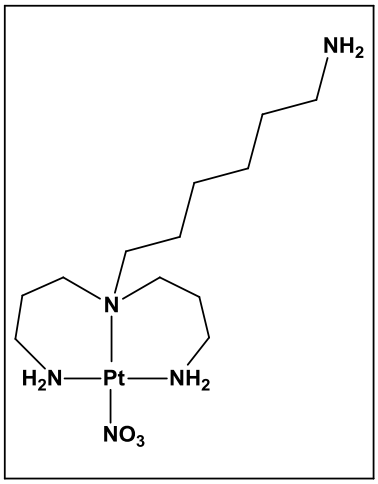

***Figure 4**. Chemical structure of the novel platinum (II)-based linker tridentate-ULS.*

Kinase inhibitor: selective versus multitargeted kinase inhibitors

Currently, the "golden" target for the treatment of tubulointerstitial fibrosis is not known. Due to the complexity of the disease and the involvement of multiple signaling cascades there are many potential targets (13-15). We focused on the inhibition of a selection of kinases that are part of the signaling cascades downstream of profibrotic growth factor receptors. In **chapter 3** we synthesized the kinase inhibitor-lysozyme conjugates LY364947-ULS-lysozyme and erlotinib-ULS-lysozyme. Although kinase inhibitors are never absolutely selective (16), the kinase inhibitors LY364947 and erlotinib relatively specific inhibit transforming growth factor-β (TGF-β) receptor kinase and epidermal growth factor (EGF) receptor kinase, respectively. TGF-β receptor kinase belongs to the most prominent kinases involved in the pathogenesis of tubulointerstitial fibrosis and activation of this kinase stimulates the inflammatory response as well as EMT and ECM production (17, 18). Activation of EGF receptor kinase contributes to EMT (19). Growth

factor receptor kinases are expressed on the proximal tubular cell membrane and, therefore, can be inhibited extracellularly as well as intracellularly. However, since the applied carrier systems in this thesis deliver their therapeutic cargo inside the cells, intracellular inhibition of membrane receptor kinases is most straightforward. The serine/ threonine kinase inhibitor LY364947 and the tyrosine kinase inhibitor erlotinib both exert their inhibitory effects at the intracellular catalytic domain of the target kinase. *In vitro* stimulation of HK-2 cells with TGF-β resulted in an enhanced activity of transcription factor Smad2, which is a direct target of TGF-β receptor kinase, and an enhanced expression of the profibrotic factors connective tissue growth factor (CTGF), procollagen 1α1 and plasminogen activator inhibitor (PAI)-1. Treatment with LY364947-ULS-lysozyme reduced the TGF-β stimulated activation of Smad2 as well as the enhanced expression of CTGF, procollagen 1α1 and PAI-1. LY364947-ULS-lysozyme furthermore reduced the expression of the profibrotic factor fibronectin, although TGF-β did not induce fibronectin expression. In a similar way, treatment with erlotinib-ULS-lysozyme reduced the EGF-stimulated activation of EGF receptor kinase.

The number of known kinases associated with the development of tubulointerstitial fibrosis is increasing. Instead of a single kinase, the profibrotic events leading to tubulointerstitial fibrosis are often triggered by a complex intracellular network of signaling cascades. This complicates the treatment of tubulointerstitial fibrosis, since alternative routes may take over when only one of the involved signaling kinases is inhibited with a single targeted drug. We therefore also designed kinase inhibitor-carrier conjugates directed to more than one target. In **chapter 4** the kinase inhibitor imatinib was coupled to lysozyme. Imatinib inhibits the platelet-derived growth factor (PDGF) receptor kinases as well as Abelson tyrosine kinase (c-Abl), which is a downstream target of the TGF-β receptor kinase. Activation of PDGF receptor kinases in tubulointerstitial fibrosis induces the proliferation, migration and survival of myofibroblasts. The multitargeted tyrosine kinase inhibitor sunitinib is less specific than imatinib and inhibits more than 50 kinases (16). Except for the PDGF receptor kinases, the role of the other targets of sunitinib in the pathogenesis of tubulointerstitial fibrosis is not clear. Nevertheless, we demonstrated in **chapter 5** that sunitinib attenuates tubulointerstitial fibrosis. Although simultaneous inhibition of multiple targets may be preferable for the treatment of tubulointerstitial fibrosis, the risk of unwanted side effects also increases when using a broad-spectrum kinase inhibitor. The toxicity observed in our efficacy studies with sunitinib, indeed, underscored the need for a cell-specific delivery approach of this drug. In **chapter 6** we showed that the novel kinase inhibitor 17864, like sunitinib, inhibits the activity of multiple tyrosine kinases. As expected, the PDGF receptor-β kinase belonged to the most inhibited kinases.

In earlier studies Prakash *et al.* successfully delivered the kinase inhibitors SB202190 (directed to p38 MAPK) and Y27632 (directed to Rho-associated kinase (ROCK)) into the proximal tubular cells by conjugation to lysozyme (20, 21). Like c-Abl, p38 MAPK and ROCK are downstream kinases of the TGF-β receptor kinase. In tubulointerstitial fibrosis p38 MAPK is strongly activated in the proximal tubular cells and induces inflammation, EMT and ECM production, while ROCK plays a crucial role in TGF-β induced EMT (22-24).

A different strategy to interfere in the profibrotic responses in proximal tubular cells is to activate antifibrotic signaling cascades. **Figure 5** shows the chemical structure of the Epac-selective cAMP analogue *para*-chlorophenylthio-2'-O-methyladenosine-3',5'-cyclic monophosphate (8-pCPT-2'-O-Me-cAMP) (25). Via activation of Rap, Epac stimulates the integrin- and cadherin-mediated adhesion of proximal tubular cells (26), thereby suppressing EMT, dedifferentiation and proliferation of proximal tubular cells. Recent studies have furthermore demonstrated that Epac decreases ECM production in fibrotic diseases, by inhibition of TGF-β induced collagen synthesis (27). The Epac agonist 8-pCPT-2'-O-Me-cAMP has been conjugated to lysozyme via the ULS linker and is currently under investigation for its potency to inhibit ischemia-induced renal fibrosis (unpublished results).

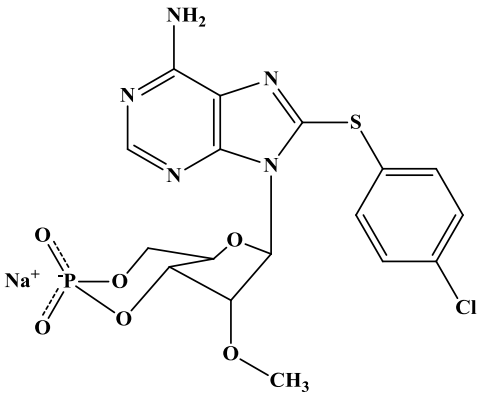

Figure 5. Chemical structure of the Epac-selective cAMP analogue 8-pCPT-2'-O-Me-cAMP (also called 007).

Future perspectives

Because of the involvement of different kinases in the progression of tubulointerstitial fibrosis we believe that the development of antifibrotic drugs needs to be focused on the simultaneously inhibition of multiple kinases. In the current thesis kinase inhibitor-carrier conjugates have been synthesized that inhibit more than one kinase, but coadministration of different kinase inhibitor-carrier conjugates would be another strategy. Treatment of tubulointerstitial fibrosis with a combination of kinase inhibitors without the use of a cell-specific delivery approach is no option due to the high risk of unwanted side effects (28, 29). It is clear that TGF-β receptor kinase mediated signaling cascades play an essential role in the development of tubulointerstitial fibrosis (13, 30). Co-administration of LY364947-ULS-lysozyme and one of the other kinase inhibitor-carrier conjugates that have been developed, for example 17864-ULS-lysozyme may therefore be a good approach to obtain a strong antifibrotic effect. If administration of a combination of kinase inhibitor-carrier conjugates yields promising effects, the treatment can be further optimized by developing conjugates in which different kinase inhibitors are conjugated to a single carrier. The NH_2-PAMAM dendritic carriers are suitable for this purpose due to the multiple functional groups on their surface.

Evaluation of the proximal tubular cell-specific delivery of kinase inhibitors directed against other target kinases is also important to gain more insight in the ideal therapeutic agent for the treatment of tubulointerstitial fibrosis. An example of a kinase inhibitor that is worthy to be investigated is the c-Jun NH_2-terminal kinase (JNK) inhibitor SP600125. The JNK inhibitor SP600125 successfully inhibited the JNK-mediated profibrotic actions of the proximal tubular cells both in vitro and in vivo (31, 32). We have conjugated SP600125 to lysozyme using the same ULS-based approach as discussed in this thesis. Further evaluation of this conjugate was not pursued since release studies showed that SP600125 was not released from ULS. In view of the later obtained results with 17864 that proved to be active in the ULS-bound form, one could rethink this decision and study the potential activity of the SP600125-ULS adduct.

In vivo models for the antifibrotic efficacy of kinase inhibitor-carrier conjugates

The efficacy of imatinib-ULS-lysozyme and 17864-ULS-lysozyme **(chapter 4 and 5)** was evaluated in the mouse ureteral obstruction (UUO) model, which is a chronic kidney disease model for tubulointerstitial fibrosis. This animal model was chosen because of the rapid occurrence of tubulointerstitial fibrosis (*i.e.* over a time course of days to weeks) and the relatively straightforward surgical procedure (33-35). The pharmacokinetic studies with imatinib-ULS-lysozyme and 17864-ULS-lysozyme demonstrated that the kidneys were exposed to active kinase inhibitor levels for at least three days. On the other hand, we did not expect that the intrarenal drug levels would persist for up to a week. Therefore we decided to evaluate their efficacy in mice subjected to three days ureteral obstruction. Three days UUO resulted in early fibrosis, characterized by an increased expression and deposition of profibrotic factors involved in inflammation, EMT and ECM production. Unfortunately, we were not able to demonstrate antifibrotic effects of both conjugates when given in a single intravenous injection before ligation of the ureter. Several explanations may exist for our results, as discussed in the **chapters 4 and 5**. Although mice received higher doses imatinib-ULS-lysozyme and 17864-ULS-lysozyme for the efficacy studies, to increase the renal exposure to active kinase inhibitor levels, the active kinase inhibitor levels in the proximal tubular cells could still have been too low to obtain a therapeutic effect. Although one might want to increase the dose frequency of the conjugates, this is not possible in the UUO model, because complete ligation of the ureter of the diseased kidney limits the possibility for proximal tubular cell-directed conjugates to reach their target cells. For the same reason, we cannot evaluate the antifibrotic effects of imatinib-ULS-lysozyme and 17864-ULS-lysozyme at later stages after ureteral obstruction, unless we adjust the animal model.

A different animal model that has been used for the evaluation of kinase inhibitor-carrier conjugates is the unilateral renal ischemia-reperfusion (I/R) model, which is an acute kidney injury model that has successfully been used by Prakash *et al*. for the investigation of the renal effects of SB202190-ULS-lysozyme and Y27632-ULS-lysozyme in rats. In this animal model the artery and vein of one of both kidneys are clamped to temporary arrest the renal blood flow and induce ischemic injury. After 45 minutes the clamps are removed again to reperfuse the kidneys (36). Although the renal I/R model is mainly used to study acute or chronic inflammation, the initial damage in the kidneys evolves into a mild model of renal fibrosis (*i.e.* over a time course of days). Four days after I/R injury a clear inflammatory and fibrotic response was observed as well as an enhanced activity of p38 MAPK and myosin light chain-2 (MLC-2, a downstream target of ROCK). Treatment with a single intravenous injection of SB202190-ULS-lysozyme, prior to I/R injury, inhibited p38 MAPK activity and reduced EMT. Daily treatment with Y27632-ULS-lysozyme strongly inhibited tubular injury, inflammation, EMT and ECM production. These favourable effects were related to the inhibition of the ROCK pathway, as demonstrated by the reduced activation of MLC-2.

Future perspectives

For future studies, when choosing an animal model to study the antifibrotic effects of the conjugates certain characteristics need to be taken into consideration. First, the animal model needs to allow repeated administration of the conjugate. This implies that the glomerular filtration as well as the capability of the proximal tubular cells to internalize the kinase inhibitor-carrier conjugates need to be preserved. Second, from a practical point of view, tubulointerstitial fibrosis should develop within weeks rather than in months or years. Third, activation of signaling pathways should be one of the key-processes in the disease model, and ideally well described in literature.

Although the UUO model used to study the efficacy of kinase inhibitor-carrier conjugates in this thesis is characterized by kinase-mediated tubulointerstitial fibrosis (37, 38), it did not allow repeated administration of the conjugate. To improve this in future studies, adjustments need to be made. Possible refinements of the UUO model are to apply partial instead of complete ureteral obstruction or by investigation of the efficacy in a UUO model in which the obstruction is reversed after inducing fibrosis. Reversing the ligation of the ureter is very complex, because adhesions can be formed around the ligature and the inner walls of the ureter can stay attached to each other thereby preventing recovery of the urinary flow. The recovery of the urinary flow can be improved by clamping the ureter and subsequently replace the clip every two days to prevent merging of the inner walls of the ureter (35), but this is still very complex and a relatively high burden for the animals. An alternative strategy to reverse the ureteral obstruction is to replace the obstructed ureter by the ureter of the contralateral (healthy) kidney (39).

The I/R model for tubulointerstitial fibrosis is a good alternative and fulfills all desired characteristics to study the efficacy of kinase inhibitor-conjugates. Besides, this animal model is a good representative of tubulointerstitial fibrosis in human, because ischemia is one of the major causes of acute kidney injury (40). Alternatively, drug-induced nephrotoxicity models may be used (34, 41, 42). An example of a drug-induced animal model characterized by kinase-mediated tubulointerstitial fibrosis is the cyclosporine A (CsA)-induced nephropathy model (34, 43). Tubulointerstitial fibrosis occurs over a time course of weeks and, like the I/R model, this animal model is a good representative of tubulointerstitial fibrosis in human (34). However, not all animal models are well characterized and future studies are needed to investigate the clinical relevance as well as the proteomics of these animal models in order to know whether the profibrotic processes are kinase-mediated.

Tubulointerstitial fibrosis is one of the hallmarks of diabetic nephropathy and the efficacy of kinase inhibitor-carrier conjugates can therefore also be studied in animal models of diabetic nephropathy (44, 45).

Kinase inhibitor-lysozyme conjugates in other renal diseases

Since tubulointerstitial fibrosis also occurs in renal transplant rejection, proximal tubular cell-targeted kinase inhibitor-carrier conjugates may also be valuable in the prevention of the organ rejection (46). ROCK plays an important role in organ rejection and earlier studies demonstrated that inhibition of the Rho/ ROCK pathway attenuated chronic allograft nephropathy (47, 48). Liu *et al.* showed that combination treatment of cyclosporine A and Y27632 in rats with chronic allograft nephropathy resulted in an improved therapeutic effect, by a remarkable reduction of inflammation and fibrosis (48). Because of the prominent role of proximal tubular cells in renal transplant rejection, local inhibition of the Rho/ ROCK pathway with Y27632 may be advantageous. Therefore, the effects of Y27632-ULS-lysozyme were studied in a rat model of acute allograft rejection (Poosti *et al.*, manuscript in preparation). Rats were treated with a daily intravenous injection of the conjugate from one day before transplantation and sacrificed at day 1

and day 4 after transplantation. At 4 days after transplantation Y27632-ULS-lysozyme remarkably reduced macrophage influx in the tubulointerstitium and glomerulus and reduced gene expression levels of vimentin and procollagen 1α1, which are markers for EMT and ECM production, respectively, were observed. Comparing the Y27632 dose used in our study with the dose administered in the study performed by Liu *et al*., we treated the transplanted animals with a more than 100 times lower dose. The favourable effects observed with this low dose underscore that delivery of Y27632 in the proximal tubular cells of the kidneys may be a very attractive and promising approach to prevent renal transplant rejection. Follow-up studies in animals with chronic allograft nephropathy should be performed to confirm that specific inhibition of the Rho/ ROCK pathway in proximal tubular cells with Y27632-ULS-lysozyme is more efficient than treatment with a high dose non-targeted Y27632.

Taken together, intracellular delivery of kinase inhibitors into the proximal tubular cells of the kidneys might be a promising strategy to reverse the progression of tubulointerstitial fibrosis. This thesis presents different strategies to improve the exposure of the proximal tubular cells to active kinase inhibitor levels, which can be applied in future studies.

References

1. P. Stenvinkel. Chronic kidney disease: a public health priority and harbinger of premature cardiovascular disease. J Intern Med. 268:456-467 (2010).
2. J. Prakash, A.M. van Loenen-Weemaes, M. Haas, J.H. Proost, D.K. Meijer, F. Moolenaar, K. Poelstra and R.J. Kok. Renal-selective delivery and angiotensin-converting enzyme inhibition by subcutaneously administered captopril-lysozyme. Drug Metab Dispos. 33:683-688 (2005).
3. R. Jevprasesphant, J. Penny, R. Jalal, D. Attwood, N.B. McKeown and A. D'Emanuele. The influence of surface modification on the cytotoxicity of PAMAM dendrimers. Int J Pharm. 252:263-266 (2003).
4. P. Singh, U. Gupta, A. Asthana and N.K. Jain. Folate and folate-PEG-PAMAM dendrimers: synthesis, characterization, and targeted anticancer drug delivery potential in tumor bearing mice. Bioconjug Chem. 19:2239-2252 (2008).
5. E.J. Franssen, J. Koiter, C.A. Kuipers, A.P. Bruins, F. Moolenaar, D. de Zeeuw, W.H. Kruizinga, R.M. Kellogg and D.K. Meijer. Low molecular weight proteins as carriers for renal drug targeting. Preparation of drug-protein conjugates and drug-spacer derivatives and their catabolism in renal cortex homogenates and lysosomal lysates. J Med Chem. 35:1246-1259 (1992).
6. V. Pinzani, F. Bressolle, I.J. Haug, M. Galtier, J.P. Blayac and P. Balmes. Cisplatin-induced renal toxicity and toxicity-modulating strategies: a review. Cancer Chemother Pharmacol. 35:1-9 (1994).
7. J.T. Hartmann and H.P. Lipp. Toxicity of platinum compounds. Expert Opin Pharmacother. 4:889-901 (2003).
8. T. Torigoe, H. Izumi, H. Ishiguchi, Y. Yoshida, M. Tanabe, T. Yoshida, T. Igarashi, I. Niina, T. Wakasugi, T. Imaizumi, Y. Momii, M. Kuwano and K. Kohno. Cisplatin resistance and transcription factors. Curr Med Chem Anticancer Agents. 5:15-27 (2005).
9. D. Wang and S.J. Lippard. Cellular processing of platinum anticancer drugs. Nat Rev Drug Discov. 4:307-320 (2005).
10. C.H. Tang, C. Parham, E. Shocron, G. McMahon and N. Patel. Picoplatin overcomes resistance to cell toxicity in small-cell lung cancer cells previously treated with cisplatin and carboplatin. Cancer Chemother Pharmacol (2010).
11. H. Kamada, Y. Tsutsumi, K. Sato-Kamada, Y. Yamamoto, Y. Yoshioka, T. Okamoto, S. Nakagawa, S. Nagata and T. Mayumi. Synthesis of a poly(vinylpyrrolidone-co-dimethyl maleic anhydride) co-polymer and its application for renal drug targeting. Nat Biotechnol. 21:399-404 (2003).
12. Y. Yamamoto, Y. Tsutsumi, Y. Yoshioka, H. Kamada, K. Sato-Kamada, T. Okamoto, Y. Mukai, H. Shibata, S. Nakagawa and T. Mayumi. Poly(vinylpyrrolidone-co-dimethyl maleic acid) as a novel renal targeting carrier. J Control Release. 95:229-237 (2004).
13. P. Boor, K. Sebekova, T. Ostendorf and J. Floege. Treatment targets in renal fibrosis. Nephrol Dial Transplant. 22:3391-3407 (2007).
14. J. Prakash, K. Poelstra, H. van Goor, F. Moolenaar, D.K.F. Meijer and R.J. Kok. Novel therapeutic targets for the treatment of tubulointerstitial fibrosis. Curr Signal Transduct Ther. 3:97-111 (2008).
15. M. Iwano and E.G. Neilson. Mechanisms of tubulointerstitial fibrosis. Curr Opin Nephrol Hypertens. 13:279-284 (2004).
16. K. Ghoreschi, A. Laurence and J.J. O'Shea. Selectivity and therapeutic inhibition of kinases: to be or not to be? Nat Immunol. 10:356-360 (2009).
17. E.P. Bottinger and M. Bitzer. TGF-beta signaling in renal disease. J Am Soc Nephrol. 13:2600-2610 (2002).
18. P. Boor, T. Ostendorf and J. Floege. Renal fibrosis: novel insights into mechanisms and therapeutic targets. Nat Rev Nephrol. 6:643-656 (2010).
19. Y. Liu. Epithelial to mesenchymal transition in renal fibrogenesis: pathologic significance, molecular mechanism, and therapeutic intervention. J Am Soc Nephrol. 15:1-12 (2004).
20. J. Prakash, M.H. de Borst, M. Lacombe, F. Opdam, P.A. Klok, H. van Goor, D.K. Meijer, F. Moolenaar, K. Poelstra and R.J. Kok. Inhibition of renal rho kinase attenuates ischemia/ reperfusion-induced injury. J Am Soc Nephrol. 19:2086-2097 (2008).
21. J. Prakash, M. Sandovici, V. Saluja, M. Lacombe, R.Q. Schaapveld, M.H. de Borst, H. van Goor, R.H. Henning, J.H. Proost, F. Moolenaar, G. Keri, D.K. Meijer, K. Poelstra and R.J. Kok. Intracellular delivery of the p38 mitogen-activated protein kinase inhibitor SB202190 [4-(4-fluorophenyl)-2-(4-hydroxyphenyl)-5-(4-pyridyl)1H-imidazole] in renal tubular cells: a novel strategy to treat renal fibrosis. J Pharmacol Exp Ther. 319:8-19 (2006).

22. F.Y. Ma, J. Liu and D.J. Nikolic-Paterson. The role of stress-activated protein kinase signaling in renal pathophysiology. Braz J Med Biol Res. 42:29-37 (2009).
23. J. Zavadil and E.P. Bottinger. TGF-beta and epithelial-to-mesenchymal transitions. Oncogene. 24:5764-5774 (2005).
24. W.C. Burns, P. Kantharidis and M.C. Thomas. The role of tubular epithelial-mesenchymal transition in progressive kidney disease. Cells Tissues Organs. 185:222-231 (2007).
25. J.L. Bos. Epac proteins: multi-purpose cAMP targets. Trends Biochem Sci. 31:680-686 (2006).
26. K.S. Lyle, J.H. Raaijmakers, W. Bruinsma, J.L. Bos and J. de Rooij. cAMP-induced Epac-Rap activation inhibits epithelial cell migration by modulating focal adhesion and leading edge dynamics. Cell Signal. 20:1104-1116 (2008).
27. U. Yokoyama, H.H. Patel, N.C. Lai, N. Aroonsakool, D.M. Roth and P.A. Insel. The cyclic AMP effector Epac integrates pro- and anti-fibrotic signals. Proc Natl Acad Sci U S A. 105:6386-6391 (2008).
28. J.T. Hartmann, M. Haap, H.G. Kopp and H.P. Lipp. Tyrosine kinase inhibitors - a review on pharmacology, metabolism and side effects. Curr Drug Metab. 10:470-481 (2009).
29. G.S. Orphanos, G.N. Ioannidis and A.G. Ardavanis. Cardiotoxicity induced by tyrosine kinase inhibitors. Acta Oncol. 48:964-970 (2009).
30. J. Rosenbloom, S.V. Castro and S.A. Jimenez. Narrative review: fibrotic diseases: cellular and molecular mechanisms and novel therapies. Ann Intern Med. 152:159-166 (2010).
31. L. Yang, T.Y. Besschetnova, C.R. Brooks, J.V. Shah and J.V. Bonventre. Epithelial cell cycle arrest in G2/ M mediates kidney fibrosis after injury. Nat Med. 16:535-543, 531p following 143 (2010).
32. M.H. de Borst, J. Prakash, M. Sandovici, P.A. Klok, I. Hamming, R.J. Kok, G. Navis and H. van Goor. c-Jun NH2-terminal kinase is crucially involved in renal tubulo-interstitial inflammation. J Pharmacol Exp Ther. 331:896-905 (2009).
33. R.L. Chevalier, M.S. Forbes and B.A. Thornhill. Ureteral obstruction as a model of renal interstitial fibrosis and obstructive nephropathy. Kidney Int. 75:1145-1152 (2009).
34. H.C. Yang, Y. Zuo and A.B. Fogo. Models of chronic kidney disease. Drug Discov Today Dis Models. 7:13-19 (2010).
35. T.S. Puri, M.I. Shakaib, A. Chang, L. Mathew, O. Olayinka, A.W. Minto, M. Sarav, B.K. Hack and R.J. Quigg. Chronic kidney disease induced in mice by reversible unilateral ureteral obstruction is dependent on genetic background. Am J Physiol Renal Physiol. 298:F1024-1032 (2010).
36. I. Stroo, G. Stokman, G.J. Teske, A. Raven, L.M. Butter, S. Florquin and J.C. Leemans. Chemokine expression in renal ischemia/ reperfusion injury is most profound during the reparative phase. Int Immunol. 22:433-442 (2010).
37. A.B. Rodriguez-Pena, M.T. Grande, N. Eleno, M. Arevalo, C. Guerrero, E. Santos and J.M. Lopez-Novoa. Activation of Erk1/ 2 and Akt following unilateral ureteral obstruction. Kidney Int. 74:196-209 (2008).
38. S. Satoh, T. Yamaguchi, A. Hitomi, N. Sato, K. Shiraiwa, I. Ikegaki, T. Asano and H. Shimokawa. Fasudil attenuates interstitial fibrosis in rat kidneys with unilateral ureteral obstruction. Eur J Pharmacol. 455:169-174 (2002).
39. T.T. Tapmeier, K.L. Brown, Z. Tang, S.H. Sacks, N.S. Sheerin and W. Wong. Reimplantation of the ureter after unilateral ureteral obstruction provides a model that allows functional evaluation. Kidney Int. 73:885-889 (2008).
40. M.E. Sabbahy and V.S. Vaidya. Ischemic kidney injury and mechanisms of tissue repair. Wiley Interdiscip Rev Syst Biol Med (2011).
41. I. Bernascone, S. Janas, M. Ikehata, M. Trudu, A. Corbelli, C. Schaeffer, M.P. Rastaldi, O. Devuyst and L. Rampoldi. A transgenic mouse model for uromodulin-associated kidney diseases shows specific tubulo-interstitial damage, urinary concentrating defect and renal failure. Hum Mol Genet. 19:2998-3010 (2010).
42. S.N. Heyman, M. Khamaisi, S. Rosen and C. Rosenberger. In vivo models of acute kidney injury. Drug Discovery Today: Disease Models. 7:51-56 (2010).
43. C. Slattery, E. Campbell, T. McMorrow and M.P. Ryan. Cyclosporine A-induced renal fibrosis: a role for epithelial-mesenchymal transition. Am J Pathol. 167:395-407 (2005).
44. C.J. Magri and S. Fava. The role of tubular injury in diabetic nephropathy. Eur J Intern Med. 20:551-555 (2009).

45. M. Morcos, A.A. Sayed, A. Bierhaus, B. Yard, R. Waldherr, W. Merz, I. Kloeting, E. Schleicher, S. Mentz, R.F. Abd el Baki, H. Tritschler, M. Kasper, V. Schwenger, A. Hamann, K.A. Dugi, A.M. Schmidt, D. Stern, R. Ziegler, H.U. Haering, M. Andrassy, F. van der Woude and P.P. Nawroth. Activation of tubular epithelial cells in diabetic nephropathy. Diabetes. 51:3532-3544 (2002).
46. N.O. Camara, W.W. Williams, Jr. and A. Pacheco-Silva. Proximal tubular dysfunction as an indicator of chronic graft dysfunction. Braz J Med Biol Res. 42:229-236 (2009).
47. J. Song, Y.P. Lu, G.H. Luo, L. Yang, X. Ma, Q.J. Xia, Y.J. Shi and Y.P. Li. Effects of mycophenolate mofetil on chronic allograft nephropathy by affecting RHO/ ROCK signal pathways. Transplant Proc. 40:2790-2794 (2008).
48. M. Liu, M. Gu, Y. Wu, P. Zhu, W. Zhang, C. Yin and W.J. Zhang. Therapeutic effect of Y-27632 on chronic allograft nephropathy in rats. J Surg Res. 157:e117-127 (2009).

Appendices

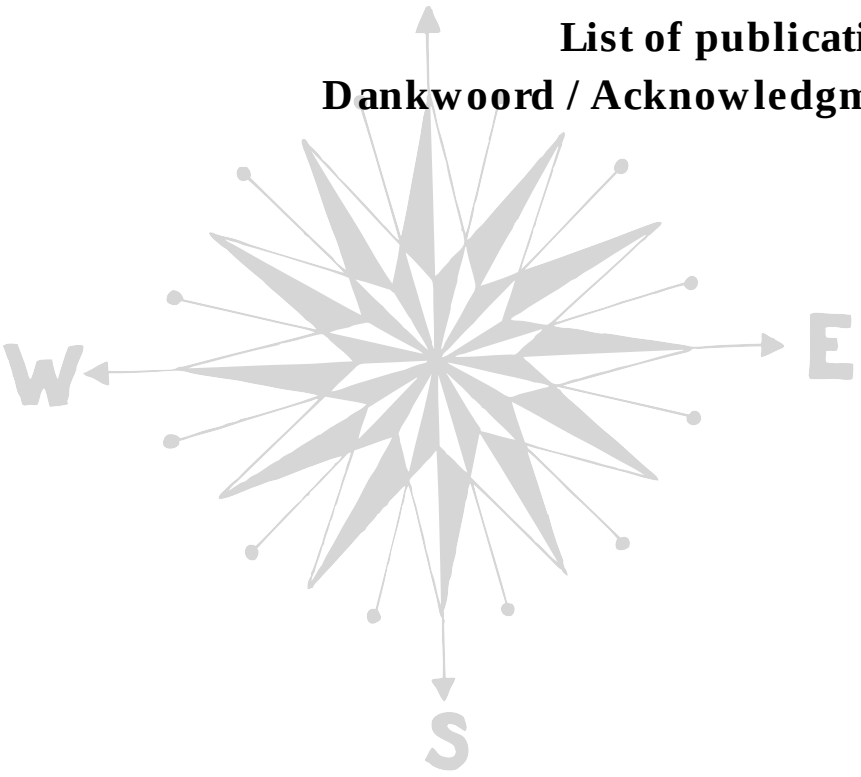

Samenvatting in het Nederlands

Wereldwijd komen chronische nierziekten steeds vaker voor. Dit komt onder andere door een toename in het aantal patiënten met andere serieuze gezondheidsproblemen zoals diabetes, hypertensie en/ of overgewicht. Deze patiënten hebben een verhoogd risico op de ontwikkeling van chronische nierziekten. In veel gevallen worden chronische nierziekten pas ontdekt in een stadium waarin de nierfunctie zo slecht is, dat nierdialyse of niertransplantatie de enige redmiddelen zijn om te overleven. Op dit moment bestaan nog geen geneesmiddelen die chronische nierziekten kunnen stoppen of ongedaan maken. De nieuwe nierspecifieke geneesmiddelen die in dit proefschrift besproken worden moeten dit wel mogelijk maken en zouden in de toekomst een bijdrage kunnen leveren aan de behandeling van chronische nierziekten.

Nierfibrose, en dan met name tubulointerstitiële fibrose, speelt een belangrijke rol in chronische nierziekten. In tubulointerstitiële fibrose vindt activatie plaats van de proximale tubulus cellen door groeifactoren. Dit leidt tot een verhoogde productie van andere profibrotische factoren die de vorming van niet-functioneel littekenweefsel induceren. Omdat dit ten koste gaat van gezond functioneel nierweefsel, gaat de nierfunctie geleidelijk aan achteruit. In de activatie van proximale tubulus cellen is een sleutelrol weggelegd voor kinases, eiwitten die een belangrijke rol spelen in intracellulaire signaleringsroutes. Geactiveerde kinases veranderen de activiteit van downstream eiwitten door een fosfaatgroep op het doeleiwit te plaatsen (= fosforylering). Vanwege de prominente rol van groeifactor geactiveerde signaleringsroutes in chronische nierziekten, ligt de focus in dit proefschrift op het nierspecifiek afleveren van stoffen die deze signaleringsroutes kunnen remmen, zogeheten kinase remmers.

In **hoofdstuk 1** wordt het nierspecifiek afleveren van geneesmiddelen naar de glomerulus en proximale tubulus cellen behandeld. Veel geneesmiddelen voor de behandeling van tubulointerstitiële fibrose hebben vervelende bijwerkingen. Dit geldt ook voor kinase remmers die de vorming van littekenweefsel in de nieren kunnen remmen. Omdat in het lichaam vrije distributie plaats vindt van dit type geneesmiddel moleculen, worden ook de signaleringsroutes in gezonde cellen geremd. Het optreden van bijwerkingen kan worden beperkt door kinase remmers specifiek af te leveren in de proximale tubulus cellen, het celtype waar het therapeutische effect gewenst is (= cel-specifieke drug targeting). Het gericht afleveren van een geneesmiddel in een celtype heeft op twee manieren een gunstige invloed op de balans tussen hoofdwerking en bijwerkingen: allereerst wordt voorkomen dat de kinase remmer wordt opgenomen in gezonde cellen buiten de nieren. Daarnaast kan een verbeterde effectiviteit van het geneesmiddel worden verkregen door het verhogen of verlengen van de lokale geneesmiddelconcentratie in de nier. Drie verschillende kinase remmers (LY364947, een remmer van transforming growth factor-β (TGFR-β) kinase; SB202190, een remmer van p38 mitogen activated protein kinase (p38 MAPK); Y27632, een remmer van Rho-associated kinase (ROCK)) zijn succesvol afgeleverd in de proximale tubulus cellen. Hierbij werd het laagmoleculaire eiwit lysozym gebruikt als niergericht dragermolecuul. Lysozym kan binden aan de megaline receptor op proximale tubulus cellen en wordt vervolgens opgenomen in de tubulus cellen via receptor-gemedieerde endocytose. Op dezelfde wijze kunnen geneesmiddel-lysozym conjugaten worden opgenomen door deze cellen. De antifibrotische effecten van LY364947-ULS-lysozym, SB202190-ULS-lysozym en Y27632-ULS-lysozym zijn aangetoond in celexperimenten en dierstudies.

Hoofdstuk 2 is een overzichtsartikel waarin het afleveren van geneesmiddelen in de proximale tubulus cellen met macromoleculaire geneesmiddel-carrier conjugaten centraal staat. De meest voor de hand liggende strategie hierbij is om een geneesmiddel conjugaat te ontwikkelen dat wordt opgenomen via receptor-gemedieerde endocytose aan de apicale zijde van de cellen, dat wil zeggen de kant van de cellen die blootgesteld wordt aan de pre-urine. Naast een uitgebreide beschrijving van alle dragermoleculen die hiervoor gebruikt kunnen worden, wordt ook uitgebreid aandacht besteed aan de technieken die gebruikt kunnen worden om geneesmiddelen te koppelen aan deze dragermoleculen. De intracellulaire verwerking van geneesmiddel conjugaten na opname in de proximale tubulus cellen is eveneens belangrijk en wordt ook behandeld in dit hoofdstuk. Hoewel geneesmiddel conjugaten stabiel moeten zijn in de circulatie, is het in de meeste gevallen noodzakelijk dat het geneesmiddel na intracellulaire opname van het conjugaat in zijn oorspronkelijke vorm wordt vrijgegeven. Daarom moet de binding tussen het geneesmiddel en het dragermolecuul biologisch afbreekbaar zijn.

In **hoofdstuk 3** wordt de koppeling van de kinase remmers LY364947 en erlotinib (gericht tegen epidermal growth factor receptor (EGFR) kinase) aan lysozym beschreven. LY364947 en erlotinib zijn gekoppeld aan lysozym via het Universal Linkage System (ULS). De ULS linker bevat een platina atoom dat coördinatieve bindingen vormt met de kinase remmers en met lysozym. Deze coördinatieve bindingen zijn stabiel, maar kunnen in de proximale tubulus cellen worden verbroken waardoor de kinase remmers vrij komen en hun therapeutisch effect kunnen uitoefenen. *In vitro* opname studies in humane proximale tubulus cellen (HK-2 cellen) bevestigden de opname van kinase remmer-lysozym conjugaten via receptor-gemedieerde endocytose. LY364947-ULS-lysozym remde de transforming growth factor-β (TGF-β) gestimuleerde fosforylering van Smad2 (een doeleiwit van TGFR-β kinase) in HK-2 cellen en de TGF-β gestimuleerde genexpressie van profibrotische factoren betrokken bij de vorming van littekenweefsel. Op gelijke wijze remde erlotinib-ULS-lysozym de epidermal growth factor (EGF) gestimuleerde fosforylering van EGFR kinase. Deze *in vitro* resultaten laten zien dat kinase remmer conjugaten in staat zijn om groeifactor gerelateerde processen te remmen in tubulointerstitiële fibrose.

In tubulointerstitiële fibrose worden veel verschillende kinase-gemedieerde signaleringsroutes geactiveerd. Gelijktijdige remming van meerdere signaleringsroutes kan daarom voordeliger zijn dan het remmen van slechts één signaleringsroute. Daarom is in **hoofdstuk 4** de kinase remmer imatinib gekoppeld aan lysozym. Imatinib remt onder anderen de platelet-derived growth factor receptor (PDGFR) kinases en Abelson tyrosine kinase (c-Abl), een downstream target van TGFR-β kinase. Zowel de PDGFR- als de TGFR-β kinase-gemedieerde signaleringsroutes zijn geactiveerd in tubulointerstitiële fibrose. De *in vivo* farmacokinetiek van imatinib-ULS-lysozym werd onderzocht in muizen. Imatinib-ULS-lysozym werd onafhankelijk van de toedieningsroute snel opgenomen (d.w.z. binnen 10 minuten) in the proximale tubulus cellen van de nieren. Het afgeleverde imatinib was drie dagen na toediening nog steeds detecteerbaar in de nieren.
Voor de effectiviteit van het conjugaat is het noodzakelijk dat imatinib intracellulair vrij komt van de linker. Vrij imatinib in de nieren was al detecteerbaar binnen 10 minuten na intraveneuze en intraperitoneale toediening van imatinib-ULS-lysozym. In vergelijking met de toediening van een gelijke dosering vrij imatinib resulteerde een enkelvoudige intraveneuze en intraperitoneale

injectie van het conjugaat in een, respectievelijk, 30- en 15-voudige verhoogde blootstelling van de nieren aan actief imatinib.
Om de potentie van imatinib-ULS-lysozym in de behandeling van tubulointerstitiële fibrose te onderzoeken, is de *in vivo* effectiviteit van het conjugaat onderzocht in muizen. Hiervoor werd het unilaterale ureterobstructie (UUO) model gebruikt, een diermodel waarbij een van de urineleiders wordt afgebonden. Hoewel na drie dagen ureterobstructie een licht verhoogde activiteit van PDGFR-β kinase en een verhoogde depositie en expressie van profibrotische factoren werd waargenomen, waren imatinib mesylaat (het vrije, niet naar de nier gerichte geneesmiddel) en imatinib-ULS-lysozym niet therapeutisch actief. Vervolgstudies in een ander diermodel waarin een grotere rol is weggelegd voor PDGFR- en c-Abl kinases zijn daarom nodig voor het onderzoek naar de potentie van imatinib-ULS-lysozym in de behandeling van tubulointerstitiële fibrose.

Sunitinib is een multitargeted kinase remmer die gelijktijdig op zeer veel verschillende signaleringsroutes aangrijpt. **Hoofdstuk 5** beschrijft de ontwikkeling van een nieuw sunitinib derivaat, 17864, dat op gelijke wijze aan lysozym geconjugeerd kan worden als de eerder genoemde kinase remmers. Het bijzondere aan dit sunitinib derivaat is dat het ook farmacologisch actief kan zijn terwijl het ULS nog aan de remmer gebonden is. Voorgaande studies met kinase remmer-ULS-lysozym conjugaten hadden laten zien dat de in de proximale tubulus cellen afgeleverde kinase remmers voornamelijk intracellulair aanwezig waren in de ULS-gebonden vorm. Omdat bij dit nieuwe type derivaat de activiteit behouden kan blijven na binding aan de ULS linker, verwachten we ook een hogere effectiviteit van het conjugaat.
In vitro studies laten zien dat de activiteit van 17864 inderdaad behouden blijft na koppeling aan lysozym en dat ULS-gebonden 17864 zelfs meer actief is dan vrij 17864. Hier wordt uitgebreider op ingegaan in hoofdstuk 6 van dit proefschrift. De *in vivo* farmacokinetiek van 17864-ULS-lysozym is onderzocht na intraveneuze toediening van een enkelvoudige injectie in gezonde muizen. In vergelijking met de toediening van een gelijke dosering sunitinib was het initiële verdelingsvolume van 17864-ULS-lysozym meer dan 15 keer kleiner, meest waarschijnlijk doordat het conjugaat (in tegenstelling tot sunitinib) niet vrij kan diffunderen in lichaamscellen en de verdeling van het conjugaat beperkt blijft tot de circulatie en extracellulaire vloeistoffen. 17864-ULS-lysozym werd net als imatinib-ULS-lysozym snel geëlimineerd uit de bloedbaan en opgenomen in de nieren. Belangrijk was de waarneming dat meer dan 95% van de 17864 gedetecteerd in de nieren aanwezig was in de meer actief ULS-gebonden vorm. In vergelijking met sunitinib resulteerde intraveneus toegediend 17864-ULS-lysozym in een 28 keer hogere renale blootstelling aan actieve kinase remmer.
De antifibrotische activiteit van 17864-ULS-lysozym werd onderzocht in het UUO model, hetzelfde diermodel als gebruikt is voor imatinib-ULS-lysozym. Dagelijkse behandeling met een therapeutische dosering sunitinib resulteerde in een verminderde activiteit van PDGFR-β kinase en een significante remming van de renale mRNA expressie van de profibrotische factoren collageen 1A2 en fibronectine, maar een aantal muizen uit deze behandelingsgroep moesten uit het experiment gehaald worden vanwege geneesmiddel gerelateerde systemische toxiciteit. De waargenomen toxiciteit van sunitinib laat zien hoe belangrijk het is om dit geneesmiddel selectief af te leveren in de proximale tubulus cellen. Tijdens de looptijd van dit promotie onderzoek kon alleen getest worden of 17864-ULS-lysozym effectief was na een enkelvoudige toediening, maar

dit leidde niet tot een antifibrotisch effect. Voor nader onderzoek naar de effectiviteit van 17864-ULS-lysozym is een aanpassing van het diermodel nodig die het mogelijk maakt om ook herhaalde doseringen te geven.

In **hoofdstuk 6** ligt de focus op de *in vitro* evaluatie van 17864-ULS-lysozym. Allereerst werd met moleculaire modellering studies onderzocht of 17864-ULS en het 17864-ULS-lysozym in de ATP-binding pocket passen van een receptor tyrosine kinase (stem cell factor receptor kinase c-KIT). Deze studies lieten zien dat 17864-ULS in staat moet zijn om dit kinase te remmen, wat ook daadwerkelijk werd aangetoond in celexperimenten. Studies in HK-2 cellysaten lieten een sterke remming van de fosforylering zien met 17864-ULS en 17864-ULS-lysozym. De remming was zelfs sterker dan was waargenomen voor 17864. Een vergelijkbaar effect werd waargenomen in een experiment waarin met een peptide microarray is onderzocht welke tyrosine kinases geremd werden door 17864 en 17864-ULS-lysozym. Tot de tyrosine kinases die het sterkste werden geremd behoorden onder anderen phosphoinositide 3-kinase (PI3K) en PDGFR-β kinase. Koppeling van 17864 aan ULS leidde niet tot een afname in de potentie van de stoffen voor PDGFR-β kinase, terwijl de potentie voor c-KIT zelfs toegenomen was.
Middels opname studies met 17864-ULS-lysozym en HK-2 cellen is aangetoond dat 17864-ULS-lysozym beter accumuleerde in HK-2 cellen dan 17864 en ook langer door de cellen werd vastgehouden. Dit resultaat was terug te zien in de remmende werking van 17864 en 17864-ULS-lysozym op de fosforylering van tyrosine kinases na opname in HK-2 cellen. De remmende activiteit van het conjugaat hield aanzienlijk langer aan. Hieruit werd geconcludeerd dat het nierspecifieke conjugaat een verbeterde werking kan hebben door enerzijds cel-specifieke herkenning van doelwitcellen, maar ook door een verbeterde retentie in de proximale tubulus cellen en door de omzetting in actieve 17864-ULS metabolieten.

Hoofdstuk 7 tenslotte, behandelt de koppeling van 17864-ULS aan poly(amidoamine) dendrimeren met eindstandige amines (NH_2-PAMAM-G3). Uit de literatuur was gebleken dat NH_2-PAMAM dendrimeren efficiënt accumuleren in de proximale tubulus cellen en dat hiermee in principe zelfs een hogere accumulatie bereikt kan worden dan met het dragereiwit lysozym. In dit hoofdstuk is daarom uitgezocht of NH_2-PAMAM-G3 dendrimeren geschikt zijn als nierspecifieke drager voor het afleveren van de kinase remmer 17864.
Allereerst werd aangetoond dat NH_2-PAMAM-G3 dendrimeren kunnen binden aan de megaline receptor, wat impliceert dat dit type dendrimeer kan worden opgenomen in de proximale tubulus cellen.Het intacte 17864-ULS-NH_2-PAMAM-G3 conjugaat remde de *in vitro* fosforylering van tyrosine kinases in HK-2 cellysaat. Blootstelling van HK-2 cellen aan 100 nM en 1 μM 17864-ULS-NH_2-PAMAM-G3 resulteerde niet in cytotoxiciteit.
Behandeling van muizen met een enkelvoudige intraveneuze injectie van 17864-ULS-NH_2-PAMAM-G3 resulteerde in een snelle nieraccumulatie van het conjugaat. De nieraccumulatie op 1 uur na toediening van het conjugaat was ongeveer tweemaal hoger dan de maximale nieraccumulatie van 17864-ULS-lysozym (13 versus 6,3% van de geïnjecteerde dosis). Daarnaast bleven de renale spiegels van de kinase remmer relatief constant tot het einde van het experiment (d.w.z. drie dagen). Deze resultaten zijn veelbelovend voor vervolgstudies gericht op de ontwikkeling van nieuwe nierspecifieke conjugaten voor het afleveren van kinase remmers.

Dit proefschrift beschrijft verschillende strategieën voor het cel-specifiek afleveren van kinase remmers in proximale tubulus cellen. Samenvattend kan gesteld worden dat ik er in geslaagd ben om met deze technieken kinase remmers in de nier af te leveren, maar dat het nog niet gelukt is om de therapeutische effectiviteit van de ontwikkelde conjugaten aan te tonen. Dit is een belangrijk aandachtspunt voor de vervolgstudies van het nu gepresenteerde onderzoek, dat uiteindelijk moet leiden tot nierspecifieke geneesmiddelen die tubulointerstitiële fibrose kunnen remmen.

List of abbreviations

8-pCPT-2'-O-Me-cAMP
= *para*-chlorophenylthio-2'-*O*-methyladenosine-3',5'-cyclic monophosphate
ABCG2 = ATP-binding cassette sub-family G member 2
c-Abl = Abelson tyrosine kinase
ACE = angiotensin-converting enzyme
ACN = acetonitrile
cis-Aco = *cis*-aconitic anhydride
AKI = acute kidney injury
ALK5 = Activin-receptor like kinase
ARF = acute renal failure
AT II = angiotensin II
ATP = adenosine triphosphate
AUC = area under the curve
BCA = bovine carbonic anhydrase
BSA = bovine serum albumin
C_{max} = maximum concentration
CHX-A"-DTPA = *trans*-(*S*,*S*)-cyclohexane-1,2-diamine-*N,N,N',N",N"*-pentaacetic acid
CDDP = *cis*-diamine-dichloroplatinum
CKD = chronic kidney disease
CKD-2 = cyclin-dependent kinase-2
CLSM = confocal laser scanning microscopy
CsA = cyclosporine A
CTGF = connective tissue growth factor
DAB = 3,3-diaminobenzidine
cDNA = complementary deoxyribonucleic acid
DMEM = Dulbecco's Modified Eagle's Medium
DMF = dimethylformamide
DTT = dithiothreitol
ECM = extracellular matrix
EDC = ethylene dichloride
EDTA = ethylenediaminetetraaetic acid
EGF = epidermal growth factor
(p-)EGFR = phosphorylated epidermal growth factor receptor
EGTA = ethyleneglycoltetraacetic acid
EMT = epithelial-to-mesenchymal transition
ERK = extracellular-signal regulated kinase
ESI = electrospray ionization
ESRD = end-stage renal disease
FA = formic acid
FCS = foetal calf serum
FITC = fluorescein isothiocyanate
FR = folate receptor
GAPDH = glyceraldehyde-3-phosphate dehydrogenase
GBM = glomerular basement membrane

GFR = glomerular filtration rate
GSH = glutathione
H_2O_2 = hydrogen peroxide
HK-2 cells = immortalized human kidney proximal tubular cells
HOBt = *N*-hydroxybenzotriazole
HPLC = high-performance liquid chromatography
HRP = horseradish peroxidase
HPMA = N-(2-hydroxypropyl)methacrylamide
ICAM-1 = intercellular adhesion molecule-1
IL-1 = interleukin-1
IPA = isopropanol
I/ R = ischemia-reperfusion
JNK = c-Jun NH_2-terminal kinase
kDa = kilo Dalton
KSCN = potassium thiocyanate
LC-MS = liguid chromatography-mass spectrometry
LMWC = low molecular weight chitosan
LMWP = low molecular weight protein
LZM = lysozyme
M-PER = Mammalian Protein Extraction Reagent
MALDI-TOF = matrix-assisted laser desorption-ionization time-of-flight
MCP-1 = monocyte chemoattractant protein-1
MeOH = methanol
MHC = major histocompatibility complex
MLC-2 = myosin light chain-2
MRI = magnetic resonance imaging
NH_2-PAMAM = amine-terminated poly(amidoamine) dendrimers
NH_2-PAMAM-G3 = generation-3 amine-terminated poly(amidoamine) dendrimers
NHS = *N*-hydroxysuccinimide
NMR = nuclear magnetic resonance
OD = optical density
P-gp = P-glycoprotein
p38 MAPK = p38 mitogen activated protein kinase
PAI-1 = plasminogen activator inhibitor-1
PAMAM = polyamidoamine
PBS = phosphate buffered saline
PDA = photodiodearray
PDGF = platelet-derived growth factor
(p-)PDGFR = (phosphorylated) platelet-derived growth factor receptor
PEG = polyethylene glycol
PI3K = phosphoinositol-3-kinase
PHEA = α,β-poly(*N*-2-hydroxyethyl)aspartamide
PVD = poly(vinylpyrrolidone-co-dimethyl maleic acid)
PVDF = polyvinylidene fluoride

PVP = polyvinylpyrrolidone
qRT-PCR = quantitative reverse transcription-polymerase chain reaction
RASA1 = Ras p21 protein activator
RCC = renal cell carcinoma
RFC = reduced folate carrier
RGDfK = Arg-Gly-Asp-D-Phe-Lys
RNA = ribonucleic acid
ROCK = Rho-associated kinase
RU = response unit
SDS = sodium dodecyl sulfate
α-SMA = alpha-smooth muscle actin
SMPT = succinimidyloxycarbonyl-α-methyl-α-(2-pyridyldithio)toluene
SOD = superoxide dismutase
SRB = sulphorodamine B
$(t_{1/2})_{\alpha}$ = initial elimination half life
$(t_{1/2})_{\beta}$ = terminal elimination half life
$(t_{1/2})_{absorption}$ = absorption half life
$(t_{1/2})_{elimination}$ = elimination half life
T_{max} = time to maximum concentration
TBME = *tert*-butyl methylether
TBS = Tris buffered saline
TBS/ T = Tris buffered saline with 0.1% (v/ v) Tween-20
TCA = trichloroacetic acid
TFA = trifluoroacetic acid
TGF-α/ β = transforming growth factor α/ β
TGFR-β = transforming growth factor-β receptor
TIMP-1 = tissue inhibitor of metalloproteinase-1
TKI = TGF-β type 1 receptor kinase inhibitor
TNF-α = tumor necrosis factor-alpha
Tris = 2-Amino-2-(hydroxymethyl)-1,3-propanediol
ULS = Universal Linkage System
UUO = unilateral ureteral obstruction
UV = ultra violet
V_d = volume of distribution
VCAM-1 = vascular cell adhesion molecule-1
VEGFR = vascular endothelial growth factor receptor

Curriculum vitae

Emmy Dolman was born on October 31st 1981 in Utrecht, the Netherlands. After graduating from the secondary school (athenaeum) in 2000 at College Blaucapel in Utrecht, the Netherlands, she started her study pharmacy at Utrecht University, the Netherlands. As a part of her study she visited Prince Henry's Institute of Medical Research in Melbourne, Australia, for a six-month research project on the effect of estradiol on the growth hormone secretion by somatotropes under the supervision of prof. Chen Chen. She furthermore did internships at several community and hospital pharmacies and at the Netherlands Pharmacovigilance Centre Lareb. After obtaining her pharmacist degree (Pharm. D.) in November 2006, she started her PhD research project in February 2007 within the Division of Biopharmacy and Pharmaceutical Technology at the same university. Under supervision of dr. Robbert Jan Kok, prof. dr. ir. Wim Hennink and prof. dr. Gert Storm she worked on the proximal tubular cell-specific delivery of kinase inhibitors for the treatment of renal diseases. This research was funded by the European Commission within the sixth framework program. The results of her PhD research project are described in the current thesis.

List of publications

M.E.M. Dolman, M.M. Fretz, G.J. Segers, M. Lacombe, J. Prakash, G. Storm, W.E. Hennink, and R.J. Kok. Renal targeting of kinase inhibitors. International Journal of Pharmaceutics 364:249-257 (2008).

M.E.M. Dolman, S. Harmsen, G. Storm, W.E. Hennink, and R.J. Kok. Drug targeting to the kidney: advances in the active targeting of therapeutics to proximal tubular cells. Advanced Drug Delivery Reviews 62:1344-1357 (2010).

M.E.M. Dolman, K.M.A. van Dorenmalen, E.H.E. Pieters, M. Lacombe, J. Pató, G. Storm, W.E. Hennink, R.J. Kok. Imatinib-ULS-lysozyme: a proximal tubular cell-targeted conjugate of imatinib for the treatment of renal diseases. Submitted for publication.

M.E.M. Dolman, S. Harmsen, R.W. Sparidans, E.H.E. Pieters, M. Lacombe, B. Szokol, L. Őrfi, G. Kéri, G. Storm, W.E. Hennink and R.J. Kok. Targeting of a platinum-bound sunitinib analogue to renal proximal tubular cells. Submitted for publication.

M.E.M. Dolman, K.M.A. van Dorenmalen, E.H.E. Pieters, R.W. Sparidans, M. Lacombe, B. Szokol, L. Őrfi, G. Kéri, N. Bovenschen, G. Storm, W.E. Hennink and R.J. Kok. NH_2-PAMAM-G3 as carrier for the intracellular delivery of a sunitinib analogue into the proximal tubular cells of the kidneys. Manuscript in preparation.

M.M. Fretz, **M.E.M. Dolman**, M. Lacombe, J. Prakash, T.Q. Nguyen, R. Goldschmeding, J. Pató, G. Storm, W.E. Hennink, and R.J. Kok. Intervention in growth factor activated signaling pathways by renally targeted kinase inhibitors. Journal of Controlled Release 132:200-207 (2008).

S. Harmsen, **M.E.M. Dolman**, Z. Nemes, M. Lacombe, B. Szokol, J. Pató, G. Kéri, L. Őrfi, G. Storm, W.E. Hennink and R.J. Kok. Development of a cell-selective and intrinsically active multikinase inhibitor bioconjugate. Bioconjugate Chemistry 22(4):540-545 (2011).

R. Haselberg, S. Harmsen, **M.E.M. Dolman**, G.J. de Jong, R.J. Kok, G.W. Somsen. Characterization of drug-lysozyme conjugates by sheathless capillary electrophoresis–time-of-flight mass spectrometry. Manuscript accepted in Analytica Chimica Acta.

Selected abstracts

Oral presentations

M.E.M. Dolman, M.M. Fretz, M. Lacombe, T.Q. Nguyen, R. Goldschmeding, G. Storm, W.E. Hennink and R.J. Kok: Inhibition of growth factor activated signaling pathways by targeting of kinase inhibitor-LZM conjugates to proximal tubular epithelial cells. Oral presentation at the "Najaarssymposium van de Nederlandse Federatie voor Nefrologie", Utrecht, the Netherlands, October 2008.

M.E.M. Dolman, J. Prakash, M. Lacombe, G. Storm, W.E. Hennink and R.J. Kok. Proximal tubular cell-targeted kinase inhibitor-lysozyme conjugates for the intervention in renal fibrosis. Globalization of Pharmaceutics Education Network (GPEN), North Carolina, USA, November 2010. ***Awarded with the second best oral presentation award.***

Poster presentations

M.E.M. Dolman, M.M. Fretz, M. Lacombe, T.Q. Nguyen, J. Pató, G. Storm, W.E. Hennink and R.J. Kok. Treatment of renal fibrosis by targeting of kinase inhibitor-LZM conjugates to proximal tubular epithelial cells. Globalization of Pharmaceutics Education Network (GPEN), Leuven, Belgium, September 2008. ***Awarded with the third best poster presentation award.***

M.E.M. Dolman, M.M. Fretz, M. Lacombe, J. Prakash, J. Pató, R. Ruijtenbeek, T.Q. Nguyen, Roel Goldschmeding, G. Storm, W.E. Hennink and R.J. Kok. Targeting of kinase inhibitor-LZM conjugates to the proximal tubular epithelial cells for the treatment of renal fibrosis. 36th Annual Meeting & Exposition of the Controlled Released Society, Copenhagen, Denmark, July 2009.

Dankwoord / Acknowledgment

U geeft mij meer dan ik nodig heb
en alles wat ik van U ontvang, geeft mij grote vreugde.
Ik loof de Here, Die mij steeds de weg wees.
Zelfs wanneer ik slaap, leidt Hij mij.
Dag en nacht is de Here de grootste in mijn leven;
omdat Hij mij leidt, struikel ik niet.
Daarom is er vreugde in mijn hart en ben ik gelukkig.

(Psalm 16)

Now that my time as a PhD student is almost finished I am regularly looking back on all experiences of the last 4 years. The nice conclusion of this "brainstorm session" is that, although the experimental results were not always the ones aimed for, I would do it all over again. This is not only because I liked the job, but also – more important – due to the persons around me with whom I worked together and/or shared a lot of nice memories. For all of you I write this acknowledgment!

Graag begin ik met het bedanken van de allerliefste en belangrijkste mensen in mijn leven: mijn familie! Lieve papa en mama, ik wil jullie super bedanken voor alles wat jullie voor mij (hebben) beteken(d)en. Jullie hebben ervoor gezorgd dat ik sta waar ik nu sta. Texel 2000…weten jullie het nog? Even gauw beslissen wat ik ging studeren, omdat ik te laat was mij op te geven voor mijn eerste keuze. Wat heeft dat goed uitgepakt … bedankt voor de tip mama! Ik vond het altijd super fijn dat ik makkelijk even langs kon komen uit mijn werk om onder het genot van een wijntje alle belevenissen met jullie te delen. Bedankt dat jullie mij altijd hebben gesteund en bereid waren om met mij mee te denken. Pap, heel erg bedankt dat je zoveel interesse toonde in de inhoud van het onderzoek en het altijd probeerde te begrijpen. Het betekent veel voor mij dat je hebt mee gedacht aan het ontwerp van de cover. De vrijdagavonden houden we er zolang mogelijk in he?!

Als ik het heb over de allerliefste en belangrijkste mensen, dan heb ik het ook over mijn zussen en schoonbroers. Liselotte, Christine, Dieuwertje, Tijmen, Doortje en Reinder, ik zou niet weten wat ik zonder jullie zou moeten! Heel erg bedankt voor alle liefde en mooie momenten die jullie mij (hebben ge)geven en dat ik altijd bij jullie terecht kon! Liselotte, ik hou van jouw manier van denken en vind de gesprekken die ik met jou kan voeren (je weet wel waarover) altijd ontzettend fijn. De middagjes shoppen, de avondjes Flikken Maastricht, de dagjes uit samen…..SUPER! Ik vind het heel lief van je dat je altijd vroeg hoe het ging op het werk. Bijna niemand weet dat je bij mij op het lab helemaal zelf (succesvol) een eiwitbepaling hebt gedaan! Lisi, jouw levensmotto "plezier maken op school" gaat je erg goed af en ik ben trots op hoe je het allemaal doet! Je weet dat er voor jou een speciaal drankje klaar staat op 27 juni! Christine, feestbeest, gelukkig vind jij exacte vakken zoals wiskunde en scheikunde en medische vakken zoals de anatomie en fysiologie van het lichaam ook erg leuk en kunnen we elkaar enthousiast maken en helpen. Soms word je aan het twijfelen gebracht, maar het liefste wil je geneeskunde studeren. Ga ervoor, je kunt het! Chris, je bent ook altijd in voor een goed avondje stappen. Nu mijn promotie er bijna op zit, moeten we maar snel weer een avond Havana plannen (en wat nemen we dan? ...). Dieuw, als ik praktische hulp nodig heb (zelfs mijn haar knippen … bedankt!) of geen beslissing kan nemen, moet ik bij jou zijn! Wij denken over veel dingen hetzelfde, waardoor het heel fijn is om deze dingen met jou te delen. En wat is een beter moment hiervoor dan de zaterdag, die we inmiddels hebben uitgeroepen tot onze "samen boodschappen doen"-dag. Hoe laat gaan we komende zaterdag? Succes met de laatste loodjes van je opleiding tot medium care verpleegkundige. Ben super trots op je! Thijmen, als het goed is ben jij op het moment dat ik mijn proefschrift verdedig net terug uit New York en heb je een rugzaak vol mooie ervaringen mee genomen! Ik vind het leuk dat je weer terug bent en kijk uit naar de volgende kanotocht in Rhijnauwen, barbecue in je achtertuin en…. Heel veel succes met je nieuwe baan! Door, wij schelen maar 1 jaar, waardoor we altijd vrijwel gelijk op zijn gegaan en elkaar goed begrepen … en konden helpen. Weet je het nog? Jij mijn Nederlands en ik jouw aardrijkskunde. We hebben andere karakters, maar vullen elkaar zo goed aan! Jij wilt ook gaan promoveren en ik weet zeker dat je het kunt en een leuke plek zult vinden! Als het zover is, ben ik daar om jou te supporten! Rein, je bent een super leuke schoonbroer! De donderdagavondjes bij jullie zorgden altijd voor de nodige ontspanning en ik kijk al uit naar onze volgende stedentrip! Als je de volgende keer weer belt of ik na mijn werk naar jullie toe kom op het terras, staat de koude rosé dan weer klaar?

Natuurlijk was dit proefschrift niet tot stand gekomen zonder mijn co-promotor Robbert Jan Kok en mijn promotoren Wim Hennink en Gert Storm. Robbert Jan, jij was het grote brein achter dit hele project. Dank je wel dat je deur altijd open stond voor mij en ik je altijd mocht lastig vallen met allerlei vragen. Jij was in staat om ook uit de negatieve resultaten het positieve te halen. Hiervan en van de vele discussies die we hebben gevoerd heb ik ontzettend veel geleerd. Ik was niet altijd blij met de rode kleur van mijn manuscripten na jouw screening, maar bij deze wil ik je bedanken dat je altijd kritisch bent geweest en het beste hebt nagestreefd. De congressen waar we allebei zijn geweest en jouw frequente aanwezigheid op borrels, etentjes en andere feestjes vond ik erg gezellig! Robbert Jan, bedankt voor je openheid en de leuke gesprekken die we hebben gevoerd. Ik hoop dat we, waar ik hierna ook terecht kom, in contact blijven.

Wim (tjongejonge ...) en Gert, de supercombi! Ik vond het fijn om jullie allebei als promotor te hebben. Mijn projecten gingen van synthese naar *in vivo* effectiviteit. Door jullie verschillende expertises werd ik op alle vlakken scherp gehouden. Bedankt! Jullie begeleiden allebei behoorlijk wat AIO's maar wisten altijd voldoende tijd voor mij vrij te maken en hoe het ervoor stond. Manuscripten werden snel van commentaar voorzien en voor vragen kon ik altijd langs komen. Super! Wim en Gert, ik wil jullie ook ontzettend bedanken voor de leuke en warme sfeer die jullie creëren in de groep en de jaarlijkse labuitjes, kerstdiners, barbecues en de maandelijkse (of meer frequente) borrels, waar jullie als het kon altijd bij waren. Een biertje doen met jullie stond garant voor leuke gesprekken en – vooral – veel grappen! Wim, jouw aanwezigheid op de GPEN zal ik niet vergeten. Dank jullie wel voor deze onvergetelijke jaren!

Marjan en Stefan, ik vond het ontzettend leuk om met jullie – postdocs - samen te werken op dit project. Naast dat ik veel van jullie heb geleerd, was het ook erg gezellig en vond ik het fijn om alle onderzoeksperikelen met jullie te kunnen delen. Marjan, wij begonnen vrijwel tegelijkertijd aan dit project en al gauw leerde ik jou kennen als één van de feestbeesten binnen biofarmacie! Ik wil je bedanken voor de vele leuke activiteiten die je organiseerde en de gezellige avondjes eten. Stefan, we kenden elkaar al toen jij nog bezig was met jouw PhD project binnen de afdeling geneesmiddelentoxicologie. Toen jij daarna als postdoc bij ons begon waren wij binnen no time op elkaar ingespeeld in het lab. Geen celexperiment was te groot voor ons … hoeveel platen namen wij op één dag onder ons hoede om het NMI van voldoende sample te voorzien? Stefan, heel erg bedankt voor je blijvende interesse in mijn verdere voortgang na jouw vertrek en je adviezen! Het boekje is af dus het afgesproken biertje moet maar snel gepland worden!

During my project I also got the help of different students! Aimee, you were my first student and started the same day I started my PhD, so we both had to find our way in the labs and to set-up experiments. You already finished your PhD in England, congratulations! Joseph, Helma, Sergio and Sabina, I also would like to thank you for all the work you did. Joseph, Helma and Sergio, you worked a lot on the production/ synthesis of a novel carrier for renal drug delivery. Although it was a difficult and time-consuming job you always were motivated to keep on going. I hope future students or other people will continue your work. (Sergio, when we moved to the new building I was confronted again with the huge number of polymers we produced …). Zoltan, you worked with Stefan, but also felt a little bit my student. It was nice to have you in Z-513 and I am happy that your research is included in my thesis and has also been published. Geert, bedankt voor de gezelligheid tijdens feestjes en borrels en voor je hulp bij het tot stand komen van hoofdstuk 1 van mijn thesis.

Collaboration knows no boundaries! Marie Lacombe, many thanks for all the kinase inhibitor-ULS adducts you synthesized and the nice discussions we always had. I will never forget me portraying how orbitals look like in the middle of the streets in Groningen after a nice dinner. Het UMC kon beschouwd worden als mijn tweede werkonderkomen naast de universiteit. Mijn speciale dank gaat uit naar Dionne, Jan Willem en Amélie die altijd voor mij klaar stonden en mij ontzettend hebben geholpen met het aanleren van verschillende technieken. Jan Willem, jij verdedigt jouw proefschrift een paar dagen voor mij. Heel veel succes en geniet van de dag! Amélie, succes met de laatste loodjes! Daarnaast wil ik ook Roel Goldschmeding, Tri Nguyen, Kevin van der Ven, Dick van Wichem en Niels Bovenschen van het UMC bedanken.

Roel, Rolf, Kim en Andrew, bedankt dat ik altijd jullie - voorheen geneesmiddelentoxicologie - lab kon binnenvallen om experimenten te doen en de -80 vriezer te bezetten met mijn samples. Het was meestal erg rustig op het lab, maar jullie waren altijd in voor een gezellig praatje (en goede muziek). Rolf, bedankt voor alle hulp bij het analyseren van mijn *in vivo* samples. Roel, bedankt voor het meedenken als ik tegen problemen aan liep.

Dank je wel Rob Ruijtenbeek voor je hulp bij de tyrosine kinase PamChip® microarray's. Rob Haselberg, leuk dat onze conjugaten uiteindelijk ook zijn gebruikt voor een hoofdstuk in jouw proefschrift.

Wat is een PhD doen binnen de vakgroep biofarmacie zonder jou Mies? Steekwoorden die bij jou horen zijn o.a.: vrolijk, koffiepauze, erwtensoep, dansen, zingen, Sinterklaas, kerstdiner … Kortom, bedankt voor de leuke sfeer die je creëerde binnen de groep. Verder wil ik je ook bedanken voor al je hulp bij de HPLC en GPC analyses. Die soms onmogelijk oplosbare kinase remmers en polymeren hebben ons aardig wat puzzels opgeleverd. Op de vijfde hield jij, Louis, de zaakjes draaiende. Dank je wel voor je hulp bij bestellingen en het verschaffen van allerlei disposables! Willemiek, bedankt voor alle hulp en gezelligheid tijdens de *in vivo* experimenten.

Luckily it was not all about work within the biopharmacy group and I had the privilege to meet a lot of nice friends that made the job unforgettable and much more easier for me!

My dear friend Roby, I am so happy and grateful to have met you! You were the person with whom I could share all my feelings and emotions and who could read my face. We made chatting our part time job besides the research. I will never forget our talks in the corridors, on our way home and in the lab while enjoying a cappuccino and cookie. Thank you Roby for your warmth and always making me feel comfortable, for your ongoing interest and always being there for me, for all the nice dinners and unforgettable holidays in Fermo, for all the laughter and fun … ! It was a great honour for me being your paranimf and I am very thankful that you are mine. It means a lot to me you draw the cover. We will both go different ways, but our friendship will stay forever. Roby remember: "se sei felice, sono felice"!
Romano, matey, I really loved your company during the nice moments I shared with Roby. We laughed a lot together about funny jokes and stories. Thanks for all the nice experiences and your kindness!

Lieve Pieter, jij bent niet veel later aan je PhD begonnen dan ik en bent ruim drie jaar mijn directe buur geweest in het gezellige Z-513! Samen met Roy begonnen we onze werkweek standaard met het doornemen van het afgelopen weekend en hadden we de leuke gewoonte om elkaar continu van koffie te voorzien. Ik wil je bedanken voor je belangstelling, de leuke gesprekken en alle gezelligheid in het lab … de laatste borrel in Z-513 voor de verhuizing naar DDW was een mooi moment. De rust die jij mee bracht in het lab was bijzonder en ik wil je bedanken dat je altijd bereid was om mee te denken met mijn project. Pieter, heel veel succes met de laatste loodjes van jouw project en heel erg bedankt dat je mijn paranimf wilt zijn!

Negar, met jou kon ik het meteen goed vinden en ik ben blij dat je na je stage binnen onze groep terug gekomen bent als AIO. Je bent een toffe, spontane meid! Bedankt voor de leuke pauzes, de gezellige "samen western blotten"-momenten, de goede gesprekken en alle andere gezellige activiteiten (etentjes, Koninginnedag, proseccootjes….). Ik ben je dankbaar dat je hebt mee geholpen met de cover en lay-out van dit proefschrift. Straks ben ik geen collega meer, maar weet dat je altijd bij mij terecht kan (je weet wat ik bedoel)! Friends forever!

Z-513 was lang niet zo gezellig geweest zonder jouw aanwezigheid Roy! Jij behoort zeker weten tot de smaakmakers binnen biofarmacie. De "privé borrels" in Z-513 en buiten – ook als het ijskoud is – en de door jou verzorgde muziek in het lab zal ik zeker niet vergeten. Super bedankt voor je vrolijkheid, enthousiasme en interesse, maar zeker ook voor al je hulp! Dankzij jou heeft mijn laptop deze 4 jaar overleefd. Anna, super leuk en gezellig dat je er vaak bij was op borrels en feestjes. Bedankt voor al het lekkers dat je voor ons mee gaf aan Roy.

Lieve Inge, twee maanden na jouw fantastische verdediging is het mijn beurt om mijn proefschrift te verdedigen. Ik vind het super leuk en fijn dat we het eindtraject samen hebben kunnen beleven en ben je dankbaar voor alle hulp en de goede en leuke gesprekken. Het was ontzettend gaaf om je paranimf te mogen zijn Inge. Ik wil je ook bedanken voor de gezellige feestjes, etentjes en sinterklaasviering! Jij ook bedankt Mike! Als jullie naar New York gaan houden jullie wel een kamer vrij he?!

Another close friend I want to thank is you, Hajar. We experienced so many good moments together … Spending time with you means having lots of fun (I am looking forward to your promotion …). Thanks a lot for your friendship, sharing the ups and downs, your generosity, listening, warmth and the dinners and parties you organized! Wish you all the best with the remaining months of your PhD and we keep in touch!

Twee mensen die ik nog niet heb bedankt voor al hun hulp zijn Kim en Ebel. Dat ik jullie hier samen noem heeft alles te maken met de leuke herinneringen die ik heb aan de effectstudies die we samen hebben uitgevoerd! Dankzij jullie waren dit de leukste studies tijdens mijn AIO periode: bedankt! Ebel, ik wil je ook bedanken voor je hulp bij alle andere dierstudies, voor je flexibiliteit, interesse en gezelligheid. Kimmiejoooooo, bedankt voor het vele werk dat je heb gedaan voor mij, zelfs toen je eigenlijk al begonnen was bij Enrico. Ik weet dat ik niet altijd de makkelijkste ben geweest om mee samen te werken omdat ik een behoorlijk pietje precies ben, maar je ging er altijd ontzettend goed mee om en gaf mij alle ruimte. Super bedankt daarvoor!

Naast het serieuze werk was jij ook altijd in voor een drankje in the basket of café België. Kim, bedankt voor alle gezelligheid, je begrip en de goede gesprekken. We hebben heel wat afgelachen samen!

Mel, thanks for organizing so many unforgettable activities such as dinners, brunches, cocktail parties and movie nights. I hope we will continue doing this! Thank you Andreas for your nice company during these activities!

Barbara, matey, dank je wel dat ik altijd even binnen kon lopen voor hulp of gewoon een leuk gesprek! Bij jou was ik vaste klant voor het aanschaffen van een nieuwe toegangspas of koffiekaart. Gelukkig heb je mij altijd zonder problemen een nieuwe verschaft, ook al was het aantal keren verlies bijna niet meer op twee handen te tellen. Barbara en Lies, jullie aanwezigheid op feestjes hebben ook voor onvergetelijk mooie momenten gezorgd. Haal je dansschoenen maar vast uit de kast Lies!

I also want to thank you, Lise and Kimberly, for your friendship, for your support when I needed it and for the good chats and nice moments in- and outside the lab. Lise and Nicolas, I liked the trips to France and Italy and I am happy you stay in the Netherlands longer! Kimberly, laat je niet gek maken, jij komt er ook! En je weet het … ik sta altijd voor je klaar.

Many others contributed to the unforgettable experience I had within the biopharmacy group by always being kind, helpful and supportive. Your friendship and company at activities in- and outside the lab was of great value to me. Writing a personal message to all of you will result in another thesis, but I would like to mention you. Thank you Albert (I really enjoyed your company in North Carolina), Marina, Markus, Karin (thanks for the nice dinners and funny moments), Amir G, Maria, Amir V, Audrey, Marion, Sabrina, Maryam, Afrouz, Isil, Grzegorz, Mehrnoosh, Peter, Bart, Tina, Cristianne, Vera, Cor, Frank, Najim, Martin L, Manuela and my Italian friends Ele, Francesca S and Laura. Ele, thanks for the unforgettable moments in Italy. Laura, good luck with your defence one week earlier! I also would like to thank the (old) students Rianne, Ralf, Susan, Volkert, Marius, Antonis, Martin P, Lieselotte, Giorgio and Evelien.
The nice atmosphere within biopharmacy was created by the whole group. Thanks Agnes, Filis, Sima, Luis, Sylvia, Alex, Abdul, Merel, Anastasia, Andhyk, Georgi, Burcin, Mazda, Farshad, Martin S, Eduardo, Neda, Chris, Yang, Erik, Ethlinn, Rolf, Roel, Marcel, Karlijn, Ellen, Joris, Niels, Joost, Holger, Birgit, Albert van H, Helena, Myrra, Nataša, Sophie, Naushad, Yu Ling, Maarten, Ray, Enrico, Rene, Herre, Twan, Lidija, Daan, Koen, Huub, Herman and … all others
Ook de mensen van het onderwijs wil ik bedanken voor hun gezelligheid en belangstelling! Nel, bedankt voor de vele leuke gesprekjes in de gang en bij het koffieapparaat en de grappige momenten als we elkaar voor de zoveelste keer weer tegen kwamen.
During my PhD I also met nice colleagues from other groups. Thank you Steffen, Francesca P, Hilde, Francisco and Marta.

Besides all persons I met at work, there were always my lovely friends I already knew who supported me and gave me so many nice memories!

Lieve Thijs, Peter, Lieke, Maartje en Annemiek, ik vind het ontzettend gaaf dat onze vriendengroep zo goed stand houdt, ondanks dat we allemaal door het land verspreid wonen. Tot begin maart was de verdeling openbaar apotheker, ziekenhuisapotheker en AIO binnen onze groep gelijk. Volgens de nieuwe statistiek zou ik nu door moeten gaan als openbaar apotheker … dat gaat niet gebeuren! Ik wil jullie en ook Annemarie, Leon, Herman en Xander bedanken voor alle gezellige etentjes, feestjes, bowlingavondjes, weekendjes weg, leuke en goede gesprekken en … ! Thijs, jij hebt het zelfde traject doorlopen en begreep daarom als geen ander de problemen waar ik af en toe tegen aan liep. Het was super fijn om jou om hulp en advies te kunnen vragen en ik wil je middels deze weg vertellen dat ik het altijd heel fijn heb gevonden dat je zo trouw belde om te informeren hoe het allemaal met me ging. Tot voor kort woonde je bij mij om de hoek en zochten we elkaar geregeld op om onder het genot van een lekkere maaltijd en een goed wijntje bij te kletsen. Door je verhuizing naar Enschede is dat minder geworden. Maar mijn boekje is nu af en dus gaan we die traditie weer oppakken. Ik kijk uit naar ons volgend reisavontuur!

Rachel, Sanne en Charlotte, als wij elkaar zien is het altijd goed en gezellig. Ik wil jullie bedanken voor alle gezellige (huis)feestjes, etentjes, borrels, meidenpraat en jullie interesse!

Andries, Remco, Laurens, Claire, Dennis, Coby, Mark, Jessica, Willem, Iris, Albert, Maaike, Josh, Marianna, Gerrit, Reinder en Doortje, bedankt voor de gezellige boothill-avondjes, terrasjes, feestjes, derde kerstdagen, vrimibo's, parkbezoekjes, etentjes, voetbalwedstrijden … dit heeft zeker voor de nodige ontspanning gezorgd!

Lastly, I would like to thank all other persons in my surrounding I did not mention, but who also expressed their interest!

Thank you all!

Emmy